Universitat Autònoma de Barcelona

Neurodevelopmental alterations in X-linked adrenoleukodystrophy

Arantxa Golbano Rodríguez

Institut de Neurociències
Departament de Bioquímica i Biologia Molecular
Unitat de Bioquímica, Facultat de Medicina
Universitat Autònoma de Barcelona

Neurodevelopmental alterations in X-linked adrenoleukodystrophy

Arantxa Golbano Rodríguez

PhD Thesis

Bellaterra, Setembre 2019

Institut de Neurociències
Departament de Bioquímica i Biologia Molecular
Unitat de Bioquímica, Facultat de Medicina
Universitat Autònoma de Barcelona

Neurodevelopmental alterations in X-linked adrenoleukodystrophy

Memòria de tesi doctoral presentada per Arantxa Golbano Rodríguez per optar al grau de doctor en neurociències per l'Institut de Neurociències de la Universitat Autònoma de Barcelona.

Treball realitzat al departament de Bioquímica i Biologia Molecular i a l'Institut de Neurociències de la Universitat Autònoma de Barcelona sota la direcció de la Dra. Elena Galea Rodríguez de Velasco i la Dra. Roser Masgrau Juanola.

Bellatera, Setembre 2019.

Doctoranda

Arantxa Golbano Rodríguez

Directores de tesi

Dra. Elena Galea

Dra. Roser Masgrau

In memoriam

¿Qué has descubierto hoy?
-Carmelo Golbano-

A la meva mare i a la meva àvia.

INDEX

ABSTRACT

X-linked adrenoleukodystrophy (X-ALD) is a rare disease caused by mutations in the peroxisomal ABCD1 transporter, with two major clinical manifestations of neurodegeneration: acute and lethal brain demyelination in the child cerebral X-ALD (CCALD), and chronic degeneration of spinal-cord tracts and peripheral neuropathy in the adult adrenomyeloneuropathy (AMN). Psychiatric alterations are an early sign of CCALD and coexist with spinal-cord and peripheral neurodegeneration in AMN, revealing concomitant brain pathology. Since X-ALD is a genetic condition, we sought to determine whether psychiatric alterations could be due, at least in part, to abnormal formation of brain circuits during brain development and not to neurodegeneration. To this end, we used a top-down approach, moving from patient transcriptome data, where we searched for dysregulated neurodevelopmental pathways, to *in vitro* murine models of X-ALD based on *Abcd1/Abcd2* silencing to dissect out astrocyte versus neurons compartmentalization. There are four major findings. First, developmental pathways are dysregulated in CCALD, CAMN and in ABCD-null neuronal cultures, associated with altered neuritogenesis, spinogenesis, and axonogenesis. Second, aberrant spine growth is in part due to alterations in canonical Wnt signalling alteration since the spinogenesis is partially rescued by activation of WNT pathways by pharmacological GSK-3 inhibition. Third, cholesterol synthesis and localization is changed in ABCD-null astrocytes. Four, silencing of ABCD transporters causes metabolic alterations in astrocytes including fatty acid oxidation impairment, increase of the ratio NAD^+/NADH, ATP depletion, decreases in total glutathione, suggesting joint impairment of antioxidant defense and bioenergetics. Fifth, X-ALD astrocytes present altered agonist-induced calcium signaling and ER stress. We conclude that i) X-ALD has a neurodevelopmental component that may account for psychiatric symptoms, and perhaps contribute to the progression of CCALD, and to the conversion of AMN into a cerebral condition, and ii) metabolic and excitability dysregulation in astrocytes support global astrocytic dysfunction that may jeopardize computational and homeostatic role of astrocytes in neural circuits.

INTRODUCTION

1. Peroxisome dysfunction causes brain diseases

Peroxisomes are single membrane-bound organelles, which harbour a variety of catabolic and anabolic reactions to contribute to normal cell function. Originally, peroxisomes were defined by the performance of oxidation reactions that produce hydrogen peroxide (H_2O_2) and its subsequent detoxification. The enzyme catalase, exclusive of peroxisomes, decomposes H_2O_2, which is harmful for cells, and produces water or uses it to oxidize another organic compound. Actually, peroxisomes are involved in many metabolic reactions.

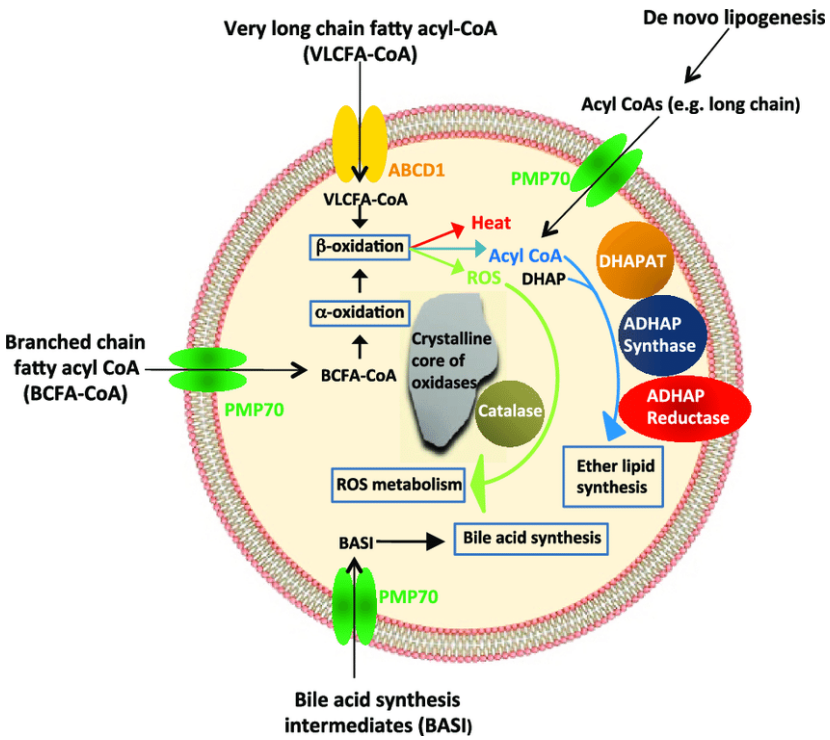

Figure 1. Peroxisome structure and functions. Peroxisome is a single membrane-bounded organelle that perform α-oxidation of branched chain fatty acids, B-oxidation of very long chain fatty acids, removal of reactive oxygen species and synthesis of bile acids. (Lodhi and Semenkovich, 2014).

In higher eukaryotes, peroxisomes carry out essential catabolic reactions using as a substrate fatty acids, amino acids, and polyamines. In particular, fatty acid β-oxidation of very long-chain fatty acids (VLCFA), which are exclusively oxidized in peroxisomes, while short- and medium-chain fatty acids are exclusively oxidized in mitochondria and long-chain fatty acids which can be oxidized in both (Singh *et al.*, 1984). VLCFA include fatty acids from 22 to 26 carbons in their chain. Mitochondrial and peroxisomal β-oxidation share similar mechanisms, although, mithocondrial products are used

directly as a major source of ATP while acetil-coA and shortened fatty acids resultant from peroxisomal β-oxidation have to be transferred to mitochondria where they will be fully oxidized and used to generate energy. Moreover, peroxisomes are involved in anabolic reactions like lipid biosynthesis, for instance, cholesterol and dolichol that are synthesized in peroxisomes as well as in the ER (James and Kandutsch, 1980) or plasmalogens that are important membrane components of heart and brain (Hajra and Bishop, 1982).

The proper peroxisomal function is necessary as the complete or partial loss of one of their functions leads to severe inherited human diseases. We can divide these diseases in two groups: **peroxisome biogenesis disorders** (PBD), in which formation of peroxisomes are disrupted, and **single enzyme and transporter deficiencies**, where different proteins are non-functional or absent disturbing different peroxisomal functions. Loss of peroxisomal activities is often linked to perturbation of brain formation and function, principally cortex and cerebellum development, axonal and synaptic transmission, inflammatory processes and early ageing. Peroxisomal disorders affecting CNS can be grouped in three categories as we have more than 17 types described: Abnormalities in neuronal migration and differentiation, defects in formation and maintenance of central white matter and post-developmental neuronal degeneration (Cantagrel and Lefeber, 2011).

Peroxisomes contribute to different biological pathways depending on cell type and tissue. In CNS, peroxisomes are notably smaller than in other tissues, calling them microperoxisomes (HOLTZMAN *et al.*, 1973). They play a role in myelin compounds biosynthesis such as ether phospholipids. They exert the last step of docosahexaenoic acid (DHA) (C22:6ω3) biosynthesis, which have an important role in nervous system (Bazinet and Layé, 2014; Dyall, 2015). DHA can be used as a structural component of membranes, especially in CNS, but also as a signalling molecule, contributing to normal cell growth and differentiation. DHA could affect either early development as well as cognitive functions throughout life (Lauritzen *et al.*, 2016). Peroxisomal enzymes also degrade D-amino acids such as D-serine, which have a role in synaptic transmission (Pollegioni, Sacchi and Murtas, 2018). D-amino acid oxidase (DAO) is responsible of this process and its activity is restricted to astrocytes (Arnold, Liscum and Holtzman, 1979).

Moreover, peroxisomes degrade potentially toxic compounds that could be detrimental for brain formation and maintenance such as phytanic acid that requires α-oxidation in peroxisomes prior to β-oxidation in mitochondria (Wanders, Komen and Ferdinandusse, 2011).

Ultimately, correct peroxisome biosynthesis and function is crucial for nervous system. Provide biosynthetic intermediates, degrade toxic products and maintain proper metabolite levels are critical activities. Disturbances on any of these processes could lead to different disorders with a wide spectrum of defects. Genetics, epigenetics and environmental factors modify disease progression and interaction of peroxisomes with other organelles might affect them secondarily (Schrader *et al.*, 2015).

2. X-linked adrenoleukodystrophy

X-linked adrenoleukodystrophy (X-ALD, OMIM #300100) is the most common peroxisomal disorder. It has an estimated incidence of 1:20,000 births (Bezman *et al.*, 2001). X-ALD is a monogenic disorder caused by mutations in *ABCD1* gene that codifies for peroxisomal transporter named Adrenoleukodystrophy protein (ALDP). ALDP is responsible for the import of free very long chain fatty acids (VLCFA) into the peroxisome for their further degradation by peroxisomal β-oxidation (Mosser *et al.*, 1993). The lack of a functional ALDP results in VLCFA accumulation in plasma and tissues which is the biochemical hallmark of the disease (Igarashi *et al.*, 1976; Kawamura, A. B. Moser, *et al.*, 1978; Kawamura, H. W. Moser, *et al.*, 1978; Moser *et al.*, 1981).

X-ALD is a neurodegenerative disease that mainly affects central nervous system (CNS) white matter, adrenal cortex and Leydig cells of the testes (Powell *et al.*, 1975; Powers *et al.*, 1982). Clinical presentation is highly complex and it is characterised by a progressive cerebral demyelination, axonopathy in the spinal cord and adrenal insufficiency (Mosser *et al.*, 1993).

2.1 History

In 1910 Haberfeld and Spieler described a clinical case of what could be X-ALD. Two brothers died at the age of 7 and 8 years old respectively. The case reported was about

the young brother who was healthy until the age of 6 when he developed hyperpigmentation, impaired visual acuity and worsen his school performance. Incontinence, loss of speech ability and spastic tetraparesis appeared later and were followed by inability to walk. At the age of 7 he died and the post-morten analysis revelled cerebral demyelination and perivascular accumulation of lymphocytes and plasmatic cells in the nervous system (Haberfeld and Spieler, 1910). Not was until 1923 when Siemerling and Creutzfeldt reported a similar case which combined cerebral demyelination and lymphocytic infiltration with atrophy of the adrenal cortex (Siemerling and Creutzfeldt, 1923). This was the first unequivocal case of X-ALD reported.

In 1993, 9 cases had been reported. All of patients were males, suggesting a possible X-linked recessive inheritance that was proposed by Fanconi based on pedigree analysis. The name X-linked adrenoleukodystrophy was introduced in 1970 by Michael Blaw.

2.2 Clinical features and phenotypes

X-ALD can be presented at different ages with a wide range of phenotypic manifestations. Neither the age of appearance nor the phenotype could be predicted by mutations as in the same family we can find very diverse clinical manifestations. Moreover, as it is a progressive disease, the same patient could have different phenotypes throughout his life. Therefore, interplay of *ABCD1* gene defect with genetic, epigenetic and environmental factors will determine initiation and progression of the disease.

Up to 7 phenotypes have been described (Moser *et al.*, 2000) with different severities. Ranging from the rapidly progressing childhood cerebral from (CCALD) to the later-onset adrenomyeloneuropathy (AMN). These two are the most frequent, and most of the patients will develop one or the other.

Table1. X-ALD phenotypes.

Table. X-Linked Adrenoleukodystrophy (X-ALD) Phenotypes

Phenotypes	Total ALD, %	Symptoms/ Signs	Age at Presentation, y	Misdiagnosed as	Diagnostic Test	Follow-up Tests	Recommended Therapy
Males							
Asymptomatic (MRI normal)	Increasing	None	0 to ≥10	Normal	VLCFA in relatives of X-ALD patients	Monitor MRI and adrenal function; family screening	Lorenzo's oil, adrenal HRT
Asymptomatic (MRI abnormal)	Increasing	None (cognition normal)	2 to ≥10	Other white matter disorders	VLCFA, brain MRI	Neurological and neuropsychological testing, adrenal function	HSCT, adrenal HRT
Addison disease only (MRI normal)	20 (decreases with age)	Primary adrenocortical insufficiency, normal neurology, MRI normal	0 to ≥10	Other causes of Addison disease	VLCFA	Monitor MRI, neurological and neuropsychological testing	Lorenzo's oil, adrenal HRT
Addison disease only (MRI abnormal)	1	Primary adrenocortical insufficiency	0 to ≥10	Other causes of Addison disease	VLCFA, brain MRI	Neurological and neuropsychological testing, MRI	HSCT, adrenal HRT
Cerebral (mild) without AMN*	45	Behavior changes, school failure, dementia, audiovisual	3-10 (common) 11-21 (intermediate) ≥21 (rare)	ADHD, psychological disorder, Asperger syndrome, autism	VLCFA, brain MRI	Neurological and neuropsychological testing, family screening, adrenal function	HSCT, adrenal HRT
Cerebral (severe) without AMN*	2-3	Dementia, psychoses, paralysis, epilepsy, loss of vision, loss of speech, bulbar palsy	5 to adulthood	Other neurodegenerative diseases, brain tumor, psychosis, epilepsy	VLCFA, brain MRI	Adrenal function, neurological and neuropsychological testing, family screening	Adrenal HRT, general support
Pure AMN†	35	Paraparesis, sphincter disturbances, sensory changes, incoordination, pain, impotence	28 (SD,9)	Multiple sclerosis, progressive spastic paraparesis, cervical spondylosis, osteoarthritis, back injury, ALS, "triple A syndrome"[14]	VLCFA	Brain MRI, adrenal function, MTS, SSEP, family screening	Adrenal HRT, possibly Lorenzo's oil,‡ physical therapy
Cerebral AMN†	15 (increases with age)	Like pure AMN plus dementia, behavioral disturbances, psychosis, epilepsy, aphasia, visual loss, bulbar palsy	28 (SD, 9)	Other causes, dementia, other neurodegenerative diseases, brain tumor, schizophrenia, Alzheimer disease, cerebrovascular disease, epilepsy, alcoholism, drug dependency	VLCFA, brain MRI	As in pure AMN plus neurological and neuropsychological testing, EEG, psychiatry, family screening	Adrenal HRT, general support, possibly HSCT§
Cerebellar	2-3	Ataxia, brainstem	Childhood; adolescence	Olivopontocerebellar degeneration	VLCFA, brain MRI	Adrenal function, neurological testing, family screening	Adrenal HRT, physical therapy
Females Heterozygous for ALD							
Asymptomatic (normal neurology)	50 (estimated)[9]	None	Any age		DNA (VLCFA)‖	Neurological examination and adrenal function, monitor MRI, family screening	Genetic counseling, general support
Heterozygotes (symptoms or neurological abnormalities)	50 (estimated)[15]	Paraparesis, sphincter disturbances, leg pain, sensory disturbances, incoordination, fatigue	Rare in women younger than 30 y	Multiple sclerosis, spastic paraparesis, peripheral neuropathy, cervical spondylosis, back injury, arthritis, herniated disk	DNA (VLCFA)‖	Adrenal function, MTS, SSEP, family screening	Genetic counseling, physical therapy, adrenal HRT, possibly Lorenzo's oil,‡ general support

Abbreviations: ADHD, attention-deficit/hyperactivity disorder; ALS, amyotrophic lateral sclerosis; DNA, *ABCD1* mutation analysis; AMN, adrenomyeloneuropathy; EEG, electroencephalogram; HRT, hormone replacement therapy; HSCT, hematopoietic stem cell transplant; MRI, magnetic resonance imaging; MTS, magnetization transfer MRI cervical cord; SSEP, somatosensory evoked potential; VLCFA, very long chain fatty acids assay in plasma.
*See Peters et al[13] for distinction between mild and severe cerebral forms.
†See text for distinction between pure and cerebral AMN.
‡Placebo-controlled trial in progress.
§HSCT being considered for mild cerebral AMN.
‖False-negative test results can occur.

(Moser *et al.*, 2000).

Adrenal insufficiency is usually the first manifestation of the disease in males, appearing during childhood (Dubey *et al.*, 2005). When patients only develop adrenal insufficiency, without other neurologic involvement, it is named Addison disease or Addison-only (Laureti *et al.*, 1996).

Myelopathy, an impairment of spinal cord**,** will appear progressively in adulthood without specific signs or symptoms, resulting in spastic paraparesis and sensory ataxia. Bladder dysfunction is also common and progressive, from urinary urgency to full incontinence (Engelen, Kemp, *et al.*, 2012). It will appear in males and females, being the main manifestation in females as other symptoms are very unusual (>1%) (Moser *et al.*, 2000; Jangouk *et al.*, 2012).

Peripheral neuropathy is also common in X-ALD. However, sometimes it is masked by myelopathy signs. Nerve conduction affectation can appear as a sensorimotor axonal neuropathy (**axonopathy**) or less frequently as a demyelinating neuropathy (Chaudhry, Moser and Cornblath, 1996; van Geel *et al.*, 1996). In AMN axonopathy and peripheral neuropathy appears prior to demyelination.

Progressive cerebral demyelination can appear at any age, as a first symptom or in addition to others (van Geel *et al.*, 2001) (Fig. 2). The youngest patient reported with cerebral disease had 3 years old. It usually appears before the age of 10 (31-35%) and the frequency is really low in adolescence (4-7%) and adulthood (2-5%) (Moser *et al.*, 2000). The age of appearance cannot be predicted as we do not know which are the factors that will determine it. White matter lesions are visible on MRI prior to appearance of symptoms. Normally, the first place affected is the splenium of the corpus callosum and they expand progressively to the periventricular and occipital white matter (van der Knaap and Valk, 2005).

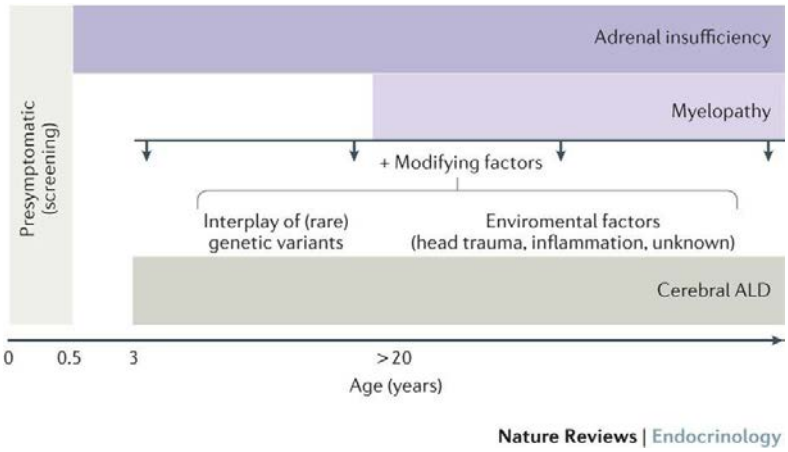

Figure 2. Clinical progression of ALD in men. All patients are asymptomatic at birth, first signs of adrenal insufficiency appear from 5 months of life. Cerebral form could occur at any age. (Kemp *et al.*, 2016).

Children affected by CCALD initially have behavioural and cognitive problems. Sometimes they are misdiagnosed as attention deficit hyperactivity disorders. Even disease progression is variable between individuals, it is usually extremely rapid. Auditory and visual impairment, hemiparesis or spastic tetraparesis, cerebral ataxia and seizures are often common symptoms. In adults, symptoms are similar; however, early clinical manifestations are usually depression or psychiatric disorders and the progression of the disease is slower. The severity of these phenotype leads to death on average 2 years after the onset of the first symptoms (Scriver, 2001). Demyelinating lesions (Fig. 3) in CALD are accompanied by a severe inflammatory process as it is observed in histopathological *post-mortem* studies. Infiltration of lymphocytes and macrophages, reactive microglia, damaged oligodendrocytes and astrocytes are surrounding demyelinated zones where axons are lost (POWERS *et al.*, 1992).

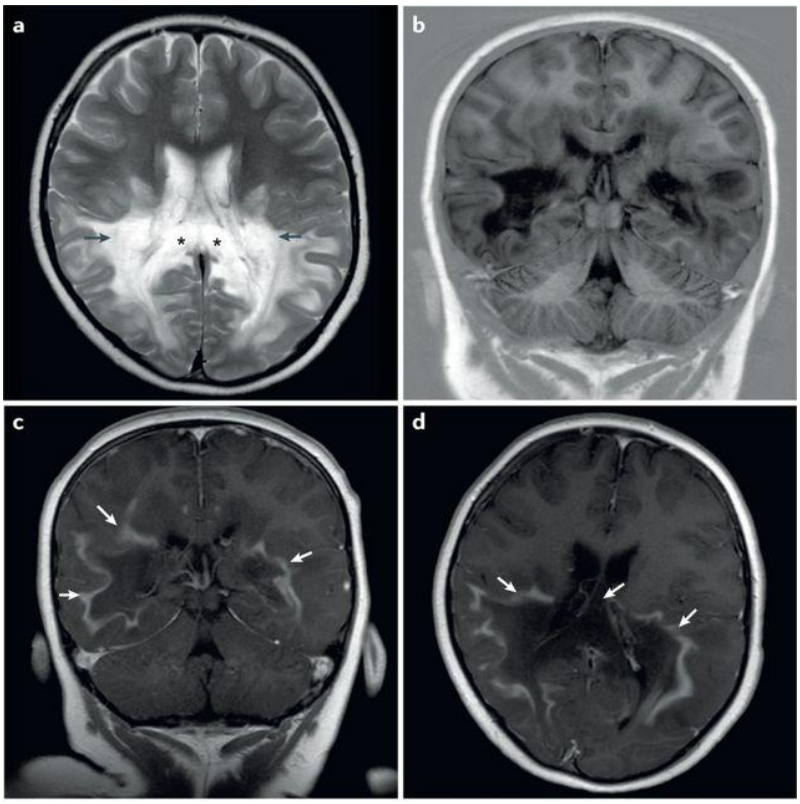

Figure 3. MRI of cerebral ALD. White matter lesions in a 6-year old boy involve parieto-occipital and splenium of the corpus callosum regions indicated with arrows and asterisks. (Kemp *et al.*, 2016)

2.3 Animal model

Abcd1-knockout mice was generated simultaneously by tree different laboratories (Forss-Petter *et al.*, 1997; Kobayashi *et al.*, 1997; Lu *et al.*, 1997). Three transgenic mice were generated by inactivation of the endogenous gene, exhibited reduced oxidation levels and accumulation of VLCFA in central nervous system (CNS) and kidney. Lipid inclusions were observed in adrenal cortex cells, testis and ovaries. However, no neurological involvement was seen up to 6 months of age and no lipid inclusions or demyelinating lesions were features in brain, spinal cord or peripheral nerves.

A few years later, Pujol A. demonstrated that at 15 months *Abcd1*$^{-}$ mice exhibit neurological, behavioural and motor abnormalities. Axonopathy and demyelination were detectable in spinal cord and sciatic nerve. Apparently brain was not affected neither by demyelination or inflammation resembling the AMN pathology rather than CCALD (Pujol *et al.*, 2002). Modulation of ALDP expression levels can change phenotype. Overexpression of *Abcd2* prevents neurodegenerative processes and accumulation of VLCFA, whereas double mutants (*Abcd1*$^{-}$*/Abcd2*$^{-}$*)* exhibit a more severe disease with an earlier onset. In this model, axonal damage precedes demyelination and lymphocytes infiltrations have been seen in spinal cord (Pujol *et al.*, 2004).

2.4 Biochemical features

Oligodendrocytes and astrocytes challenged with VLCFA (C22:0, C24:0 and C26:0) **die** within 24h (Hein *et al.*, 2008a). Moreover, lysophosphatidilcholine injection in mouse brain triggers **microglial activation and apoptosis** (Eichler *et al.*, 2008).

Depolarization of mitochondrial inner membrane (IM) and **increase of intracellular Ca^{2+} levels** are induced by VLCFA accumulation in astrocytes, oligodendrocytes and neurons (Hein *et al.*, 2008a).

Oligodendrocytes are responsible of **myelination** in CNS. Myelination of axons enables propagation of saltatory impulse saving energy. Defects in myelin not only perturb motor and sensory capacities, but also results in cognitive impairment (Saab, Tzvetanova and Nave, 2013). Ensheathing oligodendrocytes are severely affected by

lack of completely functional peroxisomes (Kassmann *et al.*, 2007). Normal myelin is composed mainly of long-chain fatty acids, while in X-ALD brain contains large amounts of VLCFA. Interestingly, myelin from CCALD contains higher levels of VLCFA than AMN patients (Asheuer *et al.*, 2005). Unfolding of myelin sheet, VLCFA induced apoptosis of oligondendrocites, microglial activation and release of cytokines and altered function of membrane receptors due to alterations in membrane composition have been proposed as a possible scenarios causing the inflammatory reactions that leads to demyelination (Singh *et al.*, 1992; Ho *et al.*, 1995).

Excess of VLCFA are incorporate into many different lipid species. Ganglioside, phosphatidilcholine and cholesterol ester fractions include the majority of these VLCFA. Glangliosides are constituents of plasmatic membrane; act as surface markers playing a role in cell-to-cell communication and recognition. They are implicated in neuroimunological disorders. Immunological properties of gangliosides vary with fatty acid composition. In normal brain, the higher amount of gangliosides is found in grey matter cells membrane and does not have VLCFA, while they are highly incremented in X-ALD patients. Phosphatidilcholine also have higher levels of VLCFA that could trigger immunological reactions, relating the amount of VLCFA with the stage of the disease. Moreover, in active demyelinating lesions cholesterol contains the highest VLCFA levels (Theda *et al.*, 1992).

ABCD1 defects also decrease plasmalogens levels. Plasmalogens have antioxidant activities and are synthesized in peroxisomes. The reduction of acyl-CoA from β-oxidation seems to be the reason of this decrease, however some studies showed plasmalogens synthesis in absence of β-oxidation (Khan, Singh and Singh, 2008).

Astrocytes from *Abcd1*$^{-/-}$ mice showed VLCFA induction of **ROS** and **mithocondria depolarization**. **Reversion of oxidated pyridine nucleotides to NAD(P)H impairment** was observed as a consequence of VLCFA accumulation in *Abcd1*$^{-/-}$ astrocytes. Accumulation of VLCFA in control and *Abcd1*$^{-/-}$ mitochondria increased ROS, impaired ATP production and diminished Ca^{2+} uptake (Kruska *et al.*, 2015a). Mitochondrial membrane potential is also decreased after VLCFA application as seen in fibroblasts (Fourcade *et al.*, 2008).

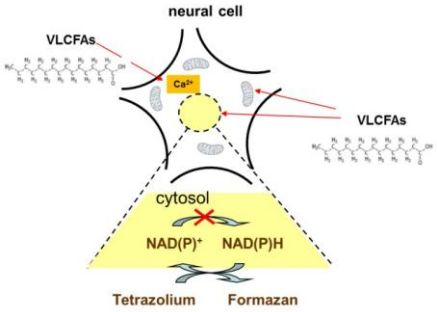

Figure 4. Altered energy dependent functions. Calcium signalling and conversion of $NAD(P)^+$ to NAD(P)H is impaired. (Kruska *et al.*, 2015a).

Protein modifications due to oxidative stress trigger cellular dysfunctions and tissue damages. Oxidative damage to proteins has been observed in Abcd1$^{-/-}$ mice and X-ALD fibroblasts prior to neuropathological signs. At 3.5 months of age, protein modifications occur in spinal cord of mice due to lipid peroxidation. Later, at 12 months of age, additional oxidative modifications of proteins arise from metal-catalyzed oxidation and glycoxidation/liposxidation (Fourcade *et al.*, 2008).

Free radicals production is a physiological situation in all cell types. Antioxidant defences maintain a balance of radical oxygen species (ROS) production and inactivation that when is disturbed leads to oxidative stress. Superoxide dismutases (SOD), gluthatione peroxidises (GPX) and peroxiredoxines (PRX) and catalase are responsible of antioxidant defence in nervous system. Expression of different SOD enzymes are repressed in spinal cords of 3.5 and 12 months old Abcd1$^{-/-}$ mice while other antioxidant enzymes do not present expression changes. In contrast, even no oxidative stress is reported in brain, SOD levels are increased in the knockout mice pointing to an incipient redox misbalance (Powers *et al.*, 2005). Catalase induction is specific of motoneurons in absence of peroxisomal proliferation (Fourcade *et al.*, 2008).

Gluthatione (GSH) plays a central role in antioxidant protection of all organs. GSH acts as a co-factor of ROS and lipid hydroperoxides reduction. Fibroblasts challenged with VLCFA presented a depletion of GSH levels suggesting a possible explanation for protein lipoxidative damage. Moreover, X-ALD fibroblasts have higher sensitivity to VLCFA exposure inducing cell death due to oxidative stress (Fourcade *et al.*, 2008).

Additionally, oxidative damage to proteins compromises 5 key enzymes of glycolisis and tricarboxilic acid cycle (TCA) in Abcd1$^{-/-}$ mice spinal cord and pyruvate kinase in

human X-ALD fibroblasts. ATP levels are decreased in these samples as well as GSH levels. NADH levels were also decreased an NADPH increased (Galino *et al.*, 2011b).

Contradictory studies have shown structural abnormalities in *Abcd1*$^{-/-}$ mice mitochondria while others showed normal size and structure (Powers *et al.*, 2001; McGuinness *et al.*, 2003; Oezen *et al.*, 2005). A diminish in mitochondrial amount (Morató *et al.*, 2013) and reduced phosphorylating respiration in *Abcd1*$^{-/-}$ mice spinal cord was observed (López-Erauskin *et al.*, 2013).

Plasma membrane inclusion of C26:0-containing lipids can disrupt its structure and interfere with serum albumin binding (Ho *et al.*, 1995). In concordance, membrane viscosity of erythrocytes and adrenocortical cells challenged with VLCFA is increased (Knazek *et al.*, 1983; Whitcomb, Linehan and Knazek, 1988).

Additional studies, showed other alterations non-directly related with VLCFA metabolism. For example, an study showed blood-brain barrier disturbances combined with endothelial tight junction proteins and adhesion molecules changes prior to VLCFA increased levels (Musolino *et al.*, 2015).

2.5 ABCD1, ALDP and VLCFA

ABCD1 gene is located in the long arm o choromosome X and maps to Xq28 (Mosser *et al.*, 1993). It is a member of the superfamily ATP-binging cassette (ABC) transporters. ABC transporters are divided into 7 families, ABC proteins transport several molecules across extra and intracellular membranes. Particularly, *ABCD1* encodes for the ATP-binging cassette transporter sub-family D member 1 also named Adrenoleukodystrophy protein (ALDP), which transports VLCFA and their CoA-esters into the peroxisome (van Roermund *et al.*, 2008).

The gene spans 19.9kb and has 10 exons that encode for 745 amino acids. More than 800 mutations have been described (*Mutations & Biochemistry - Adrenoleukodystrophy.info*, 2019) (Fig. 6). Most of them are point mutations although there are some insertions and deletions reported. *ABCD1* levels does not correlate with affected tissues as it is highly expressed in certain types of cells of liver, kidney, lung, colon, cardiac and skeletal muscle, skin, thyroid, placenta and lymph node, but

only CNS white matter, adrenal cortex and testis are severely affected. *ABCD1* mRNA levels are largely higher in fetal brains compared with adult brain (Höftberger *et al.*, 2007).

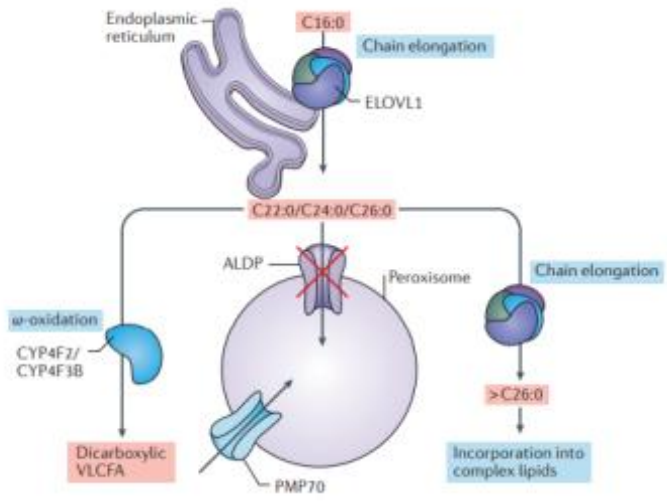

Figure 5. VLCFA elongation key enzymes. Very long-vchain fatty acids (VLCFA) synthesis takes place in the endoplasmic reticulum where long-chain fatty acids are elongated by ELOVL1. ALDP deficiency impairs import into peroxisome and β-oxidation. Accumulated VLCFA are further elongated and incorporated into more complex lipids. are (Kemp *et al.*, 2016)

ABC transporters are composed of 2 transmembrane domains and 2 nucleotide binding domains. ALDP is a half transporter, so 2 ABC half-transporters have to dimerize to form a full transporter that hydrolyse ATP and releases ADP to transport molecules across membrane (Roerig *et al.*, 2001). Apart from *ABCD1*, there are two other peroxisomal ABC transporters: ABCD2 that encodes for adrenoleukodystrofy related protein (ALDRP) and ABCD3 that encodes for PMP70 (Kamijo et al., 1990; Lombard-Platet et al., 1996). ALDP transports saturated straight chain VLCFA (C24:0 and C26:0) and monounsaturated VLCFA (C26:1) (Moser et al., 1999; Valianpour et al., 2003). ALDRP transports C24:6ω3 for the posterior synthesis of poly-unsaturated fatty acid docosohexaenoic acid (DHA, C22:6ω3) (Fourcade et al., 2009). PMP70 transports 2-methylacyl-CoA esters including pristanoyl-CoA, dihydroxycholestanoyl-CoA (DHC-CoA) and trihydroxycholestanoyl-CoA (THC-CoA) and of medium chain dicarboxylic acids presumably as CoA-esters (Wanders et al., 2001). Nonetheless, the residual β -oxidation activity (15-25%) in ALDP-deficient fibroblasts is due to PMP70. It is demonstrated that overexpression of ABCD2 and ABCD3 in X-ALD patients fibroblasts can restore β-oxidation levels (Kemp *et al.*, 1998; A Netik *et al.*, 1999; Wiesinger *et al.*, 2013).

However, ALDP and the other peroxisomal ABC transporters could have other functions and interactions not reported yet.

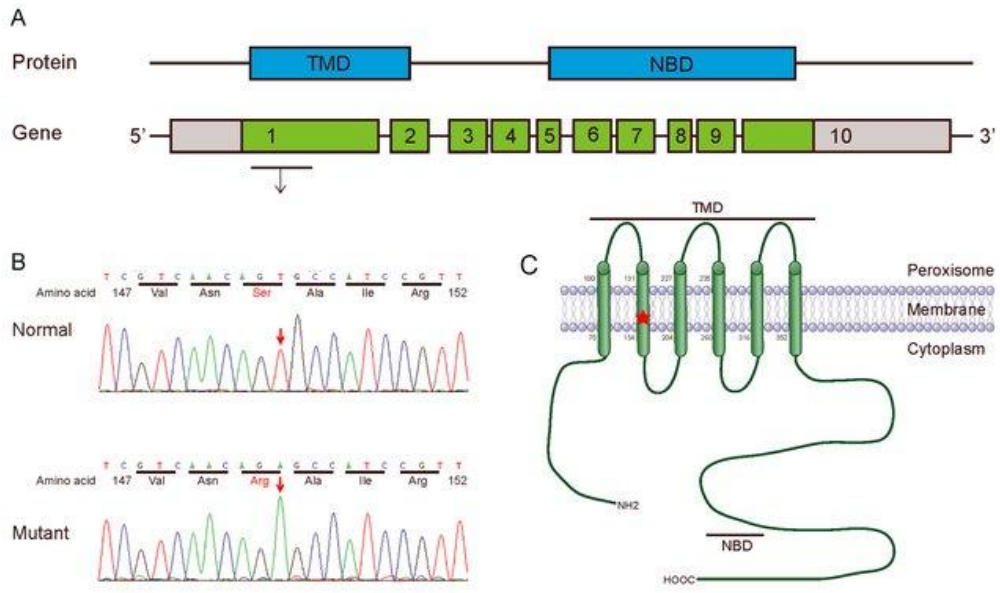

Figure 6. ABCD1 mutation, protein and gene structure. A. Protein and gene structure. B. Single nucleotide mutation indicated with a red arrow. C. Scheme of protein ALDP ant their membrane position. (Yan *et al.*, 2017)

VLCFAs are fatty acids with more than 20 carbons in their chain (C>20). C22 and C24 VLCFAs are distributed ubiquitously throughout the tissues and body fluids while C≥26 VLCFAs are found in small amounts in most of the body and have higher concentrations in skin, retina, meibomian gland, testis, and brain (Poulos, 1995; Sassa and Kihara, 2014).

2.6 VLCFA function and metabolism

Endogenous **VLCFA predominantly result from elongation** of long and less frequently very long-chain fatty acids. Only a small part comes from the diet (TSUJI *et al.*, 1981; Robinson, Johnson and Poulos, 1990). Hence, dietary restriction was not a good strategy to lower VLCFA levels, such as C26:0, as it was demonstrated by Van Duyn *et al.*, 1984. Moreover, elongation is induced in X-ALD patients, at least in fibroblasts, incrementing the amount of VLCFA accumulated (Kemp *et al.*, 2005a).

After synthesis the novo of long-chain fatty acids, up to 16 carbons, in the cytosol by the fatty acid synthase (FAS) or dietary intake, elongation of FAs occurs in the

endoplasmic reticulum (ER). Acetil-CoA FAs are elongated by the addition of two carbons in each cycle. Each cycle has 4 reactions catalized by four distinct enzymes: condensation (elongation of very long chain fatty acids (ELOVL)), reduction (3-ketoacyl-CoA reductase (HSD17B12)), dehydration (3-hydroxyacyl dehydratase (HACD)) and reduction (trans-2,3,-enoyl-CoA reductase (TECR)) (Guillou et al., 2010). First step is mediated by FA elongases, which constitute the ELOVL family of proteins with seven members (ELOVL1-7) in mammals (JAKOBSSON, WESTERBERG and JACOBSSON, 2006) (Fig. 7).

Each ELOVL exhibits characteristic substrate specificity and tissue distribution pattern. For example, ELOVL4, responsible of >C26 FAs, is restricted to the tissues where higher amounts of extremely long FAs are found like retina, skin, testis and brain (Zhang *et al.*, 2001; Agbaga, Mandal and Anderson, 2010; Sherry *et al.*, 2017).

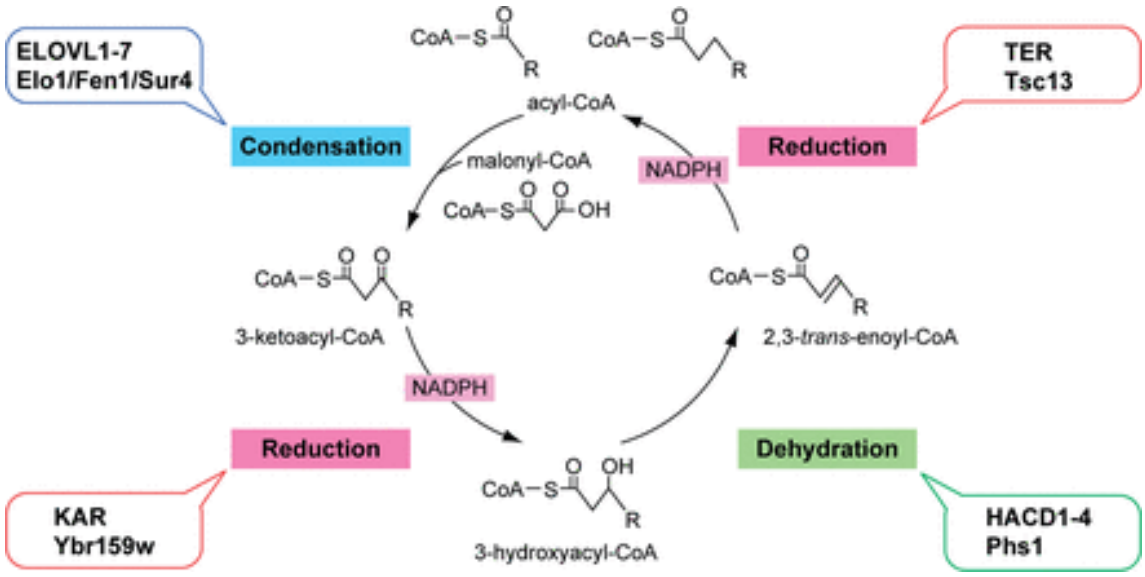

Figure 7. Fatty acid elongation cycle. Mammalian genes and yeast enzymes controlling each step are indicated. Acetil-CoA incorporate two carbon units each cycle of four steps as represented.(Kihara, 2012)

Tetracosanoic acid (C24:0) and hexacosanoic acid (C26:0) are the most abundant FAs in X-ALD patients plasma (Moser *et al.*, 1991; Korenke *et al.*, 1995). Synthesis of C24:0 and C26:0 requires two reactions. First the elongation of C16:0 to C20:0/C22:0 by ELOVL6 and then the further elongation to C24:0 and C26:0 by ELOVL1 (Ofman, Inge M

E Dijkstra, *et al.*, 2010). Inhibition of ELOVL1 in cells derived from patients leads to lower levels of C26:0 (Engelen, Schackmann, *et al.*, 2012), however, administration of benzafibrate, an inhibitor of ELOVL1, in patients was unable to lower VLCFAs levels (Engelen, Tran, *et al.*, 2012).

VLCFAs degradation by β-oxidation takes place in peroxisome. Consists of four sequential reactions: dehydrogenation, hydration, dehydrogenation, and thiolytic cleavage, and three enzymes: acyl-CoA oxidase (ACOX1 or ACOX2), bifunctional protein (DBP or LBP) and a thiolase (ACAA1 or SCPx). Substrates of β-oxidation are imported as Co-A esters though the ABC, in each cycle the backbone is shortened two carbons and acetil-CoA, propionyl-CoA, and medium-chain acyl-CoAs is released. Resultant products are processed into carnitine esters by carnitine acetyltransferases or into free acids by Acetyl-CoA thioesterase. End products of peroxisomal –oxidation are transported to mitochondria for full oxidation to CO_2 and H_2O (Wanders, Waterham and Ferdinandusse, 2016) .

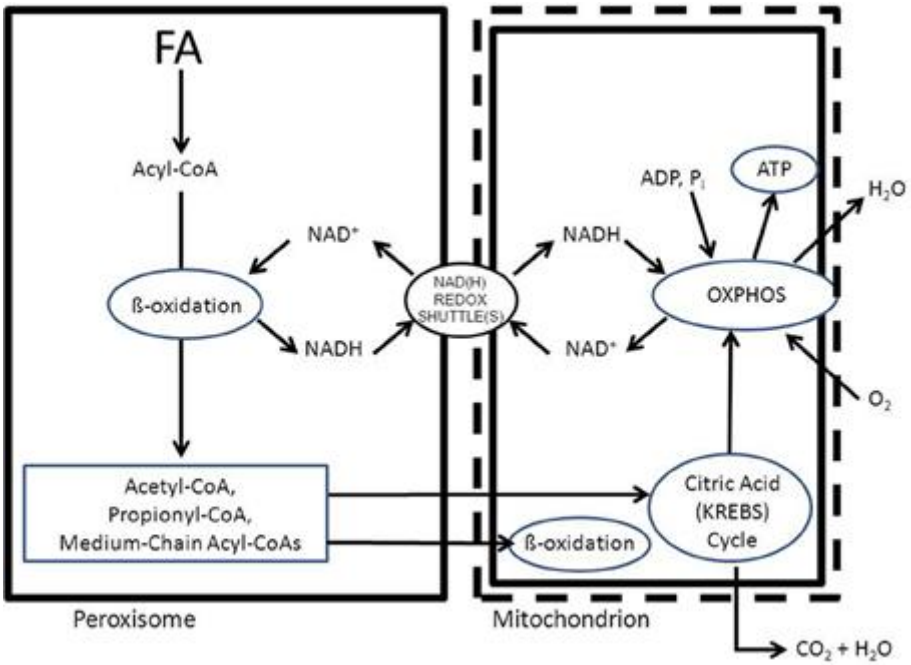

Figure 8. Scheme of β-oxidation comparison between peroxisome and mitochondria. (Wanders, Waterham and Ferdinandusse, 2016)

VLCFA play essential roles in cellular signalling and membrane structure. In mammals, most VLCFAs are found as constituents of sphingolipids. They are abundant in plasma membrane. Ceramide (Cer), the backbone of sphingolipids is converted to

sphingomyelin (SM) and glycosphingolipids. FAs in sphingolipids are usually C16:0, C24:0 and C24:1, the content of C18:0 is higher in brain and skeletal muscle (Kihara *et al.*, 2007). Neurons synthesize perdominantly C18 sphingolipids, while oligodendrocytes and Schwann cells, responsible of myelin sheath formation, synthesize C24 sphingolipids (Becker *et al.*, 2008). Ultra long-chain fatty acids (ULCFAs) (C≥26) are found in the skin (PROTTEY, 1977). VLCFAs are also found in the meibum, a mixture of lipids which protect the ocular surface in combination with tears. Meibum is mainly composed of cholesteryl esters and wax esters (WEs) (Ohashi, Dogru and Tsubota, 2006). Cholesteryl esters residues are C24-C27 VLCFAs mainly (Butovich, 2010) and WEs have C24-C26 VLC fatty alcohols (Butovich, Wojtowicz and Molai, 2009). ULCFAs and Docosahexaenoic acid (DHA) (C22:6*n*-3) is especially abundant in glycerophospholipids in the testis, brain, and retina (Sastry, 1985; Lin *et al.*, 1993; SanGiovanni and Chew, 2005), these tissues present also high amounts of ULCFAs. Mutations in the ELOVL4, responsible of the formation of ULCFAs, are related with seizures, mental retardation and spastic quadriplegia, showing the importance of these lipids in brain development and physiology (Aldahmesh *et al.*, 2011). 2-hydroxylated (2-OH) VLCFAs are abundant in epidermis, brain and kidney. 2-OH VLCFAs and C24 sulfatides are important for myelin formation and maintenance (Alderson *et al.*, 2006).

ALDP dysfunction reduces β-oxidation levels, in consequence VLCFA-CoA are accumulated in cytosol and incorporated into complex lipids changing the essential proportions of all of these lipids. Accumulated VLCFA are also substrate for further elongation to longer fatty acids by the ELOVL, increasing progressively the amount of VLCFA in the cytoplasm and membranes (Kemp *et al.*, 2005; Ofman, Inge M E Dijkstra, *et al.*, 2010).

2.7 Diagnosis and treatment

When signs and symptoms appear if a diagnosis of X-ALD is suspected, a blood test will be performed to look at VLCFA levels. In 99% of males elevated levels of VLCFA will be detected. Genetic testing on *ABCD1* will confirm the diagnosis and brain MRI will

determine the extent of the disease (Raymond, Moser and Fatemi, 1993). Adrenal function test will be also performed.

As VLCFA is the most probable cause of the pathogenesis of the disease, most of the therapeutic strategies have been addressed to reduce VLCFA levels. First approximation was the called "**Lorenzo's oil**". A combination of oleic acid (C18:1ω9) and erucic acid (C22:1ω9) dietary administrated reduced hexacosanoic acid (C26:0) levels in plasma (Rizzo *et al.*, 1989). However, its effectiveness has been object of controversy as it does not stop the progression of the disease nor prevent the appearance in asymptomatic patients. The reduction in VLCFA levels with Lorenzo's oil treatment is in part due to the inhibition of Elongation of very long chain fatty acids protein 1 (ELOV1) by the oils combination (Sassa *et al.*, 2014).

Lovastatin, a statin that reduces cholesterol levels, when combined with a certain diet, was able to reduce VLCFA levels in mice however, clinical trials has not been successful. The idea was that in plasma, VLCFA are transported as cholesterol esters and reduction of cholesterol could reduce VLCFA levels (Singh *et al.*, 1998; Engelen *et al.*, 2010).

Knockdown of ELOVL1 using **bezafibrate** reduced the VLCFA levels in X-ALD fibroblasts (Ofman, Inge M. E. Dijkstra, *et al.*, 2010). Unfortunately, benzafibrate does not reduce VLCFA levels in leukocytes and trials have not worked well (Engelen, Tran, *et al.*, 2012).

Glucocorticoid supplementation is mandatory to treat adrenal insufficiency. Male patients who have hypogonadism with low testosterone levels should be treated with **testosterone**. None of them seem to alter neurologic progression (Kanakis and Kaltsas, 2000).

Hematopoietic stem cell transplantation (HSCT) is the only option available for CALD. However, the success of the procedure depends on the stage of the disease. For advanced stages 5-year survival is 60% and increases up to 90% when only a few symptoms are visible and MRI shows only a few lesions. It is only indicated for boys and adolescents when there is evidence of brain involvement, but IQ performance is higher than 80, due to the high risk of morbidity and mortality (Shapiro *et al.*, 2000;

Peters *et al.*, 2004). HSCT for adult CALD arrest the progression of demyelination and prevent loss of neurocognition but implies deterioration of motor function in most of the cases (Kühl *et al.*, 2017). HSCT for X-ALD was implanted at 2000s, a 10 years follow up showed that not only survival rate is increased, but also neurologic function and major function disabilities are significatively preserved in patients treated at the early stages of the dieses (Raymond *et al.*, 2018). However, the effect of HSCT on AMN remains to be determined as myelopathy could appear in adulthood in these transplanted boys. Indeed, the benefits from HSCT could be due to the elimination of inflammatory processes or whether to the effect of healthy cells on VLCFA metabolism. This shows the importance of early diagnosis, which could be achieved by newborn screening. In February 2016, the US Department of Health and Human Services recommended the addition of ALD screening in routine newborn screening (Kemper et al., 2017). To date, only a few countries offer the neonatal screening.

Alternatively to allogeneic HSCT, **gene therapy** using autologous hematopoietic stem cells transduced with a healthy copy of *ABCD1* seem to be a good alternative to reduce the risk of graft-versus-host disease. No major functional disability and minimal clinical symptoms have been reported and survival rate has increased when autologous modified HSCT is done during the early stages of CALD. However, a longer follow-up is needed to confirm this safety and efficacy (Eichler *et al.*, 2017). For the AMN phenotype, transduction of adeno-asosocieted virus specifically into the spinal cord was assessed in mouse models (Gong *et al.*, 2018).

Genome editing techniques have not been tested yet in X-ALD. However, the possibility to modify gene sequences on living cells using engineered nucleases such as CRISPR-Cas9, ZFNs or TALENs, specially the first one, delivered by viral systems or other transporters, are promising tools that would be tested in a near future.

3. Is X-linked adrenoleukodystophy a developmental disorder?

Diverse psychological impairments have been described recurrently in individual case reports; attention deficit and hyperactivity in children and adolescents (Ilango and Nambi, 2015; Ray, Girimaji and Bharath, 2017; Zheng *et al.*, 2017; Rubia, 2018), and characteristic symptoms of dementia, including apathy, depression, cognitive

impairment and memory problems, in adults (Shamim and Alleyne, 2017). More severe disorders including schizophrenia, acute psychosis and bipolar-like manifestations have been also reported. All of these symptoms are recurrent in diverse neurodegenerative diseases, however we cannot rule out the possibility that they are due to developmental alterations. In fact, recent studies on different classically considered neurodegenerative diseases have shown neurodevelopmental alterations, changing completely the current view of them. Expression of neurodevelopmental-related genes like NEUROD1, NEUROG2 and ASCL1 are found diminished in Huntington disease (Consortium et al., 2017). Other classically considered neurodegenerative diseases like Parkinson disease (Corona, 2018) and some psychiatric disorders like schizophrenia and bipolar disorder (Buoli et al., 2017) also present these features combining both, the neurodegenerative component and the neurodevelopmental alterations.

3.1 Basic notions of brain development

Human brain development is a highly complex process controlled by genetics and environmental inputs. Central nervous system (CNS) formation begins at the third gestational week and extends until adolescence. Even though, brain is a structure that could suffer changes throughout the whole lifespan.

Despite being composed of different cell types, brain development studies have been focused on neurons for a long time. Nevertheless, it has been demonstrated that astrocytes, oligodendrocytes and microglia play a fundamental role in brain development appearing at particular stages (Reemst *et al.*, 2016). Microglia invasion and neurogenesis start almost simultaneously during embryonic development. Meanwhile astrogenesis, synaptogenesis and oligodendrogenesis are initiated at later stages of embryogenesis and performed mainly at postnatal stages as seen in rodents (Fig.9). Neurons, astrocytes and oligodendrocytes share the same neuroepithelial origin while microglia has a controversial origin. Most evidence supports that microglia have a macrophage origin, which is followed by brain invasion during the prenatal period. In this work we will focus on neurons and astrocytes as they are our object of study.

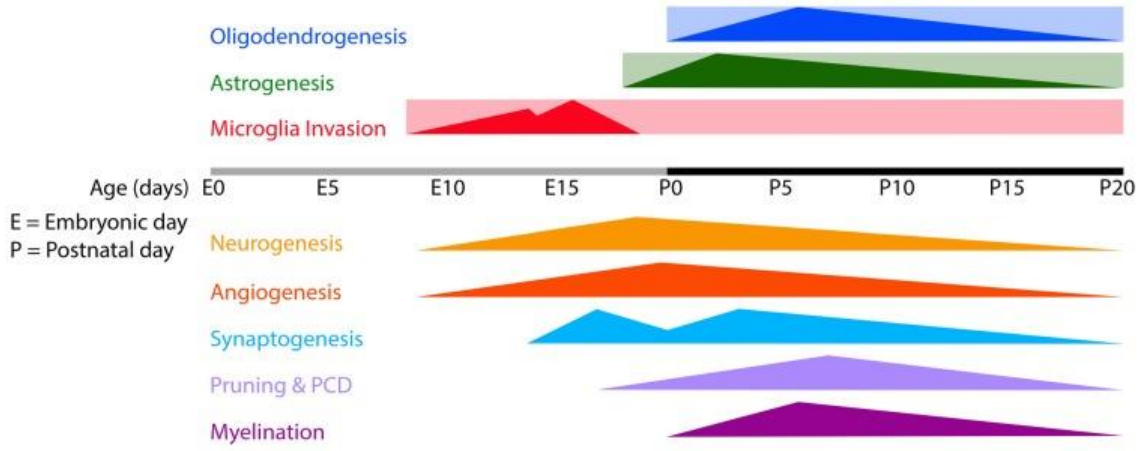

Figure 9. Timeline of developmental processes in mouse brain. PCD: programmed cell death (Reemst *et al.*, 2016)

Briefly, epiblast cells differentiate into neuroectodermal stem cells during gastrulation along the third gestational week. By the end of the third week, the first well-defined neural structure, called neural tube, is formatted and contains the neural progenitors in a zone called neural plate. Signals controlling cell migration during this period will determine which neural progenitors will produce the primary structures depending on their location; forebrain, midbrain, hindbrain and spinal cord. Subsequent genetic signalling processes will lead to neural stem cells differentiation, segment division and subdivision. By the end of embryonic period, at week 8, primary organization of central nervous system will be established. Patterning and refinement of previous established regions will continue for fetal period and extend to adolescence (Stiles and Jernigan, 2010).

Until embryonic day 25 (E25), neuroepithelial cells (NECs) in the ventricular zone (VZ) experience symmetrical divisions. At E42, after the formation of neural tube, NECs convert to radial glia and start asymmetrical divisions resulting in progenitor cells and neurons. Neural progenitors stays at VZ and neurons migrate to take its place in the developing neocortex (Weissman *et al.*, 2003). Neurons use three main strategies to move, somal translocation, used by the first neurons produced for short distances, glia-guided locomotion, in which radial glial cells have their soma in the VZ and

neurons migrate along their process, and tangential migration, to travel larger distances which is used by motoneurons from basal ganglia (Nadarajah *et al.*, 2003).

As we have mentioned before, unlike neurogenesis, that occurs mainly prenatally, astrocyte proliferation, migration and differentiation starts at final stages of prenatal period and extends throughout childhood. Extrinsic signals combined with intrinsic epigenetic mechanisms control the switch of radial cells from neurogenesis to astrogenesis (Bayraktar *et al.*, 2014) (Fig. 10).

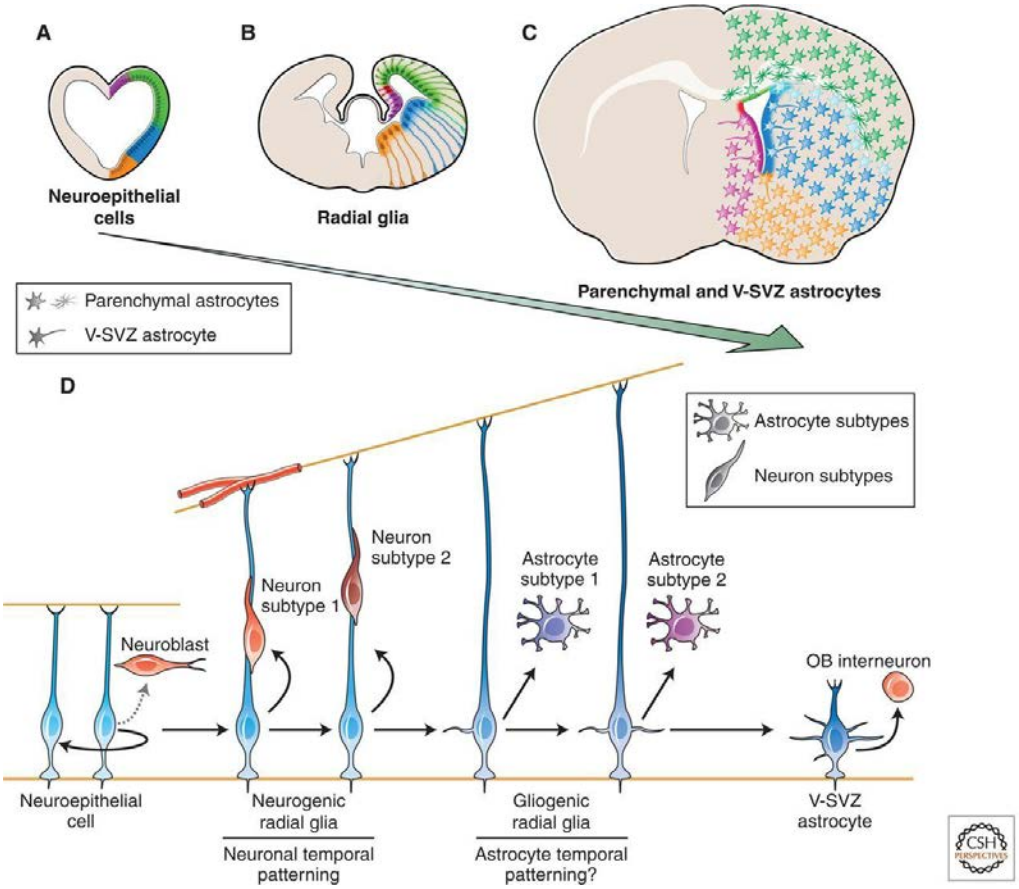

Figure 10. Origins in development of adult V-SVZ and parenchymal astrocyte heterogeneity. (Bayraktar *et al.*, 2014)

Among genetic signals controlling cell differentiation and patterning we find *WNT*, Janus kinase/signal transducers and activators of transcription (JAK-*STAT*) and *NOTCH*. *WNT* signalling activates Neurogenin 1 (*NEUROG1*) and Neurogenin 2 (*NEUROG2*) expression when chromatin is open leading to neuron formation while astrocyte genes are repressed by the DNA (cytosine-5)-methyltransferase 1 (*DNMT1*) action on glial fibrillary acidic protein (*GFAP)* promoter (Namihira *et al.*, 2009). Later, the proastrocitic

factor *CT-1*, secreted by neurons, activates *JAK-STAT* and *NOTCH* signalling, increasing the levels of nuclear factor I A (NFIA), an inhibitor of DNMT1 promoting chromatin opening and leading to astrocyte generation (Fig. 11) (Morrow, Song and Ghosh, 2001; Hirabayashi *et al.*, 2004; Freeman, 2010).

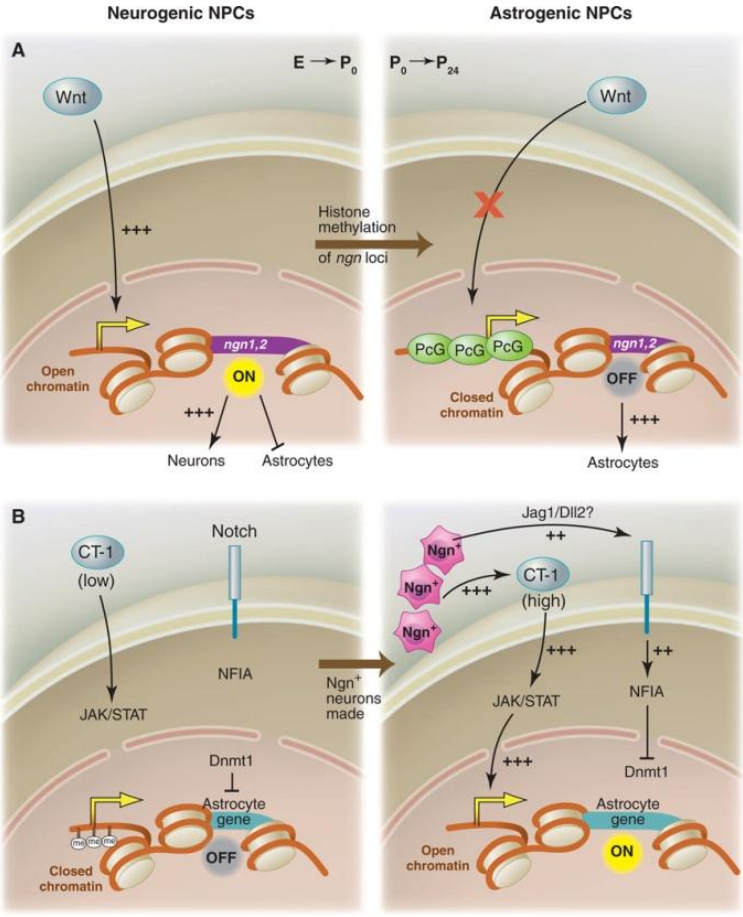

Figure 11. Neurogenic and astrogeneic signalling pathways. (Freeman, 2010)

Although they have different timings, neurogenesis and astrogenesis are highly coordinated processes where growth and refinement of both cell types depend on each other. Once neurons reach their positions, they need to develop dendrites, axons and form synapses to become integrated into neural networks. Synapse formation and maturation occurs at the same time as astrocytes differentiate and maturate. Astrocytes initially extend large filopodial processes and lately give rise to refined fine processes which are closely related with synapse formation, maturation, maintenance and elimination.

Immature astrocytes secrete different molecules, including thrombospondins (TSPs) that promote synaptogenesis (Karen S. Christopherson *et al.*, 2005b). Astrocytes contribute to spine maturation through direct contact using ephrin signalling (Nishida and Okabe, 2007) and by cholesterol secretion. Astrocytic cholesterol are the primary source of cholesterol in the CNS and is controlled by sterol regulatory element binding proteins (SREBPs) (van Deijk *et al.*, 2017). During synaptogenesis there is a peak of cholesterol synthesis, a reduction in cholesterol synthesis during this period leads to more immature dendritic spines (Ferris *et al.*, 2017). Ephrin signalling is also involved in axonal outgrowth as ephrin receptors are localized on axonal growth cones an astrocyte processes, which mediates contact repulsion (Murai and Pasquale, 2011), while laminin and fibronectin expressed by astrocytes attract the growth cone (Liesi and Silver, 1988; Tonge *et al.*, 2012).

During axonogenesis and synaptogenesis, there is an axonal and synaptic overgrown followed by selective pruning (Chechik, Meilijson and Ruppin, 1998). Inappropriate synapses and axons are eliminated by astrocytes and microglia (Stevens *et al.*, 2007) and, more recently, it has been demonstrated that there is similar process where astrocytic fine processes are also pruned (Bushong, Martone and Ellisman, 2004).

As well as synapses that are eliminated postnataly, around 50% of neurons will be lost prenatally (Kuan *et al.*, 2000). There are two major forms of cell death, necrosis which is a mechanism to eliminate damaged tissue and cells, and apopotosis which is a programmed process where DNA and cell are fragmented and eliminated. Intrinsic and environmental factors can promote or prevent apoptosis. The useless neurons will suffer apoptosis, different signals determine which neurons have to stay and which ones have to be removed. Among these factors, uptake of neurotrophic substances promotes survival (Oppenheim, 1989).

As well as oligodendrogenesis that occurs mainly postnatally, myelination takes place during this period and depends on oligodendrocyte progenitor cells (OPCs). When they reach their destinations, begin to differentiate and starts to insulate axons by myelin sheath production, which is essential for the rapid conduction of electrical impulses

along axons, maintain axon integrity and provide trophic support to them (Zalc, Goujet and Colman, 2008).

Correct coordination and performance of all processes are essential for the correct brain formation. Any change or disturbance during this period will be a challenge that could have severe consequences for the invidual.

3.2 Peroxisomes during development

Importantly, the number of peroxisomes and their activity changes over time. While peroxisomal activity during development, measured as catalase activity, remains constant in cerebral cortex, there is a peak in white matter all along myelination phase (Adamo, Aloise and Pasquini, 1986). Moreover, mRNA levels of different peroxisomal β-oxidation enzymes (*ACOX1, DBP, ACAA1a*), transporters (*ABCD2* and *ABCD3*) and ether phospholipid biosynthesis enzymes, reached a maximum during the first postnatal weeks and then declined. Meanwhile α-oxidation enzymes are not detected during the first postnatal weeks. In contrast, *ABCD1* mRNA levels in brain are higher during embryonic development (Berger *et al.*, 1999; Huyghe *et al.*, 2001).

3.3 Interplay between neurons and astrocytes in circuit formation

Astrocytes are crucial for the proper brain functioning as they provide several metabolic and trophic factors to neurons (Banker, 1980). However, they are more than mere supporting cells, changes of calcium concentrations in fine processes of astrocytes modulate neuronal synapses by altering the uptake of astrocyte transmitters and sodium calcium pump. Changes in astrocyte calcium levels have been also attributed to gliotransmiters release that could modulate synapses (Perea, Navarrete and Araque, 2009). However, further studies are needed to confirm if astrocytes could modulate synapses by gliotransmitters release (Bazargani and Attwell, 2016). Spatial domains differ in their calcium transients origin, being calcium of the soma mainly changed by internal calcium release and processes calcium uptake come largely from extracellular sapace (Bazargani and Attwell, 2016) (Fig. 12).

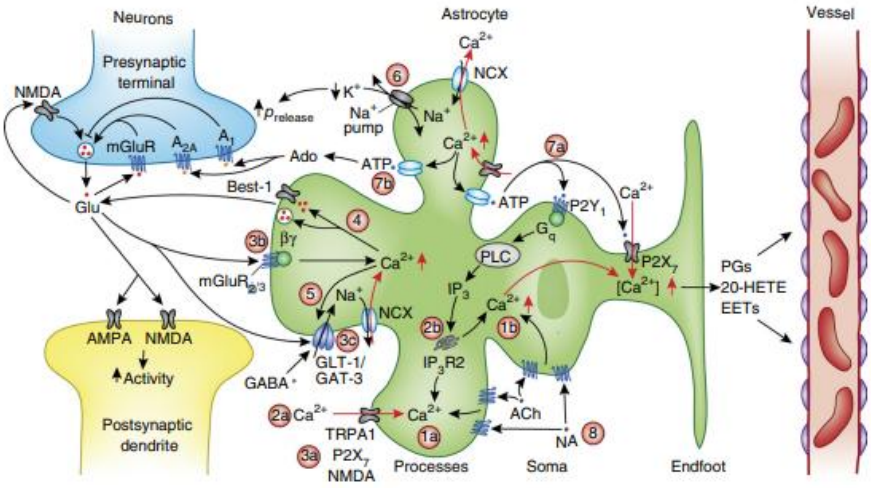

Figure 12. Differences in calcium transients in soma compared to processes. Calcium in processes depends largely on extracellular calcium entry and calcium in the soma depend mainly on calcium internal stores. (Bazargani and Attwell, 2016)

Importantly, astrocyte generation takes place at the same time of neurogenesis and neuronal migration in the brain (Miller and Gauthier, 2007) and glial-derived lipids, especially cholesterol, are described as essential for correct elaboration of dendritic structures (Camargo, Smit and Verheijen, 2009). Moreover, a large list of astrocyte-derived factors play a role in synapse formation and maintenance and they are altered in divers neurodevelopmental diseases (Allen and Eroglu, 2017).

Therefore, the study of astrocyte-neuron communication as well as neuronal and astrocytic alterations is key for understanding the origin of sings and symptoms of several diseases and their possible therapies.

WORKING HYPOTHESIS AND OBJECTIVES

Our working hypothesis is that the abnormal formation and maintenance of neural circuits due to altered neuronal and/or astrocyte pathways during development caused by mutations in the *Abcd* transporters and lipid dyshomeostasis may cause neuropsychiatric symptoms observed in X-ALD, both in children and adults. The overarching, long-term goal is to identify molecular targets that may alleviate cognitive symptoms in adult X-ALD, and perhaps arrest progression to deathly forms of X-ALD, by restoring proper neural-circuit function.

Specific objectives are:

1. To search for non-reported dysregulated biological processes related to neural circuit formation in publicly available transcriptomic data of X-ALD children and adults in order to identify dysregulated developmental pathways and molecular culprits.
2. To establish *in vitro* modes of X-ALD neurons and X-ALD astrocytes devoid of microglia to validate the dysregulation of developmental programs predicted from the mining of the transcriptomic analysis.
3. To dissect out the neuronal versus astrocyte compartmentalisation of dysregulated pathways in X-ALD with a battery of morphometric, molecular and functional assays, as well as the crosstalk between neurons and astrocytes using astrocyte-conditioned media.

MATERIALS AND METHODS

1. Cell culture and treatments

1.1 Primary rat hippocampal neuron and cortical astrocyte cultures

Neuronal and astrocytic cultures were obtained from a poll of hippocampi and cortices of 0-1 day-old Sprague Dawley rats. Pups were decapitated and brains extracted. Using a microscope meninges were removed and brain structures separated. Cortices and hippocampi were processed separately. A minimum of 3 pubs were used in each experiment. Brain parts were fragmented with a scalpel and transferred to a solution composed of 35ml of Calcium-free Krebs Ringer Buffer (KRB), 120 mM NaCl, 4.8 mM KCl, 1.2 mM KH_2PO_4, 25 mM $NaHCO_3$, 14.3 mM glucose, 0.03% Mg_2SO_4 and 0.3% bovine serum albumin (BSA). Tissue was centrifuged for 1 minute at 300g and supernatant removed. 10ml of calcium-free KRB solution with 0.025% of trypsin was added at cells and cells were incubated at 37ºC for 10 minutes, to allow tissue dissociation. To inhibit trypsin we added 10ml of calcium-free KRB containing 0.052% of soybean trypsin inhibitor (Gibco), 0.008% DNAse (Sigma) and 0.03% extra of Mg_2SO_4. Next, cells were centrifuged for 1 minute at 300g, supernatant was removed and cells resuspended in 5ml of KRB. Cells were mechanically separated using a glass pipet and filtered through a 40µM nylon mesh. Cells obtained were centrifuged for 5 minutes at 250g. After removal of supernatant, neurons were resuspended in Neurobasal A (NBA) medium containing 1x serum-free B27 supplement (ThermoFisher), 1x GlutaMAX^{TM} (ThermoFisher) and 20U mL^{-1} penicillin and 20µg mL^{-1} streptomycin. Astrocytes were resuspended in Dulbecco's Modified Eagle's medium (DMEM) (Thermo Fisher) containing 10% Fetal Bovine Serum (FBS), 20U mL^{-1} penicillin and 20µg mL^{-1} streptomycin.

Cells resuspended in Trypan Blue were counted in a Neubauer chamber. Astrocytes were seeded at 300,000 cells/mL in T150 flasks and neurons were seeded at 80,000-125,000 cells/mL in polylysine-containing plates. Cells were maintained in an incubator at 37ºC with 55 of CO_2 in a humidified atmosphere.

Astrocyte medium was changed at 3h to avoid excessive oligodendrocyte and microglial growth. After this, medium was changed every 7 days until they reach

confluence (10 days approximately). Then, flasks were agitated in a mechanical shaker at 400rpm for 3 hours to eliminate superficial microglia. Cells were washed twice with Phosphate buffered Saline (PBS) containing 2.5 mM KCl, 136.87 mM NaCl, 1.47 mM K_2HPO and 40.8 mM NaH_4PO_4 at pH 7.4 supplemented with 20U mL-1 penicillin and 20µg mL-1 streptomycin. Next, 3ml of Trypsin/EDTA (Sigma) was added to the flask and incubated for 5 minutes at 37ºC. Manual shake was used to facilitate cells deattaachement, anf full DMEM was added to stop the reaction. Cells were collected and centrifuged at 250g for 5 minutes, supernatant was removed and cells were seeded at 80,000 cells/mL and maintained in the incubator in the same conditions. 50% of neuronal media was changed every 3 days for fresh medium and neurons were cultured for 5-14 days.

1.2 *Abcd1*/*Abcd2* silencing in astrocytes

Abcd1 and *Abcd2* genes were silenced in primary rat cortical astrocytes using RNA interference purchased from Ambion (s170867 and s136468). Each siRNA was chosen from two different synthetic siRNAs depending on the efficiency. A scrambled-synthetic-siRNA was used as a negative control (Ambion, Catalog#: 489043).

Table 2. siRNA sequence.	**Sense**	**Antisense**
Abcd1	GCUGGUUAGUGAACGUACAtt	UGUACGUUCACUAACCAGCtc
Abcd2	GCAUGAGAAAGGUUAUACAtt	UGUAUAACCUUUCUCAUGCat

Transfection was performed as follows; for each mL of DMEM FBS-free and antibiotics-free either 1µL of 20µM s*iAbcd1* and *siAbcd2* or 20µM siScramble was combined with 3µL Lipofectamine®RNAiMAX (Invitrogen). Lipofectamine was added to 50 µL of medium, siRNAs to 50 50 µL of medium of medium and incubated for 5 minutes. After that lipofectamine containing media and siRNA containing media were incubated for 20 minutes to facilitate complex formation. Resultant mixture was added to cells drop by drop containing 900µL of DMEM and treated after 48h.

Astrocytes were silenced when they reach 60% of confluence after microglia removal.

1.3 *Abcd1*/*Abcd2* silencing in neurons

Using the synthetics siRNAs that we previously identified that are active in triggering knockdown of our target genes, we designed the corresponding shRNAs by adding a common loop and slightly modifying the sequence. We delivered the shRNAs using an adenovirus 5 (Ad5) (Fig. 13). Plasmids and viruses were generated by the Viral Vector Production Unit of Autonomous University of Barcelona. The efficiency was checked by transfecting neurons with a Scrambled-shRNA. The scrambled did not downregulate the expression of either *Abcd1* or *Abcd2* genes, showing that the silencing was specific.

Neurons were silenced at 0 days *in vitro* (DIV) for axonal growth experiments and 7 DIV for the rest of the experiments. For viral transduction 50% of medium was removed and viral particles added at multiplicity of infection (MOI) 50, for sh*Abcd1* and sh*Abcd2* and MOI 100 for shScramble as the first two go together. Viral infection was carried out overnight and medium were replaced for 50% of neuronal conditioned medium and 50% of fresh medium.

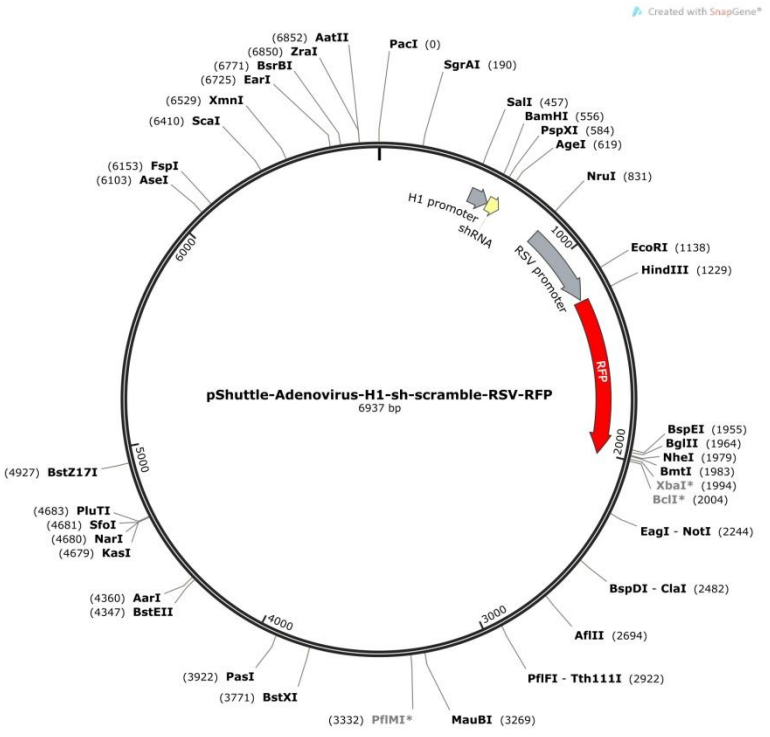

Figure 13 . pShuttle-shRNA scheme. Plasmid backbone of sh*Abcd1*, sh*Abcd2* and shScramble adenovirus 5 RFP of the scheme was removed.

1.4 VLCFA treatment

Hexacosanoic acid (C26:0) (sigma-Aldrich) 50 µM was added a day 1-10 (DIV) and maintained for 96h in neurons, neuronal medium was exchanged completely at the time of treatment for NBA medium containing 1x serum-free B27 supplement minus antioxidants (minus AO) (ThermoFisher), 1x GlutaMAX^{TM} (ThermoFisher) and 20U mL^{-1} penicillin and 20µg mL^{-1} streptomycin. In astrocytes after 48 hours, to allow genes silencing, of silencing treatment was applied. For ACM media experiments acute treatment of astrocytes with 100 µM C26:0 was done for 4h in DMEM without glucose containing containing 1% FBS, 20U mL^{-1} penicillin and 20µg mL^{-1} streptomycin and medium replacement for NBA medium containing 1x serum-free B27 supplement minus antioxidants (minus AO) (ThermoFisher), 1x GlutaMAX^{TM} (ThermoFisher) and 20U mL^{-1} penicillin and 20µg mL^{-1} streptomycin.

As a vehicle we used a synthetic carrier, α-cyclodextrin (α-cyclo). A stock of C26:0 was prepared in chloroform and stored at -80ºC. For usage, chloroform was evaporated with gas nitrogen and the resultant powder was sonicated for 20 seconds at 30% power, after addition of correspondent media with α-cyclodextrin.

2. Molecular biology methods

2.1 RNA extraction, reverse transcription and real-time qPCR

Total RNA extraction was performed using Trizol reagent (ThermoFisher). Cells were washed twice on a cold surface with PBS. Next, 1mL of TRIzol was added for 6-well plates, and cells were separated by strongly pipetting. Cells were collected and sample was kept at -80ºC. For RNA extraction, samples were kept in ice to allow defreezing. 200µL of chloroform were added to 1ml of sample. Tubs were agitated manually and centrifuged at 12000 g for 15 minutes at 4ºC for DNA separation. Separation will result in three layers, the upper layer contain the RNA and represent 50% of the original volume. To RNA extracted we added 500µL of isopropanol and kept in ice for 10 minutes. Next, samples were centrifuged at 12000g for 10 minutes at 4ºC. Afterwards, the RNA pellet was washed with 1mL cold 75% ethanol and centrifuged for at 7500 g for 5 minutes at 4ºC. After centrifugation, Ethanol was removed and RNA pellet was

kept at RT to allow air dry. 30µL of TE was used to resuspended pellet and tubs were incubated in a heat block at 55ºC for 10 minutes to facilitate the elution.

An RT-PCR was performed to reverse transcribe mRNA to cDNA. A final volume of 50µL containing 0.5-2µg of RNA was prepared with , 1µM of dNTPs, 1µM Oligo(dT) primers, 0.45mM of DTT, 10U of RNAse out, 1x RT buffer and 200U SuperScript reverseaid transcriptase (all the products from ThermoFisher). First, a mix containing RNA, primers and dNTPs was heated to 65ºC for 10 minutes in a thermocycler before adding the rest of the reagents. Afterwards, samples were incubated for 10 minutes at 25ºC, for 1 hour at 42ºC an 10 minutes at 72ºC to allow reverse transcription reaction. cDNA obtained was maintained at -20ºC until use.

For, mRNA expression quantification, cDNA was diluted from 1:2 to 1:10 to obtain a appropriate Ct curves between 15 and 30 cycles. We used primers or Taqman proves. For primers 2.5µL of diluted cDNA, 0.5µM of primers forward and reverse (Tab. 3), 5µL of Syber green and 1.7 µL of nuclease-free water was used. For Taqman proves we used 4µL of diluted cDNA plus 1µL of Taqman primer (Table. 4), 10µL of Taqman Universal Master Mix and 5µL of nuclease-free water. Triplicate samples were analyzed per condition and amplified in a 7500 Fast System (Applied biosystems). Comparative Cq and PCR efficiencies were obtained using LinReg software and Cq method was used to analyse results.

Table 3. Primer sequences

Gene	Primer forward	Primer reverse
Syp	5'-TTTGCTACGTGCGGCAGCTA-3'	5'-TTGGTAGTGCCCCCTTTGAC-3'
Gapdh	5'-GAAGCTCATTTCCTGGTATGAC-3'	5'-TCTCTTGCTCTCAGTATCCT-3'

Table 4. Taqman proves

Gene	Model	Taqman Reference
Abcd1	Rat	Rn01529709_m1
Abcd2	Rat	Rn00583723_m1
Wnt2	Rat	Rn01500736_m1
Wnt6	Rat	Rn00437351_m1
Notch3	Rat	Rn00571731_m1
Stat3	Rat	Rn00680715_m1

Ntrk2	Rat	Rn01441749_m1
Ntrk3	Rat	Rn00570389_m1
Ephb2	Rat	Rn01181017_m1
Shh	Rat	Rn00568129_m1
Gapdh	Rat	Rn01476455_m1

2.2 Microarray analysis

Non-demyelinated brain tissue samples were obtained from patients and their respective controls. Total RNA was extracted from frontal and parietal white matter samples, RNA quantity and quality were determined and samples with an insufficient RNA yield were rejected. After selection, samples were processed and hybridized to Affimetrix HG-U133 Gene Chips. Finally, only 24 (3 cALD, 3 child control, 8 adult cAMN and 10 adult controls) out of 41 initial samples were acceptable to proceed with transcriptomic analysis.

First, row data from publicly available microarray was pre-processed and LIMMA statistics analysis was used to obtain fold change, logFC, p-value and adjusted p-value of the different groups comparisons. Second, we choose Gene Set Enrichment Analysis (GSEA) to investigate transcriptome changes and evaluate positive and negative enrichment of different pathways/concepts using Gene Ontology (GO) (*Gene Ontology Resource*) annotation. GSEA compare two different gene expression datasets of two phenotypes and revels witch groups of genes are enriched and the gene set they belong to. Cytoskepe pluging Enrichment map was used to plot GSEA results and Autoannotate clustered them according to their similarity coefficient. Heat maps were obtained using Orange software.

3. Cell biology methods

3.1 Calcium imaging

Cytosolic calcium signalling was measured using a ratiometric calcium dye, Fura-2AM (Thermo Fisher, F1221). Fura-2AM emit fluorescence at 510nm upon excitation at two different wavelengths, 340nm and 380nm. Fluorescence upon excitation at 340nm (calcium saturated) is proportional to calcium concentration while fluorescence upon

excitation at 380nm (calcium free) decreases. Therefore the ratio 340/380 is proportional to the calcium concentration.

Cells were seeded in a coverslip and after treatments; cells were incubated for 1 hour with 2µM Fura-2AM in KRB in the dark. Next, coverslips were mounted on an O-ring chamber with 1mLof KRB and placed on the stages of a Nikon TE2000-U microscope using a 40x oil objective. Cells were excited at the two wavelengths thanks to a monochromator (Cairns) and resultant fluorescence were processed every two seconds by a high sensitivity CCD EG-ORCA camera (Humamatsu Photonics). MetaFluore software was used to collect images (universal Imaging). Regions of interest (ROI) were selected to analyse data. A minimum of 3 different coverslips per condition were analysed.

3.2 ATP, NAD/NADH, GSH, ROS and cholesterol production

Adenosine triphosphate (ATP) production was measured with ATPlite Luminiscense Assay kit (6016943, PerkinElmer).
GSH production was measured using GSH/GSSG Ratio detection Assay kit (Fluorometric –Green).

NAD/NADH measurements were done using a colorimetric comertial kit from Abcam (ab65348).

ROS production was measured using DCFDA- cellular Reactive Oxygen Species Detection Assay kit (Abcam, ab113851).

Cholesterol production was measured with Amplex Red cholesterol Kit (Thermo, catalogue number. A12216)

3.3 Immunocytochemistry protocol and stainings

After treatments, cells were washed twice with PBS and fixed using 4% paraformaldehyde (Electron Microscopy Science, 15714) for 15 minutes at room temperature. Then, cells were washed twice with PBS for 5 minutes a 150rmp in a mechanical shaker. Plates could be stored at 4ºC or used immediately, if keepet at 4ºC cells must be washed twice as before with PBS before the immunohistochemistry (IHQ). Then, cells membranes were permeabilized for 15 minutes at 150rpm in 0.1%

Triton X-100 (Alfa Aesar, A16046) diluted in PBS. To reduce non-specific binding of antibodies we blocked the cells with PBS-NGS 5% (GibcoTM 16210-064) for 30 minutes at 150 rpm. Next, glass coverslips containing cells were incubated face-down on 10µL of antibody in a humidified chamber at 37ºC overnight. Afterwards, cells were returned to the plate and washed three times with PBS for 10 minutes at room temperature RT. The corresponding secondary antibody diluted in PBS-NGS 5% was added for 1 hour at 150rpm and RT. Cells were covered to create a dark space, cells were washed three times with PBS at 150 rpm for 10 minutes and incubated with DAPI 1:20,000 for 5 minutes. Then, DAPI mixture was removed and cells washed twice for 10 minutes at 150rpm and RT. Coverslips were mounted using 8µL Fluoromont-G (southern Biotech, catalogue number: 0100-00) on slides. Cells were air-dried and kept in dark boxes.

Table 5. Antibodies and dyes

Antibody	**Reference**
Neuronal nuclei (NeuN)	Chemicon international, MAB377
Glial Fibrillary Acidic Protein (GFAP)	Dako, Z0334
Purified anti-neurofilament marker (pan axonal, cocktail) SMI 312	BioLegend, 837904
PDI rabbit mAb	Cell signalling technology, C81H6
Filipin III	Sigma Aldrich, F4767
Nile Red	Santa cruz biotechnology, 7385-67-3
DAPI	Ambion, Thermo Fisher Scientific, D1306
ActinGreen™ 488 ReadyProbes™ Reagent	Thermo Fisher Scientific, R37110
Goat anti-Mouse IgG 594	Thermo Fisher Scientific, A-11032
Goat anti-Rabbit IgG 488	Thermo Fisher Scientific, A-11034

For lipid droplets (LD) staining we used Nile Red, a selective dye for intracellular lipid droplets. cells were washed twice with PBS and incubated with Nile Red (2.5µg/mL) for 10 minutes at RT, cells were washed again at 150rpm and coverslips mounted as described before.

Cholesterol staining was done with Filipin III, and antibiotic capable to unesterified cholesterol that emits fluorescence at ultraviolet spectrum. After washing cells twice

with PBS, 25µg/mL of Filipin II was added for 30 minutes at RT in the dark. Afterwards, cells were washed twice with PBS and coverslips mounted as described before.

Actin green staining was performed washing cells twice with PBS and adding two drops of ActinGreen^{TM} 488 ReadyProbes^{TM} Reagent per mL of medium. Cells were incubated with the reagent for 30 minutes. Afterwards, stain solution were removed and cells washed twice with PBS, cells were stained with 1:20000 of DAPI for 5 minutes and washed twice with PBS. Afterwards, cells were washed twice with PBS and coverslips mounted as described before.

3.4 Image acquisition and analysis

Images were acquired in a fluorescence microscope Nikon Eclipse TE2000-E coupled to a camera and thanks to metamorph Universal imaging software. Images with higher magnification were obtained using a Confocal microscope as needed.

Image G was used to process images and cell counter plugging to count cell death and lipid droplets.

IMARIS Software and Filament tracer plugin was used to create a mask on confocal images to evaluate pine formation, dendrite arborisation and thickness and axonal growth. Minimum dendrites' thickness was established at 0.35µM as it is the minimum distance detectable in the dendrite thickness. Minimum spine diameter was established at 0.5µM and maximum at 1.5µM.

3.5 Cellular death assay

Neuronal death was assessed using TUNEL Apo-Green kit (Biotool), that detect fragmented DNA. After fixation described in IHC, cells were washed twice for 5 minutes at 150rpm. Cells were permeabilized with 0.2% Triton X-100 for 5 minutes at RT. Then, cells were washed once for 5' at 150 rpm, and a mixture containing, 34µL of ddH_2O, 10 µL 5x equilibrium buffer, 5µL Apo-Green labelling mix and 1µLrecombinant TdT Enzyme was added for 1 hour at 37ºC in a humidified chamber. Control positive was Tris-HCL 50mM, and negative control, the same mixture without enzyme. Afterwards, cells were washed twice with PBA for 5 minutes at 150 rpm and immunohistochemistry protocol followed.

4. Radioactive methods

4.1 Fatty acid oxidation measurement (^{3}H-Palmitate)

Fatty acid oxidation measurements were done using ^{3}H-palmitic acid (Perkin Elmer). Extracellular ^{3}H-H_2O was used as an indirect measure of fatty acid oxidation as at the end of the process H2O is released. Astrocytes were incubated overnight with 1µCi/mL of ^{3}H-palmitic acid (30nM). ^{3}H-palmitic acid was mixed with DMEM supplemented with 10% FBS, containing delipidated BSA 0.5% to allow fatty acid absorption. Afterwards, cells were washed once with KRB with 0.5% of delipidated BSA and twice with KRB. Posterior incubation of astrocytes was done with KRB containing glucose (Sigma) or not. An inhibitor of carnitine palmitoyltransferase I, etomoxir (ETX) (Sigma) 30µM was used to block fatty acid oxidation. 8 h later 400µL of KRB medium were transferred to 1mL o 1:2 slurry of Dowey (chloride form) anionic exchange resin (Sigma) in dd$H_2$0. Resin captured other labelled products than ^{3}H-H_2O. Tubs with the resin and KRB were vortexed and centrifuged at 1,000 rpm for 2 minutes. 100 µL of the supernatant were transferred to scintillation tubes and 3mL of Emulsifier-Safe scintillation cocktail (perkin Elmer) were added. A Scintillation Counter TRI-CARB 2810TR (Perkin Elmer) was used to measure radioactivity.

4.2 Cholesterol synthesis measurement (^{14}C-Acetate) and lipid extraction and separation

Cholesterol synthesis was measured using ^{14}C-Acetate a precursor of cholesterol formation. Cells were incubated overnight with medium containing ^{14}C-Acetate 1µCi/mL. Cells were washed with PBS and then a protocol for lipid extraction and separation was followed. The same protocol was used for intracellular and extracellular cholesterol measurements.

After washing 0.6mL of chloroform/methanol (1:2, v/v) was added to solubilise lipids. 0.6mL was transferred to a polypropylene tube and 0.5mL of chloroform added followed by 0.5mL H_2O addition. Tubs were agitated vigorously and centrifuged for 5 minutes at 1000rpm. Two fases appear after centrifugation, one aqueous phase (superior) and one organic phase (inferior). Organic phase was collected and transferred to a new tube. Chloroform was evaporated using a speed-vac for 1h.

Lipidic button was resuspended in 10µl of chloroform/methanol 1:1 and applied to the concentration area of a HPTLC. Plate were developed using hexane/ethylic eter/acetic (70:30:1, v/v/v). Plate was air dried and sprayed with primuline (5mg in 100mL acetone/H_20 (80:20, v/v). Bands were visualized wit UV light and marked with a pencil. Chemidoc^{TM} gel Imaging System was used to obtain images for quantification in the case of intracellular and extracellular cholesterol, known concentrations of cholesterol were used as a control. For radioactively labelled samples, bands were scratched with a scalpel and 3mL of Emulsifier-Safe scintillation cocktail (Perkin Elmer) were added. A Scintillation Counter TRI-CARB 2810TR (Perkin Elmer) was used to measure radioactivity.

5. Statistical analysis

Sample size was at least 3 different cell cultures of a mixture of 3 rats. Unpaired student's T-test was applied to compare one variable. One way analysis of variance ANOVA with multiple comparisons Tukey's pothoc test was used to compare two variables and two-way ANOVA with the same posthoc test to compare more than two variables. Interval of confidance was 955 and data were represented as mean ± standard error of the mean (SEM). P-value< 0.05 was considered statistically significant. Other statistical significances were indicated as follows: *p<0.05, **p<0.01, *** p<0.001 and **** p<0.0001.

RESULTS

CHAPTER I: Re-analysis of X-ALD transcriptomic data reveals novel dysregulated biological processes

1. Re-analysis of X-ALD transcriptomic data

The hallmarks of demyelination and inflammation in X-ALD have focused the attention of most of the research projects and therapeutic strategies on these two processes, masking other possible features equally relevant but less aggressive in the progression and symptoms of the disease. Specifically, psychiatric alterations are an early sign of CCALD (Berger, Forss-Petter and Eichler, 2014), and a chronic symptom in AMN (van Geel *et al.*, 1996), revealing, in the latter, the existence of brain pathology concomitant to spinal-cord and peripheral neurodegeneration. Molecular profiling allows one to identify molecular signatures of brain dysfunction unbiasedly. Here, we sought to profit from publicly available transcriptomic data from children and adults suffering X-ALD (Schlüter, Espinosa, Fourcade, Galino, Lśpez, *et al.*, 2012)in order to gain insight into the molecular features explaining how genetic changes may lead to psychiatric symptoms of X-ALD patients.

Previous studies of X-ALD brains have reported alterations in pathways related to oxidative phosphorylation, insulin signalling pathways, adipocytokine and protein synthesis between others (Schlüter, Espinosa, Fourcade, Galino, López, *et al.*, 2012). To gain insight into additional biological changes, we performed a GSEA to associate the differentially expressed genes into biological processes. GSEA determines whether a given set of genes shows statistically significant differences between two datasets, in this case CCALD versus healthy children, and AMN versus healthy subjects. GSEA identifies enriched gene sets that are overrepresented at the top (upregulated) or the bottom (downregulated) of a pre-ranked list of genes (p-value < 0.05), giving an enrichment score (ES). The most deregulated genes will be responsible for the ES. The ES can be positive or negative, depending on whether the term is globally upregulated or downregulated (i.e., whether upregulated or downregulated genes predominate). In this chapter, we will focus on statistically significant dysregulated pathways not reported and studied before. Gene ontology (GO) annotations were used to gain insight into the altered functions. Enriched GOs obtained by GSEA were filtered by false discovery rate q-value (FDR q-val < 0.25), subsequently clustered into groups according to their similarity-coefficient, and clusters were in turn manually classified into general categories (Fig. 14).

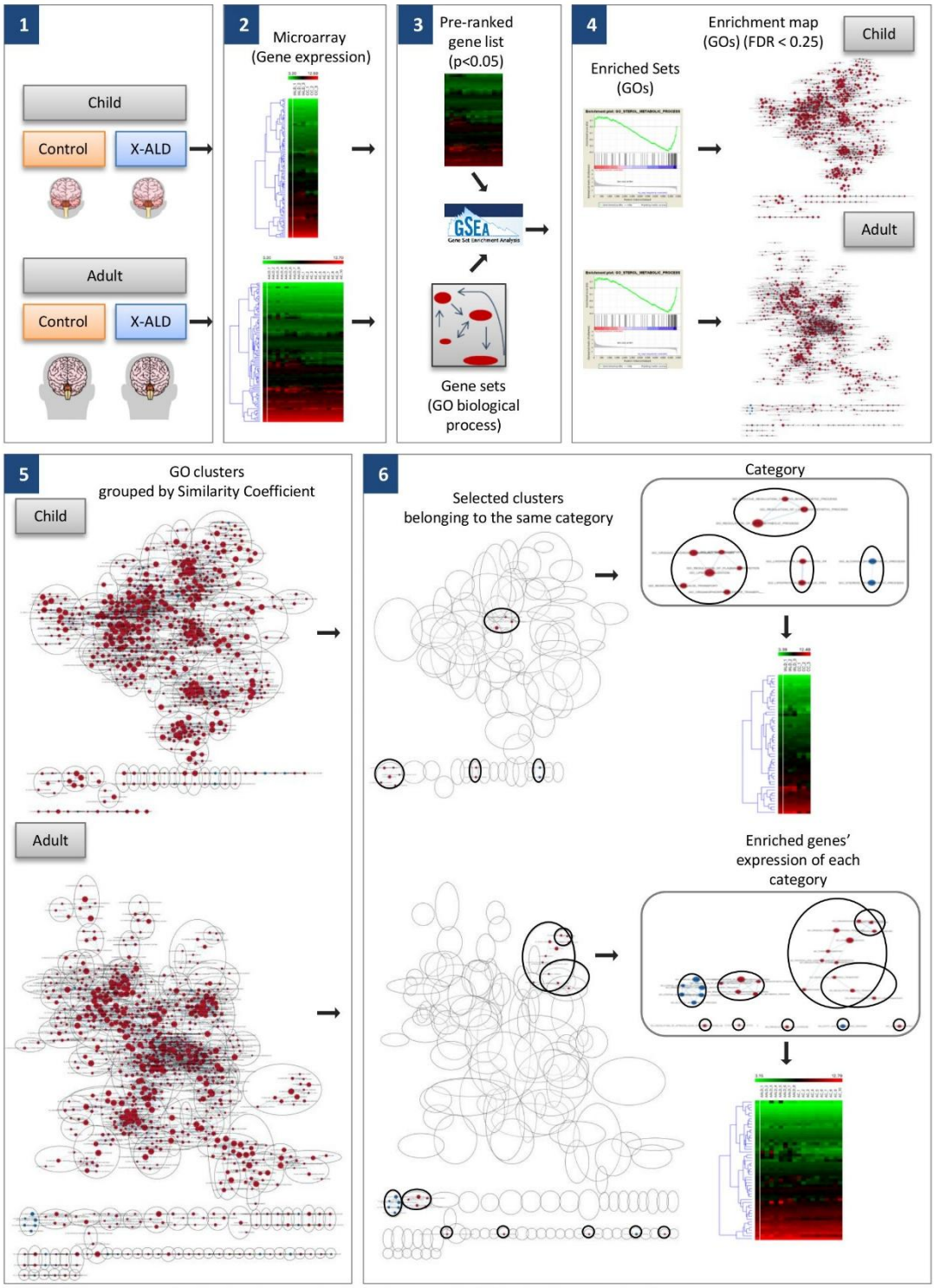

Figure 14. Microarray analysis and GSEA. Procedural workflow to study novel enriched biological process in X-ALD patients. 1. Extraction and processing from children and adult brain samples. RNA. 2. Microarray analysis and hierarchically clustered heat-map of the whole transcriptome. 3. GSEA was performed with differentially expressed genes between genotypes (p-value < 0.05) and Gene Ontology (GO) gene sets.4. Enriched gene sets (GOs) were obtained and enrichment maps of the enriched GOs with a FDR < 0.25 were plotted using e'nrichment map' plugin of Cytoscape. Each red and blue node represents a GO and edges represent the overlap between GOs. 5. GOs were clustered by 'Autoannotate' plugin of Cytoscape according to 'similarity coefficient'. GOs belonging to the same cluster are shown grouped inside acircle. 5. Clusters corresponding to the same category were selected,

and enriched gene expressionswere plotted in a hierarchically clustered heat-map. (Step 1 and 2 were performed by the group of A. Pujol and reported in (Schlüter, Espinosa, Fourcade, Galino, López, *et al.*, 2012)

A pre-ranked list of differentially expressed genes (p-value < 0.05) from the X-ALD transcriptomes was used to generate the enriched GOs list (Annex I, Supplementary Tab. 1) by GSEA. A higher number of GOs and clusters appear enriched in X-ALD adults (2121 GOs / 151 clusters) than in X-ALD children (1621 GOs / 78 clusters) (Fig. 2). This could be explained by the greater number of deregulated genes in children (3683) as compared to adults (5394). However, the subsequent classification into categories exhibits a similar number of altered processes—only a category related to aging appeared in adults and not in children (Fig. 14 and Tab. 6), ranked according to the number of clusters/GOs). Interestingly, while the number of down-regulated genes was greater than the number of down-regulated genes (Children: 1270 UP / 2413 DOWN. Adults: 2021 UP / 3373 DOWN), the number of up-regulated GOs was much lower than the number of down-regulated ones (Children: 1504 UP / 117 DOWN. Adults: 1848 UP / 237 DOWN). Clusters were classified into categories as shown in figure 14.

Previous studies have reported and emphasized differences in 'Immune system', 'General Metabolism', 'Signal Transduction', 'Stress response', 'Proteostasis', 'Cell junction', 'Transcription/replication/gene expression' and 'Death' (Schlüter, *et al.*, 2012). However, 'Development/regeneration/differentiation/proliferation' ('Development' from now on), 'Synaptic transmission and calcium signalling', 'Lipid Metabolism and Transport', 'Cytoskeleton and Motility', 'Membrane dynamics', 'Cell cycle', 'Circadian rhythm' and 'Ageing' were overlooked.

Although all categories except 'Ageing' appear deregulated in children and adults, GOs included in these categories are different (Annex I, Supplementary Tab. 1 and 2) meaning that, different pathways related included the same category are affected at each age. Therefore it is necessary to study which GOs include each category in both ages separately.

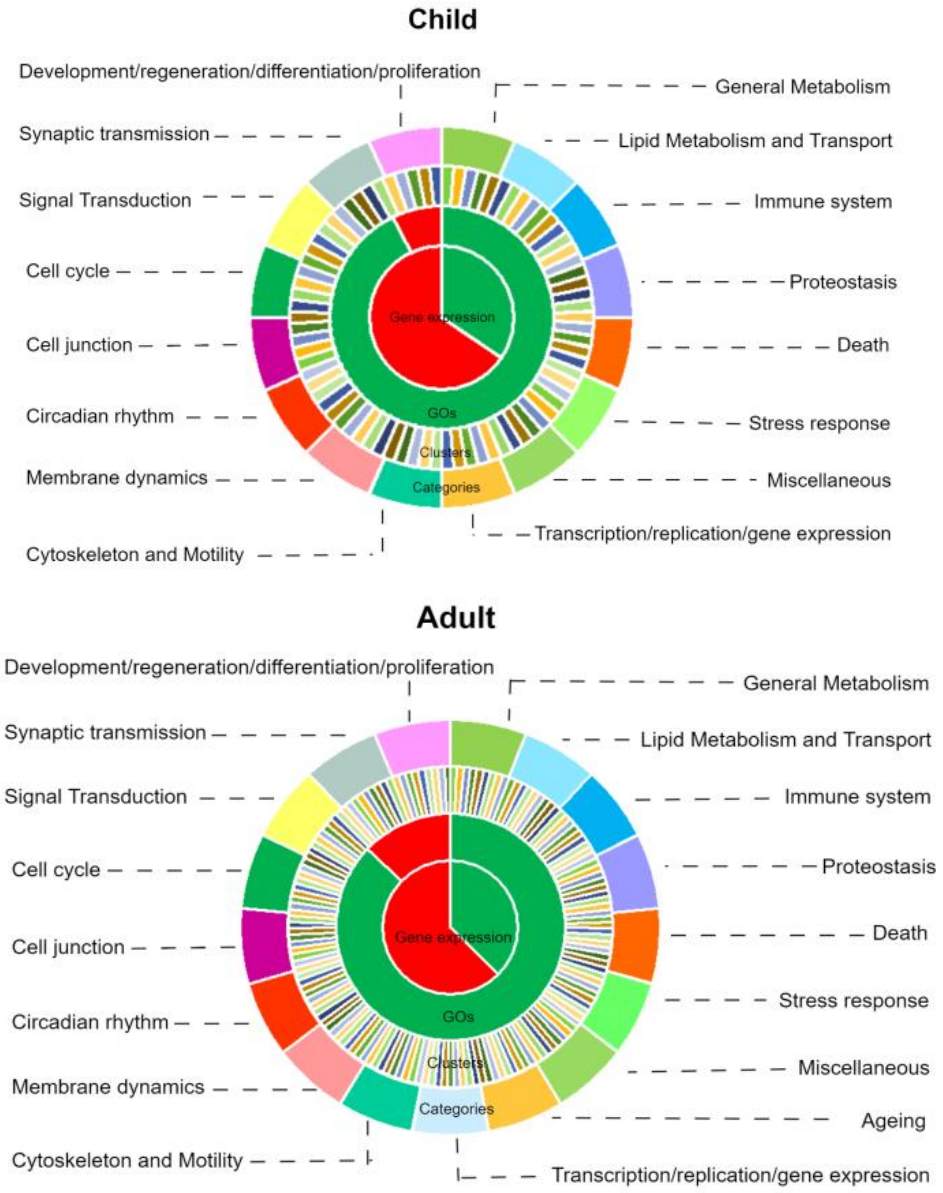

Figure 14. Transcriptomic differences of adult and children with X-ALD *versus* healthy counterparts at-a-glance. From the inner to the outer circle: GSEA analysis of differential gene expression (p-value < 0.05, inner circle enriched GOs, clusters according to the similarity coefficient of GOs. Clusters were classified into 17 functional categories, each one represented with a different colour in the outer circle. clustering was done using the 'Autoannotate' plugin of Cytoscape.

Of all the dysregulated categories, because we aim to gain insight into neurodevelopmental alterations, we will directed our analysis to three categories: 'Development' and 'Synaptic transmission' 'Lipid Metabolism and Transport' as lipids are relevant not only as fuel but also as important structural and signalling molecules during development

Table 6. Categories and clusters enriched n X-ALD children and adults versus healthy counterparts

Cluster (ADULTS)	Number of Nodes/GOs	Cluster (CHILDREN)	Number of Nodes/GOs
		Immune system	
cell regulation activation	99	antigen wnt pathway	46
immune response humoral	30	somatic recombination immune	19
cytokine chemokine production	20	leukocyte proliferation fibroblast	10
gamma interleukin 1	12	interferon gamma cytokine	10
growth factor beta	11	type interferon production	2
presentation antigen mhc	5	superfamily cytokine production	2
peptide polysaccharide antigen	3	interspecies interaction organisms	2
tumor necrosis factor	2	viral genome replication	6
transforming growth stimulus	2		
production molecular immune	2		
nik kappab signaling	2		
lymphocyte apoptotic process	2		
cytokine secretion production	2		
viral genome replication	6		
		Development/regeneration/differentiation/proliferation	
projection regeneration platelet	12	regulation muscle differentiation	37
projection negative differentiation	8	pancreas development morphogenesis	25
mesenchymal transition stem	8	neuron projection morphogenesis	14
morphogenesis branching kidney	19	regulation organ growth	6
formation valve angiogenesis	8	growth involved developmental	6
utero embryonic placenta	6	circulatory system angiogenesis	5
osteoclast hemopoiesis myeloid	6	glial oligodendrocyte gliogenesis	4
ossification biomineral osteoblast	6	reproductive primary sexual	3
muscle tissue development	6	central neural midbrain	3
connective tissue development	5	cellular size extent	3
vasculature development shape	4	skin epidermis development	2
prostate gland hepaticobiliary	4	osteoblast differentiation ossification	2
fibroblast regulation proliferation	4	organ regeneration	2
female maternal placenta	4	muscle structure development	2
cell size growth	4	antigen wnt pathway	46
regulation endothelial proliferation	3		
organ growth cell	3		
cartilage development chondrocyte	3		
astrocyte differentiation glial	3		
smooth muscle proliferation	2		

regulation remodeling bone	2		
osteoblast differentiation ossification	2		
negative muscle differentiation	2		
muscle hypertrophy adaptation	2		
epithelial cell proliferation	2		
endocrine pancreas development	2		
tissue remodeling	1		
neuromuscular junction development	1		
post embryonic development	1		
lens development camera	1		
positive regulation cell	1		
fat cell differentiation	1		
renal homeostasis number	52		
General Metabolism			
cysteine type endopeptidase	5	nucleoside triphosphate metabolic	34
amide posttranscriptional gene	5	macromolecular complex organization	7
tetramerization oligomerization homotetramerization	4	snrna metabolic process	2
chondroitin sulfate proteoglycan	3	regulation protein binding	2
carbohydrate derivative organonitrogen	3	oxide synthase monooxygenase	2
regulation stabilization stability	2	cellular biogenesis complex	2
regulation phospholipase lipase	2	homeostasis water transition	21
regulation glucose import	2		
regulation atpase activity	2		
peptidyl serine phosphorylation	2		
oxidoreduction coenzyme nad	2		
nucleoside monophosphate biosynthetic	2		
multicellular organismal macromolecule	2		
lipoprotein metabolic biosynthetic	2		
ammonium ion amine	2		
water soluble vitamin	1		
thioester metabolic process	1		
oxidative phosphorylation	1		
cyclic nucleotide metabolic	1		
isoprenoid biosynthetic process	1		
amino sugar metabolic	1		
organic hydroxy compound	1		
regulation hydrolase activity	1		
regulation protein deacetylation	1		
Lipid Metabolism and Transport			
biosynthetic sterol steroid	6	regulation lipid biosynthetic	3

lipid biosynthetic metabolic	5	steroid biosynthetic alcohol	2
fatty acid biosynthetic	1	lipoprotein metabolic biosynthetic	2
neutral lipid metabolic	1	particle sterol ester	6
particle complex subunit	7		
sterol transport lipid	3		
organophosphate ester phospholipid	2		
toxin transport	1		
regulation lipid storage	1		
regulation intracellular steroid	1		
Signal Transduction			
retinoic acid response	31	response purine cellular	50
radiation abiotic ionizing	14	detection light mechanical	6
insulin nitrogen glucagon	11	communication negative stimulus	3
starvation nutrient extracellular	8	response toxic substance	2
toxic detoxification antibiotic	3	response exogenous dsrna	2
response drug	1	external starvation biotic	12
negative function catalytic	12	rho protein kinase	26
camp messenger nucleotide	3	mediated signaling messenger	6
stat cascade	1	peptidyl autophosphorylation phosphorylation	4
map kinase activity	21		
kappab kinase nf	3		
protein kinase signaling	2		
rho transduction ras	2		
Cytoskeleton and Motility			
filament actin reorganization	6	migration subcellular motility	6
contraction striated muscle	5	smooth migration locomotion	3
lamellipodium organization	1	single cell adhesion	11
migration leukocyte chemotaxis	12	filament bundle actin	6
epithelial migration locomotion	9	actin contraction muscle	4
collagen fibril disassembly	3	cytoskeleton dependent intracellular	2
Membrane dynamics			
membrane biogenesis assembly	2	mitochondrial membrane permeability	4
regulation mitochondrial membrane	1	regulation mitochondrion transport	30
plasma membrane organization	1	localization membrane budding	28
regulation localization secretion	39	regulated exocytosis secretion	7
regulated exocytosis secretion	9	vacuole organization autophagy	2
endocytosis internalization phagocytosis	8	positive regulation endocytosis	2
phagocytosis engulfment clearance	6		
nuclear import nucleus	3		

monosaccharide transport carbohydrate	2		
maintenance location cell	2		
bicarbonate transport	1		
regulation vesicle fusion	1		
lytic vacuole organization	1		
Stress response			
endoplasmic reticulum stress	8	stress hydrolase peptidase	23
reactive oxygen species	5	reactive oxygen species	3
synthase oxidoreductase monooxygenase	4		
cellular response oxygen	1	wound healing coagulation	3
reactive oxygen species	1		
response fluid shear	1		
erad catabolic process	6		
hydrogen peroxide response	14		
Proteostasis			
maturation proteolysis peptidase	8	catabolic proteasomal process	13
catabolic small conjugation	11	macromolecule catabolic polyubiquitination	12
erad catabolic process	6	regulation stabilization stability	2
chaperone refolding folding	3		
topologically incorrect ire1	5		
Synaptic transmission and calcium signalling			
regulation postsynaptic membrane	2	regulation ion calcium	20
neuron synaptic transmission	1	nanoparticle inorganic substance	6
canonical wnt coupled	5	divalent cation calcium	3
regulation depolarization homeostatic	4		
sodium ion transmembrane	4		
anion negative transport	3		
Death			
apoptotic pathway extrinsic	12	apoptotic death neuron	16
extrinsic apoptotic intrinsic	8	apoptotic pathway intrinsic	6
neuron process death	5		
apoptotic process epithelial	3		
muscle cell death	2		
Cell junction			
substrate junction assembly	12	substrate junction assembly	5
		adherens junction matrix	4
Transcription/replication/gene expression			

sequence specific binding	4	telomere organelle chromosome	8
telomere maintenance lengthening	3	ire1 topologically incorrect	8
regulation dna binding	3	rna splicing mrna	6
templated polymerase promoter	2	posttranscriptional gene expression	4
amino acid activation	1	sequence specific binding	3
		nucleobase compound transport	2
Cell cycle			
regulation cell cycle	2		
		mitotic nuclear cycle	4
Circadian rhythm			
circadian rhythm ovulation	3	circadian rhythm rhythmic	2
Ageing			
cell aging	2		
Miscellaneous			
vasodilation circulation vasoconstriction	5	positive regulation vasodilation	2
systemic arterial pressure	2	cardiac conduction contraction	5
digestive system process	1	digestive system process	2
heart rate conduction	3		
regulation body fluid	1		
involved symbiotic interaction	8		

Cytoscape plugin 'Enrichment map' in combination with 'Autoannotate' plugin was used to cluster significantly enriched GOs (FDR q-value < 0.25) according to their similarity coefficient. Clusters were classified in categories depending on the GOs they contain.

2. Altered biological processes in children

All the clustered GOs belonging to 'development' category as well as the edges indicating the overlapping between them are shown in Fig. 3. Differentially expressed genes contributing to these GOs are represented in the hierarchically clustered heat-map revealing different patterns (Fig. 15).

The **'development'** category encompasses enriched GOs related to development and differentiation of several cells and tissues, morphogenesis of different structures, organ and cell growth, and WNT signalling pathway regulation. Regarding development of CNS*, nervous system development, neuron projection development,*

neuron development, glial cell development, neural nucleus development, dendrite development, *central nervous system development, midbrain development, gliogenesis* and *neurogenesis* are featured GOs. *Neuron projection morphogenesis, dendrite morphogenesis* and *morphogenesis involved in neuron differentiation, negative regulation of neuron differentiation, glial cell differentiation, neuron projection guidance* and *neuron differentiation* are dysregulated pathways. Suggesting that the whole brain formation could be affected by changes in gene expression (Annex I, Supplementary Tab. 1).

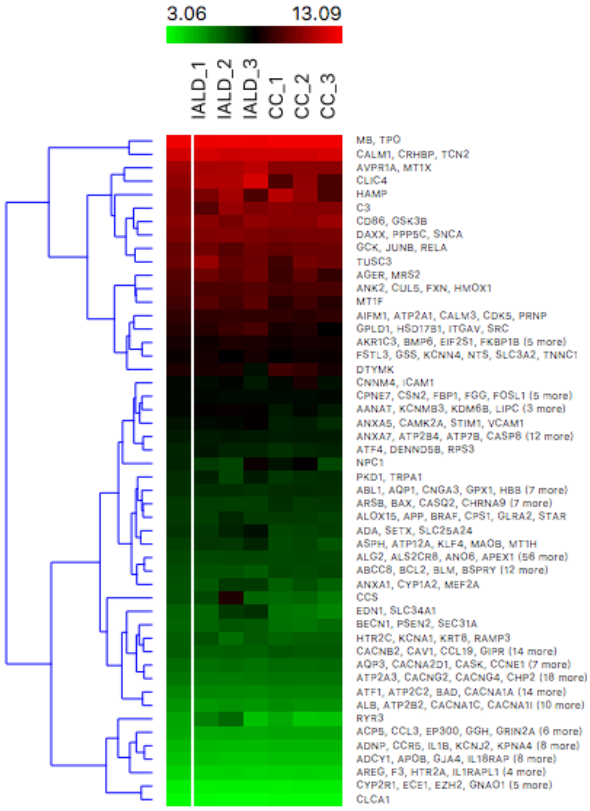

Figure 15. Children'Development/regeneration/differentiation/proliferation' gene expression. Hierarchically clustered heat-map of enriched genes contributing to GOs belonging to 'development'. Genes in each row are representative genes of each cluster IALD: child X-ALD. CC: child control. The program Orange was used to generate the heat-map.

WNT signalling pathway is a key route in development of all tissues and regulation of it is impaired in X-ALD children according to GSEA. Actually, children immune system category, apart from GOs directly related to immunity and inflammation, also includes canonical and non-canonical WNT signalling pathway. WNT signalling and WNT ligands play essential roles in differentiation, proliferation, death and regulate immune

responses through T-cell development, immune cell infiltration in cancer and macrophage-mediated tissue injury and repair between others (Hirabayashi *et al.*, 2004; Chae and Bothwell, 2018). However, how canonical and non-canonical WNT signalling pathway modulates the immune response depending on the context remains unclear. As WNT signalling could participate in both, 'immune system' and 'development', the cluster will appear in the two categories.

Fig 16. 'Development/regeneration/differentiation/proliferation' nodes (GOs) in children. Cytoscape plugin 'Enrichment map' was used to plot significantly enriched GOs (FDR q-value < 0.25). Size of nodes represents the number of enriched genes in each GO. Up-regulated GOs are showing in red and down-regulated GOs in blue.

N*egative regulation of canonical WNT signalling pathway* GO and *neural precursor cell proliferation* GO are between the top 40 GOs deregulated (Fig. 17). Notwithstanding both biological processes are enriched positively, up-regulated genes contribute more to *negative regulation of canonical WNT signalling pathway* GO, and *neural precursor cell proliferation* GO are influenced by up and down-regulated genes.

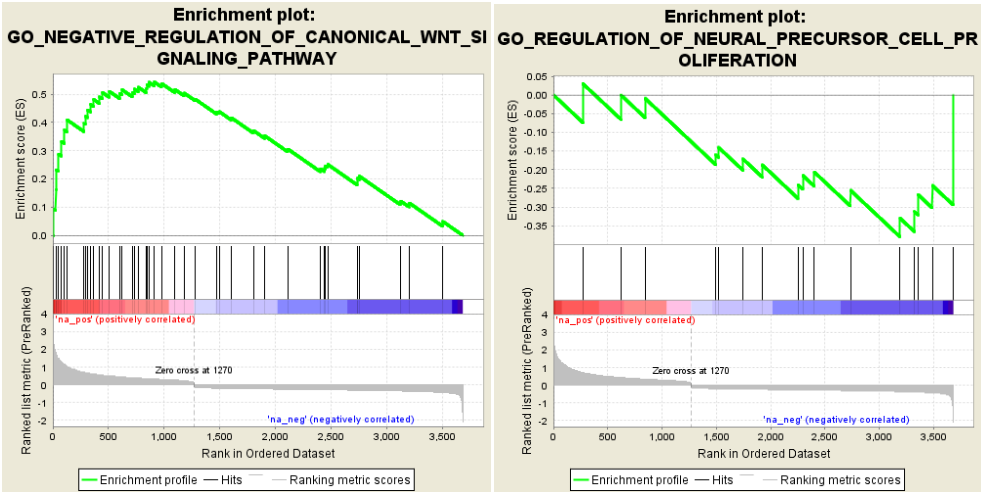

Figure 17. *Negative regulation of canonical WNT signalling pathway* GO and *Neural precursor cell proliferation* GO enrichment gene set. Enrichment plot of top 40 'Development' GO's situated in the top 40 enriched in X-ALD children compared to healthy controls. Results were obtained by GSEA analysis.

'Synaptic transmission and calcium signalling' are crucial to the correct function of the brain and responsible for thinking and movement control. Wherefore, dysregulation of genes controlling synaptic transmission will compromise the functionality of developing brain circuits in X-ALD children.

Regulation of cation channel activity, regulation of ion transport and more specifically *calcium ion transport* and *regulation of calcium ion transport* are deregulated. Transport into the cytosol, the release of sequestered calcium into the cytosol, transmembrane transporter activity, and import are some of the processes altered related with calcium ion (Annex I, Supplementary Tab. 1).

Calcium signalling triggers the release of synaptic vesicles neurotransmitters and is base of astrocyte excitability and potentially lead to gliotransmitters release that could act on neurons and modulate synapses (Perea, Navarrete and Araque, 2009). Ergo, the synaptic transmission will suffer changes in these individuals affecting normal neuron and astrocyte functions.

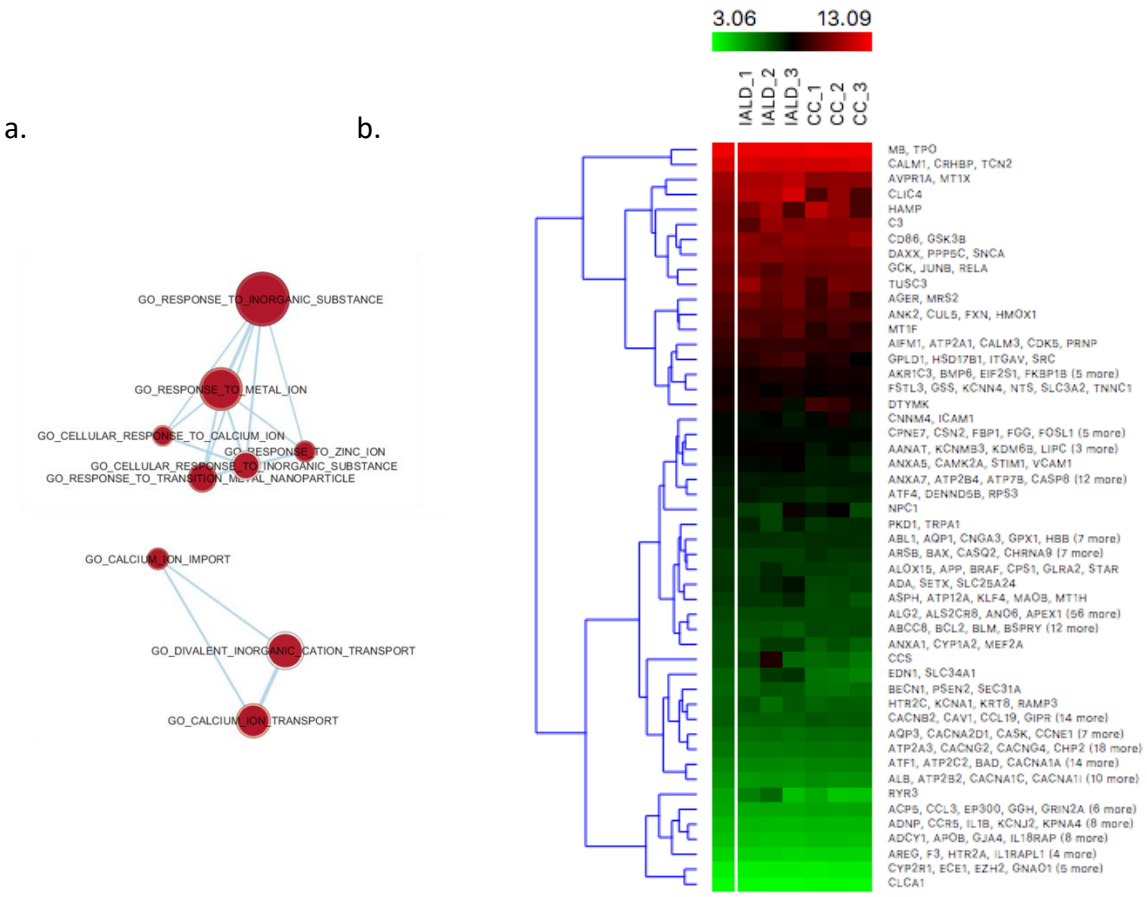

Figure 18. 'Synaptic transmission' nodes (GOs) and gene expression in children. a. Cytoscape plugin Enrichment map was used to plot significantly enriched GOs (FDR q-value < 0.25). Size of nodes represents the number of enriched genes in each GO. Up-regulated GOs are showing in red and down-regulated GOs in blue. b. Gene expression hierarchically clustered heat-map of enriched genes contributing to GOs belonging to 'synaptic transmission' category. Representative genes in each column are annotated. IALD: child X-ALD. CC: child control. Orange was used to generate the heat-map.

All the deregulated GOs of 'synaptic transmission' category, their edges and, the differentially expressed genes responsible for the GOs enrichment and their expression are shown in figure 18.

X-ALD is characterised by the accumulation of specific lipids; however, how other lipids and their metabolism could be affected by this lipid dyshomeostasis is barely known.

'Lipid metabolism and transport' category includes enriched GOs of *regulation of lipid metabolic and biosynthetic process, lipoprotein metabolic and biosynthetic process, regulation of plasma lipoprotein particle levels* and, *steroid biosynthetic process.* As

well as metabolism and biosynthesis*, lipid localisation and sterol transport* are compromised according to GSEA (Annex I, Supplementary Tab. 1).

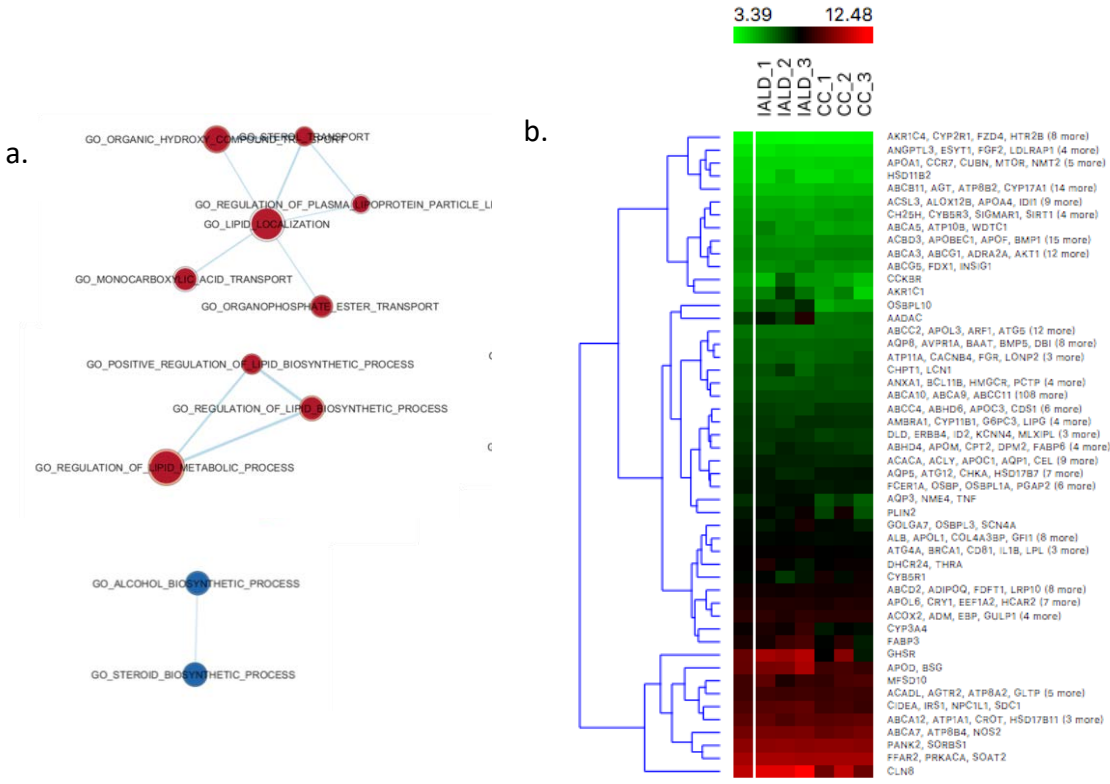

Figure 19. 'Lipid metabolism and transport' nodes (GOs) and gene expression in children. a. Cytoscape plugin Enrichment map was used to plot significantly enriched GOs (FDR q-value < 0.25). Size of nodes represents the number of enriched genes in each GO. Up-regulated GOs are showing in red and down-regulated GOs in blue. b. Gene expression hierarchically clustered heat-map of enriched genes contributing to GOs belonging to 'lipid metabolism and transport' category. Representative genes in each column are annotated. IALD: child X-ALD. CC: child control. Orange was used to generate the heat-map.

Deregulated GOs of 'lipid metabolism and transport' category, their edges and, the differentially expressed genes responsible for the GOs enrichment and their expression are shown in figure 19.

3. Altered biological processes in adults

Unlike children brains, adult brain circuits and synapses are established, synaptic plasticity is dramatically reduced, and the capacity of neurogenesis is restricted to certain areas. Hence, pathways and biological process occurring will be different, acquiring synaptic transmission a higher relevance compared to development.

In adults, **'Synaptic transmission'** is affected not only by changes in *regulation of calcium ion transport* but also by *negative regulation of synaptic transmission*, *regulation of membrane depolarisation*, *regulation of postsynaptic membrane potential* and *neuron neuron synaptic transmission* (Annex I, Supplementary tab. 2). In fact, *regulation of postsynaptic membrane potential* GO, and *neuron neuron synaptic transmission* GO are two of the top 40 enriched GOs in adults (Fig. 20).

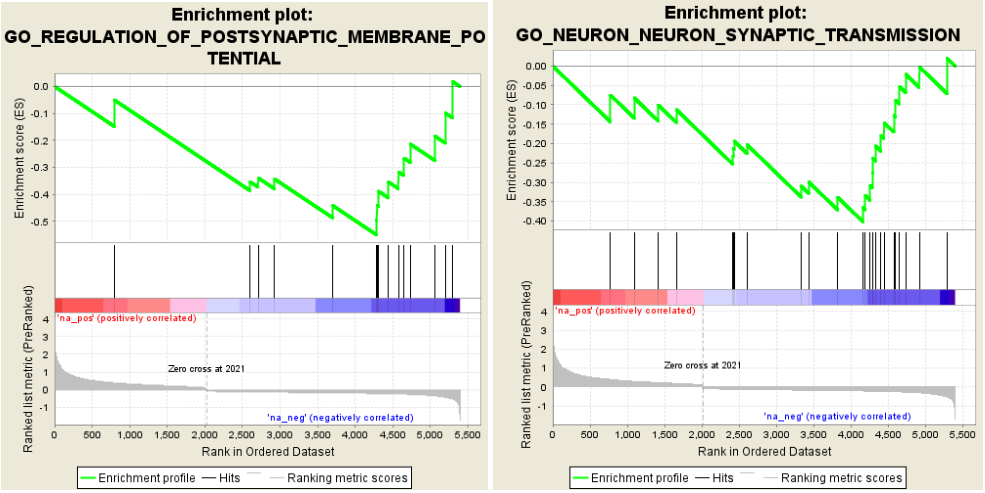

Figure 20. *Regulation of postsynaptic membrane potential* GO, and *Neuron neuron synaptic transmission* GO enrichment gene set. Enrichment plot of top 40 'Synaptic transmission' GOs situated in the top 40 enriched in X-ALD adults compared to healthy controls. Results were obtained by GSEA analysis.

Enriched GOs of 'synaptic transmission' and their leading genes expression are plotted in figures 9 and 10.

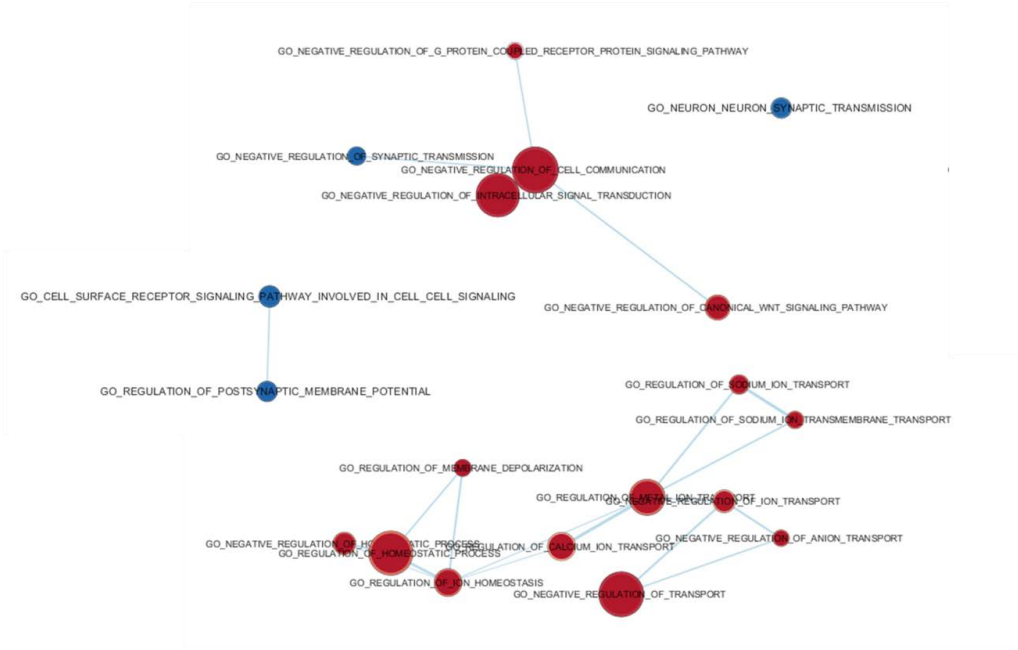

Figure 9. Synaptic transmission nodes (GOs) in adults. Cytoscape plugin Enrichment map was used to plot significantly enriched GOs (FDR q-value < 0.25). Size of nodes represents the number of enriched genes in each GO. Up-regulated GOs are showing in red and down-regulated GOs in blue.

Regarding 'Lipid metabolism and transport', more clusters and GOs are enriched in adults compared to children. *Sterol metabolic and biosynthetic process, steroid metabolic and biosynthetic process, fatty acid biosynthetic process, neutral lipid metabolic process* and regulation of them appear deregulated. *Transport of sterols, fatty acids and their regulation, sterol homeostasis, lipid localisation, regulation of lipid storage* are also enriched GOs (Annex I, Supplementary tab. 2). Suggesting that lipids and sterols metabolism, synthesis, storage and transport could be malfunctioning.

Curiously, *Sterol biosynthetic process* GO, and *Sterol metabolic process* GO belong to the top 40 GOs enriched in adults and both have over-represented genes in both extremes of the graph (Fig. 11). Figures 12 and 13 show GOs altered in lipid metabolism and transport and their leading-edge gene expressions.

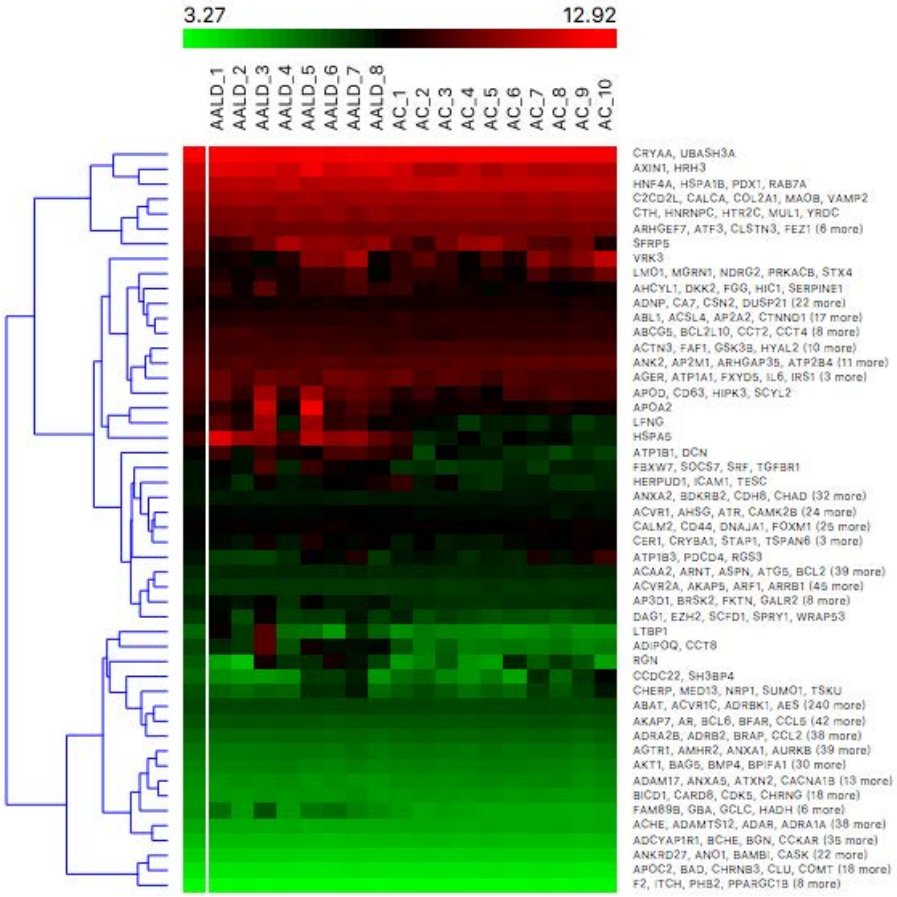

Figure 10. 'Synaptic transmission' gene expression in adults. Gene expression hierarchically clustered heat-map of enriched genes contributing to GOs belonging to 'development'. Representative genes in each column are annotated. AALD: adult X-ALD. AC: adult control. Orange was used to generate the heat-map.

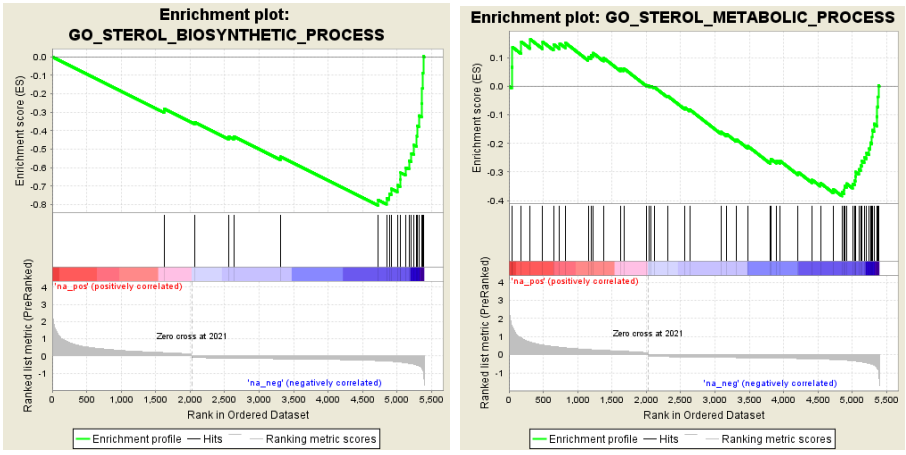

Figure 11. *Sterol biosynthetic process* GO, and *Sterol metabolic process* GO enrichment gene set. Enrichment plot of top 40 'Lipid metabolism and transport' GOs situated in the top 40 enriched in X-ALD adults compared to healthy controls. Results were obtained by GSEA analysis.

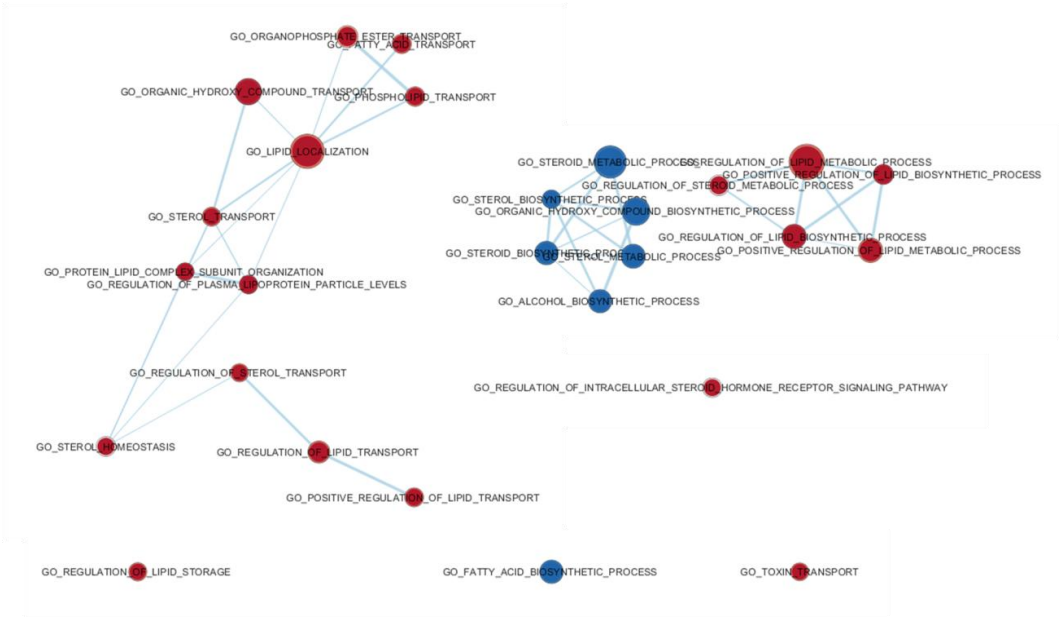

Figure 12. 'Lipid metabolism and transport' nodes (GOs) in adults. Cytoscape plugin Enrichment map was used to plot significantly enriched GOs (FDR q-value < 0.25). Size of nodes represents the number of enriched genes in each GO. Up-regulated GOs are showing in red and down-regulated GOs in blue.

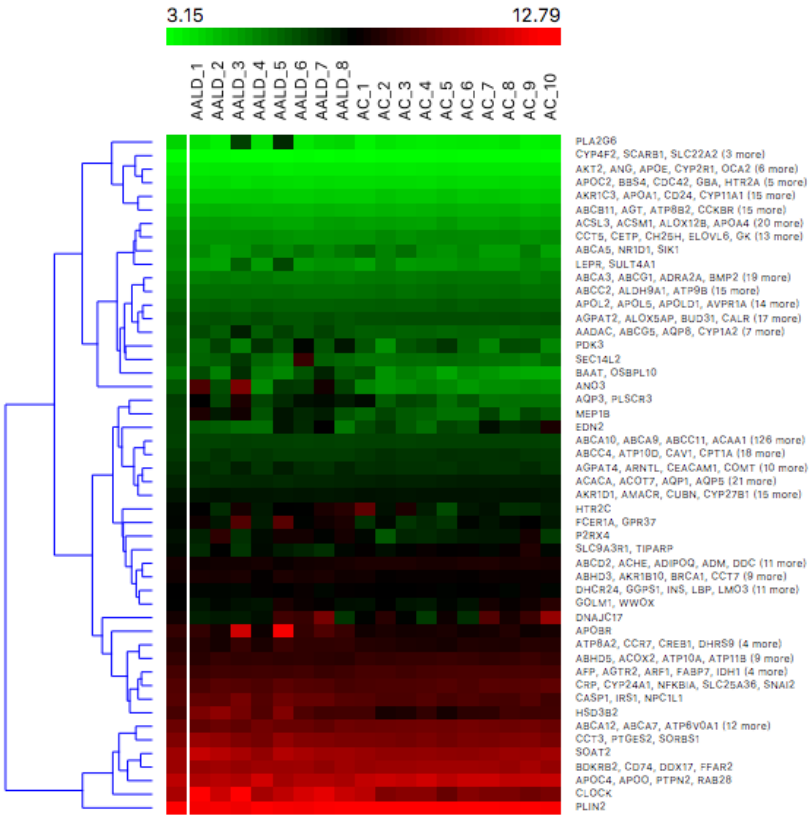

Figure 13. Adults 'Lipid metabolism and transport' gene expression. Gene expression hierarchically clustered heat-map of enriched genes contributing to GOs belonging to 'development'. Representative genes in each column are annotated. AALD: adult X-ALD. AC: adult control. Orange was used to generate the heat-map.

Even we have called the category 'Development', it includes development, regeneration, differentiation and proliferation. Different situations will require one of these processes and therefore, maintain these capacities regulated are essential especially for brain repair and maintenance.

A long list of enriched GOs are included in this category, however, most of them are related to organs others than the central nervous system. *Response to axon injury, neuron projection regeneration, positive regulation of stem cell differentiation, regulation of cell size and growth, gliogenesis, glial cell development*, *astrocyte differentiation,* and *postembryonic development* are some of the highlighted GOs (Annex I, Supplementary tab. 2). Of particular interest is regeneration, as most of the patients are suffering from neuronal damage.

Fig 14. Development/regeneration/differentiation/proliferation nodes in adults. Cytoscape plugin Enrichment map was used to plot significantly enriched GOs (FDR q-value<0.25). Size of nodes represents the number of enriched genes in each GO. Upregulated GOs are showing in red and down-regulated GOs in blue.

In image 14, we can see the huge amount of GOs included in this category and image 15 shows the differentially expressed genes of these GOs.

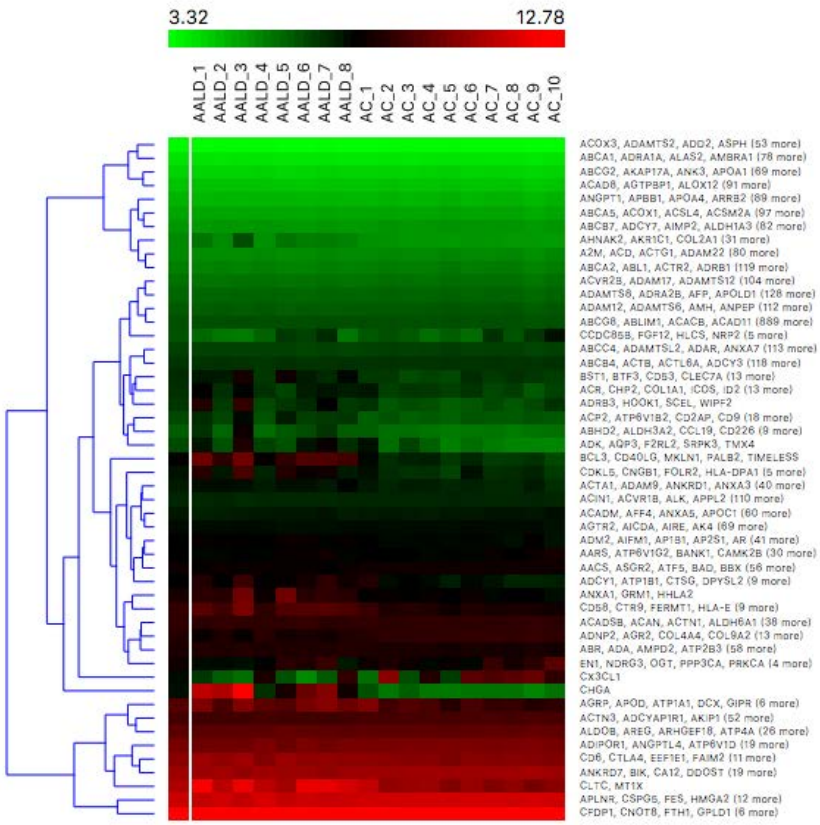

Figure 15. 'Development/regeneration/differentiation/proliferation' gene expression in adults. Gene expression hierarchically clustered heat-map of enriched genes contributing to GOs belonging to 'development'. Representative genes in each column are annotated. AALD: adult X-ALD. AC: adult control. Orange was used to generate the heat-map.

4. Cholesterol transport gene candidates

Considering that children and adults with X-ALD exhibit biological pathways related with sterols metabolism synthesis and transport, and astrocyte-derived cholesterol supply to neurons is critical for synapse formation and maintenance, we decided to deepen in cholesterol transport. This leads us to study how genes related to cholesterol transport are in patients.

Taking advantage of the study done by (Chu *et al.*, 2015a), where 341 hits were identified for intracellular cholesterol transport trough a genome-wide pooled shRNA screen on cells that only survive when cholesterol transport is impaired. We crosschecked their list with our transcriptomic data to see if any of their candidates are affected in X-ALD brains.

Interestingly, we found out that 106 genes of the candidates' list are differentially expressed in X-ALD (Tab. 7). in the original article, hits were classified bioinformatically into biological processes. We used the same classification to see if any categories are particularly enriched. Neurodisease is the category with more genes affected in our analysis which includes *Abcd1*. We have to mention that the same gene could appear in different categories, and that is the case of *Abcd1* that appears in cellular transport, neurodisease and peroxisome.

This result suggests that *Abcd1* could have other functions apart from VLCFA transport that could affect the progression of the disease.

Table 7. Gene candidates involved in cholesterol transport and altered in CCALD.

Symbol	logFC	Z-score
Lipid metabolism:		
S100G	-0.317	1.980
ACACB	0.710	2.745
SLC27A2	-0.163	2.091
SMPD1	-0.240	2.072
SCAP	0.200	2.309
SREBF2	-0.250	2.316
GK	-0.263	1.968
Cellular transport:		
Cellular transport:		
AAK1	-0.383	5.517
SPTBN1	0.607	2.613
LDLR	-0.327	1.137
TRIM3	-0.293	2.241
OCA2	-0.347	2.027
EHD4	-0.213	2.033
RAB22A	0.253	2.222
TRPC4	-0.177	2.458
NUMB	0.240	2.567
GTP binding protein:		
SOS1	-0.323	2.865
RALGDS	0.393	2.713
RGS1	-0.113	3.085
GNAQ	-0.290	2.021
RAPGEF2	-0.130	2.349
Cytoskeleton:		
ARPC5	-0.267	2.401
ABC family:		
ABCD1	-0.360	2.074
SLC family:		
SLC6A20	-0.320	2.157
SLC39A9	-0.233	2.067
SLC27A2	-0.163	2.091
Neurodisease:		
KIF11	-0.330	1.974
ESR2	-0.247	1.965
CXCL12	-0.370	2.243
SPG11	0.383	2.368
TDP1	-0.280	1.981
MET	-0.327	2.234
KCNMA1	-0.290	1.760
HPS1	-0.203	2.288
SMAD3	-0.250	2.464

MTMR10	-0.230	2.152
IL1A	-0.200	2.193
SMPD1	-0.240	2.072
UBE3A	0.320	3.070
ABCD1	-0.360	2.074
PDE11A	-0.270	2.281

Calcium:

PCDHB1	-0.380	2.183
DSG3	-0.283	1.977
S100G	-0.317	1.980
F2	-0.330	2.699
CRELD1	0.710	2.265
KCNMA1	-0.290	1.760
TGM1	-0.237	2.104
EHD4	-0.213	2.033
TRPC4	-0.177	2.458
DMP1	-0.110	2.144

Peroxisome:

PEX6	1.120	-
BAAT	-0.360	1.920
PEX3	0.193	-
ABCD1	-0.360	2.074
PEX1	-0.413	-

Immune system:

TNFRSF1A	0.770	2.173
CXCL12	-0.370	2.243
RFX5	-0.243	3.195
CD80	-0.360	2.015
IL1A	-0.200	2.193
IL21	-0.193	2.007
KLRC4	-0.123	1.684

Cell adhesion:

PCDHB1	-0.380	2.183
DSG3	-0.283	1.977
CRELD1	0.710	2.265
TGM1	-0.237	2.104

Ubl conjugation pathway:

CYLD	-0.297	2.427
UBE2D3	0.457	2.279
UBE3A	0.320	3.070
UBE2B	0.383	2.062

Purine metabolism:

PDE3B	-0.360	2.180
PDE1A	-1.117	2.048
PDE11A	-0.270	2.281

Hhh pathway:

PTCH1	0.587	2.259
BMP4	-0.307	2.304

Transcription:

ESR2	-0.247	1.965
GTF2A1	-0.303	2.604
RFX5	-0.243	3.195
ZNF3	-0.253	2.192
SMAD3	-0.250	2.464
KLF12	-0.303	2.037
IRX5	-0.227	1.842
LHX5	-0.187	3.537

FHL5	-0.217	2.002
HR	-0.363	2.172
RNA processing:		
RBM12B	-0.393	2.356
PAPOLB	-0.210	2.279
SSB	0.297	2.650
Cell cycle:		
HCFC1	-0.320	2.030
Cell death:		
TNFSF8	-0.253	1.357
Unclassified:		
Unknown:		
SAYSD1	-0.257	2.147
Others:		
AKT3	-0.323	1.616
ACOT13	0.823	2.095
ALDH4A1	0.913	1.050
MUSK	-0.313	2.100
PPM1J	0.517	2.689
BHMT	-0.437	3.440
F2	-0.330	2.699
PDPR	-0.343	2.076
CA12	-0.270	2.248
SULT1C4	0.430	2.420
CDY1	-0.253	2.204
HYDIN	-0.233	2.489
LCMT1	0.297	2.125
PTPRF	0.307	2.595

Candidate genes obtained from Genome-wide RNAi Screen and their correspondent z-score found deregulated in children with X-ALD. logFC corresponds to gene expression in children X-ALD. Gene classification according to gene functions. FC: fold change.

5. Astrocytes factors that induce synaptogenesis

According to GSEA results, synaptic transmission as well as the whole neuron development seems to be altered. Gliogenesis and calcium signalling also appear deregulated. Then brain circuits are changed. We want to gain insight into functional consequences of these perturvances and see if synaptogenesis is altered in X-ALD. Likewise we want to see if the astrocytic changes are affecting how they could promote and modulate synapse formation.

As we have mentioned before, one astrocyte could contact more than 2,000,000 synapses (Bushong *et al.*, 2002; Oberheim *et al.*, 2009) however not all synapses are ensheathed by astrocytes (Genoud *et al.*, 2006). These covering could be altered during development and astrocyte clearance of neurotransmitters modificated. Therefore, synapse development, elimination, and plasticity could be modified by different astrocytic- secreted molecules. A

targeted analysis of different genes responsible for these molecules release and expression will be performed (Tab. 8).

Cholesterol was one of the first identified astrocyte-released molecules that when is diminished impairs synapse development (Mauch *et al.*, 2001). SREBP1 (also known as SREBF1) and SREBP2 (also known as SREBF2) are responsible for cholesterol synthesis by astrocytes (Madison, 2016), that is secreted in complex with APOE (Kim *et al.*, 2014). SREBP2 and APOE show statistically significant differences in gene expression in both, children and adults with X-ALD.

Thrombospondin secreted by astrocytes (Karen S Christopherson *et al.*, 2005) and SPARCL1/hevin induce formation of glutamatergic synapses, pre-synaptically active and post-synaptically silent (Kucukdereli *et al.*, 2011). An antagonist of hevin, SPARC is also produced by astrocytes, blocking synapse formation. THBS1 expression is decreased in children with X-ALD while in adults is increased. SPOCK3, a form of SPARC is also down-regulated in X-ALD children.

Several astrocyte-derived signals modulating AMPA receptors have been identified. Heparan sulfate proteoglycans glypicans 1 and 4 (GPC 1 and GPC4) reclute GluA1 AMPA receptors and postsynaptic density proteins to new synapses (Allen *et al.*, 2012). However, they aren't changed in our samples. At already formed synapses, TNF-α increases AMPA receptors levels and decreased GABAA receptors at inhibitory synapses, leading to a higher neuronal activity (Beattie *et al.*, 2002). In adults, TNF expression is statistical significantly reduced in X-ALD, while in children remains stable.

Wnt secreted from astrocytes cluster glutamate receptors in Drosophila. In mammals, similar effects have been observed; however the origin of Wnt is not well known (He, Liao and Pan, 2018). The study of different Wnt molecules revealed that expression of WNT2, WNT2B, WNT6, WNT7A, WNT10B and WNT16 in children, and WNT2B, WNT5A, WNT6, WNT7A, WNT10B, and WNT11 in adults is changed.

Synaptic pruning is directly regulated by Mertk receptors that promote phagocytosis of the excess of synapses (Chung *et al.*, 2013) and indirectly regulated by transforming growth factor β (TGF-β) (Bialas and Stevens, 2013). MERTK and TGF-β expression are down-regulated in X-ALD adults but not in X-ALD children. Moreover, synaptic remodelling by ephrins is altered as, expression of EPHB2 and EPHB4 is diminished in both adults and children.

Table 8. Astrocytic genes involved in synapse-modifying signals.

Child X-ALD vs Child control					Adult x-ALD vs Adult control				
Gene	**logFC**	**P.Value**	**adj.P.Val**		**Gene**	**logFC**	**P.Value**	**adj.P.Val**	
THBS1	-0.393	0.0798	0.080	**	THBS1	0.520	0.041	0.138	*
THBS2	0.193	0.7872	0.787		THBS2	-0.136	0.502	0.654	
THBS3	-0.090	0.5321	0.532		THBS3	-0.072	0.129	0.277	
THBS4	0.097	0.7525	0.752		THBS4	-0.010	0.915	0.951	
SPOCK1	0.160	0.7874	0.787		SPOCK1	0.010	0.952	0.973	
SPOCK2	0.517	0.3364	0.336		SPOCK2	-0.042	0.493	0.647	
SPOCK3	-0.547	0.1934	0.193	*	SPOCK3	-0.206	0.144	0.295	
SPARCL1	1.050	0.0978	0.098	**	SPARCL1	0.516	0.012	0.069	*
GPC1	0.173	0.4042	0.404		GPC1	-0.088	0.148	0.301	
GPC4	-0.180	0.5638	0.564		GPC4	0.088	0.327	0.498	
WNT1	-0.147	0.4795	0.480		WNT1	-0.001	0.991	0.994	
WNT2	-0.323	0.1784	0.178	*	WNT2	-0.149	0.067	0.185	
WNT2B	-0.253	0.0702	0.070	**	WNT2B	-0.235	0.001	0.018	**
WNT3	-0.150	0.3533	0.353		WNT3	-0.071	0.193	0.356	
WNT4	-0.043	0.8638	0.864		WNT4	-0.127	0.065	0.182	
WNT5A	0.030	0.8385	0.839		WNT5A	0.184	0.008	0.055	**
WNT5B	-0.093	0.6801	0.680		WNT5B	-0.095	0.178	0.339	
WNT6	-0.403	0.1156	0.116	**	WNT6	-0.172	0.014	0.074	*
WNT7A	-0.203	0.2045	0.204	*	WNT7A	-0.129	0.021	0.093	*
WNT7B	-0.130	0.3440	0.344		WNT7B	-0.065	0.163	0.321	
WNT8B	-0.130	0.4033	0.403		WNT8B	-0.093	0.080	0.207	
WNT10B	-0.377	0.1092	0.109	**	WNT10B	-0.262	0.001	0.020	**
WNT11	-0.137	0.3121	0.312		WNT11	-0.118	0.014	0.075	*
WNT16	-0.187	0.1824	0.182	*	WNT16	0.015	0.739	0.837	
TNF	-0.153	0.5263	0.526		TNF	-0.183	0.026	0.106	*
SREBF1	0.130	0.8455	0.845		SREBF1	-0.239	0.191	0.354	
SREBF2	-0.250	0.2275	0.227	*	SREBF2	-0.350	0.000	0.002	***
APOE	1.783	0.1124	0.112	**	APOE	1.609	2.58E-05	0.002	****
TGFB1	-0.123	0.8369	0.837		TGFB1	-0.216	0.002	0.025	**
TGFB2	-0.153	0.4522	0.452		TGFB2	-0.184	0.001	0.017	**
TGFB3	-0.153	0.7083	0.708		TGFBR3	0.856	0.000	0.512	***
EPHB1	-0.060	0.7995	0.800		EPHB1	-0.070	0.293	0.464	
EPHB2	-0.457	0.0631	0.063	**	EPHB2	-0.204	0.001	0.014	**
EPHB4	-0.263	0.1845	0.185	*	EPHB4	-0.247	0.001	0.014	**
MERTK	-0.153	0.4502	0.450		MERTK	0.198	0.016	0.078	*

Comparative expression of selected genes related with astrocyte mediated spynogenesis in X-ALD children and x-ALD adults versus controls. *p-value <0.05, **p-value <0.01, and ***p-value <0.001.

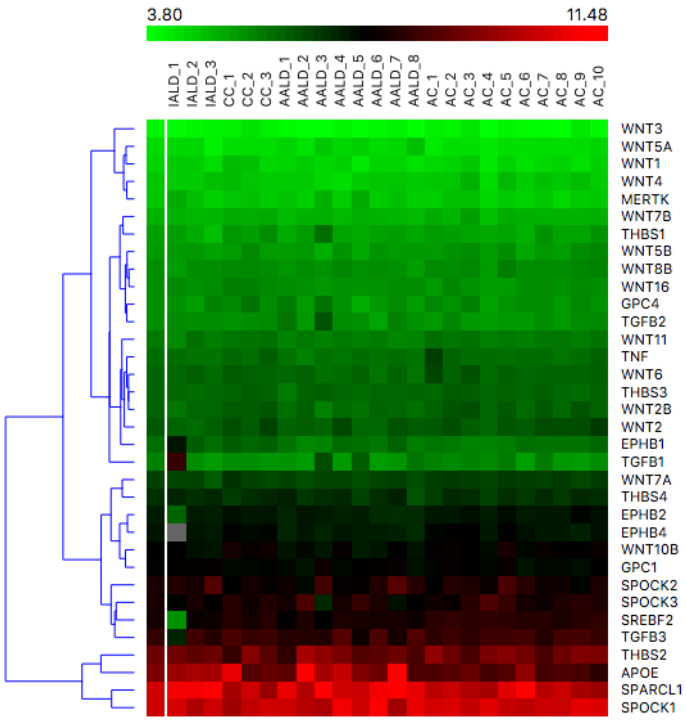

Figure 16. Expression of astrocytic genes involved in synapse-modifying signals. Hierarchically clustered heat-map of gene expression of selected genes related with astrocyte mediated spynogenesis in X-ALD children and X-ALD adults.

Chapter II: Neurodevelopmental alterations in X-ALD

1. Establishment of in vitro models of X-ALD

Prompted by the discovery of developmental alterations in X-ALD children revealed by GSEA, we sought to validate the pathways changed using *in vitro* models of X-ALD generated and three strategies. First, and most importantly, we silenced the *Abcd1* and *Abcd2* genes in primary rat hippocampal neurons and cortical astrocytes (Fig. 17). The independent study of neurons and astrocytes helps to dissect out the cellular origin of dysregulated pathways in whole brains. Because *Abcd2* overexpression has been shown to compensate for the lack of function of *Abcd1* (A. Netik *et al.*, 1999), we designed interference RNAs targeted to *Abcd1* or *Abcd2* to downregulate the expression of both genes at the same time. The expression of both genes was successfully reduced in neurons and astrocytes prepared from brains of WT rats (Fig. 17).

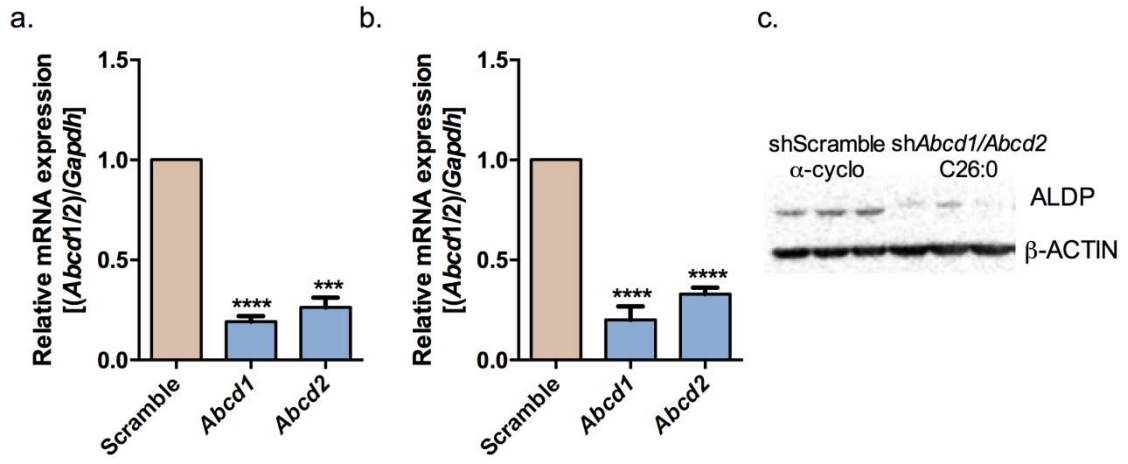

Figure 17. Decreased expression of *Abcd1* and *Abcd2* with interference RNA strategies. Primary cultures of neurons and astrocytes were treated with scrambled sRNAi, or a cocktail containing sRNAi for *Abcd1* and *Abcd2* to knock down both genes in unison. *Abcd1* and *Abcd2* mRNA expressions were measured with qPCR and normalised by *Gapdh* expression. a. Expression in neurons (n=3). b. Expression in astrocytes (n=4). c. ALDP and β-ACTIN protein expression quantified by Western blot (n=3). Data are the mean ± SEM, n=3-4, ***p<0.001 and ****p<0.0001 (Unpaired T-test).

Second, we exacerbated the accumulation of VLCFA by adding exogenous C26:0 (vehicle α-cyclodextrin), as previously described in Vargas *et al.*, 2004. Treatments were done at different time points depending on the objective of the study, as described in figure 18. Third, as molecules secreted by astrocytes have been shown to regulate neuronal plasticity (Clarke and Barres, 2013), and because there is a precedent in Amyotrophic Lateral Sclerosis (ALS) in that astrocyte-secreted factors kill neurons (Basso *et al.*, 2013), we explored the relationship between astrocytes and neurons in our X-ALD model by adding astrocyte-conditioned media (ACM) to neurons in order to mimic neuronal-astrocyte interactions (Fig. 18). ACM form WT

astrocytes (ACM^{Ctrl}) was used as a control, and ACM from astrocytes with *Abcd1* and *Abcd2* genes silenced and treated with C26:0 ($ACM^{X\text{-}ALD}$) to explore changes in the secretome caused by the disease.

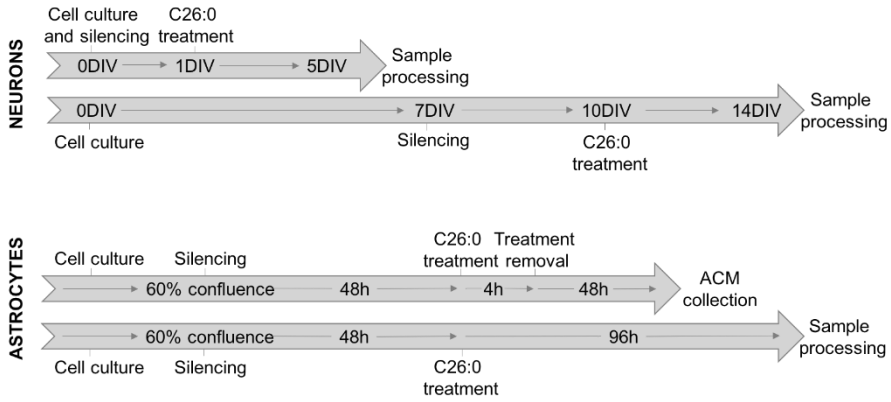

Figure 18. Experimental timeline. Neurons and astrocytes were seeded at 0 days *in vitro* (DIV). *Abcd1* and *Abcd2* were silenced at 0 DIV (for axonal growth experiments) or 7DIV in neurons (for the rest of the experiments), and in astrocytes at an approximately 60% of confluence. Treatments with VLCFA C26:0 were administered at 1DIV, 10 DIV or after 48h of silencing respectively. Treatments were removed only in astrocytes to change de media for posterior astrocyte-conditioned media (ACM) collection after 48h. ACM were administered at the same time as C26:0 when appropriate. Cells were processed at 5DIV and 14DIV in the case of neurons, or after 96h in the case of astrocytes.

2. Neuronal death due to loss of function of Abcd transporters

Neurodegenerative processes feature chronic and progressive loss of brain and spinal cord cells, neuronal death being one of the most remarkable pathological hallmarks. Apoptosis and necroptosis, a novel form of programmed necrosis (Zhang *et al.*, 2017), have been described as the two main forms of cellular death, although the particular mechanisms by which these processes are activated are still partially known. The study of cellular death in X-ALD has been traditionally focused on spinal cord cells because motor problems derived from of axonal degeneration of motor neurons are arguably the most visible symptoms in patients (Shamim and Alleyne, 2017). Thus, the possibility that CNS regions other than the spinal cord, and cells other than motor neurons, are affected by the accumulation of VLCFA has been overlooked. This existence of neuronal death in brains of X-ALD patients is supported by the observation that apoptosis as well as other pathways related with cellular death, particularly neuronal death, appear dysregulated in arrays (Annex I, Supplementary Tab. 1 and 2) performed in brain materials from both CCALD and AMN. Moreover, VLCFAs toxicity has been reported in

fibroblasts isolated from X-ALD patients (Fourcade *et al.*, 2008), and astrocyte demise has been described in brain rat cultures (Hein *et al.*, 2008b). Here, we have examined cellular death in brain-derived astrocytes and neurons brain using TUNEL staining, an assay based on the detection of DNA fragmentation.

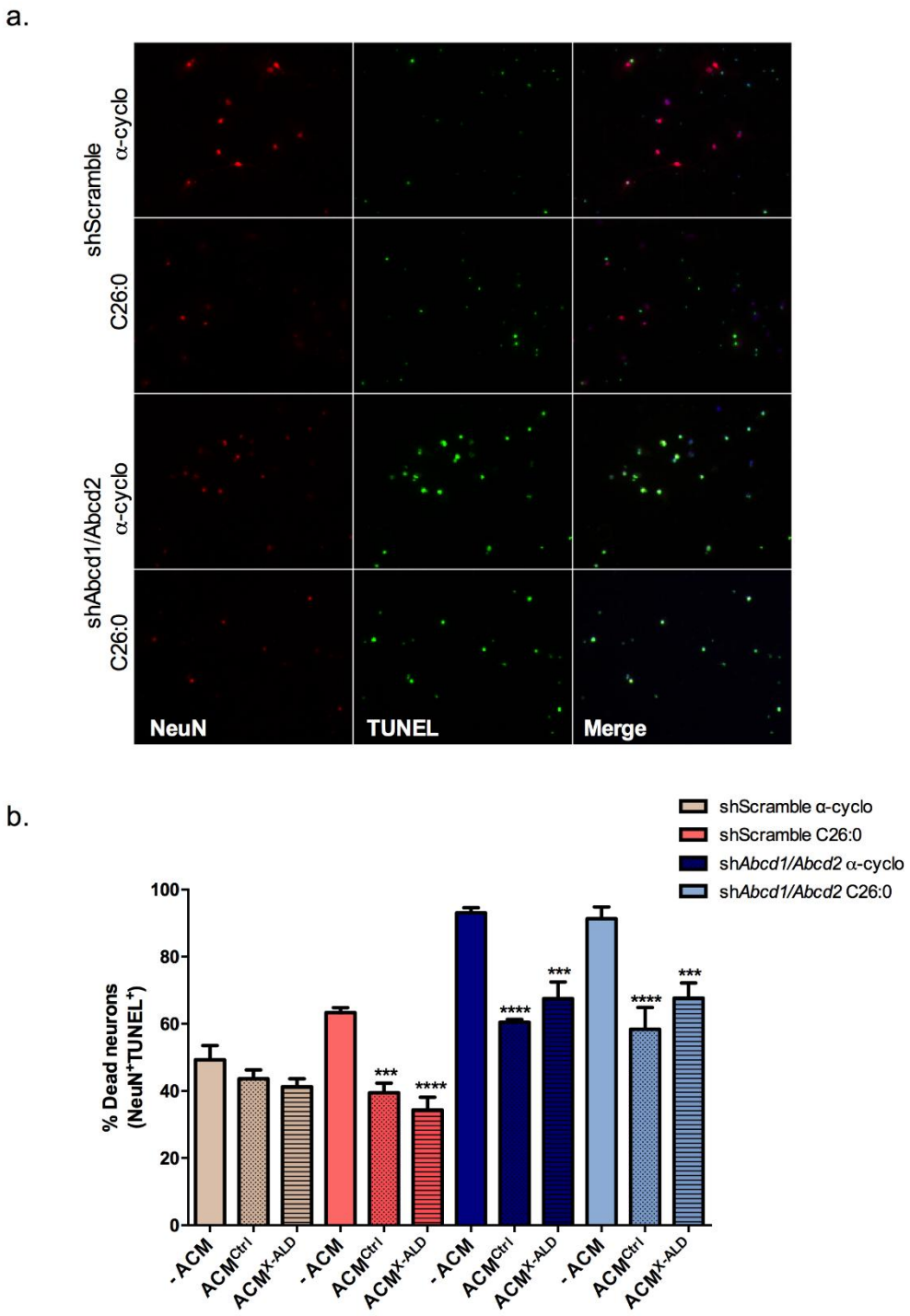

Figure 19. Assessment of death in X-ALD neurons. shScramble and sh*Abcd1/Abcd2* neurons were treated with α-cyclodextrin or C26:0. Neuronal media, control astrocyte conditioned media (ACM) (ACM^{Ctrl}) and ACM from X-ALD (ACM^{X-ALD}) were added to neurons. Neuronal nuclei (NeuN) was used to

stain neurons (red) and TUNEL assay to stain fragmented DNA (green). a. Representative images. b. Quantification of the percentage of dead neurons. A minimum of 300 cells for each experiment was analysed. Data are the mean ± SEM, n=3, and *p < 0.05 (Two-way ANOVA and post-hoc Tukey's multiple comparisons test).

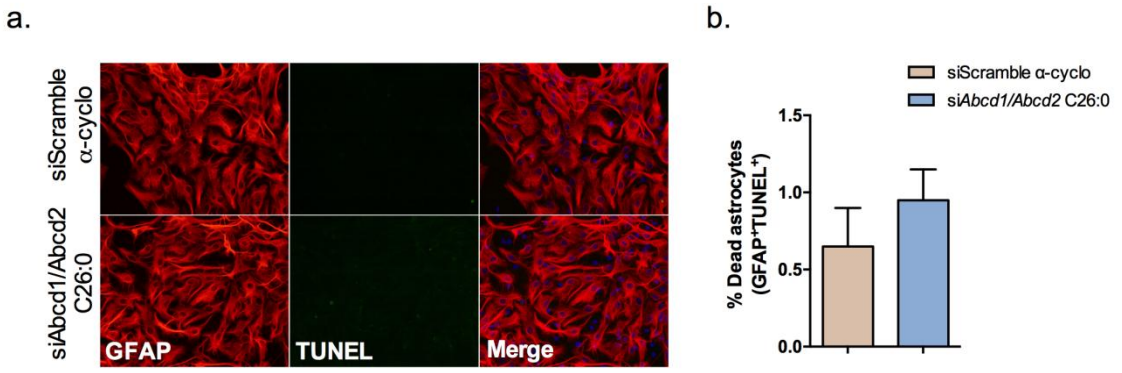

Figure 20. Assessment of death in X-ALD astrocytes. siScramble and si*Abcd1/Abcd2* astrocytes were treated with α-cyclodextrin or C26:0. Glial fibrillary acidic protein (GFAP) was used to stain astrocytes and TUNEL assay to stain fragmented DNA. a. Representative images. b. Quantification of the percentage of dead astrocytes. A minimum of 300 cells for each experiment was analysed. Data are the mean ± SEM, n=3, *p<0.05 (Unpaired T-test).

We have evaluated the viability of hippocampal X-ALD neurons under different scenarios: plus/minus C26:0 (timing in Fig. 18), and plus/minus ACM^{Ctrl} and $ACM^{X\text{-}ALD}$. The most relevant results are shown in Fig. 19 and Fig. 20.:

(i) Neuronal death was approximately 50% in control conditions, and there was a statistically significant increase up to 90% in X-ALD neurons in the absence of C26:0 or ACM (Fig. 19). That is, silencing the transporters *per se* causes neuronal demise. C26:0 slightly but non significantly potentiated cellular death in shScrambled neurons, and had no additional effect on silenced neurons (Fig. 19).

(ii) ACM was protective even if it derived from X-ALD astrocytes. Thus ACM^{Crtl} reduced from 60% to 40% the neuronal death caused by C26:0, 90 to 65% the death in silenced neurons (Fig. 19). The protective effect of $ACM^{X\text{-}ALD}$ was slightly lower than ACM^{Ctrl} in silenced neurons, but not statistically significant (Fig. 19). All in all, X-ALD astrocytes do not appear to be neurotoxic as shown for ALS astrocytes,

(iii) Astrocytes did not die, neither when the *Abcd* transporters were silenced nor when treated with C26:0 (Fig. 20), at variance with previous data (Hein *et al.*, 2008b).

Altogether, the data thus far suggest that neurons account for pathways related to cellular death found enriched in GSEA. Still, neuronal death in the most extreme conditions (silenced neurons plus ACM$^{X\text{-}ALD}$ plus C26:0) is enhanced at most 30% with respect to control conditions, neurons cultured in ACM$^{X\text{-}ALD}$ did not present such a big diference suggesting that detrimental pathway dysregulation other than death ought to exist affecting neuronal function.

3. Decreased spinogenesis and neurite thickness in X-ALD neurons

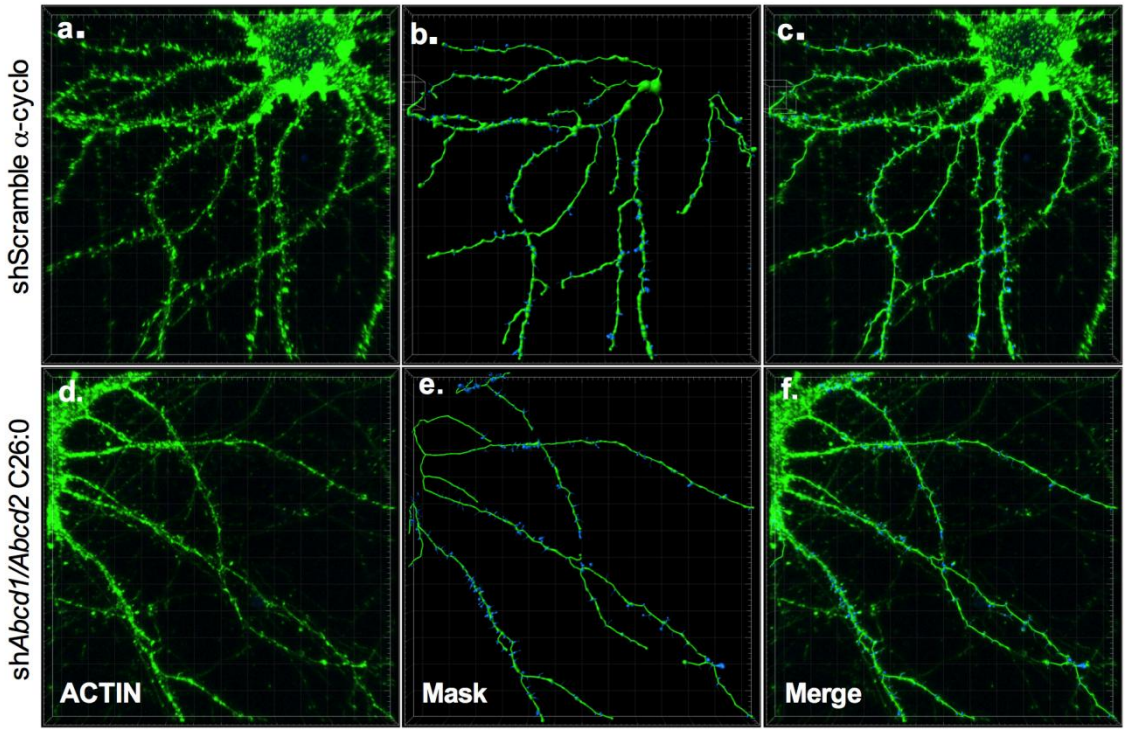

Figure 21. Defective spine formation in hippocampal X-ALD neurons. Representative confocal-microscope images of 14 DIV shScramble neurons treated with α-cyclodextrin (control neurons), and *shAbcd1/Abcd2 neurons* treated with C26:0 (X-ALD neurons). (a, d) Neurons labelled with ActinGreen™ 488. (b, e). Masks generated with the 'Filament tracer' and (c,d) 'Merge' applications (IMARIS software).

The molecular data presented in Chapter I suggested dysregulated synaptogenesis. To confirm this prediction, we performed a morphological analysis. Neurons were cultured at a low density, labelled with Actingreen™488 Ready Probes® Reagent, and images taken with a confocal microscope were analysed using the 'Filament tracer' software in the IMARIS software (Fig. 21). Furthermore, we studied the effect of silencing the transporters, with or without exacerbation of lipid accumulation by the addition of exogenous C26:0, as well as the effect of ACM$^{X\text{-}ALD}$ as compared to ACM^{ctrl}.

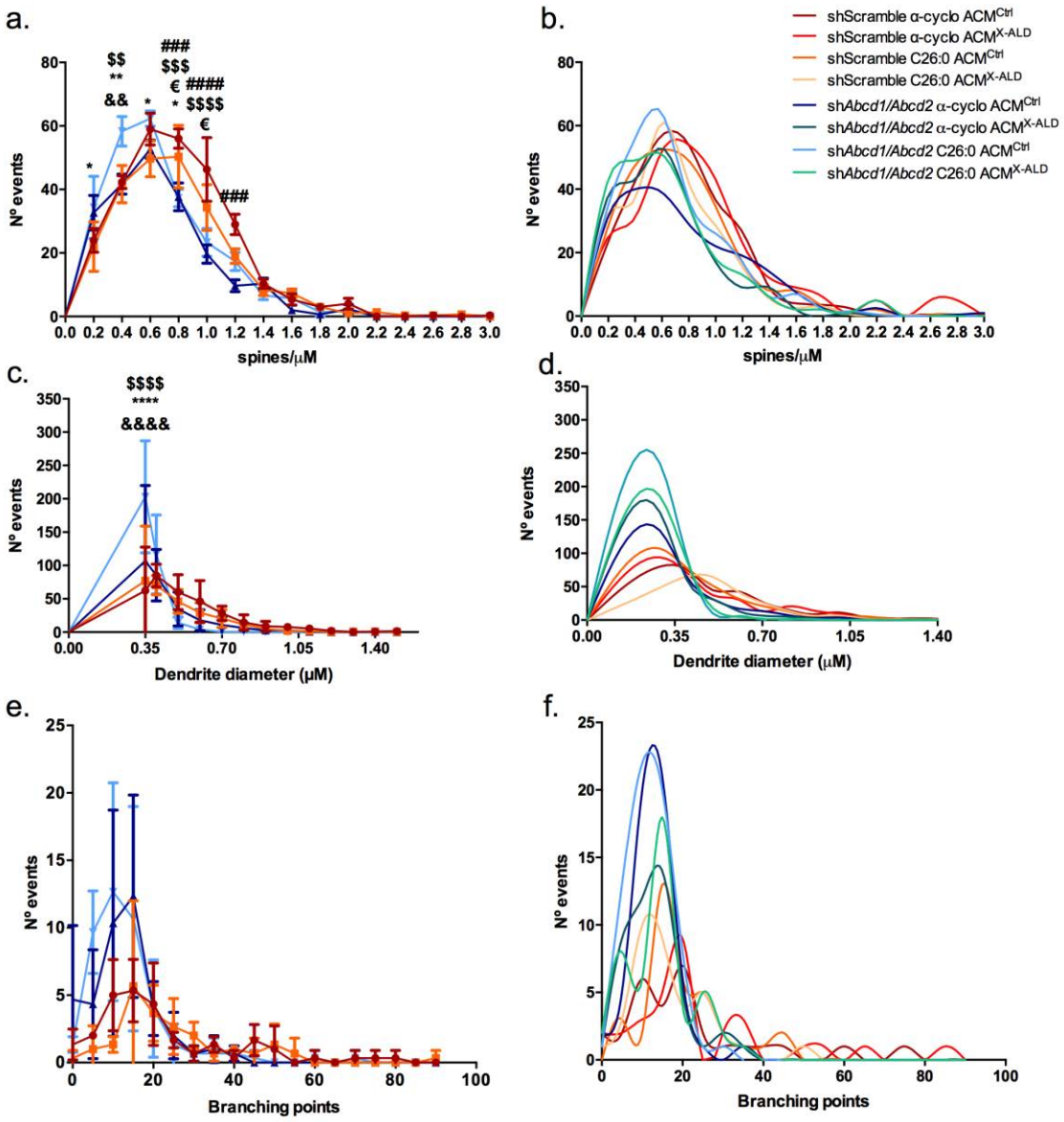

Figure 22. Quantification of spine and neurite formation in hippocampal X-ALD neurons. The analyses were performed using images of control (shScramble, red-based colours) and X-ALD neurons (sh*Abcd1/Abcd2,* blue-based colours) plus or minus C26:0/α-cyclodextrin (α-cyclo), stained with ActinGreen™ 488. (a) Spines per μM, (c) Dendrite diameter, (e) Neurite branching points. (a, c, e). Neurons grown in control astrocyte conditioned media (ACM^{Ctrl}). (b, d, and f) Smoothing of curves comparing neurons developed in ACM^{Ctrl} versus ACM^{X-ALD}. Data are the means ± SEM of n=3 independent experiments, each experiment s the mean of 15 neurons,*p<0.05, **p<0.01, *** p<0.001 and **** p<0.0001 (Two-way ANOVA and post-hoc Tukey's multiple comparisons test). Symbols: @ shScramble α-cyclo vs shScramble C26:0, # shScramble α-cyclo vs sh*Abcd1/Abcd2* α-cyclo, $ shScramble α-cyclo vs sh*Abcd1/Abcd2* C26:0, € shScramble C26:0 vs sh*Abcd1/Abcd2* α-cyclo, * shScramble C26:0 vs sh*Abcd1/Abcd2* C26:0, & sh*Abcd1/Abcd2* α-cyclo vs sh*Abcd1/Abcd2* C26:0).

The number of spines per micrometre (μM) was represented as the distribution of the total amount of events, considering an event the number of dendrites with this number of spines/μM (i.e. 20 dendrites with an average of 0 to 0.2 spines/μM are 20 events in the graph). In the X-axis we have 15 groups according to the interval of spines/μM (0.00 - 0.20, 0.21 - 0.40,

0.41 - 0.60, etc.). There are two spine densities: from 0.00 to 0.60 spines/μM, low spine density, and from 0.80 to 3.00 spines/μM, high spine density (Fig. 22 b.). The vast majority of the dendrites in our cells have around 0.6 spines/μM. There were three findings when comparing control and X-ALD conditions. First, silencing of *Abcd* transporters reduced the number of spines, as shown by the global displacement of density distributions to the left, and the detection of individual statistical significance differences between silence and not silenced neurons at several intervals. Second, C26:0 per se had no effect, but worsened spine loss at several intervals. Fig. 23 shows representative images of spine decreases. Third, $ACM^{X\text{-}ALD}$ had no statistically significant effect, but tended to.

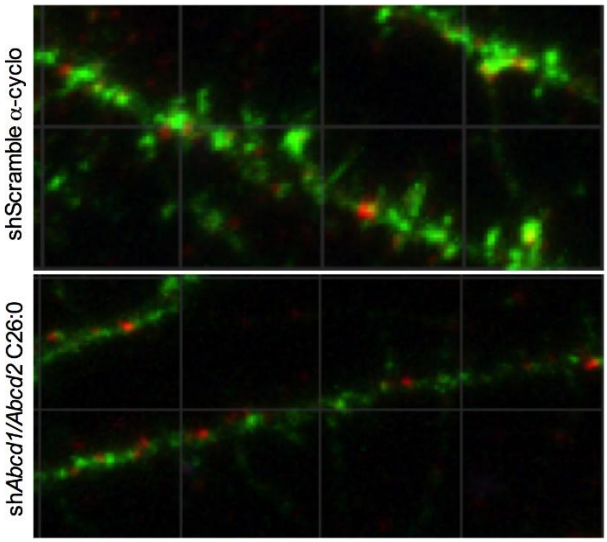

Figure 23. Magnification of hippocampal neurons neurites and spines. Representative confocal images of 14 days *in vitro* shScramble neurons treated with α-cyclodextrin, and *shAbcd1/Abcd2* neurons treated with C26:0. Neurons were labelled with ActinGreen™ 488.

Neurite diameter was assessed with the 'Filament mascara' of IMARIS software. The minimum diameter was fixed at 0.35 μM, the thinner neurite detected by the program. Neurite diameters of neurons shScramble α-cyclo vs sh*Abcd1/Abcd2* C26:0, shScramble C26:0 vs sh*Abcd1/Abcd2* C26:0, and sh*Abcd1/Abcd2* α-cyclo vs sh*Abcd1/Abcd2* C26:0 showed statistically significant differences at 0.35 μM, while the following measures keep up the same tendency. Thicker dendrites are found in the control conditions (in reds) and thinner dendrites in the X-ALD conditions (in blues) (Fig. 22c). Curve displacement to the right is showed by shScramble neurons indicating a larger neurite diameter (Fig. 22d); however no differences were observed due to ACM origin. At the minimum diameter, most of the neurites were from neurons with *Abcd1,* and *Abcd2* silenced. The combination of the silencing with the addition of VLCFA resulted in thinner neurites. As the diameter increases, the number of the events form controls increases, and only the control dendrites had the largest diameters represented (Fig. 22c).

In conclusion, X-ALD neurons developed fewer spines and thinner dendrites due to silencing of *Abcd1* and *Abcd2* without the need to add extra VLCFA, suggesting that depletion of transporters triggers a cell-autonomous impairment of spinogenesis and neuritogenesis. The phenomena is worsened by the administration of C26:0 in excess.

4. Poor arborization and reduced neurite length in X-ALD neurons

Analysis of the dendritic tree, including arborisation and neurite length, was performed in 10 images per condition using the Sholl technique whereby we quantified the number of intersections from the nucleus to the farthest neurite by tracing circles every single micrometre from the nucleus to the end of neurites (Fig. 24c).

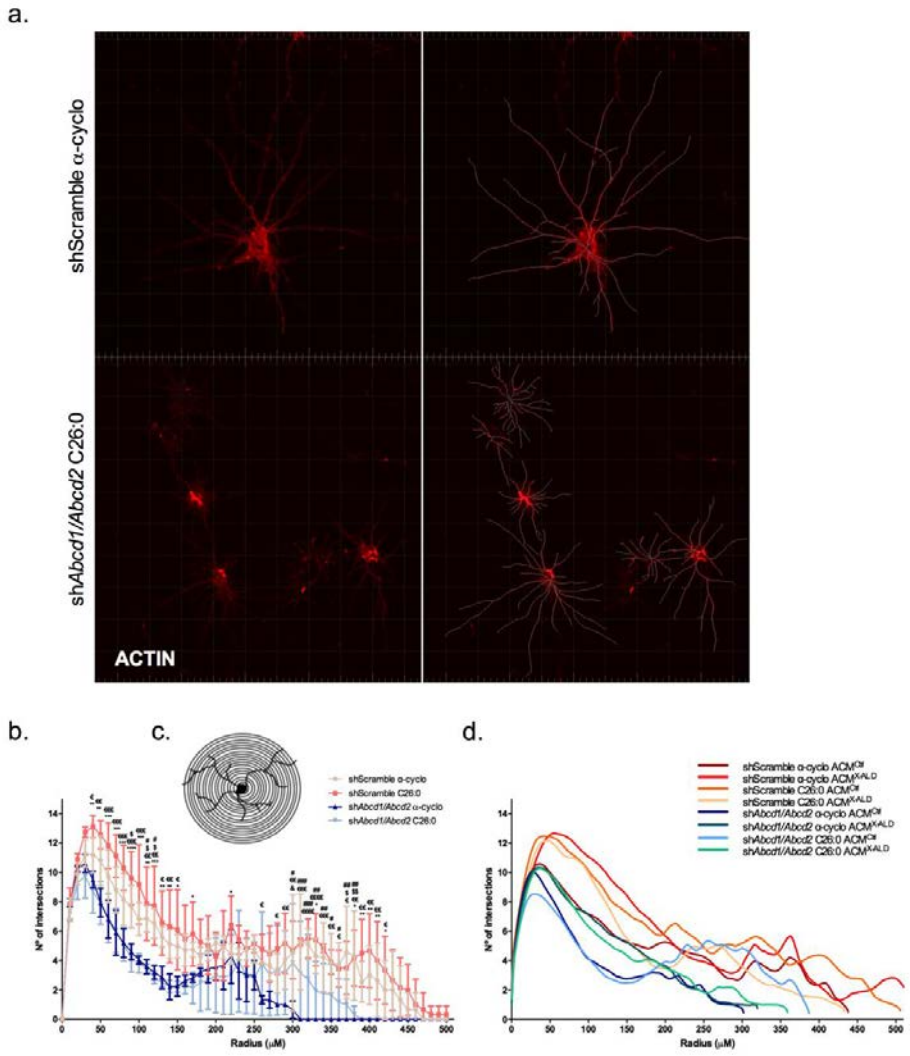

Figure 24. Representative images and quantification of neurons arborization. Images of neurons shScramble or sh*Abcd1/Abcd2* treated with α-cyclodextrin or C26:0 were collected. a. Representative confocal images and mask generated with filament tracer application of IMARIS software. b. Sholl quantification. Number of neurite intersections every each µM with concentrical circles from the nucleus quantified using filament tracer of IMARIS software. c. Representative image of concentrical

circles used for measurements. Data are the means ± SEM of n=3 independent experiments, each experiment s the mean of 15 neurons,*p<0.05, **p<0.01, *** p<0.001 and **** p<0.0001 (Two-way ANOVA and post-hoc Tukey's multiple comparisons test). Symbols: @ shScramble α-cyclo vs shScramble C26:0, # shScramble α-cyclo vs sh*Abcd1/Abcd2* α-cyclo, $ shScramble α-cyclo vs sh*Abcd1/Abcd2* C26:0, € shScramble C26:0 vs sh*Abcd1/Abcd2* α-cyclo, * shScramble C26:0 vs sh*Abcd1/Abcd2* C26:0, & sh*Abcd1/Abcd2* α-cyclo vs sh*Abcd1/Abcd2* C26:0).

Control conditions showed a higher complexity, having more intersections from the beginning and presenting longer neurites. Differences were specially marked between scrambled conditions and silenced conditions; that is, there is no need to add extra VLCFA to see the effect (Fig. 24).

Moreover, X-ALD neurons showed a lower number of neurite branching points. among the neurons analysed, we had more X-ALD neurons with 0 to 20 branching points per cell than control neurons. A similar number of neurons had from 20 to 40 branching points, less X-ALD neurons had from 40 up to 60 branching points, and almost any X-ALD neuron had from 60 to 90 (Fig. 22e).

These results indicate that X-ALD neurons have shorter and less complex neuritis, as neurite length is reduced, and they have less branching points.

5. Reduced axonal length in X-ALD

As synaptogenesis and axonogenesis are closely related processes, and we have observed differences in axonogenesis regulation in the transcriptomic data, we decided to examine axon length. Neurons were cultured at a low density for 5DIV to allow the complete traceability of axons. Experimental timings were adapted to the length of the experiment; silencing was done at the time of seeding and treatment were done at 2DIV. Axons were labelled with purified anti-neurofilament Marker (pan axonal cocktail) (SMI 312), and axons were traced using 'Filament tracer' of IMARIS software.

Axon length of neurons analysed spanned from 0.36 to 370.10 μM in controls and from 0.337 to 309.87μM in X-ALD neurons extreme conditions. The average was 49.55 and 34.10 μM, respectivel, with the axons being statistically significant shorter in X-ALD (Fig. 25c). Moreover, there is a greater number of long axons in controls, while only a few axons reached long lengths in X-ALD neurons (Fig. 25b).

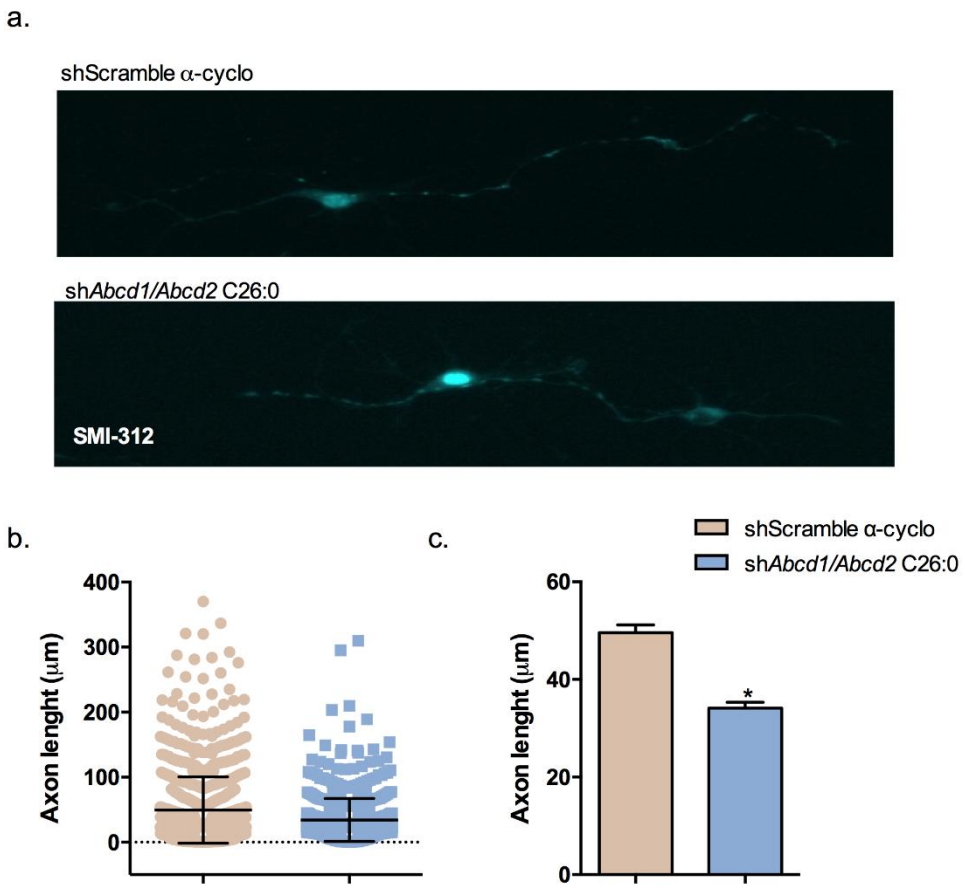

Figure 25. Representative images and quantification of axonal length. Images of neurons shScramble treated with α-cyclodextrin or sh*Abcd1/Abcd2treated with* C26:0 were collected. a. Representative confocal images. b. Individual measures of axon length (200-300 neurons per experiment). c. Axon length quantification using filament tracer of IMARIS software. Data are the mean ± SEM, n=3, *p<0.05 (Unpaired T-test).

Axonal growth is reduced due to *Abcd1* and *Abcd2* silencing and treatment with VLCFA such as C26:0.

6. Validation of differentially expressed genes of enriched pathways

Since the understanding of cellular compartmentalisation is critical to tailor therapies— there is no such thing as whole-brain specific pathways for drugs always act upon cell-specific pathways—we measured gene expression in astrocytes and neurons separately by qRT-PCR. We validated differentially-expressed genes (DEGs) of pathways directly-related with neuronal development; *Wnt2* (Sousa *et al.*, 2010), *Wnt6* (Schmidt *et al.*, 2007), *Notch3* (Lasky and Wu, 2005), *Shh* (Charytoniuk *et al.*, no date) and *Stat3* (Yan *et al.*, 2004a), and neurotrophic receptors (*Ntrk2* and *Ntrk3*) (Bartkowska, Paquin, Andrée S Gauthier, *et al.*, 2007). *Ephb2*(Katakowski *et al.*, 2005), because of its relevance in differentiation and the relation with mood disorders (Katakowski *et al.*, 2005; Dong, Wong and Licinio, 2009). *Syn* expression was

used as a widely-used marker of spine content (Ichikawa *et al.*, 1991). The p-values of the validated genes in the whole-brain of children and adults X-ALD arrays are represented in Table 4. Validations were performed in the extreme conditions: control (siScrambled+α-cylco) and X-ALD (silenced+C26:0).

Table 9. Expression of candidate genes.

Child X-ALD vs Child control					Adult x-ALD vs Adult control				
Gene	**logFC**	**P.Value**	**adj.P.Val**		**Gene**	**logFC**	**P.Value**	**adj.P.Val**	
WNT2	-0.323	0.024	0.178	*	WNT2	-0.149	0.067	0.185	
WNT6	-0.403	0.007	0.116	**	WNT6	-0.172	0.014	0.074	*
NOTCH3	-0.193	0.006	0.111	**	NOTCH3	-0.126	0.003	0.029	**
STAT3	0.717	0.000	0.038	***	STAT3	0.443	0.000	0.003	***
NTRK2	-0.210	0.049	0.243	*	NTRK2	0.931	0.011	0.063	*
EPHB2	-0.457	0.001	0.063	**	EPHB2	-0.204	0.001	0.014	**
SHH	-0.183	0.033	0.206	*	SHH	-0.069	0.157	0.313	
SYN1	0.023	0.955	0.981		SYN1	-0.204	0.405	0.570	
SYN2	-0.173	0.302	0.570		SYN2	-0.112	0.253	0.423	
SYN3	-0.153	0.161	0.421		SYN3	-0.080	0.209	0.375	

Comparative expression of selected genes related with astrocyte and neuron development and synaptogenesis in X-ALD children and x-ALD adults versus controls. *p-value <0.05, **p-value <0.01, and ***p-value <0.001.

The most relevant results are: in neurons, genes directly related to development such as WNT and NOTCH3 are downregulated, the effect of conditioned media from X-ALD astrocytes on neuronal gene expression is the downregulation of neurotrophic factors. Moreover, SYN expression is downregulated in X-ALD and this downregulation is exacerbated by the presence of $ACM^{X\text{-}ALD}$ indicating that synapse formation could be altered.

The expression of *Syn*, *Wnt2* and *Wnt6* is especially diminished in X-ALD neurons and astrocytes (Fig. 26). *Wnt2* neurons exposed to $ACM^{X\text{-}ALD}$ presented a lower diminution of *Wnt2* mRNA levels; while, *Wnt6* was not affected by the presence of ACM. *Notch3* expression was also diminished in neurons but only in the presence of $ACM^{X\text{-}ALD}$.

Stat3 expression was lower in neurons but not statistically significant, and the same happened with *Notch3* in astrocytes. *Shh* expression was variable between experiments but not different from controls (Fig. 26). A higher sample will be required to further confirm these results.

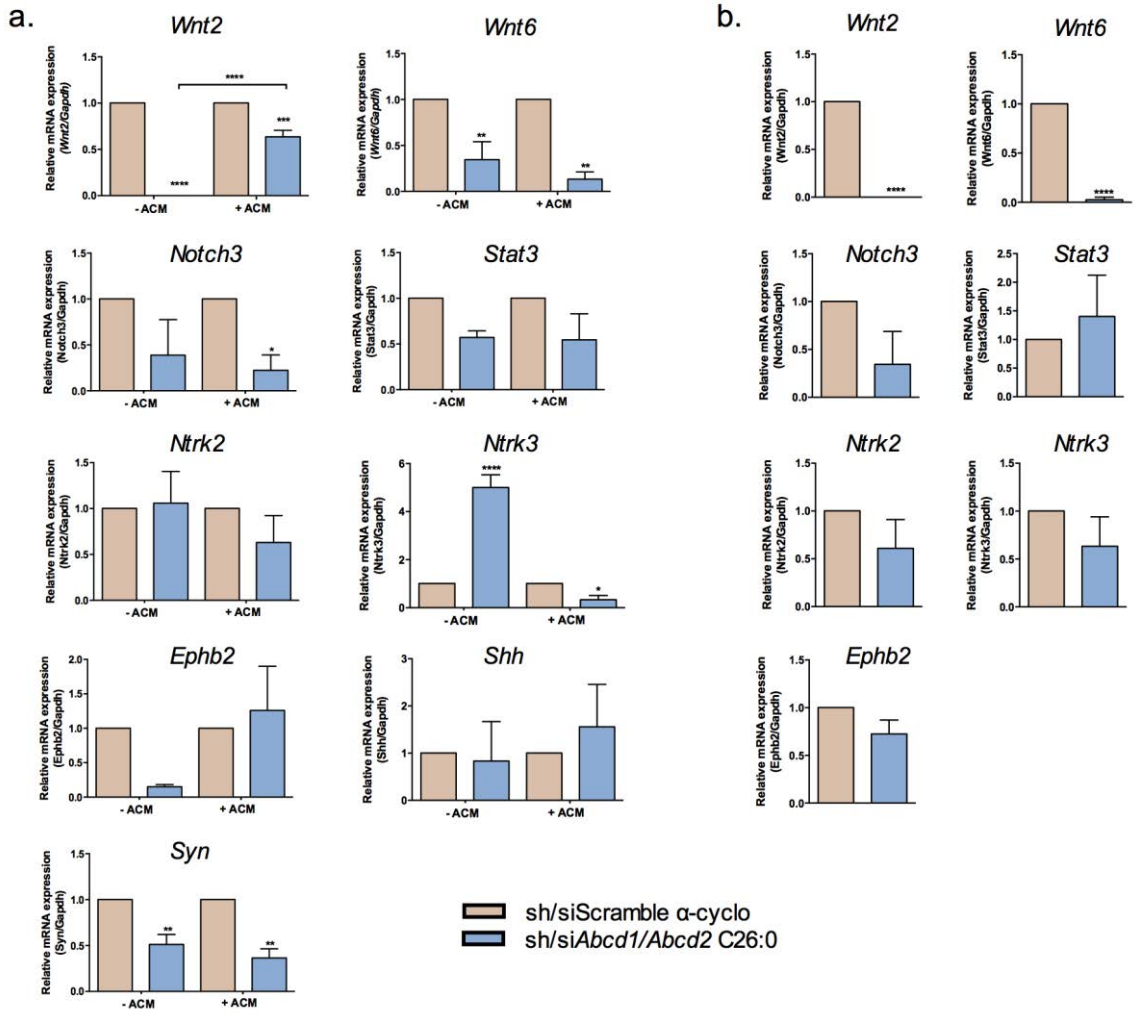

Figure 26. *Gene* expression validation in X-ALD neurons and astrocytes. Quantification of mRNA expression of *Wnt2, Wnt6, Notch3, Stat3, Ntrk2, Ntrk3, Ephb2, Shh and Syn* normalised to *Gapdh* expression. siScramble neurons and astrocytes treated with α-cyclodextrin or *Abcd1*$^{-}$ *and Abcd2*$^{-}$ *treated with* C26:0. a. Expression in neurons with and without astrocyte conditioned media (ACM). b. Expression in astrocytes. Data are the mean ± SEM, n=3, *p<0.05, **p<0.01, *** p<0.001 and **** p<0.0001 (Unpaired T-test).

While *Ntrk2* levels are stable between conditions, *Ntrk3* expression is diminished in X-ALD neurons in the presence of ACM$^{X\text{-}ALD}$ and increased with ACMctrl?. However, the expression of *Ntrk3* in astrocytes is similar between X-ALD and control. Contrarily, *Ephb2* levels are increased

in X-ALD neurons in the presence of ACM$^{X\text{-}ALD}$ and diminished in the absence of ACM$^{X\text{-}ALD}$, while astrocytic levels are similar to controls (Fig. 26).

In brief, *Wnt2* and *Wnt6* expressions are diminished in both *Abcd*$^{-}$ neurons and astrocytes. *Wnt6 and Notch3* expression are lower in X-ALD neurons in the presence of ACM $^{X\text{-}ALD}$, and *Ntrk3* and *Eph2* levels are modulated upon ACM presence. ACM $^{X\text{-}ALD}$ reduces the expression o these genes while ACM ^{Ctrl} increases them (Fig. 26).

7. *Gsk3* inhibition partially restores *Syn* expression in X-ALD neurons

WNT secreted proteins are highly important factors for synapse formation and maintenance. Since *Wnt-related* pathways are deregulated in human child X-ALD arrays, and *the expression of* Wnt-related proteins such as WNT6 and WNT2 is reduced in neurons upon deletion of abcd transporters, we reason that the therapeutic rescue of *Wnt* pathway signalling could improve some of the neuron-autonomous neurodevelopmental alterations observed. In the absence of *Wnt* ligands, we aimed to potentiate Wnt pathways by inhibiting Glycogen synthase kinase 3 (GSK-3), since GSK-3 negatively regulates the canonical *Wnt* signalling by phosphorylating β-catenin, thereby promoting its proteasome-dependent degradation (Wu and Pan, 2010). Thus, the inhibition of GSK-3 results in β-catenin stabilisation and transfer to the nucleus to activate transcription (Huang *et al.*, 2017). Here, we used a GSK-3 inhibitor (SB216763) as a constitutive activator of the *Wnt* pathway. For simplicity, the experiments were carried out with the extreme *in vitro* conditions: shScrambled neurons plus α-cyclodextrin and *Abcd* silenced neurons plus C26:0. 5µM GSK-3 inhibitor was administered at time 0 and re-administered every 24h, and mRNA was obtained after 96h. *Syn* expression was used as the readout of synaptogenesis. SB216763 partially rescued *Syn* expression in *Abcd*$^{-}$ neurons and increased *Syn* levels in control neurons (Fig. 27).

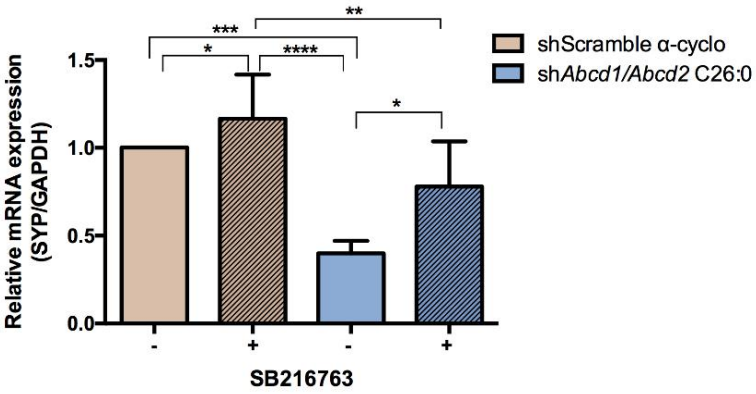

Figure 27. Synaptophysin *mRNA* expression in X-ALD neurons upon GSK-3 inhibition. Synaptophysin (*Syn*) expression in shScramble neurons treated with α-cyclodextrin and in sh*Abcd1/Abcd2* neurons *treated with* C26:0 and normalised to *Gapdh* expression. Neurons were

treated (+) or not (–) with 5 µM SB216763, an inhibitor of GSK-3, every 24h. Data are the means ± SEM, n=3, *p<0.05, **p<0.01, *** p<0.001 and **** p<0.0001 (One-way ANOVA and post-hoc Tukey's multiple comparisons test).

8. Changes in cholesterol production, localisation and transport in X-ALD astrocytes

Since it is well demonstrated that factors secreted by astrocytes regulate spinogenesis ((Allen and Eroglu, 2017), and our data showed that *Syn, Wnt6 and Ntrk3* expression are reduced in the presence of ACM$^{X\text{-}ALD}$, we looked at GSEA analysis to find possible candidates to modulate these genes and the resultant neuritogenesis and spinogenesis. As described in Chapter I, factors such as *SREBP2* were decreased in X-ALD chidren brain transcriptomes.

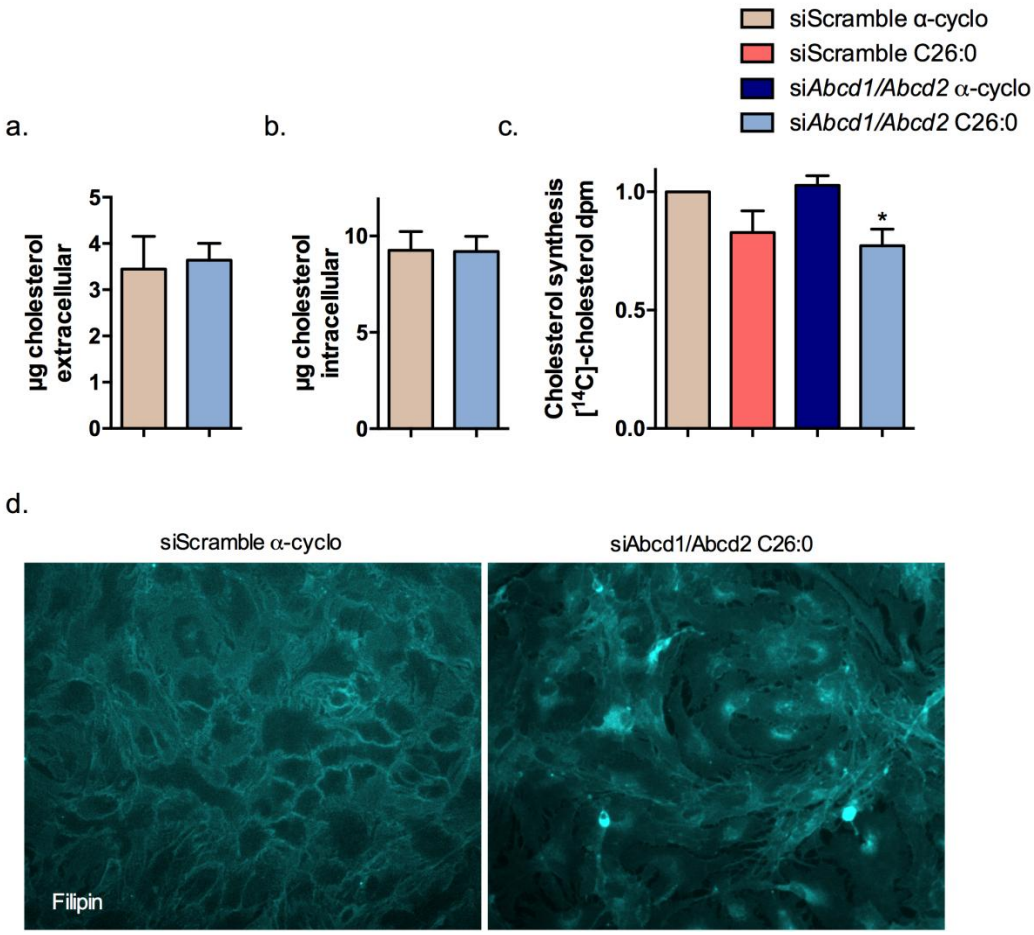

Figure 28. Cholesterol production and localisation in astrocytes. siScramble and si*Abcd1/*Abcd2 astrocytes treated with α-cyclodextrin or C26:0 were studied. (a) and (b) Intracellular and extracellular cholesterol was quantified using thin-layer chromatography. (c) Cholesterol synthesis was measured by the conversion of the 14-C-acetate precursor in cholesterol. (d). Representative images of cholesterol distribution stained with Filipin dye. Data are the means ± SEM, n=3 and *p<0.05. (Unpaired T-test or One-way ANOVA and post-hoc Tukey's multiple comparisons test).

Moreover, cholesterol metabolism and transport appeared as part one of the top enriched categories in whole-brain enrichment analysis. As astrocyte-derived cholesterol is crucial for synaptic formation and maintenance (Pfrieger and Ungerer, 2011), we determined whether X-ALD conditions altered cholesterol metabolism and transport in astrocytes. Analysis ofa biguer number of samples is pending to undubtely confirm this result.

First, we looked at cholesterol production using ^{14}C-acetate, the precursor of cholesterol synthesis; we measured the amount of labelled cholesterol after 48h of treatment with C26:0. X-ALD astrocytes in the presence of C26:0 produced 20 % less cholesterol than controls. Neither the silencing of the transporters nor the presence of C26:0 in excess resulted in decreased production of cholesterol (Fig. 28d).

Second, we examined intracellular and extracellular cholesterol by extracting and separating cholesterol with thin-layer chromatography. (Fig 28a and b). None of the conditions presented differences over control. By contrast, cholesterol localisation in these astrocytes measured with Filipin staining showed a different distribution inside the cell (Fig. 28d). While control astrocytes showed more pronounced staining in the plasmatic membrane and diffuse staining inside the cell, X-ALD astrocytes showed a higher amount of perinuclear cholesterol and reduced staining in the plasma membrane. Although, this different distribution pattern in X-ALD cultures appears in some clusters of cells, even in the same well while other cells looked like controls (Fig. 28d).

Finally, we measured astrocyte-secreted cholesterol in ACM. Measurements were done using a fluorimetric commercial kit. Notwithstanding synthesis, localisation and gene expression pointed to a decreased secretion, measurements in collected media were similar in all samples (Fig. 29), suggesting that cholesterol secretion was not impaired in X-ALD astrocytes.

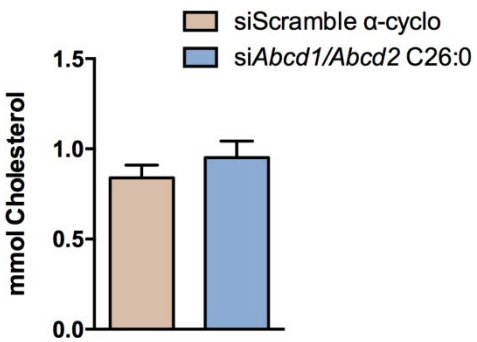

Figure 29. Cholesterol secretion in astrocytes. siScramble and si*Abcd1/Abcd2 astrocytes treated* with α-cyclodextrin or C26:0 were studied. Cholesterol secreted to media during 48h was quantified using a fluorimetric kit. Data are the means ± SEM, n=3 and (One-way ANOVA and post-hoc Tukey's multiple comparisons test).

Chapter III: Impairment of energy metabolism and excitability in X-ALD astrocytes

Results obtained with the GSEA, as well as previous studies(Schlüter, Espinosa, Fourcade, Galino, Lśpez, *et al.*, 2012), support the existence of global metabolic impairment the brains of patients with ALD cells. Protein metabolism, lipid metabolism and transport, energy production and ion transport are top hits in the array analysis. Likewise, calcium signalling and synaptic transmission are dysregulated in X-ALD according to the GSEA; Astrocyte exitability, metabolism and storage of fatty acids, oxidative stress and antioxidant defense, and endoplasmic reticulum stress are enriched biological processes in X-ALD transcriptomic data (Annex I, Supplementary Tab. 2). However cellular compartmentalisation of these phenomena remains unclear. In this section we sought to determine if processes dysregulated in X-ALD arise, in part, from astrocytes.

1. Mitochondrial fatty-acid oxidation impairment in X-ALD astrocytes

We have recently shown that fatty acid β-oxidation (FAO) coexists with glycolysis in astrocytes (Eraso-Pichot *et al.*, 2018). As X-ALD is a condition with lipid dyshomeostasis and *regulation of fatty acid metabolic process* GO is enriched in the GSEA analysis, we reasoned that astrocytic FAO may be disturbed.

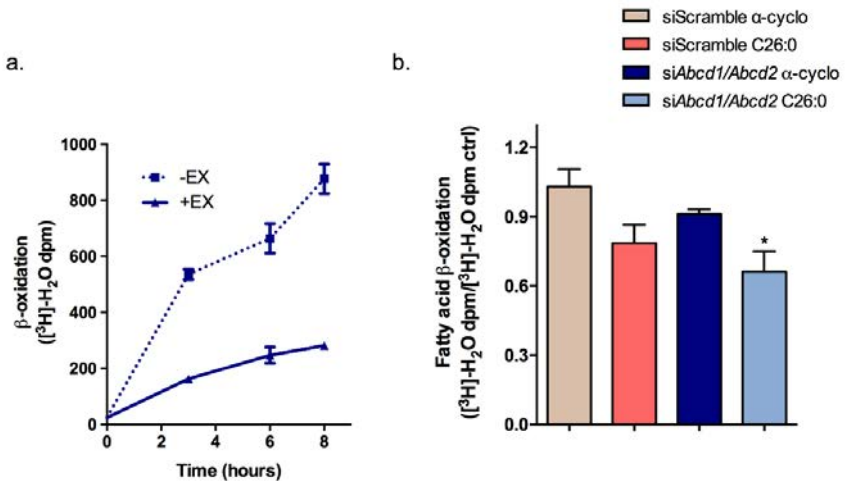

Figure 30. Fatty acid β-oxidation in cortical astrocytes. a) Time course of fatty acid β-oxidation (FAO) in *wild type* astrocytes after addition of ^{3}H-palmitate in the presence and absence of glucose (adapted from Eraso-Pichot et al., 2017). b) FAO in X-ALD-like conditions (e.g., exposure to excess of C26:0 and/or decreased activity of *Abcd* transporters caused by genetic silencing) 8h after ^{3}H-palmitate addition in the absence of glucose. Significance to control condition, siScramble α-cyclo. Data are the mean ± SEM, n=3, and *p < 0.05 (Two-way ANOVA and post-hoc Tukey's multiple comparisons test).

Hence, in previous studies in our lab FAO was measured in rat cortical astrocytes. After 96h of treatment with C26:0, in a medium without glucose to enhance FAO, we labelled astrocytes

with [^{3}H]palmitic acid and used etomoxir (ETX), an inhibitor of FAO, as a negative control. The production of [^{3}H]H_2O from [^{3}H]palmitic acid β-oxidation was the readout quantified. FAO is detected at 3, 6 and 8h after the addition of [^{3}H]palmitic acid, the greatest difference being observed at 8h (Eraso-Pichot, Braso-Vives, Golbano *et al.*, 2018). For this reason, we chose to measure FAO in X-ALD-like conditions at 8h. The amount of [^{3}H]H_2O was statistically significant lower in astrocytes when the silencing of both transporters was combined with the addition of C26:0, as compared to control astrocytes (shScrambled plus vehicle). Although there is no statistically significant difference between silenced condition without adition of C26:0 and scramble condition with C26:0 compared with the control, we can observe that, in both cases, the addition of C26:0 to the scramble condition there is a small reduction in FAO (adjust p-val 0.15). The results suggest that mitochondrial FAO in astrocytes is impaired in X-ALD as a consequence of VLCFA accumulation, and further reduced when *Abcd* transporters are silenced.

2. Reduced ATP production in X-ALD astrocytes

To determine if the dysregulation in energy metabolism in X-ALD astrocytes has functional consequences, we studied mitochondrial adenosine-5'-triphosphate (ATP) production. ETX was used to determine ATP production as a result of reactions other than mitochondrial FAO (e.g., glycolysis and aminoacids' catabolism). ATP measurements were performed in the presence and absence of glucose should the possible decrease in ATP due to decreased mitochondrial FAO be compensated by increased glycolysis.

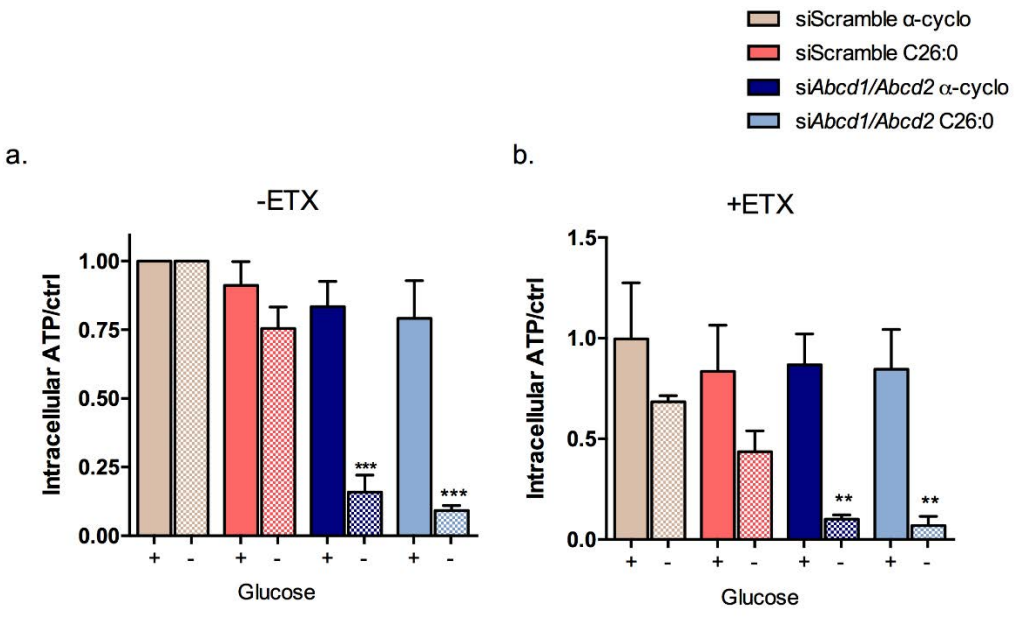

Figure 31. ATP content in X-ALD astrocytes. a) Determination of ATP production in the presence or absence of glucose, and b) after inhibition of fatty acid β-oxidation (+ etomoxir (ETX)) in control astrocytes and when C26:0 is accumulated. Data are the means ± SEM, n=3, and (*) $p < 0.05$ (significance compared to control) (Two-way ANOVA and post-hoc Tukey's multiple comparisons test).

The main result was that, although there is a trend of reduced content of ATP upon addition of C26:0 and/or the silencing of *Abcd* transporters, the production of ATP is dramatically reduced in silenced astrocytes only in the absence of glucose, both in the presence or absence of ETX (Fig. 31). The data suggest that impaired FAO is compensated by increased glycolysis in X-ALD astrocytes, that is, X-ALD astrocytes show reprogramming of energy metabolism, which may explain by they survive.

3. Imbalance of NAD/NADH contents in X-ALD astrocytes

Mitochondria are the main responsible for energy metabolism in cells. Within mitochondria occur several metabolic pathways, citric acid cycle and oxidative phosphorylation being responsible for the final production of ATP. Intermediate substrates generated in citric acid cycle such as NADH, which provide reducing equivalents to the electron transport chain, are decreased in spinal cords of *Abcd1*$^{-/-}$ mice (Galino *et al.*, 2011b), suggesting that the brain could be affected as well. For this reason, we analysed NADH in X-ALD astrocytes.

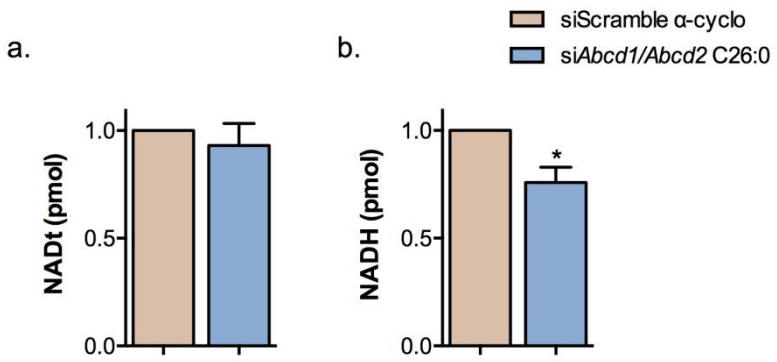

Figure 32. Total NAD and NADH quantification in X-ALD astrocytes. Total amount of NAD and NADH measured in siScramble astrocytes treated with α-cyclodextrin and si*Abcd1/Abcd2* astrocytes treated with C26:0 using a quantification kit. a) Total intracellular NAD. b) Intracellular NADH. Data are the mean ± SEM, n=3 and *$p<0.05$ (Unpaired T-test).

NAD^+ and NADH were measured in astrocytes after silencing of *Abcd1* and *Abcd2* and C26:0 treatment. Although the total levels of NAD were similar in X-ALD astrocytes compared with controls (Fig. 32a), the ratio NAD^+/NADH was different in a statistically significant fashion, NADH being lower in X-ALD conditions (Fig. 32b).

4. Slight changes in lipid droplets size in X-ALD astrocytes

Since lipid droplets are the main substrates for FAO and possible storage for extra fatty acids, and because we observed a reduction in FAO and ATP production in astrocytes, we examined if lipid-droplet accumulation was altered in X-ALD astrocytes. Lipid droplets were revealed with Nile red, a dye that binds to most lipids. Lipid droplets were quantified using the 'Cell counter' plugin in image G, and the counts were normalized to the number of cells. The number of lipid droplets was not changed in X-ALD astrocytes as compared to controls, but the size of each lipid droplet appeared to be increased, suggesting increased lipid content (Fig. 33)

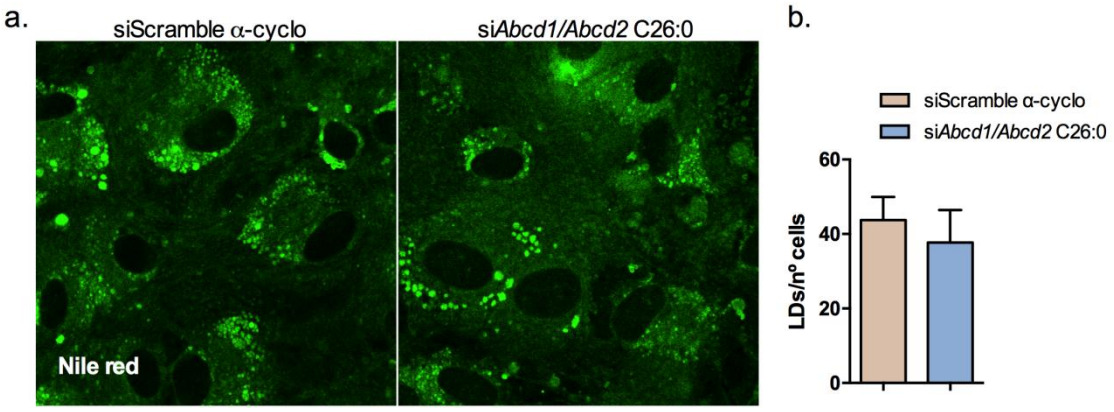

Figure 33. Lipid droplets in X-ALD astrocytes. Lipid droplets in siScramble astrocytes treated with α-cyclodextrin and si*Abcd1/Abcd2* astrocytes treated with C26:0 stained with Nile Red a) Representative images. b) Total number of lipid droplets. c) Percentage of small and big lipid droplets. Data are the mean ± SEM, n=3 and *p<0.05 (Unpaired T-test).

5. Reduced GSH production in X-ALD astrocytes

Energy homeostasis and oxidative stress are intertwined (Schlüter, Espinosa, Fourcade, Galino, López, *et al.*, 2012) such that bioenergetics failure in X-ALD is critically associated with oxidative stress, as seen in fibroblasts, lymphocytes and plasma of X-ALD patients (Vargas *et al.*, 2004; Petrillo *et al.*, 2013), as well as in astrocytes from the mouse model of X-ALD (Kruska *et al.*, 2015a). Here, oxidative stress was measured in astrocytes using the permeant non-fluorescent reagent 2',7' –dichlorofluorescin diacetate (DCFDA), which is oxidated by ROS to 2', 7' –dichlorofluorescein (DCF) to become fluorescent. It measures peroxyl, hydroxyl and other ROS within the cell. *Abcd1* and *Abcd2* were silenced and astrocytes were treated for 96h with C26:0, cells were collected and stained for 30 min at 37°C before flow cytometry assay. Exposure to 50 µM of Tert-Butyl Hydrogen Peroxide (TBHP), an organic peroxide that induces

oxidative stress, was used as a control. Surprisingly, we did not detect ROS or other superoxide species in X-ALD astrocytes using the DCFDA approach (Fig. 34).

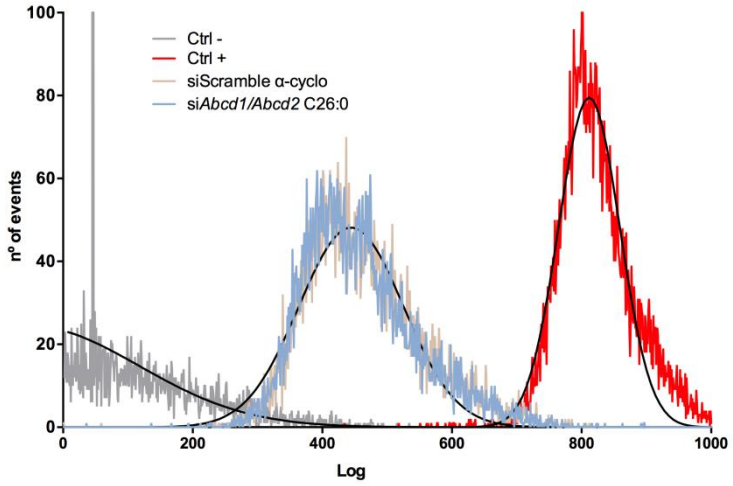

Figure 34. ROS/Superoxide production in X-ALD astrocytes. Representative quantification of DCF fluorescence intensity measured by flow cytometry assay in SiScramble astrocytes treated with α-cyclodextrin and si*Abcd1/Abcd2* astrocytes treated with C26:0. A total of 10000 events were measured for each sample and represented in the graph according to their fluorescence. 50µ M tert-butyl hydrogen peroxide (TBHP) was used as a positive control and cells without staining as a negative control.

Although X-ALD astrocytes seem to have similar levels of ROS compared to control at the time point studied, antioxidant defence could be compromised. Glutathione peroxidases (GSH-Pxs) play an important role in antioxidant defence. The ratio between the reduced and oxidized glutathione (GSH/GSSG) is indicative of the redox status of the cell as GSH-Pxs use GSH as a co-substrate. Because antioxidant molecules secreted by astrocytes such as glutathione (Wang and Cynader, 2000) are decreased in neurodegenerative diseases such as Alzheimer's disease (Markesbery, 1999; Ballatori *et al.*, 2009), and since total and reduced GSH was found decreased in lymphocytes of patients (Petrillo *et al.*, 2013), we studied glutathione production in X-ALD astrocytes.

A colorimetric compound, 5,5'-dithiobis (2-nitrobenzoic acid) (DTNB), was used to measure total GSH and GSSG, after degradation of GSH. GSH and GSSG levels were lower in silenced astrocytes (Fig. 35 a and b). The total amounts of both ghs and GSSG were reduced (Fig. 35c), such that GSH/GSSG ratios were similar between conditions (Fig. 35d).

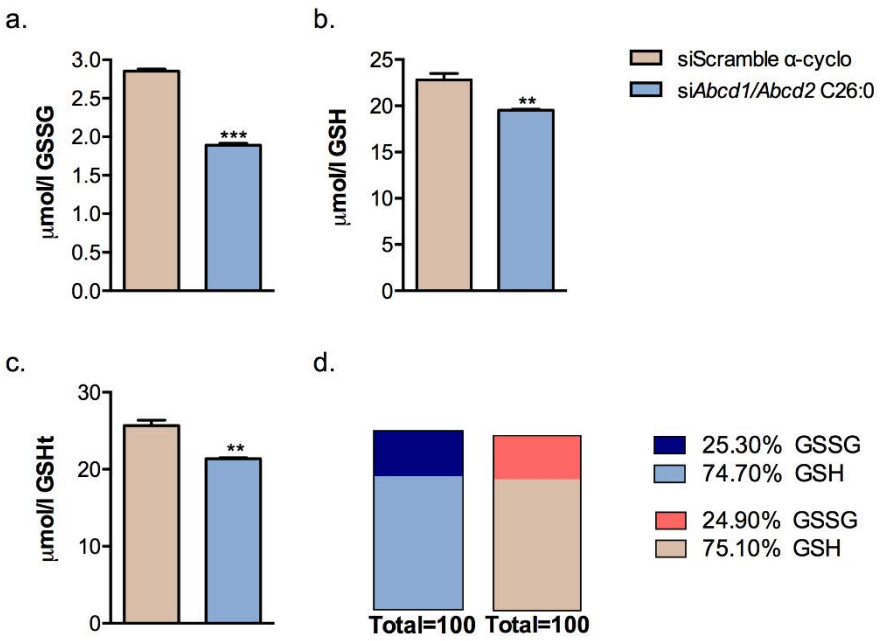

Figure 35. Total GSH and GSH/GSSH ratio measurement in X-ALD astrocytes. Total amount of GSSG, and GSH were measured in SiScramble astrocytes treated with α-cyclodextrin and si*Abcd1/Abcd2* astrocytes treated with C26:0, using a quantification colorimetric kit (Sigma-Aldrich 38185). a) Intracellular oxidized form GSSG b). Intracellular reduced form GSH c) Total intracellular GSH d). GSH/GSSG ratio. Data are the means ± SEM, n=3, **p<0.01 and ***p<0.001 (Unpaired T-test).

6. VLCFAs accumulation decreases purinergic-induced calcium responses in astrocytes

Given the physiological relevance of calcium fluxes in astrocytes (Bazargani and Attwell, 2016), we examined whether the amplitude or duration of calcium transients are altered in X-ALD astrocytes. We measured intracellular calcium concentration and recovery after ATP stimulation using FURA 2-AM, a cell-permeable ratiometric fluorescent indicator that is excited at 340 nm of light when free, and excited at 380 nm of light when bound to intracellular calcium.

Other authors have shown that acute application of VLCFA such as C26:0 potentiates intracellular calcium transients, reaching maximal intracellular calcium levels higher than controls, with non-synchronous and irregular calcium concentration increases (Hein *et al.*, 2008b). In our hands, astrocytes challenged with C26:0 had high variability in responses, ranging from no response in most of the cells, to small irregular responses in a few responding astrocytes. Due to the lack of consistency in acute responses, and the lack of relevance of

acute exposure to C26:0, since VLCFA accumulation is chronic, these data were not analysed. Rather, we focused on chronic exposure to C26:0.

Silenced X-ALD astrocytes exposed to C26:0 during 96 hours showed diminished ATP-induced peak calcium responses, as compared to non treated X-ALD astrocytes, and to control siScrambled astrcocytes (Fig. 36 a and b). The cells also showed aberrant recovery of basal calcium levels, having a lower peak followed by a progressive increase of intracellular calcium, and a slower mobilisation of cytoplasmic calcium (Fig. 36 a and b).

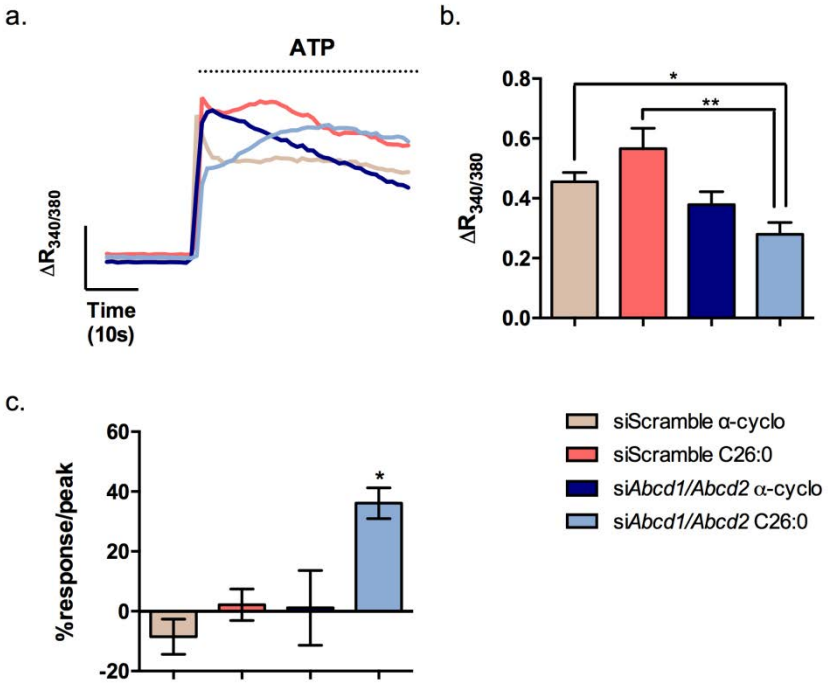

Figure 36. X-ALD astrocyte excitability. siScramble and si*Abcd1/Abcd2* astrocytes were treated with α-cyclodextrin or C26:0 and labelled with FURA2-AM, a ratiometric calcium dye. a) Single cell traces, b) quantification of neurotransmitter-induced calcium responses (peak), and c) quantification of % response/peak after 20 seconds of stimulation (significance to siScramble α–cyclo) and c). Calcium responses to ATP 100µM were monitored, and 50 cells for each experiment were analyzed. One-way ANOVA were used in all sections (n=3, mean ± SEM, *p<0.05, **p<0.01).

7. Increased endoplasmic-reticulum stress in X-ALD astrocytes

The interplay between organelles inside the cell is crucial for the normal cell function. Every organelle plays a particular role that when altered, starts a cascade of events disturbing cellular homeostasis. In the case of X-ALD, peroxisomal malfunction and the subsequent VLCFA accumulation exerts a negative effect on the performance of other organelles (Schrader, Kamoshita and Islinger, 2019). Further, concomitant oxidative stress and ER stress has been observed in fibroblasts from patients (van de Beek *et al.*, 2017). However, neither ER stress nor oxidative stress has been evaluated in brain cells individually—indeed it is assumed that ER and oxidative stresses are always neuronal. Since we found signs of oxidative stress in X-ALD astrocytes such as decreased content of GSH and reducing equivalents, we reasoned that ER may be altered, too.

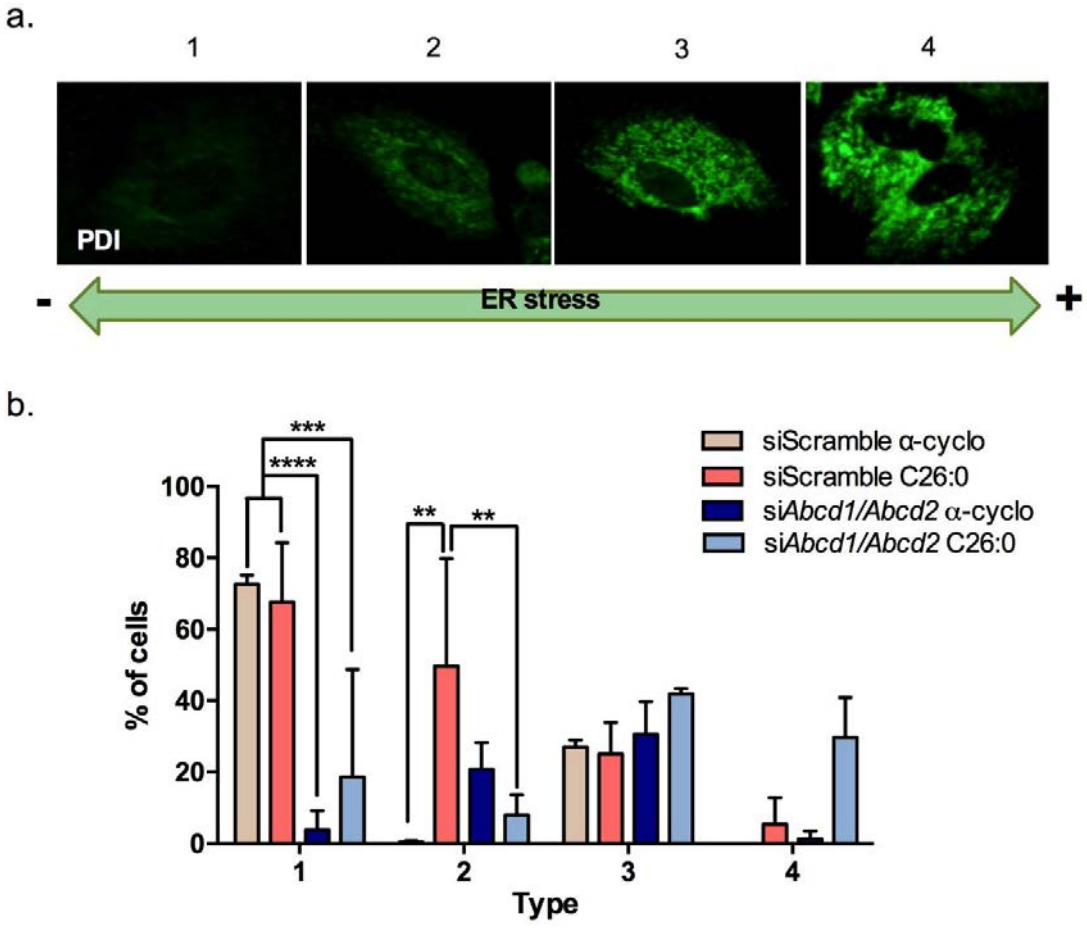

Figure 37. Protein disulfide isomerase (PDI) distribution as a marker of ER stress in X-ALD astrocytes. a) Classification of PDI differential staining pattern; type 1) low staining, type 2) medium intensity staining, type 3) dotty staining and type 4) clumpy staining (ER stress-associated pattern). b) Percentage of cells presenting different expression patterns of PDI. Data are the means ± SEM, n=3, and *$p < 0.05$ (One-way ANOVA and post-hoc Tukey's multiple comparisons test).

We assessed ER stress in astrocytes by measuring the expression of PDI by immunohistochemistry. PDI expression and localization changes in ER stress (Grek and Townsend, 2013). According to the intensity and distribution of PD staining, we classified cells in 4 different groups: no staining, low staining, punctuated staining, and clumpy staining. While control cells have a statistically significant higher amount of type 1 and 2 cells, the percentage of X-ALD astrocytes is higher in groups 3 and 4, indicating ER stress (Fig. 37).

DISCUSSION

The study of human brain transcriptomes to test the hypothesis of abnormal brain circuits formation in X-ALD and performance of morphological and biochemical analysis of the data obtained have guided this thesis. Four main results have been obtained, first, neurodevelopmental pathways were found deregulated in cCALD brains and this results were confirmed in neuronal and astrocyte cultures in which ABCD transporters have been silenced, second, astrocyte conditioned media worse the downregulation of genes implied in neurodevelopment, suggesting that direct and indirect alterations are happening in neurons and astrocytes, third, cholesterol metabolism and localization is altered in astrocytes but not cholesterol release to de medium, four, synaptic transmission and calcium signalling have been deregulated and results were confirmed in astrocytic cultures, and five, astrocytes metabolism is impaired at different levels, however they do not present oxidative stress.

The classical view of X-ALD could be overlooking important characteristics for the disease treatment such as cellular compartmentalization of pathological cascades, and mechanisms underling phyquiatric symptoms. For this, we used a top-down approach to first, study biological processes related with behavioural and psychiatric symptoms in X-ALD, second, look at this particular processes in neurons and astrocytes separately and, third, study the interaction between neurons and astrocytes in X-ALD.

Re-analysis of public X-ALD transcriptomic data by GSEA using gene ontology annotation reveled three main enriched categories; 'development', 'synaptic transmission' and 'lipid metabolism and transport' related to neural circuit formation and maintenance (Fig. 38).

1. Neurodevelopmental alterations in X-ALD neurons

Children's brain is a tissue that is still developing and remodelling. In consequence, 'development' should be highly controlled to grow correct brain structures and circuits. Surprisingly, neuron and glial development and morphogenesis are enriched in GSEA of both cCALD and AMN patients, indicating that brain circuits' formation could be altered in X-ALD. This is consistent with cognitive symptoms described in patients, and could explain most of the psychiatric features observed.

We validated some the differentially expressed genes leading to the enrichment of developmental dysregulation in human transcriptomic data of whole brain according to their significance and their importance in GO enrichment. We found that *Wnt2* and *Wnt6* expression is diminished in *in vitro* neuronal models of X-ALD. *Wnt2* regulate dendritic spine formation through interaction with brain derived-neurotrophic factor (BDNF) (Hiester *et al.*, 2013). Although, *Wnt6* have not been related to neuronal development directly, it appears as a top gene in the gene expression array. *Wnt6* intervenes in somite and neural crest formation in chicks, its intervention in early stages of development being critical for whole body formation (Schmidt *et al.*, 2008). The targeted analysis of gene expression of all Wnt family reveled that, apart from *Wnt*2 and *Wnt6, Wnt2B, Wnt7A, Wnt10B* and *Wnt16* are downregulated in cCALD. Of special interest for synaptogenesis is *Wnt7A* which could be secreted by astrocytes, and capted by neurons. It is involved in promotion of dendritic spine growth, synapse formation, and clustering of synaptophysin (*SYN*) between other funtions (Sahores, Gibb and Salinas, 2010; Ciani *et al.*, 2011; Tabatadze *et al.*, 2012). SYN is an integral membrane glycoprotein that is localized in presynaptic vesicles of neurons (Wiedenmann *et al.*, 1986), and is a marker of fibre outgrowth as well as synapse formation (Bergmann *et al.*, 1991). In our neuronal cultures Syn expression is downregulated in X-ALD conditions suggestin an aberrant generation of post-synaptic terminals. *STAT3* mediates cell growth differentiation and survival in CNS (Yan *et al.*, 2004b). SHH participate in neuroprotective and neurotrophic activities during brain development and in adulthood (Charytoniuk *et al.*, 2002). *STAT3 and SHH* are downregulated in transcriptomic data however, we had not observed changes in rat neuronal and astrocytic cultures. In addition, neuron projection guidance is also enriched in GSEA analysis. The axonal length was measured in rat sh*Abcd1/Abcd2* neurons treated with C26:0 at 5DIV and exhibit shorter axons (Fig. 25). Axon guidance and synapse formation are essential for brain circuits' formation. The growth cone of an axon is guided by different molecules to the target area where the synaptic formation will occur. Thinner processes coming from the terminal, grow at the targeted area and synapses are formed at the end of the axon (Chen and Cheng, 2009). It suggests that not only the expression of molecules like SYN or WNTs are responsible

for a number of synapse reduction, but also axonal growth will compromise synapse formation in X-ALD as axons could not reach their targeted areas.

2. Developmental alterations in X-ALD astrocytes

Neurodevelopmental pathways studied could share genes that interfere with synaptogenesi and astrocytic development (Allen and Eroglu, 2017). *Wnt2* and *Wnt6* expression is diminished in astrocytes. WNT secreted from astrocytes are responsible for clustering of glutamate receptors in *Dropsohila* (Kerr *et al.*, 2014), however further studies are needed to confirm if similar processes are happening in humans. Therefore, Wnt reduction could be affecting directly astrocytes or indirectly neurons throw Wnt ligands release to the extracellular space.

Supporting the idea that *ABCD1* could have functions other than transporting VLCFA into the peroxisome, we found that a genome-wide shRNA screen for LDL-cholesterol transport genes, identified *ABCD1* as a possible candidate (Chu *et al.*, 2015b). Moreover they confirmed that modulation of cholesterol transport is due to lysosome-peroxisome membrane contacts where ABCD1 localization is higher (Chu *et al.*, 2015b).Crooscheking the data from this study with our data we found that 106 out of 341 are differentially expressed in children with X-ALD. Gene candidates include *ABCD1* as we mentioned before, and even they have to be validated, the high number of genes deregulated in the array indicate that cholesterol transport could be a relevant biological process in X-ALD. Moreover, we found that sterol transport is deregulated in children and adults with X-ALD, and metabolism and synthesis is deregulated in adults when we performed GSEA. Astrocyte secreted-factors including cholesterol promote synapse formation,(Mauch *et al.*, 2001). Although neurons produce a small amount of cholesterol that allow them to survive, in order to differentiate axons and dendrites, and form new synapses, they require additional cholesterol supplied by astrocytes by lipoproteins that contain ApoE (Pfrieger, 2003). The expression of ApoE is upregulated in X-ALD children and adult transcriptomes. SREBP2 expression, responsible for cholesterol synthesis, is reduced, indicating a possible imbalance in cholesterol formation.

Moreover, our in rat astrocytes with ABCD transporters silenced, and treated with VLCFA, exhibit different localization of cholesterol, which shows a perinuclear pattern in the silenced condition, while control neurons had more cholesterol in membranes. Intracellular and extracellular cholesterol amount was not changed, but cholesterol synthesis was confirmed to be reduced. Surprisingly, the cholesterol content in ACM is similar between X-ALD rat astrocytes and controls, suggesting that, despite the alteration in cholesterol distribution, changes in cholesterol release are non detectable. The amount of cholesterol in membranes is tightly regulated, and changes on them could modify membrane characteristics, therefore, lack of cholesterol or accumulation unphysiologicaly in other places could lead to astrocytic dysfunctions.

3. ACM implication in neurodevelopmental processes

Expression of *Syn* in our neuronal cultures is decresed, interestingly, this decrease is higher in presence of $ACM^{X\text{-}ALD}$. Notch expression is maintained in adulthood, suggesting roles in adult brain plasticity (Presente, Andres and Nye, 2001). Notch signalling pathway, regulate CNS development and play roles in neural stem cells (NSC) proliferation and differentiation (Temple S, 2001; Merkle *et al.*, 2004). *NOTCH3* is mutated in Alzheimer'ds disease (Guerreiro *et al.*, 2012). Transcriptomic data of children and adults revealed *NOTCH3* downregulation. In concordance, *Notch3* expression is diminished in our rat X-ALD neurons, but only in presence of ACM form rat X-ALD astrocytes suggesting that some astrocyte-secreted factors could be modulating gene expression in neurons. Moreover, *NTRK3* is involved in cell proliferation and differentiation in cortical tissue (Bartkowska, Paquin, Andrée S. Gauthier, *et al.*, 2007), mutations in *NTRK3* could lead to anxiety and suscebility to panic (Bosch, 2001). *NTRK3* expresion is statistically significant changed in children and adults with X-ALD and reduced in rat neurons upon exposure to $ACM^{X\text{-}ALD}$.

Morphologic analysis of rat neurons with *Abcd1* and *Abcd2* genes silenced showed reduction in spine formation, thinner dendrites, and a poor arborisation as measured with sholl analysis and branching points (Fig. 22 and 24). Alteration of all the parameters were independent from VLCFA, and only certain measures are exacerbated by C26:0 addition, meaning that the observed effects are caused by the lack of *Abcd*

transporters *per se*. It could be due to two reasons: i) accumulation of endogenous VLCFA at 7DIV post-silencing is sufficient to disturb neuritogenesis and synaptogenesis, without need to add exogen C26:0, or ii) ABCD transporters have other functions than transporting VLCFA to the peroxisome that could modulate spynogenesis and neuritogenesis. Contradictory to our gene expression data, $ACM^{X\text{-}ALD}$ did not exhibited differences with control ACM. As morphological analysis is a less refined study than gene expression studies, we hypothesise that morphological analysys are not fine enought to detect difereces. The so-considered 'pure' neuronal cultures may contain a small proportion of astrocytes, running from 10 to 20%, as measured in our neuronal cultures. This fact hampers our understanding of what is happening exclusively in neurons, and the effect of ACM when values are changed drastically.

Altogether, suggest that basic brain formation will be compromised in X-ALD as critical genes involved in early development as Wnts are downregulated. Resultant modifications could be responsible for brain circuits' defects. However, further validation in independent human samples is needed to corroborete this hypothesis.

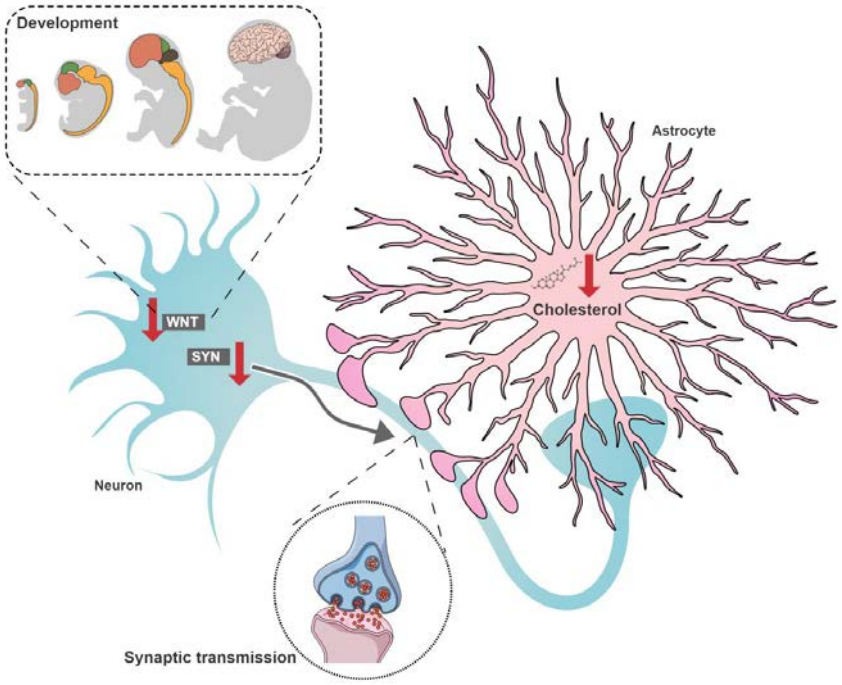

Figure 38. Neurodevelopmental alterations, synaptic transmission and cholesterol changes in X-ALD. Wnt singnalig and Synaptophisyn downregulation and reduced cholesterol synthesis.

4. Partial recovery of spinogensis

In order to restore synapse formation and as the relevance of Wnt signalling pathway alteration, we decided to activate the canonical Wnt signalling pathway throw inhibition of GSK-3. Inhibition of GSK-3 drives β-catenin to activate gene dependent transcription (Wu and Pan, 2010). GSK-3 inhibition partially rescues Syn expression in X-ALD neurons. Syn was used as a readout of spine formation; however further analysis, such as morphologial analysis, will be needed to confirm partial restoring of synaptogenes. Combination of canonical Wnt signalling pathway activation with other mechanisms participating in synapse formation could be a good strategy to treat patients. This reaffirms the importance of alterations in the Wnt signalling pathway refered to synaptogenesis disruption.

Among other candidates to restore neuronal development, astrocyte-derived synaptogenic factors are of our interest. We find thrombospondins that promote synaptogenesis in combination with other synaptogenic molecules (Karen S. Christopherson *et al.*, 2005a). *THBS1* expression is statistically significantly reduced in children with X-ALD while they are a statistically significant increase in adults with X-ALD. The same occurs in other neurodevelopmental diseases as X-Fragile in which THBS1 is decreased in knockout mice astrocytes (Cheng, Lau and Doering, 2016). Acute aplication of THSB to neurons will confirm if morphological changes could be restored.

It is clear that *ABCD1* mutations are present from the beginning of patients' life and therefore, dysregulation of neurodevelopment will be carried through adulthood. While Wnt signalling pathway seem to be the major responsible for neurodevelopmental alterations, cholesterol supply from astrocytes do not seem to be responsible for changes in synapse formation; however, further studies are needed to confirm these results and other possible candidates such as thrombospondin could restore synapse formation.

5. Synaptic transmission deregulation and calcium signalling

Action potentials open calcium channels leading to calcium increases in presynaptic spines triggering neurotransmitters release (Südhof, 2012). However, calcium

signalling does not occur in neurons exclusively, in fact, astrocyte calcium signalling is the base of their excitability and controls several processes related to brain information processing. Release of gliotransmiters upon transient elevations of calcium concentration has been proposed to modulate synapses, however this hypothesis has been questioned (Bazargani and Attwell, 2016). Recent studies have shown that calcium transients are different in fine processes than in the soma and for this reason, calcium signalling occurring in the fine process could modulate particular synapses (Bazargani and Attwell, 2016).

The transcriptomic data reveals that synaptic transmission is impaired in X-ALD patients. In children, biological processes related to calcium ion transport and their regulation appear enriched. In adults, calcium ion transport and regulation is also altered. Membrane potential and neuron neuron synaptic transmission are the top enriched GOs in adults. It means that synaptic transmission is specially impaired in adults, and calcium signalling changes could affect both neurons and astrocytes. On the one hand, astrocytic cultures excitability is reduced when *Abcd* transporters are silenced and C26:0 is accumulated. Other groups have shown hyperexcitability upon C26:0 stimulation (Kruska *et al.*, 2015b). However, we had not observed consistent responses to acute application of VLCFAs. On the other hand, recovery of basal calcium levels is slower in X-ALD astrocytes showing a progressive increase of cytosolic calcium levels after the first peak and a slow recovery of basal calcium levels. As these fine mechanisms are altered in whole astrocytes, we hypothesise that astrocytic calcium domains could suffer changes in calcium transients as well compromising astrocytic functions. In turn, the interaction of astrocytic processes with synapses will be also modified and, in consequence, brain circuits processing of information will be altered.

6. Functional changes in X-ALD astrocytes

As bioenergetic's failure and oxidative stress were reported as clue biological dysfunctions in X-ALD (Vargas *et al.*, 2004). Several studies point to oxidative stress as a possible target for disease treatment. However, different clinical trials have failed to improve motor and non-motor symptoms using antioxidant drugs (Berger *et al.*, 2010). In our studies, astrocytes do not present oxidative stress, as shown by the failed

detection of ROS. However, mitochondrial β-oxidation is impaired, ATP levels reduced, ER strees increased, NAD/NADH ratio changed and total GSH reduced.

FAO have been postulated recently as an available fuel for astrocytes (Eraso-Pichot *et al.*, no date). In our cultures, FAO levels are decreased in X-ALD and the efect is dependent on C26:0 accumulation. As FAO is a major source of energy and reduced ATP levels where reported in *Abcd1*$^{-}$mice spinal cords (Galino *et al.*, 2011a). We studied ATP formation in all the possible schenarios. Lack of glucose drastically reduce ATP levels at silenced conditions. Indicating that FAO is unable to compensate lack of glycolisis when ABCD transporters are not functional.

Surprisingly, GSH/GSSG ratio did not presented differences between X-ALD astrocytes and controls as it happen in other neurodegenerative disease (Saharan and Mandal, 2014)**.** GSH reduction was also observed in fibroblasts from X-ALD (Galino *et al.*, 2011b), and total amount was also reduced. In our experiments with astrocytes, total amount was also reduced indicating that oxidazed and reduced forms of gluthation are diminished (Fig. 33) the lack of appropiate values of total GSH and not only the ratio could be indicative of defects in antioxidant defense. As astrocytes provide GSH to neurons further vaidation of neuons redox state will be needed.

NADH levels are reduced in favor of NAD+ in astrocitic cultures. Therefore, the lack of reduction equivalents could be the cause of final oxidative stress, and as GSH is reduced and oxidative stress has not been observed in astrocytic cultures with the methods used.

Silencing of C26:0 transporters causes mitochondrial FAO (mit-FAO) impairment thereby causing depletion of reducing equivalents, which, in turn, depletes ATP and GSH in astrocytes. That is, oxidative stress, if any, is a consequence not a cause of mit-FAO impairment.

CONCLUSIONS

1. Pathways regulating formation, maintenance and/or function of neural circuits are dysregulated in cCALD and AMN according to non-targeted and targeted re-analyses of publicly available transcriptomic data using GSEA and GO annotation.

    1.1. The non-targeted analysis shows dysregulation in:

    i) Brain development in CCALD, canonical Wnt signalling being a top deregulated pathway.

    ii) Cell proliferation and regeneration in AMN.

    iii) Lipid metabolism and transport, especially of sterols, in AMN.

    iv) Synaptic transmission and calcium signaling in both CCALD and AMN.

    1.2. The targeted analysis shows dysregulation in:

    i) Astrocyte-mediated synaptogenesis, as suggested by the dysregulated expression of astrocyte-secreted molecules including trombospondins, SPARCL1 and their inhibitor, ephrines, tumor necrosis factor and synaptic pruning related genes.

    ii) Cholesterol metabolism and transport, as suggested by the dysregulation of 106 out of 341 genes previously identified in a genome-wide shRNA screen of LDL-cholesterol transport gene candidates. Dysregulated genes include gens related with lipid metabolism, cellular transport, peroxisome, immune system, neurodisease, cell adhesion, Ubl conjugation pathway, purine metabolism, Hhh pathway, and transcription.

2. X-ALD neurons present survival and developmental deficits, as shown by molecular and morphological observations in a novel *in vitro* model of CCALD generated by joint depletion of *Abcd* transporters using silencing strategies based on interference RNA. Specifically:

    2.1. Demise in hippocampal X-ALD neurons is increased in the absence of astrocyte-mediated neuroprotection provided by ACM, suggesting that *Abdc* depletion renders neurons more vulnerable.

    2.2. Sinaptogenesis, neuritogenesis and axon growth are impaired in hippocampal X-ALD neurons, which show a reduction in spine

formation, thinner dendrites, poor arborisation, and decreased expression of the mRNAs encoding for the synaptic marker SYN, as well as in factors involved in development including *WNT2, WNT6, NOTCH3 and NTRK3.*

2.3. The increased demise and developmental impairment of X-ALD neurons were mostly due to the silencing of *Abcd* transporters. The addition of external C26:0 only partially exacerbated the cell-autonomous damage.

2.4. Constitutive activation of canonical Wnt signalling pathway through GSK-3 inhibition partially restored the cell-autonomous deficit in synaptogenesis, assessed by *Syn* expression.

3. X-ALD astrocytes present metabolic, functional and secretion deficits, as shown in a novel *in vitro* model of cCALD generated by joint depletion of *Abcd* transporters using silencing strategies based on interference RNA. Specifically:

3.1. ACM from X-ALD astrocytes maintains the capacity to support neuronal survival, but partially contributes to the decreased synaptogenesis in X-ALD neurons, since ACM from X-ALD astrocytes aggravates the cell-autonomous downregulation of *Syn* in X-ALD neurons.

3.2. Cholesterol synthesis and distribution, but not release, are altered in X-ALD astrocytes, suggesting that the contribution of astrocytes to the impaired synaptogenesis of X-ALD neurons is not due to decreased secretion of cholesterol.

3.3. Mitochondrial FAO and ATP production are reduced in X-ALD astrocytes, associated with decreased production of glutathione and increasd NAD^+/NADH, pointing to intertwined bioenergetic failure and reduction of anti-oxidant defence. X-ALD astrocytes also show ER stress, as shown by altered PDI distribution.

3.4. Calcium-based excitability is altered in X-ALD astrocytes, a shown by a reduced response to ATP stimulation, and a slower recovery of basal calcium levels.

LIST OF ABREVIATIONS

ABC	ATP-binging cassette
ABCD	Binging cassette transporter sub-family D
ACOX	Acyl-CoA oxidase
ALDP	Adrenoleukodystrophy protein
AMN	Adrenomyeloneuropathy
ANOVA	Analysis of variance
ATP	Adenosine triphosphate
CCALD	Childhood cerebral adrenoleukodystrophy
Cer	Ceramide
CNS	Central nervous system
DHA	Docosohexaenoic acid
DHC	Dihydroxycholestanoyl
DIV	Days in vitro
DMEM	Dulbecco's Modified Eagle's medium
DNMT1	DNA (cytosine-5)-methyltransferase 1
ELOVL	Elongation of very long chain fatty acids
ER	Endoplasmic reticulum
FAS	Fatty acid synthase
FBS	Fetal Bovine Serum
GFAP	Glial fibrillary acidic protein
GO	Gene Ontology
GPX	Gluthatione peroxidises
GSEA	Gene Set Enrichment Analysis
GSH	Gluthatione
HSCT	Hematopoietic stem cell transplantation
IHC	Immunohistochemistry
IM	Inner membrane
JAK-*STAT*	Janus kinase/signal transducers and activators of transcription
MOI	Multiplicity of infection
NBA	Neurobasal A
NECs	Neuroepithelial cells
NEUROG	Neurogenin
NFIA	Nuclear factor I A
PCD	Programmed cell death
PRX	Peroxiredoxines
ROS	Radical oxygen species
SEM	Standard error of the mean
SM	Sphingomyelin
SOD	Superoxide dismutases
TCA	Tricarboxilic acid cycle
TSPs	Thrombospondins
VLCFA	Very long chain fatty acids
VZ	Ventricular zone
X-ALD	X-linked adrenoleukodystrophy

BIBLIOGRAPHY

Adamo, A. M., Aloise, P. A. and Pasquini, J. M. (1986) 'A possible relationship between concentration of microperoxisomes and myelination.', *International journal of developmental neuroscience : the official journal of the International Society for Developmental Neuroscience*, 4(6), pp. 513–7. Available at: http://www.ncbi.nlm.nih.gov/pubmed/3455609 (Accessed: 19 March 2019).

Agbaga, M.-P., Mandal, M. N. A. and Anderson, R. E. (2010) 'Retinal very long-chain PUFAs: new insights from studies on ELOVL4 protein', *Journal of Lipid Research*, 51(7), pp. 1624–1642. doi: 10.1194/jlr.R005025.

Aldahmesh, M. A. *et al.* (2011) 'Recessive Mutations in ELOVL4 Cause Ichthyosis, Intellectual Disability, and Spastic Quadriplegia', *The American Journal of Human Genetics*, 89(6), pp. 745–750. doi: 10.1016/j.ajhg.2011.10.011.

Alderson, N. L. *et al.* (2006) 'FA2H-dependent fatty acid 2-hydroxylation in postnatal mouse brain', *Journal of Lipid Research*, 47(12), pp. 2772–2780. doi: 10.1194/jlr.M600362-JLR200.

Allen, N. J. *et al.* (2012) 'Astrocyte glypicans 4 and 6 promote formation of excitatory synapses via GluA1 AMPA receptors.', *Nature*, 486(7403), pp. 410–4. doi: 10.1038/nature11059.

Allen, N. J. and Eroglu, C. (2017) 'Cell Biology of Astrocyte-Synapse Interactions', *Neuron*. Cell Press, pp. 697–708. doi: 10.1016/j.neuron.2017.09.056.

Arnold, G., Liscum, L. and Holtzman, E. (1979) 'Ultrastructural localization of D-amino acid oxidase in microperoxisomes of the rat nervous system.', *Journal of Histochemistry & Cytochemistry*, 27(3), pp. 735–745. doi: 10.1177/27.3.39097.

Asheuer, M. *et al.* (2005) 'Decreased expression of ABCD4 and BG1 genes early in the pathogenesis of X-linked adrenoleukodystrophy', *Human Molecular Genetics*, 14(10), pp. 1293–1303. doi: 10.1093/hmg/ddi140.

Ballatori, N. *et al.* (2009) 'Glutathione dysregulation and the etiology and progression of human diseases', *Biological Chemistry*, pp. 191–214. doi: 10.1515/BC.2009.033.

Banker, G. A. (1980) 'Trophic interactions between astroglial cells and hippocampal neurons in culture.', *Science (New York, N.Y.)*, 209(4458), pp. 809–10. doi: 10.1126/science.7403847.

Bartkowska, K., Paquin, A., Gauthier, Andrée S, *et al.* (2007) 'Trk signaling regulates neural precursor cell proliferation and differentiation during cortical development.', *Development (Cambridge, England)*, 134(24), pp. 4369–80. doi: 10.1242/dev.008227.

Bartkowska, K., Paquin, A., Gauthier, Andrée S., *et al.* (2007) 'Trk signaling regulates neural precursor cell proliferation and differentiation during cortical development', *Development*, 134(24), pp. 4369–4380. doi: 10.1242/dev.008227.

Basso, M. *et al.* (2013) 'Mutant copper-zinc superoxide dismutase (SOD1) induces protein secretion pathway alterations and exosome release in astrocytes: implications for disease spreading and motor neuron pathology in amyotrophic lateral sclerosis.', *The Journal of biological chemistry*, 288(22), pp. 15699–711. doi: 10.1074/jbc.M112.425066.

Bayraktar, O. A. *et al.* (2014) 'Astrocyte development and heterogeneity.', *Cold Spring Harbor perspectives in biology*. Cold Spring Harbor Laboratory Press, 7(1), p. a020362. doi: 10.1101/cshperspect.a020362.

Bazargani, N. and Attwell, D. (2016) 'Astrocyte calcium signaling: The third wave', *Nature Neuroscience*. Nature Publishing Group, pp. 182–189. doi: 10.1038/nn.4201.

Bazinet, R. P. and Layé, S. (2014) 'Polyunsaturated fatty acids and their metabolites in brain function and disease', *Nature Reviews Neuroscience*, 15(12), pp. 771–785. doi: 10.1038/nrn3820.

Beattie, E. C. *et al.* (2002) 'Control of synaptic strength by glial TNFalpha.', *Science (New York, N.Y.)*, 295(5563), pp. 2282–5. doi: 10.1126/science.1067859.

Becker, I. *et al.* (2008) 'Differential expression of (dihydro)ceramide synthases in mouse brain: oligodendrocyte-specific expression of CerS2/Lass2', *Histochemistry and Cell Biology*, 129(2), pp. 233–241. doi: 10.1007/s00418-007-0344-0.

van de Beek, M. C. *et al.* (2017) 'Lipid-induced endoplasmic reticulum stress in X-linked adrenoleukodystrophy', *Biochimica et Biophysica Acta - Molecular Basis of Disease*. Elsevier B.V., 1863(9), pp. 2255–2265. doi: 10.1016/j.bbadis.2017.06.003.

Berger, J. *et al.* (1999) 'The four murine peroxisomal ABC-transporter genes differ in constitutive, inducible and developmental expression.', *European journal of biochemistry*, 265(2), pp. 719–27. Available at: http://www.ncbi.nlm.nih.gov/pubmed/10504404 (Accessed: 19 March 2019).

Berger, J. *et al.* (2010) 'Current and future pharmacological treatment strategies in X-linked adrenoleukodystrophy', in *Brain Pathology*. Blackwell Publishing Ltd, pp. 845–856. doi: 10.1111/j.1750-3639.2010.00393.x.

Berger, J., Forss-Petter, S. and Eichler, F. S. (2014) 'Pathophysiology of X-linked adrenoleukodystrophy', *Biochimie*, 98, pp. 135–142. doi: 10.1016/j.biochi.2013.11.023.

Bergmann, M. *et al.* (1991) 'Expression of synaptophysin during the prenatal development of the rat spinal cord: Correlation with basic differentiation processes of neurons', *Neuroscience*, 42(2), pp. 569–582. doi: 10.1016/0306-4522(91)90399-9.

Bezman, L. *et al.* (2001) *Adrenoleukodystrophy: Incidence, New Mutation Rate, and Results of Extended Family Screening*, *Ann Neurol*. Available at:

https://xpv.uab.cat/doi/pdf/10.1002/,DanaInfo=.aoonlrjrpj0k2-M-x1vESw98,SSL+ana.101 (Accessed: 15 March 2019).

Bialas, A. R. and Stevens, B. (2013) 'TGF-β signaling regulates neuronal C1q expression and developmental synaptic refinement', *Nature Neuroscience*, 16(12), pp. 1773–1782. doi: 10.1038/nn.3560.

Bosch, X. (2001) 'Anxiety disorders linked to gene abnormality', *BMJ : British Medical Journal*. BMJ Publishing Group, 323(7309), p. 360.

Buoli, M. *et al.* (2017) 'Neurodevelopmental Versus Neurodegenerative Model of Schizophrenia and Bipolar Disorder: Comparison with Physiological Brain Development and Aging.', *Psychiatria Danubina*, 29(1), pp. 24–27. Available at: http://www.ncbi.nlm.nih.gov/pubmed/28291970 (Accessed: 10 May 2019).

Bushong, E. A. *et al.* (2002) 'Protoplasmic Astrocytes in CA1 Stratum Radiatum Occupy Separate Anatomical Domains', *The Journal of Neuroscience*, 22(1), pp. 183–192. doi: 10.1523/JNEUROSCI.22-01-00183.2002.

Bushong, E. A., Martone, M. E. and Ellisman, M. H. (2004) 'Maturation of astrocyte morphology and the establishment of astrocyte domains during postnatal hippocampal development', *International Journal of Developmental Neuroscience*, 22(2), pp. 73–86. doi: 10.1016/j.ijdevneu.2003.12.008.

Butovich, I. A. (2010) 'Fatty acid composition of cholesteryl esters of human meibomian gland secretions', *Steroids*, 75(10), pp. 726–733. doi: 10.1016/j.steroids.2010.04.011.

Butovich, I. A., Wojtowicz, J. C. and Molai, M. (2009) 'Human tear film and meibum. Very long chain wax esters and (O-acyl)-omega-hydroxy fatty acids of meibum', *Journal of Lipid Research*, 50(12), pp. 2471–2485. doi: 10.1194/jlr.M900252-JLR200.

Camargo, N., Smit, A. B. and Verheijen, M. H. G. (2009) 'SREBPs: SREBP function in glia-neuron interactions.', *The FEBS journal*, 276(3), pp. 628–36. doi: 10.1111/j.1742-4658.2008.06808.x.

Cantagrel, V. and Lefeber, D. J. (2011) 'From glycosylation disorders to dolichol biosynthesis defects: a new class of metabolic diseases', *Journal of Inherited Metabolic Disease*, 34(4), pp. 859–867. doi: 10.1007/s10545-011-9301-0.

Chae, W.-J. and Bothwell, A. L. M. (2018) 'Canonical and Non-Canonical Wnt Signaling in Immune Cells.', *Trends in immunology*. Elsevier, 39(10), pp. 830–847. doi: 10.1016/j.it.2018.08.006.

Charytoniuk, D. *et al.* (2002) 'Sonic hedgehog signalling in the developing and adult brain', *Journal of Physiology Paris*, 96(1–2), pp. 9–16. doi: 10.1016/S0928-4257(01)00075-4.

Charytoniuk, D. *et al.* (no date) 'Sonic Hedgehog signalling in the developing and adult brain.', *Journal of*

physiology, Paris, 96(1–2), pp. 9–16. Available at: http://www.ncbi.nlm.nih.gov/pubmed/11755778 (Accessed: 23 September 2019).

Chaudhry, V., Moser, H. W. and Cornblath, D. R. (1996) 'Nerve conduction studies in adrenomyeloneuropathy.', *Journal of neurology, neurosurgery, and psychiatry*, 61(2), pp. 181–5. Available at: http://www.ncbi.nlm.nih.gov/pubmed/8708687 (Accessed: 17 March 2019).

Chechik, G., Meilijson, I. and Ruppin, E. (1998) 'Synaptic pruning in development: a computational account.', *Neural computation*, 10(7), pp. 1759–77. Available at: http://www.ncbi.nlm.nih.gov/pubmed/9744896 (Accessed: 7 April 2019).

Chen, S. Y. and Cheng, H. J. (2009) 'Functions of axon guidance molecules in synapse formation', *Current Opinion in Neurobiology*, pp. 471–478. doi: 10.1016/j.conb.2009.09.005.

Cheng, C., Lau, S. K. M. and Doering, L. C. (2016) 'Astrocyte-secreted thrombospondin-1 modulates synapse and spine defects in the fragile X mouse model', *Molecular Brain*. BioMed Central Ltd., 9(1). doi: 10.1186/s13041-016-0256-9.

Christopherson, Karen S *et al.* (2005) 'Thrombospondins are astrocyte-secreted proteins that promote CNS synaptogenesis.', *Cell*, 120(3), pp. 421–33. doi: 10.1016/j.cell.2004.12.020.

Christopherson, Karen S. *et al.* (2005a) 'Thrombospondins are astrocyte-secreted proteins that promote CNS synaptogenesis', *Cell*. Cell Press, 120(3), pp. 421–433. doi: 10.1016/j.cell.2004.12.020.

Christopherson, Karen S. *et al.* (2005b) 'Thrombospondins Are Astrocyte-Secreted Proteins that Promote CNS Synaptogenesis', *Cell*. Cell Press, 120(3), pp. 421–433. doi: 10.1016/J.CELL.2004.12.020.

Chu, B.-B. *et al.* (2015a) 'Cholesterol Transport through Lysosome-Peroxisome Membrane Contacts', *Cell*, 161(2), pp. 291–306. doi: 10.1016/j.cell.2015.02.019.

Chu, B.-B. *et al.* (2015b) 'Cholesterol Transport through Lysosome-Peroxisome Membrane Contacts', *Cell*. Cell Press, 161(2), pp. 291–306. doi: 10.1016/J.CELL.2015.02.019.

Chung, W.-S. *et al.* (2013) 'Astrocytes mediate synapse elimination through MEGF10 and MERTK pathways.', *Nature*, 504(7480), pp. 394–400. doi: 10.1038/nature12776.

Ciani, L. *et al.* (2011) 'Wnt7a signaling promotes dendritic spine growth and synaptic strength through Ca^{2+}/Calmodulin-dependent protein kinase II.', *Proceedings of the National Academy of Sciences of the United States of America*, 108(26), pp. 10732–7. doi: 10.1073/pnas.1018132108.

Clarke, L. E. and Barres, B. A. (2013) 'Emerging roles of astrocytes in neural circuit development.', *Nature reviews. Neuroscience*. NIH Public Access, 14(5), pp. 311–21. doi: 10.1038/nrn3484.

Consortium, T. H. iPSC *et al.* (2017) 'Developmental alterations in Huntington's disease neural cells and

pharmacological rescue in cells and mice', *Nature Neuroscience*. Nature Publishing Group, 20(5), pp. 648–660. doi: 10.1038/nn.4532.

Corona, J. C. (2018) 'Natural Compounds for the Management of Parkinson's Disease and Attention-Deficit/Hyperactivity Disorder', *BioMed Research International*, 2018, pp. 1–12. doi: 10.1155/2018/4067597.

van Deijk, A.-L. F. *et al.* (2017) 'Astrocyte lipid metabolism is critical for synapse development and function in vivo', *Glia*. John Wiley & Sons, Ltd, 65(4), pp. 670–682. doi: 10.1002/glia.23120.

Dong, C., Wong, M.-L. and Licinio, J. (2009) 'Sequence variations of ABCB1, SLC6A2, SLC6A3, SLC6A4, CREB1, CRHR1 and NTRK2: association with major depression and antidepressant response in Mexican-Americans.', *Molecular psychiatry*, 14(12), pp. 1105–18. doi: 10.1038/mp.2009.92.

Dubey, P. *et al.* (2005) 'Adrenal insufficiency in asymptomatic adrenoleukodystrophy patients identified by very long-chain fatty acid screening.', *The Journal of pediatrics*. Elsevier, 146(4), pp. 528–32. doi: 10.1016/j.jpeds.2004.10.067.

Van Duyn, M. A. *et al.* (1984) 'The design of a diet restricted in saturated very long-chain fatty acids: therapeutic application in adrenoleukodystrophy', *The American Journal of Clinical Nutrition*, 40(2), pp. 277–284. doi: 10.1093/ajcn/40.2.277.

Dyall, S. C. (2015) 'Long-chain omega-3 fatty acids and the brain: a review of the independent and shared effects of EPA, DPA and DHA', *Frontiers in Aging Neuroscience*, 7, p. 52. doi: 10.3389/fnagi.2015.00052.

Eichler, F. *et al.* (2017) 'Hematopoietic Stem-Cell Gene Therapy for Cerebral Adrenoleukodystrophy', *New England Journal of Medicine*. Massachusetts Medical Society, 377(17), pp. 1630–1638. doi: 10.1056/NEJMoa1700554.

Eichler, F. S. *et al.* (2008) 'Is microglial apoptosis an early pathogenic change in cerebral X-linked adrenoleukodystrophy?', *Annals of Neurology*. John Wiley & Sons, Ltd, 63(6), pp. 729–742. doi: 10.1002/ana.21391.

Engelen, M. *et al.* (2010) 'Lovastatin in X-Linked Adrenoleukodystrophy', *New England Journal of Medicine*, 362(3), pp. 276–277. doi: 10.1056/NEJMc0907735.

Engelen, M., Tran, L., *et al.* (2012) 'Bezafibrate for X-Linked Adrenoleukodystrophy', *PLoS ONE*. Edited by O. Baud, 7(7), p. e41013. doi: 10.1371/journal.pone.0041013.

Engelen, M., Schackmann, M. J. A., *et al.* (2012) 'Bezafibrate lowers very long-chain fatty acids in X-linked adrenoleukodystrophy fibroblasts by inhibiting fatty acid elongation', *Journal of Inherited Metabolic Disease*. Springer Netherlands, 35(6), pp. 1137–1145. doi: 10.1007/s10545-012-9471-4.

Engelen, M., Kemp, S., *et al.* (2012) 'X-linked adrenoleukodystrophy (X-ALD): clinical presentation and guidelines for diagnosis, follow-up and management', *Orphanet Journal of Rare Diseases*. BioMed Central, 7(1), p. 51. doi: 10.1186/1750-1172-7-51.

Eraso-Pichot, A. *et al.* (2018) 'GSEA of mouse and human mitochondriomes reveals fatty acid oxidation in astrocytes', *Glia*, 66(8), pp. 1724–1735. doi: 10.1002/glia.23330.

Eraso-Pichot, A. *et al.* (no date) 'GSEA of mouse and human mitochondriomes reveals fatty acid oxidation in astrocytes'. doi: 10.1002/glia.23330.

Ferris, H. A. *et al.* (2017) 'Loss of astrocyte cholesterol synthesis disrupts neuronal function and alters whole-body metabolism', *Proceedings of the National Academy of Sciences*. National Academy of Sciences, 114(5), pp. 1189–1194. doi: 10.1073/PNAS.1620506114.

Forss-Petter, S. *et al.* (1997) 'Targeted inactivation of the X-linked adrenoleukodystrophy gene in mice', *Journal of Neuroscience Research*. John Wiley & Sons, Ltd, 50(5), pp. 829–843. doi: 10.1002/(SICI)1097-4547(19971201)50:5<829::AID-JNR19>3.0.CO;2-W.

Fourcade, S. *et al.* (2008) 'Early oxidative damage underlying neurodegeneration in X-adrenoleukodystrophy', *Human Molecular Genetics*. Oxford University Press, 17(12), pp. 1762–1773. doi: 10.1093/hmg/ddn085.

Fourcade, S. *et al.* (2009) 'A key role for the peroxisomal *ABCD2* transporter in fatty acid homeostasis', *American Journal of Physiology-Endocrinology and Metabolism*, 296(1), pp. E211–E221. doi: 10.1152/ajpendo.90736.2008.

Freeman, M. R. (2010) 'Specification and morphogenesis of astrocytes.', *Science (New York, N.Y.)*. NIH Public Access, 330(6005), pp. 774–8. doi: 10.1126/science.1190928.

Galino, J. *et al.* (2011a) 'Oxidative damage compromises energy metabolism in the axonal degeneration mouse model of X-adrenoleukodystrophy', *Antioxidants and Redox Signaling*, 15(8), pp. 2095–2107. doi: 10.1089/ars.2010.3877.

Galino, J. *et al.* (2011b) 'Oxidative Damage Compromises Energy Metabolism in the Axonal Degeneration Mouse Model of X-Adrenoleukodystrophy', *Antioxidants & Redox Signaling*, 15(8), pp. 2095–2107. doi: 10.1089/ars.2010.3877.

van Geel, B. M. *et al.* (1996) 'Peripheral nerve abnormalities in adrenomyeloneuropathy: a clinical and electrodiagnostic study.', *Neurology*, 46(1), pp. 112–8. Available at: http://www.ncbi.nlm.nih.gov/pubmed/8559356 (Accessed: 17 March 2019).

van Geel, B. M. *et al.* (2001) 'Evolution of phenotypes in adult male patients with X-linked adrenoleukodystrophy.', *Annals of neurology*, 49(2), pp. 186–94. Available at:

http://www.ncbi.nlm.nih.gov/pubmed/11220738 (Accessed: 16 March 2019).

Gene Ontology Resource (no date). Available at: http://geneontology.org/ (Accessed: 10 May 2019).

Genoud, C. *et al.* (2006) 'Plasticity of astrocytic coverage and glutamate transporter expression in adult mouse cortex.', *PLoS biology*, 4(11), p. e343. doi: 10.1371/journal.pbio.0040343.

Gong, Y. *et al.* (2018) 'Intrathecal Adeno-Associated Viral Vector-Mediated Gene Delivery for Adrenomyeloneuropathy', *Human Gene Therapy*. Mary Ann Liebert, Inc., publishers 140 Huguenot Street, 3rd Floor New Rochelle, NY 10801 USA , p. hum.2018.079. doi: 10.1089/hum.2018.079.

Grek, C. and Townsend, D. M. (2013) 'Protein Disulfide Isomerase Superfamily in Disease and the Regulation of Apoptosis', *Endoplasmic Reticulum Stress in Diseases*. Walter de Gruyter GmbH, 1(1). doi: 10.2478/ersc-2013-0001.

Guerreiro, R. J. *et al.* (2012) 'Exome sequencing reveals an unexpected genetic cause of disease: NOTCH3 mutation in a Turkish family with Alzheimer's disease.', *Neurobiology of aging*, 33(5), pp. 1008.e17–23. doi: 10.1016/j.neurobiolaging.2011.10.009.

Guillou, H. *et al.* (2010) 'The key roles of elongases and desaturases in mammalian fatty acid metabolism: Insights from transgenic mice', *Progress in Lipid Research*, 49(2), pp. 186–199. doi: 10.1016/j.plipres.2009.12.002.

Haberfeld, W. and Spieler, F. (1910) 'Zur diffusen Hirn-Rückenmarksklerose im Kindesalter', *Deutsche Zeitschrift für Nervenheilkunde*. Springer-Verlag, 40(5–6), pp. 436–463. doi: 10.1007/BF01629013.

Hajra, A. K. and Bishop, J. E. (1982) 'GLYCEROLIPID BIOSYNTHESIS IN PEROXISOMES VIA THE ACYL DIHYDROXYACETONE PHOSPHATE PATHWAY', *Annals of the New York Academy of Sciences*, 386(1 Peroxisomes a), pp. 170–182. doi: 10.1111/j.1749-6632.1982.tb21415.x.

He, C.-W., Liao, C.-P. and Pan, C.-L. (2018) 'Wnt signalling in the development of axon, dendrites and synapses.', *Open biology*, 8(10). doi: 10.1098/rsob.180116.

Hein, S. *et al.* (2008a) 'Toxic effects of X-linked adrenoleukodystrophy-associated, very long chain fatty acids on glial cells and neurons from rat hippocampus in culture', *Human Molecular Genetics*, 17(12), pp. 1750–1761. doi: 10.1093/hmg/ddn066.

Hein, S. *et al.* (2008b) 'Toxic effects of X-linked adrenoleukodystrophy-associated, very long chain fatty acids on glial cells and neurons from rat hippocampus in culture', *Human Molecular Genetics*, 17(12), pp. 1750–1761. doi: 10.1093/hmg/ddn066.

Hiester, B. G. *et al.* (2013) 'Neurotrophin and Wnt signaling cooperatively regulate dendritic spine formation', *Molecular and Cellular Neuroscience*, 56, pp. 115–127. doi: 10.1016/j.mcn.2013.04.006.

Hirabayashi, Y. *et al.* (2004) 'The Wnt/ -catenin pathway directs neuronal differentiation of cortical neural precursor cells', *Development*, 131(12), pp. 2791–2801. doi: 10.1242/dev.01165.

Ho, J. K. *et al.* (1995) 'Interactions of a very long chain fatty acid with model membranes and serum albumin. Implications for the pathogenesis of adrenoleukodystrophy.', *Journal of Clinical Investigation*, 96(3), pp. 1455–1463. doi: 10.1172/JCI118182.

Höftberger, R. *et al.* (2007) 'Distribution and cellular localization of adrenoleukodystrophy protein in human tissues: Implications for X-linked adrenoleukodystrophy', *Neurobiology of Disease*. Academic Press, 28(2), pp. 165–174. doi: 10.1016/J.NBD.2007.07.007.

HOLTZMAN, E. *et al.* (1973) 'NOTES ON SYNAPTIC VESICLES AND RELATED STRUCTURES, ENDOPLASMIC RETICULUM, LYSOSOMES AND PEROXISOMES IN NERVOUS TISSUE AND THE ADRENAL MEDULLA', *Journal of Histochemistry & Cytochemistry*, 21(4), pp. 349–385. doi: 10.1177/21.4.349.

Huang, J. *et al.* (2017) 'Activation of Wnt/β-catenin signalling via GSK3 inhibitors direct differentiation of human adipose stem cells into functional hepatocytes', *Scientific Reports*. Nature Publishing Group, 7. doi: 10.1038/srep40716.

Huyghe, S. *et al.* (2001) 'Prenatal and postnatal development of peroxisomal lipid-metabolizing pathways in the mouse.', *The Biochemical journal*. Portland Press Ltd, 353(Pt 3), pp. 673–80. Available at: http://www.ncbi.nlm.nih.gov/pubmed/11171065 (Accessed: 19 March 2019).

Ichikawa, M. *et al.* (1991) 'Expression of synaptophysin during synapse formation between dissociated cortical neurons', *Neuroscience Research*. Elsevier, 12(3), pp. 452–458. doi: 10.1016/0168-0102(91)90077-C.

Igarashi, M. *et al.* (1976) 'Fatty acid abnormality in adrenoleukodystrophy.', *Journal of neurochemistry*. Wiley-Blackwell, 26(4), pp. 851–60. doi: 10.1111/J.1471-4159.1976.TB04462.X.

Ilango, Ts. and Nambi, S. (2015) 'X-linked adrenoleukodystrophy presenting as attention deficit hyperactivity disorder', *Indian Journal of Psychiatry*, 57(2), p. 208. doi: 10.4103/0019-5545.158198.

JAKOBSSON, A., WESTERBERG, R. and JACOBSSON, A. (2006) 'Fatty acid elongases in mammals: Their regulation and roles in metabolism', *Progress in Lipid Research*, 45(3), pp. 237–249. doi: 10.1016/j.plipres.2006.01.004.

James, M. J. and Kandutsch, A. A. (1980) 'Evidence for independent regulation of dolichol and cholesterol synthesis in developing mouse brain', *Biochimica et Biophysica Acta (BBA) - Lipids and Lipid Metabolism*, 619(2), pp. 432–435. doi: 10.1016/0005-2760(80)90094-6.

Jangouk, P. *et al.* (2012) 'Adrenoleukodystrophy in female heterozygotes: Underrecognized and undertreated', *Molecular Genetics and Metabolism*, 105(2), pp. 180–185. doi:

10.1016/j.ymgme.2011.11.001.

Kamijo, K. *et al.* (1990) 'The 70-kDa peroxisomal membrane protein is a member of the Mdr (P-glycoprotein)-related ATP-binding protein superfamily.', *The Journal of biological chemistry*, 265(8), pp. 4534–40. Available at: http://www.ncbi.nlm.nih.gov/pubmed/1968461 (Accessed: 17 March 2019).

Kanakis, G. and Kaltsas, G. (2000) *Adrenal Insufficiency Due to X-Linked Adrenoleukodystrophy*, *Endotext*. MDText.com, Inc. Available at: http://www.ncbi.nlm.nih.gov/pubmed/25905179 (Accessed: 18 March 2019).

Kassmann, C. M. *et al.* (2007) 'Axonal loss and neuroinflammation caused by peroxisome-deficient oligodendrocytes', *Nature Genetics*, 39(8), pp. 969–976. doi: 10.1038/ng2070.

Katakowski, M. *et al.* (2005) 'EphB2 induces proliferation and promotes a neuronal fate in adult subventricular neural precursor cells', *Neuroscience Letters*, 385(3), pp. 204–209. doi: 10.1016/j.neulet.2005.05.060.

Kawamura, N., Moser, H. W., *et al.* (1978) 'Excess C-26 fatty acid in cultured skin fibroblasts from adrenoleukodystrophy and adrenomyeloneuropathy patients.', *Transactions of the American Neurological Association*, 103, pp. 113–5. Available at: http://www.ncbi.nlm.nih.gov/pubmed/757032 (Accessed: 16 March 2019).

Kawamura, N., Moser, A. B., *et al.* (1978) 'High concentration of hexacosanoate in cultured skin fibroblast lipids from adrenoleukodystrophy patients.', *Biochemical and biophysical research communications*, 82(1), pp. 114–20. Available at: http://www.ncbi.nlm.nih.gov/pubmed/666828 (Accessed: 16 March 2019).

Kemp, S. *et al.* (1998) 'Gene redundancy and pharmacological gene therapy: Implications for X-linked adrenoleukodystrophy', *Nature Medicine*. Nature Publishing Group, 4(11), pp. 1261–1268. doi: 10.1038/3242.

Kemp, S. *et al.* (2005a) 'Elongation of very long-chain fatty acids is enhanced in X-linked adrenoleukodystrophy', *Molecular Genetics and Metabolism*, 84(2), pp. 144–151. doi: 10.1016/j.ymgme.2004.09.015.

Kemp, S. *et al.* (2005b) 'Elongation of very long-chain fatty acids is enhanced in X-linked adrenoleukodystrophy', *Molecular Genetics and Metabolism*. Academic Press, 84(2), pp. 144–151. doi: 10.1016/J.YMGME.2004.09.015.

Kemp, S. *et al.* (2016) 'Adrenoleukodystrophy – neuroendocrine pathogenesis and redefinition of natural history', *Nature Reviews Endocrinology*, 12(10), pp. 606–615. doi: 10.1038/nrendo.2016.90.

Kemper, A. R. *et al.* (2017) 'Newborn screening for X-linked adrenoleukodystrophy: evidence summary

and advisory committee recommendation', *Genetics in Medicine*. Nature Publishing Group, 19(1), pp. 121–126. doi: 10.1038/gim.2016.68.

Kerr, K. S. *et al.* (2014) 'Glial wingless/Wnt regulates glutamate receptor clustering and synaptic physiology at the Drosophila neuromuscular junction.', *The Journal of neuroscience : the official journal of the Society for Neuroscience*, 34(8), pp. 2910–20. doi: 10.1523/JNEUROSCI.3714-13.2014.

Khan, M., Singh, J. and Singh, I. (2008) 'Plasmalogen deficiency in cerebral adrenoleukodystrophy and its modulation by lovastatin.', *Journal of neurochemistry*. NIH Public Access, 106(4), pp. 1766–79. doi: 10.1111/j.1471-4159.2008.05513.x.

Kihara, A. *et al.* (2007) 'Metabolism and biological functions of two phosphorylated sphingolipids, sphingosine 1-phosphate and ceramide 1-phosphate', *Progress in Lipid Research*, 46(2), pp. 126–144. doi: 10.1016/j.plipres.2007.03.001.

Kihara, A. (2012) 'Very long-chain fatty acids: elongation, physiology and related disorders', *Journal of Biochemistry*. Narnia, 152(5), pp. 387–395. doi: 10.1093/jb/mvs105.

Kim, Jaekwang *et al.* (2014) 'Apolipoprotein E in synaptic plasticity and alzheimer's disease: Potential cellular and molecular mechanisms', *Molecules and Cells*. Korean Society for Molecular and Cellular Biology, pp. 833–840. doi: 10.14348/molcells.2014.0248.

van der Knaap, M. S. and Valk, J. (2005) *Magnetic Resonance of Myelination and Myelin Disorders*. Berlin, Heidelberg: Springer Berlin Heidelberg. doi: 10.1007/3-540-27660-2.

Knazek, R. A. *et al.* (1983) 'Membrane microviscosity is increased in the erythrocytes of patients with adrenoleukodystrophy and adrenomyeloneuropathy.', *The Journal of clinical investigation*. American Society for Clinical Investigation, 72(1), pp. 245–8. doi: 10.1172/JCI110963.

Kobayashi, T. *et al.* (1997) 'Adrenoleukodystrophy Protein-Deficient Mice Represent Abnormality of Very Long Chain Fatty Acid Metabolism', *Biochemical and Biophysical Research Communications*, 232(3), pp. 631–636. doi: 10.1006/bbrc.1997.6340.

Korenke, G. C. *et al.* (1995) 'Glyceroltrioleate/glyceroltrierucate therapy in 16 patients with X-chromosomal adrenoleukodystrophy/adrenomyeloneuropathy: effect on clinical, biochemical and neurophysiological parameters.', *European journal of pediatrics*, 154(1), pp. 64–70. Available at: http://www.ncbi.nlm.nih.gov/pubmed/7895759 (Accessed: 25 July 2019).

Kruska, N. *et al.* (2015a) 'Astrocytes and mitochondria from adrenoleukodystrophy protein (ABCD1)-deficient mice reveal that the adrenoleukodystrophy-associated very long-chain fatty acids target several cellular energy-dependent functions', *Biochimica et Biophysica Acta (BBA) - Molecular Basis of Disease*, 1852(5), pp. 925–936. doi: 10.1016/j.bbadis.2015.01.005.

Kruska, N. *et al.* (2015b) 'Astrocytes and mitochondria from adrenoleukodystrophy protein (ABCD1)-deficient mice reveal that the adrenoleukodystrophy-associated very long-chain fatty acids target several cellular energy-dependent functions', *Biochimica et Biophysica Acta - Molecular Basis of Disease*. Elsevier, 1852(5), pp. 925–936. doi: 10.1016/j.bbadis.2015.01.005.

Kuan, C. Y. *et al.* (2000) 'Mechanisms of programmed cell death in the developing brain.', *Trends in neurosciences*, 23(7), pp. 291–7. Available at: http://www.ncbi.nlm.nih.gov/pubmed/10856938 (Accessed: 31 March 2019).

Kucukdereli, H. *et al.* (2011) 'Control of excitatory CNS synaptogenesis by astrocyte-secreted proteins Hevin and SPARC.', *Proceedings of the National Academy of Sciences of the United States of America*, 108(32), pp. E440-9. doi: 10.1073/pnas.1104977108.

Kühl, J.-S. *et al.* (2017) 'Long-term outcomes of allogeneic haematopoietic stem cell transplantation for adult cerebral X-linked adrenoleukodystrophy', *Brain*, 140(4), pp. 953–966. doi: 10.1093/brain/awx016.

Lasky, J. L. and Wu, H. (2005) 'Notch signaling, brain development, and human disease.', *Pediatric research*, 57(5 Pt 2), pp. 104R-109R. doi: 10.1203/01.PDR.0000159632.70510.3D.

Laureti, S. *et al.* (1996) 'X-linked adrenoleukodystrophy is a frequent cause of idiopathic Addison's disease in young adult male patients.', *The Journal of Clinical Endocrinology & Metabolism*, 81(2), pp. 470–474. doi: 10.1210/jcem.81.2.8636252.

Lauritzen, L. *et al.* (2016) 'DHA Effects in Brain Development and Function', *Nutrients*, 8(1), p. 6. doi: 10.3390/nu8010006.

Liesi, P. and Silver, J. (1988) 'Is astrocyte laminin involved in axon guidance in the mammalian CNS?', *Developmental biology*, 130(2), pp. 774–85. Available at: http://www.ncbi.nlm.nih.gov/pubmed/3143614 (Accessed: 11 April 2019).

Lin, D. S. *et al.* (1993) 'Unique lipids of primate spermatozoa: desmosterol and docosahexaenoic acid.', *Journal of lipid research*, 34(3), pp. 491–9. Available at: http://www.ncbi.nlm.nih.gov/pubmed/8468532 (Accessed: 25 July 2019).

Lodhi, I. J. and Semenkovich, C. F. (2014) 'Peroxisomes: A Nexus for Lipid Metabolism and Cellular Signaling', *Cell Metabolism*, 19(3), pp. 380–392. doi: 10.1016/j.cmet.2014.01.002.

Lombard-Platet, G. *et al.* (1996) 'A close relative of the adrenoleukodystrophy (ALD) gene codes for a peroxisomal protein with a specific expression pattern.', *Proceedings of the National Academy of Sciences of the United States of America*, 93(3), pp. 1265–9. Available at: http://www.ncbi.nlm.nih.gov/pubmed/8577752 (Accessed: 17 March 2019).

López-Erauskin, J. *et al.* (2013) 'Impaired mitochondrial oxidative phosphorylation in the peroxisomal

disease X-linked adrenoleukodystrophy', *Human Molecular Genetics*, 22(16), pp. 3296–3305. doi: 10.1093/hmg/ddt186.

Lu, J. F. *et al.* (1997) 'A mouse model for X-linked adrenoleukodystrophy.', *Proceedings of the National Academy of Sciences of the United States of America*, 94(17), pp. 9366–71. Available at: http://www.ncbi.nlm.nih.gov/pubmed/9256488 (Accessed: 18 March 2019).

Madison, B. B. (2016) 'Srebp2: A master regulator of sterol and fatty acid synthesis1', *Journal of Lipid Research*. American Society for Biochemistry and Molecular Biology Inc., pp. 333–335. doi: 10.1194/jlr.C066712.

Markesbery, W. R. (1999) 'The role of oxidative stress in Alzheimer disease', *Archives of Neurology*. American Medical Association, pp. 1449–1452. doi: 10.1001/archneur.56.12.1449.

Mauch, D. H. *et al.* (2001) 'CNS synaptogenesis promoted by glia-derived cholesterol.', *Science (New York, N.Y.)*, 294(5545), pp. 1354–7. doi: 10.1126/science.294.5545.1354.

McGuinness, M. C. *et al.* (2003) 'Role of ALDP (ABCD1) and mitochondria in X-linked adrenoleukodystrophy.', *Molecular and cellular biology*, 23(2), pp. 744–53. Available at: http://www.ncbi.nlm.nih.gov/pubmed/12509471 (Accessed: 20 March 2019).

Merkle, F. T. *et al.* (2004) 'Radial glia give rise to adult neural stem cells in the subventricular zone.', *Proceedings of the National Academy of Sciences of the United States of America*, 101(50), pp. 17528–32. doi: 10.1073/pnas.0407893101.

Miller, F. D. and Gauthier, A. S. (2007) 'Timing is everything: making neurons versus glia in the developing cortex.', *Neuron*, 54(3), pp. 357–69. doi: 10.1016/j.neuron.2007.04.019.

Morató, L. *et al.* (2013) 'Pioglitazone halts axonal degeneration in a mouse model of X-linked adrenoleukodystrophy.', *Brain : a journal of neurology*, 136(Pt 8), pp. 2432–43. doi: 10.1093/brain/awt143.

Morrow, T., Song, M. R. and Ghosh, A. (2001) 'Sequential specification of neurons and glia by developmentally regulated extracellular factors.', *Development (Cambridge, England)*, 128(18), pp. 3585–94. Available at: http://www.ncbi.nlm.nih.gov/pubmed/11566862 (Accessed: 7 April 2019).

Moser, A. B. *et al.* (1999) 'Plasma very long chain fatty acids in 3,000 peroxisome disease patients and 29,000 controls.', *Annals of neurology*, 45(1), pp. 100–10. Available at: http://www.ncbi.nlm.nih.gov/pubmed/9894883 (Accessed: 17 March 2019).

Moser, H. W. *et al.* (1981) 'Adrenoleukodystrophy: increased plasma content of saturated very long chain fatty acids.', *Neurology*, 31(10), pp. 1241–9. Available at: http://www.ncbi.nlm.nih.gov/pubmed/7202134 (Accessed: 16 March 2019).

Moser, H. W. *et al.* (1991) 'Adrenoleukodystrophy.', *Endocrinology and metabolism clinics of North America*, 20(2), pp. 297–318. Available at: http://www.ncbi.nlm.nih.gov/pubmed/1879401 (Accessed: 25 July 2019).

Moser, H. W. *et al.* (2000) 'X-Linked Adrenoleukodystrophy: Overview and Prognosis as a Function of Age and Brain Magnetic Resonance Imaging Abnormality. A Study Involving 372 Patients', *Neuropediatrics*, 31(5), pp. 227–239. doi: 10.1055/s-2000-9236.

Mosser, J. *et al.* (1993) 'Putative X-linked adrenoleukodystrophy gene shares unexpected homology with ABC transporters', *Nature*. Nature Publishing Group, 361(6414), pp. 726–730. doi: 10.1038/361726a0.

Murai, K. K. and Pasquale, E. B. (2011) 'Eph receptors and ephrins in neuron-astrocyte communication at synapses', *Glia*, 59(11), pp. 1567–1578. doi: 10.1002/glia.21226.

Musolino, P. L. *et al.* (2015) 'Brain endothelial dysfunction in cerebral adrenoleukodystrophy.', *Brain : a journal of neurology*. Oxford University Press, 138(Pt 11), pp. 3206–20. doi: 10.1093/brain/awv250.

Mutations & Biochemistry - Adrenoleukodystrophy.info (no date). Available at: https://adrenoleukodystrophy.info/mutations-biochemistry/mutations-biochemistry (Accessed: 17 March 2019).

Nadarajah, B. *et al.* (2003) 'Neuronal migration in the developing cerebral cortex: observations based on real-time imaging.', *Cerebral cortex (New York, N.Y. : 1991)*, 13(6), pp. 607–11. Available at: http://www.ncbi.nlm.nih.gov/pubmed/12764035 (Accessed: 30 March 2019).

Namihira, M. *et al.* (2009) 'Committed Neuronal Precursors Confer Astrocytic Potential on Residual Neural Precursor Cells', *Developmental Cell*, 16(2), pp. 245–255. doi: 10.1016/j.devcel.2008.12.014.

Netik, A *et al.* (1999) 'Adrenoleukodystrophy-related protein can compensate functionally for adrenoleukodystrophy protein deficiency (X-ALD): implications for therapy.', *Human molecular genetics*, 8(5), pp. 907–13. Available at: http://www.ncbi.nlm.nih.gov/pubmed/10196381 (Accessed: 17 March 2019).

Netik, A. *et al.* (1999) 'Adrenoleukodystrophy-Related Protein Can Compensate Functionally for Adrenoleukodystrophy Protein Deficiency (X-ALD): Implications for Therapy', *Human Molecular Genetics*, 8(5), pp. 907–913. doi: 10.1093/hmg/8.5.907.

Nishida, H. and Okabe, S. (2007) 'Direct Astrocytic Contacts Regulate Local Maturation of Dendritic Spines', *Journal of Neuroscience*, 27(2), pp. 331–340. doi: 10.1523/JNEUROSCI.4466-06.2007.

Oberheim, N. A. *et al.* (2009) 'Uniquely hominid features of aHan, X., Chen, M., Wang, F., Windrem, M., Wang, S., Shanz, S., Xu, Q., et al. (2013). Forebrain engraftment by human glial progenitor cells enhances synaptic plasticity and learning in adult mice. Cell stem cell, 12(3), 342–5', *The Journal of neuroscience :*

the official journal of the Society for Neuroscience, 29(10), pp. 3276–87. doi: 10.1523/JNEUROSCI.4707-08.2009.

Oezen, I. *et al.* (2005) 'Accumulation of very long-chain fatty acids does not affect mitochondrial function in adrenoleukodystrophy protein deficiency', *Human Molecular Genetics*, 14(9), pp. 1127–1137. doi: 10.1093/hmg/ddi125.

Ofman, R., Dijkstra, Inge M E, *et al.* (2010) 'The role of ELOVL1 in very long-chain fatty acid homeostasis and X-linked adrenoleukodystrophy.', *EMBO molecular medicine*. Wiley-Blackwell, 2(3), pp. 90–7. doi: 10.1002/emmm.201000061.

Ofman, R., Dijkstra, Inge M. E., *et al.* (2010) 'The role of ELOVL1 in very long-chain fatty acid homeostasis and X-linked adrenoleukodystrophy', *EMBO Molecular Medicine*, 2(3), pp. 90–97. doi: 10.1002/emmm.201000061.

Ohashi, Y., Dogru, M. and Tsubota, K. (2006) 'Laboratory findings in tear fluid analysis', *Clinica Chimica Acta*, 369(1), pp. 17–28. doi: 10.1016/j.cca.2005.12.035.

Oppenheim, R. W. (1989) 'The neurotrophic theory and naturally occurring motoneuron death.', *Trends in neurosciences*, 12(7), pp. 252–5. Available at: http://www.ncbi.nlm.nih.gov/pubmed/2475935 (Accessed: 31 March 2019).

Perea, G., Navarrete, M. and Araque, A. (2009) 'Tripartite synapses: astrocytes process and control synaptic information.', *Trends in neurosciences*, 32(8), pp. 421–31. doi: 10.1016/j.tins.2009.05.001.

Peters, C. *et al.* (2004) 'Cerebral X-linked adrenoleukodystrophy: the international hematopoietic cell transplantation experience from 1982 to 1999', *Blood*, 104(3), pp. 881–888. doi: 10.1182/blood-2003-10-3402.

Petrillo, S. *et al.* (2013) 'Glutathione imbalance in patients with X-linked adrenoleukodystrophy', *Molecular Genetics and Metabolism*, 109(4), pp. 366–370. doi: 10.1016/j.ymgme.2013.05.009.

Pfrieger, F. W. (2003) 'Role of cholesterol in synapse formation and function', *Biochimica et Biophysica Acta - Biomembranes*. Elsevier, pp. 271–280. doi: 10.1016/S0005-2736(03)00024-5.

Pfrieger, F. W. and Ungerer, N. (2011) 'Cholesterol metabolism in neurons and astrocytes', *Progress in Lipid Research*, 50(4), pp. 357–371. doi: 10.1016/j.plipres.2011.06.002.

Pollegioni, L., Sacchi, S. and Murtas, G. (2018) 'Human D-Amino Acid Oxidase: Structure, Function, and Regulation', *Frontiers in Molecular Biosciences*, 5, p. 107. doi: 10.3389/fmolb.2018.00107.

Poulos, A. (1995) 'Very long chain fatty acids in higher animals—A review', *Lipids*, 30(1), pp. 1–14. doi: 10.1007/BF02537036.

Powell, H. *et al.* (1975) 'Adrenoleukodystrophy. Electron microscopic findings.', *Archives of neurology*, 32(4), pp. 250–60. Available at: http://www.ncbi.nlm.nih.gov/pubmed/164848 (Accessed: 16 March 2019).

Powers, J. M. *et al.* (1982) 'Fetal adrenoleukodystrophy: The significance of pathologic lesions in adrenal gland and testis', *Human Pathology*. W.B. Saunders, 13(11), pp. 1013–1019. doi: 10.1016/S0046-8177(82)80093-2.

Powers, J. M. *et al.* (2001) 'The dorsal root ganglia in adrenomyeloneuropathy: neuronal atrophy and abnormal mitochondria.', *Journal of neuropathology and experimental neurology*, 60(5), pp. 493–501. Available at: http://www.ncbi.nlm.nih.gov/pubmed/11379824 (Accessed: 20 March 2019).

Powers, J. M. *et al.* (2005) 'Adreno-leukodystrophy: Oxidative Stress of Mice and Men', *Journal of Neuropathology and Experimental Neurology*. Oxford University Press, 64(12), pp. 1067–1079. doi: 10.1097/01.jnen.0000190064.28559.a4.

POWERS, J. M. *et al.* (1992) 'The Inflammatory Myelinopathy of Adreno-Leukodystrophy', *Journal of Neuropathology and Experimental Neurology*. Oxford University Press, 51(6), pp. 630–643. doi: 10.1097/00005072-199211000-00007.

Presente, A., Andres, A. and Nye, J. S. (2001) 'Requirement of Notch in adulthood for neurological function and longevity', *NeuroReport*. Lippincott Williams and Wilkins, 12(15), pp. 3321–3325. doi: 10.1097/00001756-200110290-00035.

PROTTEY, C. (1977) 'Investigation of functions of essential fatty acids in the skin', *British Journal of Dermatology*, 97(1), pp. 29–38. doi: 10.1111/j.1365-2133.1977.tb15424.x.

Pujol, A. *et al.* (2002) 'Late onset neurological phenotype of the X-ALD gene inactivation in mice: a mouse model for adrenomyeloneuropathy.', *Human molecular genetics*, 11(5), pp. 499–505. Available at: http://www.ncbi.nlm.nih.gov/pubmed/11875044 (Accessed: 18 March 2019).

Pujol, A. *et al.* (2004) 'Functional overlap between ABCD1 (ALD) and ABCD2 (ALDR) transporters: a therapeutic target for X-adrenoleukodystrophy', *Human Molecular Genetics*. Oxford University Press, 13(23), pp. 2997–3006. doi: 10.1093/hmg/ddh323.

Ray, A., Girimaji, S. C. and Bharath, R. D. (2017) 'Adolescent-onset X-linked Adrenoleukodystrophy Presenting as Treatment-resistant Bipolar Disorder.', *Indian journal of psychological medicine*, 39(5), pp. 685–687. doi: 10.4103/IJPSYM.IJPSYM_36_17.

Raymond, G. V. *et al.* (2018) 'Survival and Functional Outcomes in Boys with Cerebral Adrenoleukodystrophy with and without Hematopoietic Stem Cell Transplantation', *Biology of Blood and Marrow Transplantation*. Elsevier. doi: 10.1016/J.BBMT.2018.09.036.

Raymond, G. V, Moser, A. B. and Fatemi, A. (1993) *X-Linked Adrenoleukodystrophy*, *GeneReviews®*. University of Washington, Seattle. Available at: http://www.ncbi.nlm.nih.gov/pubmed/20301491 (Accessed: 17 March 2019).

Reemst, K. *et al.* (2016) 'The Indispensable Roles of Microglia and Astrocytes during Brain Development.', *Frontiers in human neuroscience*. Frontiers Media SA, 10, p. 566. doi: 10.3389/fnhum.2016.00566.

Rizzo, W. B. *et al.* (1989) 'Dietary erucic acid therapy for X-linked adrenoleukodystrophy.', *Neurology*, 39(11), pp. 1415–22. Available at: http://www.ncbi.nlm.nih.gov/pubmed/2682348 (Accessed: 17 March 2019).

Robinson, B. S., Johnson, D. W. and Poulos, A. (1990) 'Metabolism of hexacosatetraenoic acid ($C_{26:4,n-6}$) in immature rat brain', *Biochemical Journal*, 267(2), pp. 561–564. doi: 10.1042/bj2670561.

Roerig, P. *et al.* (2001) 'Characterization and functional analysis of the nucleotide binding fold in human peroxisomal ATP binding cassette transporters', *FEBS Letters*, 492(1–2), pp. 66–72. doi: 10.1016/S0014-5793(01)02235-9.

van Roermund, C. W. T. *et al.* (2008) 'The human peroxisomal ABC half transporter ALDP functions as a homodimer and accepts acyl-CoA esters', *The FASEB Journal*. Federation of American Societies for Experimental Biology, 22(12), pp. 4201–4208. doi: 10.1096/fj.08-110866.

Rubia, K. (2018) 'Cognitive Neuroscience of Attention Deficit Hyperactivity Disorder (ADHD) and Its Clinical Translation.', *Frontiers in human neuroscience*. Frontiers Media SA, 12, p. 100. doi: 10.3389/fnhum.2018.00100.

Saab, A. S., Tzvetanova, I. D. and Nave, K.-A. (2013) 'The role of myelin and oligodendrocytes in axonal energy metabolism', *Current Opinion in Neurobiology*, 23(6), pp. 1065–1072. doi: 10.1016/j.conb.2013.09.008.

Saharan, S. and Mandal, P. K. (2014) 'The emerging role of glutathione in Alzheimer's disease.', *Journal of Alzheimer's disease : JAD*, 40(3), pp. 519–29. doi: 10.3233/JAD-132483.

Sahores, M., Gibb, A. and Salinas, P. C. (2010) 'Frizzled-5, a receptor for the synaptic organizer Wnt7a, regulates activity-mediated synaptogenesis', *Development*, 137(13), pp. 2215–2225. doi: 10.1242/dev.046722.

SanGiovanni, J. P. and Chew, E. Y. (2005) 'The role of omega-3 long-chain polyunsaturated fatty acids in health and disease of the retina', *Progress in Retinal and Eye Research*, 24(1), pp. 87–138. doi: 10.1016/j.preteyeres.2004.06.002.

Sassa, T. *et al.* (2014) 'Lorenzo's oil inhibits ELOVL1 and lowers the level of sphingomyelin with a

saturated very long-chain fatty acid', *Journal of Lipid Research*, 55(3), pp. 524–530. doi: 10.1194/jlr.M044586.

Sassa, T. and Kihara, A. (2014) 'Metabolism of very long-chain Fatty acids: genes and pathophysiology.', *Biomolecules & therapeutics*. Korean Society of Applied Pharmacology, 22(2), pp. 83–92. doi: 10.4062/biomolther.2014.017.

Sastry, P. S. (1985) 'Lipids of nervous tissue: composition and metabolism.', *Progress in lipid research*, 24(2), pp. 69–176. Available at: http://www.ncbi.nlm.nih.gov/pubmed/3916238 (Accessed: 25 July 2019).

Schlüter, A., Espinosa, L., Fourcade, S., Galino, J., López, E., *et al.* (2012) 'Functional genomic analysis unravels a metabolic-inflammatory interplay in adrenoleukodystrophy', *Human Molecular Genetics*, 21(5), pp. 1062–1077. doi: 10.1093/hmg/ddr536.

Schlüter, A., Espinosa, L., Fourcade, S., Galino, J., Lśpez, E., *et al.* (2012) 'Functional genomic analysis unravels a metabolic-inflammatory interplay in adrenoleukodystrophy', *Human Molecular Genetics*, 21(5), pp. 1062–1077. doi: 10.1093/hmg/ddr536.

Schmidt, C. *et al.* (2007) 'Wnt6 controls amniote neural crest induction through the non-canonical signaling pathway.', *Developmental dynamics : an official publication of the American Association of Anatomists*, 236(9), pp. 2502–11. doi: 10.1002/dvdy.21260.

Schmidt, C. *et al.* (2008) 'The role of Wnt signalling in the development of somites and neural crest.', *Advances in anatomy, embryology, and cell biology*, 195, pp. 1–64. Available at: http://www.ncbi.nlm.nih.gov/pubmed/18637521 (Accessed: 24 September 2019).

Schrader, M. *et al.* (2015) 'The different facets of organelle interplay—an overview of organelle interactions', *Frontiers in Cell and Developmental Biology*, 3(September), pp. 1–22. doi: 10.3389/fcell.2015.00056.

Schrader, M., Kamoshita, M. and Islinger, M. (2019) 'Organelle interplay—peroxisome interactions in health and disease', *Journal of Inherited Metabolic Disease*. John Wiley and Sons Inc. doi: 10.1002/jimd.12083.

Scriver, C. R. (2001) *The metabolic & molecular bases of inherited disease*. McGraw-Hill. Available at: https://books.google.es/books/about/The_Metabolic_Molecular_Bases_of_Inherit.html?id=ud5pAAAAMAAJ&redir_esc=y (Accessed: 17 March 2019).

Shamim, D. and Alleyne, K. (2017) 'X-linked adult-onset adrenoleukodystrophy: Psychiatric and neurological manifestations.', *SAGE open medical case reports*. SAGE Publications, 5, p. 2050313X17741009. doi: 10.1177/2050313X17741009.

Shapiro, E. *et al.* (2000) 'Long-term effect of bone-marrow transplantation for childhood-onset cerebral X-linked adrenoleukodystrophy', *The Lancet*, 356(9231), pp. 713–718. doi: 10.1016/S0140-6736(00)02629-5.

Sherry, D. M. *et al.* (2017) 'Distribution of ELOVL4 in the Developing and Adult Mouse Brain', *Frontiers in Neuroanatomy*, 11. doi: 10.3389/fnana.2017.00038.

Siemerling, E. and Creutzfeldt, H. G. (1923) 'Bronzekrankheit und sklerosierende Encephalomyelitis', *Archiv für Psychiatrie und Nervenkrankheiten*. Springer-Verlag, 68(1), pp. 217–244. doi: 10.1007/BF01835678.

Singh, H. *et al.* (1992) 'Peroxisomal beta-oxidation of branched chain fatty acids in human skin fibroblasts.', *Journal of lipid research*, 33(11), pp. 1597–605. Available at: http://www.ncbi.nlm.nih.gov/pubmed/1464743 (Accessed: 20 March 2019).

Singh, I. *et al.* (1984) 'Lignoceric acid is oxidized in the peroxisome: implications for the Zellweger cerebro-hepato-renal syndrome and adrenoleukodystrophy.', *Proceedings of the National Academy of Sciences*, 81(13), pp. 4203–4207. doi: 10.1073/pnas.81.13.4203.

Singh, I. *et al.* (1998) 'Lovastatin for X-Linked Adrenoleukodystrophy', *New England Journal of Medicine*, 339(10), pp. 702–703. doi: 10.1056/NEJM199809033391012.

Sousa, K. M. *et al.* (2010) 'Wnt2 regulates progenitor proliferation in the developing ventral midbrain', *Journal of Biological Chemistry*, 285(10), pp. 7246–7253. doi: 10.1074/jbc.M109.079822.

Stevens, B. *et al.* (2007) 'The Classical Complement Cascade Mediates CNS Synapse Elimination', *Cell*. Cell Press, 131(6), pp. 1164–1178. doi: 10.1016/J.CELL.2007.10.036.

Stiles, J. and Jernigan, T. L. (2010) 'The basics of brain development.', *Neuropsychology review*. Springer, 20(4), pp. 327–48. doi: 10.1007/s11065-010-9148-4.

Südhof, T. C. (2012) 'Calcium control of neurotransmitter release', *Cold Spring Harbor Perspectives in Biology*. Cold Spring Harbor Laboratory Press, 4(1). doi: 10.1101/cshperspect.a011353.

Tabatadze, N. *et al.* (2012) 'Wnt transmembrane signaling and long-term spatial memory.', *Hippocampus*, 22(6), pp. 1228–41. doi: 10.1002/hipo.20991.

Temple S (2001) 'The development of neural stem cells', *Nature*, 414(6859), pp. 112–117. Available at: http://www.ncbi.nlm.nih.gov/entrez/query.fcgi?cmd=Retrieve&db=PubMed&dopt=Citation&list_uids=11689956 (Accessed: 24 September 2019).

Theda, C. *et al.* (1992) 'Phospholipids in X-linked adrenoleukodystrophy white matter: fatty acid abnormalities before the onset of demyelination.', *Journal of the neurological sciences*, 110(1–2), pp. 195–204. Available at: http://www.ncbi.nlm.nih.gov/pubmed/1506859 (Accessed: 20 March 2019).

Tonge, D. A. *et al.* (2012) 'Fibronectin supports neurite outgrowth and axonal regeneration of adult brain neurons in vitro', *Brain Research*, 1453, pp. 8–16. doi: 10.1016/j.brainres.2012.03.024.

TSUJI, S. *et al.* (1981) 'Increased Synthesis of Hexacosanoic Acid (C26 :0) by Cultured Skin Fibroblasts from Patients with Adrenoleukodystrophy (ALD) and Adrenomyeloneuropathy (AMN)1', *The Journal of Biochemistry*, 90(4), pp. 1233–1236. doi: 10.1093/oxfordjournals.jbchem.a133578.

Valianpour, F. *et al.* (2003) 'Analysis of very long-chain fatty acids using electrospray ionization mass spectrometry.', *Molecular genetics and metabolism*, 79(3), pp. 189–96. Available at: http://www.ncbi.nlm.nih.gov/pubmed/12855224 (Accessed: 17 March 2019).

Vargas, C. . *et al.* (2004) 'Evidence that oxidative stress is increased in patients with X-linked adrenoleukodystrophy', *Biochimica et Biophysica Acta (BBA) - Molecular Basis of Disease*, 1688(1), pp. 26–32. doi: 10.1016/j.bbadis.2003.10.004.

Wanders, R. J. *et al.* (2001) 'Peroxisomal fatty acid alpha- and beta-oxidation in humans: enzymology, peroxisomal metabolite transporters and peroxisomal diseases.', *Biochemical Society transactions*, 29(Pt 2), pp. 250–67. Available at: http://www.ncbi.nlm.nih.gov/pubmed/11356164 (Accessed: 17 March 2019).

Wanders, R. J. A., Komen, J. and Ferdinandusse, S. (2011) 'Phytanic acid metabolism in health and disease', *Biochimica et Biophysica Acta (BBA) - Molecular and Cell Biology of Lipids*, 1811(9), pp. 498–507. doi: 10.1016/j.bbalip.2011.06.006.

Wanders, R. J. A., Waterham, H. R. and Ferdinandusse, S. (2016) 'Metabolic Interplay between Peroxisomes and Other Subcellular Organelles Including Mitochondria and the Endoplasmic Reticulum', *Frontiers in Cell and Developmental Biology*. Frontiers, 3, p. 83. doi: 10.3389/fcell.2015.00083.

Wang, X. F. and Cynader, M. S. (2000) 'Astrocytes provide cysteine to neurons by releasing glutathione.', *Journal of neurochemistry*, 74(4), pp. 1434–42. doi: 10.1046/j.1471-4159.2000.0741434.x.

Weissman, T. *et al.* (2003) 'Neurogenic radial glial cells in reptile, rodent and human: from mitosis to migration.', *Cerebral cortex (New York, N.Y. : 1991)*, 13(6), pp. 550–9. Available at: http://www.ncbi.nlm.nih.gov/pubmed/12764028 (Accessed: 30 March 2019).

Whitcomb, R. W., Linehan, W. M. and Knazek, R. A. (1988) 'Effects of long-chain, saturated fatty acids on membrane microviscosity and adrenocorticotropin responsiveness of human adrenocortical cells in vitro.', *Journal of Clinical Investigation*, 81(1), pp. 185–188. doi: 10.1172/JCI113292.

Wiedenmann, B. *et al.* (1986) 'Synaptophysin: A marker protein for neuroendocrine cells and neoplasms', *Proceedings of the National Academy of Sciences of the United States of America*, 83(10), pp. 3500–3504. doi: 10.1073/pnas.83.10.3500.

Wiesinger, C. *et al.* (2013) 'Impaired Very Long-chain Acyl-CoA β-Oxidation in Human X-linked Adrenoleukodystrophy Fibroblasts Is a Direct Consequence of ABCD1 Transporter Dysfunction', *Journal of Biological Chemistry*, 288(26), pp. 19269–19279. doi: 10.1074/jbc.M112.445445.

Wu, D. and Pan, W. (2010) 'GSK3: a multifaceted kinase in Wnt signaling', *Trends in Biochemical Sciences*, pp. 161–168. doi: 10.1016/j.tibs.2009.10.002.

Yan, F. *et al.* (2017) 'S149R, a novel mutation in the ABCD1 gene causing X-linked adrenoleukodystrophy', *Oncotarget*. Impact Journals LLC, 8(50), pp. 87529–87538. doi: 10.18632/oncotarget.20974.

Yan, Y. *et al.* (2004a) 'Stat3 Signaling Is Present and Active During Development of the Central Nervous System and Eye of Vertebrates', *Developmental Dynamics*, 231, pp. 248–257. doi: 10.1002/dvdy.20126.

Yan, Y. *et al.* (2004b) 'Stat3 Signaling Is Present and Active During Development of the Central Nervous System and Eye of Vertebrates', *Developmental Dynamics*, 231, pp. 248–257. doi: 10.1002/dvdy.20126.

Zalc, B., Goujet, D. and Colman, D. (2008) 'The origin of the myelination program in vertebrates', *Current Biology*, 18(12), pp. R511–R512. doi: 10.1016/j.cub.2008.04.010.

Zhang, K. *et al.* (2001) 'A 5-bp deletion in ELOVL4 is associated with two related forms of autosomal dominant macular dystrophy', *Nature Genetics*, 27(1), pp. 89–93. doi: 10.1038/83817.

Zhang, S. *et al.* (2017) 'Necroptosis in neurodegenerative diseases: a potential therapeutic target', *Cell Death and Disease*. Nature Publishing Group, 8(6), p. e2905. doi: 10.1038/cddis.2017.286.

Zheng, F. *et al.* (2017) 'Unusual brain images of a boy with adolescent cerebral X-linked adrenoleukodystrophy presenting with exhibitionism', *Medicine*, 96(51), p. e9481. doi: 10.1097/MD.0000000000009481.

Annex 1

Supplementary table 1. Categories and clusters enriched in X-ALD children.

Cluster	Nodes (GOs)	GO	ES	FDR q-val
Immune system				
antigen wnt pathway	46	GO_WNT_SIGNALING_PATHWAY	0.349	0.179
		GO_T_CELL_RECEPTOR_SIGNALING_PATHWAY	0.494	0.052
		GO_TOLL_LIKE_RECEPTOR_SIGNALING_PATHWAY	0.534	0.050
		GO_REGULATION_OF_WNT_SIGNALING_PATHWAY	0.440	0.054
		GO_REGULATION_OF_PROTEIN_UBIQUITINATION_INVOLVED_IN_UBIQUITIN_DEPENDENT_PROTEIN_CATABOLIC_PROCESS	0.425	0.179
		GO_REGULATION_OF_PROTEIN_MODIFICATION_BY_SMALL_PROTEIN_CONJUGATION_OR_REMOVAL	0.440	0.078
		GO_REGULATION_OF_LIGASE_ACTIVITY	0.436	0.150
		GO_REGULATION_OF_LEUKOCYTE_MEDIATED_IMMUNITY	0.374	0.217
		GO_REGULATION_OF_INNATE_IMMUNE_RESPONSE	0.409	0.077
		GO_REGULATION_OF_IMMUNE_RESPONSE	0.315	0.188
		GO_REGULATION_OF_IMMUNE_EFFECTOR_PROCESS	0.315	0.229
		GO_REGULATION_OF_ESTABLISHMENT_OF_PLANAR_POLARITY	0.539	0.056
		GO_REGULATION_OF_CELLULAR_KETONE_METABOLIC_PROCESS	0.379	0.175
		GO_REGULATION_OF_CELLULAR_AMINO_ACID_METABOLIC_PROCESS	0.499	0.093
		GO_REGULATION_OF_CELLULAR_AMINE_METABOLIC_PROCESS	0.454	0.115
		GO_REGULATION_OF_CANONICAL_WNT_SIGNALING_PATHWAY	0.492	0.028
		GO_PROTEIN_UBIQUITINATION	0.387	0.086
		GO_PROTEIN_MODIFICATION_BY_SMALL_PROTEIN_CONJUGATION_OR_REMOVAL	0.350	0.136
		GO_POSITIVE_REGULATION_OF_WNT_SIGNALING_PATHWAY	0.382	0.213
		GO_POSITIVE_REGULATION_OF_PROTEIN_MODIFICATION_BY_SMALL_PROTEIN_CONJUGATION_OR_REMOVAL	0.452	0.103
		GO_POSITIVE_REGULATION_OF_LYMPHOCYTE_MEDIATED_IMMUNITY	0.423	0.244
		GO_POSITIVE_REGULATION_OF_LIGASE_ACTIVITY	0.437	0.172
		GO_POSITIVE_REGULATION_OF_LEUKOCYTE_MEDIATED_IMMUNITY	0.440	0.176
		GO_POSITIVE_REGULATION_OF_INNATE_IMMUNE_RESPONSE	0.451	0.051
		GO_POSITIVE_REGULATION_OF_IMMUNE_SYSTEM_PROCESS	0.298	0.233
		GO_POSITIVE_REGULATION_OF_IMMUNE_RESPONSE	0.359	0.125
		GO_POSITIVE_REGULATION_OF_DEFENSE_RESPONSE	0.377	0.118
		GO_POSITIVE_REGULATION_OF_CELL_KILLING	0.488	0.172
		GO_POSITIVE_REGULATION_OF_CANONICAL_WNT_SIGNALING_PATHWAY	0.403	0.201
		GO_PATTERN_RECOGNITION_RECEPTOR_SIGNALING_PATHWAY	0.458	0.115
		GO_NON_CANONICAL_WNT_SIGNALING_PATHWAY	0.436	0.139
		GO_NIK_NF_KAPPAB_SIGNALING	0.408	0.210
		GO_NEGATIVE_REGULATION_OF_WNT_SIGNALING_PATHWAY	0.490	0.040

		GO_NEGATIVE_REGULATION_OF_CANONICAL_WNT_SIGNALING_PATHWAY	0.543	0.015
		GO_INNATE_IMMUNE_RESPONSE_ACTIVATING_CELL_SURFACE_RECEPTOR_SIGNALING_PATHWAY	0.575	0.026
		GO_IMMUNE_RESPONSE_REGULATING_CELL_SURFACE_RECEPTOR_SIGNALING_PATHWAY	0.355	0.173
		GO_FC_RECEPTOR_SIGNALING_PATHWAY	0.373	0.174
		GO_FC_EPSILON_RECEPTOR_SIGNALING_PATHWAY	0.431	0.108
		GO_B_CELL_RECEPTOR_SIGNALING_PATHWAY	0.463	0.241
		GO_ANTIGEN_RECEPTOR_MEDIATED_SIGNALING_PATHWAY	0.415	0.122
		GO_ANTIGEN_PROCESSING_AND_PRESENTATION_OF_PEPTIDE_ANTIGEN_VIA_MHC_CLASS_I	0.575	0.019
		GO_ANTIGEN_PROCESSING_AND_PRESENTATION_OF_PEPTIDE_ANTIGEN	0.493	0.049
		GO_ANTIGEN_PROCESSING_AND_PRESENTATION_OF_EXOGENOUS_PEPTIDE_ANTIGEN_VIA_MHC_CLASS_I	0.610	0.029
		GO_ANTIGEN_PROCESSING_AND_PRESENTATION	0.469	0.050
		GO_ACTIVATION_OF_INNATE_IMMUNE_RESPONSE	0.494	0.036
		GO_ACTIVATION_OF_IMMUNE_RESPONSE	0.400	0.076
somatic recombination immune	19	GO_RESPONSE_TO_TYPE_I_INTERFERON	0.566	0.030
		GO_PROTEIN_ACTIVATION_CASCADE	0.545	0.044
		GO_LYMPHOCYTE_MEDIATED_IMMUNITY	0.589	0.012
		GO_LEUKOCYTE_MEDIATED_IMMUNITY	0.555	0.015
		GO_INNATE_IMMUNE_RESPONSE	0.411	0.049
		GO_INFLAMMATORY_RESPONSE	0.411	0.056
		GO_IMMUNE_RESPONSE	0.338	0.141
		GO_IMMUNE_EFFECTOR_PROCESS	0.395	0.081
		GO_HUMORAL_IMMUNE_RESPONSE_MEDIATED_BY_CIRCULATING_IMMUNOGLOBULIN	0.670	0.027
		GO_HUMORAL_IMMUNE_RESPONSE	0.451	0.067
		GO_DEFENSE_RESPONSE	0.360	0.089
		GO_COMPLEMENT_ACTIVATION	0.626	0.039
		GO_CELL_ACTIVATION_INVOLVED_IN_IMMUNE_RESPONSE	-0.338	0.206
		GO_CELLULAR_DEFENSE_RESPONSE	-0.426	0.165
		GO_B_CELL_MEDIATED_IMMUNITY	0.610	0.024
		GO_ADAPTIVE_IMMUNE_RESPONSE_BASED_ON_SOMATIC_RECOMBINATION_OF_IMMUNE_RECEPTORS_BUILT_FROM_IMMUNOGLOBULIN_SUPERFAMILY_DOMAINS	0.627	0.006
		GO_ADAPTIVE_IMMUNE_RESPONSE	0.406	0.081
		GO_ACUTE_PHASE_RESPONSE	0.575	0.056
		GO_ACUTE_INFLAMMATORY_RESPONSE	0.625	0.014
leukocyte proliferation fibroblast	10	GO_REGULATION_OF_LEUKOCYTE_PROLIFERATION	0.398	0.126
		GO_REGULATION_OF_HOMOTYPIC_CELL_CELL_ADHESION	0.341	0.190
		GO_REGULATION_OF_FIBROBLAST_PROLIFERATION	0.496	0.118
		GO_REGULATION_OF_ENDOTHELIAL_CELL_PROLIFERATION	0.464	0.087
		GO_REGULATION_OF_CELL_PROLIFERATION	0.311	0.184
		GO_POSITIVE_REGULATION_OF_LEUKOCYTE_PROLIFERATION	0.386	0.193

		GO_POSITIVE_REGULATION_OF_FIBROBLAST_PROLIFERATION	0.451	0.230
		GO_NEGATIVE_REGULATION_OF_EPITHELIAL_CELL_PROLIFERATION	0.427	0.128
		GO_NEGATIVE_REGULATION_OF_CELL_PROLIFERATION	0.389	0.078
		GO_NEGATIVE_REGULATION_OF_CELL_ACTIVATION	0.408	0.174
interferon gamma cytokine	10	GO_TUMOR_NECROSIS_FACTOR_MEDIATED_SIGNALING_PATHWAY	0.435	0.125
		GO_RESPONSE_TO_TUMOR_NECROSIS_FACTOR	0.359	0.179
		GO_RESPONSE_TO_INTERLEUKIN_1	0.482	0.092
		GO_RESPONSE_TO_INTERFERON_GAMMA	0.589	0.004
		GO_RESPONSE_TO_CYTOKINE	0.357	0.118
		GO_INTERFERON_GAMMA_MEDIATED_SIGNALING_PATHWAY	0.622	0.015
		GO_CYTOKINE_MEDIATED_SIGNALING_PATHWAY	0.332	0.174
		GO_CELLULAR_RESPONSE_TO_INTERLEUKIN_1	0.510	0.077
		GO_CELLULAR_RESPONSE_TO_INTERFERON_GAMMA	0.553	0.013
		GO_CELLULAR_RESPONSE_TO_CYTOKINE_STIMULUS	0.343	0.142
type interferon production	2	GO_REGULATION_OF_TYPE_I_INTERFERON_PRODUCTION	0.420	0.192
		GO_POSITIVE_REGULATION_OF_TYPE_I_INTERFERON_PRODUCTION	0.431	0.230
superfamily cytokine production	2	GO_REGULATION_OF_TUMOR_NECROSIS_FACTOR_SUPERFAMILY_CYTOKINE_PRODUCTION	0.649	0.015
		GO_POSITIVE_REGULATION_OF_TUMOR_NECROSIS_FACTOR_SUPERFAMILY_CYTOKINE_PRODUCTION	0.619	0.050
interspecies interaction organisms	2	GO_MODIFICATION_OF_MORPHOLOGY_OR_PHYSIOLOGY_OF_OTHER_ORGANISM	0.443	0.150
		GO_INTERSPECIES_INTERACTION_BETWEEN_ORGANISMS	0.366	0.109
viral genome replication	6	GO_REGULATION_OF_SYMBIOSIS_ENCOMPASSING_MUTUALISM_THROUGH_PARASITISM	0.459	0.057
		GO_REGULATION_OF_VIRAL_GENOME_REPLICATION	0.614	0.029
		GO_POSITIVE_REGULATION_OF_VIRAL_PROCESS	0.473	0.173
		GO_NEGATIVE_REGULATION_OF_VIRAL_PROCESS	0.517	0.076
		GO_REGULATION_OF_MULTI_ORGANISM_PROCESS	0.329	0.197
		GO_NEGATIVE_REGULATION_OF_MULTI_ORGANISM_PROCESS	0.429	0.121
Development/regeneration/differentiation/proliferation				
regulation muscle differentiation	37	GO_REGULATION_OF_VASCULATURE_DEVELOPMENT	0.434	0.067
		GO_REGULATION_OF_STEM_CELL_DIFFERENTIATION	0.485	0.084
		GO_REGULATION_OF_OSTEOBLAST_DIFFERENTIATION	0.534	0.035
		GO_REGULATION_OF_OSSIFICATION	0.522	0.019
		GO_REGULATION_OF_MYELOID_CELL_DIFFERENTIATION	0.371	0.192
		GO_REGULATION_OF_MUSCLE_TISSUE_DEVELOPMENT	0.405	0.203
		GO_REGULATION_OF_MUSCLE_CELL_DIFFERENTIATION	0.366	0.240
		GO_REGULATION_OF_MULTICELLULAR_ORGANISMAL_DEVELOPMENT	0.297	0.217
		GO_REGULATION_OF_LEUKOCYTE_DIFFERENTI	0.337	0.228

		ATION		
		GO_REGULATION_OF_GLIOGENESIS	0.425	0.203
		GO_REGULATION_OF_GLIAL_CELL_DIFFERENTIATION	0.494	0.175
		GO_REGULATION_OF_FAT_CELL_DIFFERENTIATION	0.476	0.121
		GO_REGULATION_OF_EPITHELIAL_CELL_DIFFERENTIATION	0.402	0.144
		GO_REGULATION_OF_ENDOTHELIAL_CELL_MIGRATION	0.402	0.186
		GO_REGULATION_OF_CELL_SHAPE	0.428	0.144
		GO_REGULATION_OF_CELL_MORPHOGENESIS	0.329	0.176
		GO_REGULATION_OF_CELL_DIFFERENTIATION	0.301	0.212
		GO_REGULATION_OF_BLOOD_VESSEL_ENDOTHELIAL_CELL_MIGRATION	0.513	0.155
		GO_REGULATION_OF_BIOMINERAL_TISSUE_DEVELOPMENT	0.437	0.227
		GO_REGULATION_OF_ANATOMICAL_STRUCTURE_MORPHOGENESIS	0.300	0.216
		GO_POSITIVE_REGULATION_OF_VASCULATURE_DEVELOPMENT	0.499	0.049
		GO_POSITIVE_REGULATION_OF_STRIATED_MUSCLE_CELL_DIFFERENTIATION	0.427	0.245
		GO_POSITIVE_REGULATION_OF_OSTEOBLAST_DIFFERENTIATION	0.586	0.035
		GO_POSITIVE_REGULATION_OF_OSSIFICATION	0.521	0.049
		GO_POSITIVE_REGULATION_OF_MUSCLE_TISSUE_DEVELOPMENT	0.472	0.140
		GO_POSITIVE_REGULATION_OF_MUSCLE_CELL_DIFFERENTIATION	0.403	0.233
		GO_NEGATIVE_REGULATION_OF_OSSIFICATION	0.576	0.054
		GO_NEGATIVE_REGULATION_OF_NEURON_DIFFERENTIATION	0.428	0.084
		GO_NEGATIVE_REGULATION_OF_NERVOUS_SYSTEM_DEVELOPMENT	0.379	0.136
		GO_NEGATIVE_REGULATION_OF_MYELOID_CELL_DIFFERENTIATION	0.484	0.130
		GO_NEGATIVE_REGULATION_OF_MULTICELLULAR_ORGANISMAL_PROCESS	0.372	0.079
		GO_NEGATIVE_REGULATION_OF_LEUKOCYTE_DIFFERENTIATION	0.436	0.177
		GO_NEGATIVE_REGULATION_OF_HEMOPOIESIS	0.451	0.111
		GO_NEGATIVE_REGULATION_OF_DEVELOPMENTAL_PROCESS	0.354	0.122
		GO_NEGATIVE_REGULATION_OF_CELL_PROJECTION_ORGANIZATION	0.380	0.185
		GO_NEGATIVE_REGULATION_OF_CELL_DIFFERENTIATION	0.379	0.086
		GO_NEGATIVE_REGULATION_OF_CELL_DEVELOPMENT	0.364	0.149
pancreas development morphogenesis	25	GO_UROGENITAL_SYSTEM_DEVELOPMENT	0.398	0.091
		GO_TISSUE_MORPHOGENESIS	0.302	0.244
		GO_TISSUE_DEVELOPMENT	0.294	0.217
		GO_RESPIRATORY_SYSTEM_DEVELOPMENT	0.348	0.205
		GO_RENAL_TUBULE_DEVELOPMENT	0.437	0.196
		GO_REGULATION_OF_KIDNEY_DEVELOPMENT	0.561	0.066
		GO_PANCREAS_DEVELOPMENT	0.452	0.144
		GO_ODONTOGENESIS	0.402	0.183
		GO_NEPHRON_DEVELOPMENT	0.446	0.121
		GO_METANEPHROS_DEVELOPMENT	0.440	0.136

		GO_MESONEPHROS_DEVELOPMENT	0.396	0.217
		GO_MESONEPHRIC_TUBULE_MORPHOGENESIS	0.522	0.131
		GO_MESODERM_MORPHOGENESIS	0.405	0.233
		GO_MESODERM_DEVELOPMENT	0.392	0.185
		GO_KIDNEY_MORPHOGENESIS	0.601	0.035
		GO_GLOMERULUS_DEVELOPMENT	0.502	0.151
		GO_GLAND_MORPHOGENESIS	0.438	0.106
		GO_GASTRULATION	0.362	0.221
		GO_EPITHELIAL_CELL_DIFFERENTIATION	0.304	0.230
		GO_EPITHELIAL_CELL_DEVELOPMENT	0.372	0.160
		GO_EMBRYONIC_SKELETAL_SYSTEM_MORPHOGENESIS	-0.305	0.230
		GO_DORSAL_VENTRAL_PATTERN_FORMATION	0.415	0.188
		GO_CONNECTIVE_TISSUE_DEVELOPMENT	0.344	0.206
		GO_CARTILAGE_DEVELOPMENT	0.341	0.243
		GO_APPENDAGE_DEVELOPMENT	0.379	0.174
neuron projection morphogenesis	14	GO_NEURON_PROJECTION_MORPHOGENESIS	0.434	0.050
		GO_NEURON_PROJECTION_GUIDANCE	0.385	0.136
		GO_NEURON_PROJECTION_DEVELOPMENT	0.419	0.050
		GO_NEURON_DIFFERENTIATION	0.367	0.088
		GO_NEURON_DEVELOPMENT	0.355	0.122
		GO_NEUROGENESIS	0.302	0.211
		GO_DENDRITE_MORPHOGENESIS	0.578	0.077
		GO_DENDRITE_DEVELOPMENT	0.479	0.100
		GO_CELL_PROJECTION_ORGANIZATION	0.364	0.093
		GO_CELL_PART_MORPHOGENESIS	0.398	0.070
		GO_CELL_MORPHOGENESIS_INVOLVED_IN_NEURON_DIFFERENTIATION	0.389	0.085
		GO_CELL_MORPHOGENESIS_INVOLVED_IN_DIFFERENTIATION	0.399	0.069
		GO_CELL_DEVELOPMENT	0.303	0.198
		GO_CELLULAR_COMPONENT_MORPHOGENESIS	0.370	0.084
regulation organ growth	6	GO_REGULATION_OF_ORGAN_GROWTH	0.473	0.216
		GO_REGULATION_OF_GROWTH	0.331	0.166
		GO_REGULATION_OF_DEVELOPMENTAL_GROWTH	0.351	0.164
		GO_REGULATION_OF_CELL_GROWTH	0.353	0.153
		GO_NEGATIVE_REGULATION_OF_GROWTH	0.363	0.173
		GO_NEGATIVE_REGULATION_OF_CELL_GROWTH	0.356	0.197
growth involved developmental	6	GO_ORGAN_GROWTH	0.409	0.207
		GO_GROWTH	0.428	0.050
		GO_DEVELOPMENTAL_GROWTH_INVOLVED_IN_MORPHOGENESIS	0.470	0.119
		GO_DEVELOPMENTAL_GROWTH	0.389	0.092
		GO_DEVELOPMENTAL_CELL_GROWTH	0.558	0.068
		GO_CELL_GROWTH	0.584	0.020
circulatory system angiogenesis	5	GO_VASCULATURE_DEVELOPMENT	0.330	0.179
		GO_HEART_DEVELOPMENT	0.330	0.174
		GO_CIRCULATORY_SYSTEM_DEVELOPMENT	0.329	0.164

		GO_BLOOD_VESSEL_MORPHOGENESIS	0.367	0.132
		GO_ANGIOGENESIS	0.338	0.197
glial oligodendrocyte gliogenesis	4	GO_OLIGODENDROCYTE_DIFFERENTIATION	0.479	0.172
		GO_GLIOGENESIS	0.412	0.125
		GO_GLIAL_CELL_DIFFERENTIATION	0.388	0.184
		GO_GLIAL_CELL_DEVELOPMENT	0.474	0.138
reproductive primary sexual	3	GO_REPRODUCTIVE_SYSTEM_DEVELOPMENT	0.316	0.216
		GO_OVULATION_CYCLE	0.427	0.126
		GO_DEVELOPMENT_OF_PRIMARY_SEXUAL_CHARACTERISTICS	0.337	0.226
central neural midbrain	3	GO_NEURAL_NUCLEUS_DEVELOPMENT	0.507	0.125
		GO_MIDBRAIN_DEVELOPMENT	0.539	0.066
		GO_CENTRAL_NERVOUS_SYSTEM_DEVELOPMENT	0.300	0.224
cellular size extent	3	GO_REGULATION_OF_EXTENT_OF_CELL_GROWTH	0.387	0.216
		GO_REGULATION_OF_CELL_SIZE	0.412	0.118
		GO_REGULATION_OF_CELLULAR_COMPONENT_SIZE	0.335	0.206
skin epidermis development	2	GO_SKIN_EPIDERMIS_DEVELOPMENT	0.440	0.177
		GO_MOLTING_CYCLE	0.410	0.216
osteoblast differentiation ossification	2	GO_OSTEOBLAST_DIFFERENTIATION	0.417	0.129
		GO_OSSIFICATION	0.344	0.175
organ regeneration	2	GO_REGENERATION	0.505	0.028
		GO_ORGAN_REGENERATION	0.418	0.165
muscle structure development	2	GO_MYOBLAST_DIFFERENTIATION	0.456	0.233
		GO_MUSCLE_STRUCTURE_DEVELOPMENT	0.364	0.132
antigen wnt pathway	46	GO_WNT_SIGNALING_PATHWAY	0.349	0.179
		GO_T_CELL_RECEPTOR_SIGNALING_PATHWAY	0.494	0.052
		GO_TOLL_LIKE_RECEPTOR_SIGNALING_PATHWAY	0.534	0.050
		GO_REGULATION_OF_WNT_SIGNALING_PATHWAY	0.440	0.054
		GO_REGULATION_OF_PROTEIN_UBIQUITINATION_INVOLVED_IN_UBIQUITIN_DEPENDENT_PROTEIN_CATABOLIC_PROCESS	0.425	0.179
		GO_REGULATION_OF_PROTEIN_MODIFICATION_BY_SMALL_PROTEIN_CONJUGATION_OR_REMOVAL	0.440	0.078
		GO_REGULATION_OF_LIGASE_ACTIVITY	0.436	0.150
		GO_REGULATION_OF_LEUKOCYTE_MEDIATED_IMMUNITY	0.374	0.217
		GO_REGULATION_OF_INNATE_IMMUNE_RESPONSE	0.409	0.077
		GO_REGULATION_OF_IMMUNE_RESPONSE	0.315	0.188
		GO_REGULATION_OF_IMMUNE_EFFECTOR_PROCESS	0.315	0.229
		GO_REGULATION_OF_ESTABLISHMENT_OF_PLANAR_POLARITY	0.539	0.056
		GO_REGULATION_OF_CELLULAR_KETONE_METABOLIC_PROCESS	0.379	0.175
		GO_REGULATION_OF_CELLULAR_AMINO_ACID_METABOLIC_PROCESS	0.499	0.093
		GO_REGULATION_OF_CELLULAR_AMINE_METABOLIC_PROCESS	0.454	0.115
		GO_REGULATION_OF_CANONICAL_WNT_SIGNALING_PATHWAY	0.492	0.028
		GO_PROTEIN_UBIQUITINATION	0.387	0.086

		GO_PROTEIN_MODIFICATION_BY_SMALL_PROTEIN_CONJUGATION_OR_REMOVAL	0.350	0.136
		GO_POSITIVE_REGULATION_OF_WNT_SIGNALING_PATHWAY	0.382	0.213
		GO_POSITIVE_REGULATION_OF_PROTEIN_MODIFICATION_BY_SMALL_PROTEIN_CONJUGATION_OR_REMOVAL	0.452	0.103
		GO_POSITIVE_REGULATION_OF_LYMPHOCYTE_MEDIATED_IMMUNITY	0.423	0.244
		GO_POSITIVE_REGULATION_OF_LIGASE_ACTIVITY	0.437	0.172
		GO_POSITIVE_REGULATION_OF_LEUKOCYTE_MEDIATED_IMMUNITY	0.440	0.176
		GO_POSITIVE_REGULATION_OF_INNATE_IMMUNE_RESPONSE	0.451	0.051
		GO_POSITIVE_REGULATION_OF_IMMUNE_SYSTEM_PROCESS	0.298	0.233
		GO_POSITIVE_REGULATION_OF_IMMUNE_RESPONSE	0.359	0.125
		GO_POSITIVE_REGULATION_OF_DEFENSE_RESPONSE	0.377	0.118
		GO_POSITIVE_REGULATION_OF_CELL_KILLING	0.488	0.172
		GO_POSITIVE_REGULATION_OF_CANONICAL_WNT_SIGNALING_PATHWAY	0.403	0.201
		GO_PATTERN_RECOGNITION_RECEPTOR_SIGNALING_PATHWAY	0.458	0.115
		GO_NON_CANONICAL_WNT_SIGNALING_PATHWAY	0.436	0.139
		GO_NIK_NF_KAPPAB_SIGNALING	0.408	0.210
		GO_NEGATIVE_REGULATION_OF_WNT_SIGNALING_PATHWAY	0.490	0.040
		GO_NEGATIVE_REGULATION_OF_CANONICAL_WNT_SIGNALING_PATHWAY	0.543	0.015
		GO_INNATE_IMMUNE_RESPONSE_ACTIVATING_CELL_SURFACE_RECEPTOR_SIGNALING_PATHWAY	0.575	0.026
		GO_IMMUNE_RESPONSE_REGULATING_CELL_SURFACE_RECEPTOR_SIGNALING_PATHWAY	0.355	0.173
		GO_FC_RECEPTOR_SIGNALING_PATHWAY	0.373	0.174
		GO_FC_EPSILON_RECEPTOR_SIGNALING_PATHWAY	0.431	0.108
		GO_B_CELL_RECEPTOR_SIGNALING_PATHWAY	0.463	0.241
		GO_ANTIGEN_RECEPTOR_MEDIATED_SIGNALING_PATHWAY	0.415	0.122
		GO_ANTIGEN_PROCESSING_AND_PRESENTATION_OF_PEPTIDE_ANTIGEN_VIA_MHC_CLASS_I	0.575	0.019
		GO_ANTIGEN_PROCESSING_AND_PRESENTATION_OF_PEPTIDE_ANTIGEN	0.493	0.049
		GO_ANTIGEN_PROCESSING_AND_PRESENTATION_OF_EXOGENOUS_PEPTIDE_ANTIGEN_VIA_MHC_CLASS_I	0.610	0.029
		GO_ANTIGEN_PROCESSING_AND_PRESENTATION	0.469	0.050
		GO_ACTIVATION_OF_INNATE_IMMUNE_RESPONSE	0.494	0.036
		GO_ACTIVATION_OF_IMMUNE_RESPONSE	0.400	0.076
General Metabolism				
nucleoside triphosphate metabolic	34	GO_RIBONUCLEOSIDE_DIPHOSPHATE_METABOLIC_PROCESS	0.432	0.232
		GO_POLYSACCHARIDE_METABOLIC_PROCESS	0.463	0.141
		GO_PHENOL_CONTAINING_COMPOUND_METABOLIC_PROCESS	0.414	0.240
		GO_PEPTIDE_METABOLIC_PROCESS	0.363	0.122
		GO_OXIDATIVE_PHOSPHORYLATION	0.480	0.201

		GO_OXIDATION_REDUCTION_PROCESS	0.301	0.232
		GO_ORGANOPHOSPHATE_METABOLIC_PROCESS	0.295	0.241
		GO_ORGANONITROGEN_COMPOUND_METABOLIC_PROCESS	0.303	0.201
		GO_ORGANONITROGEN_COMPOUND_BIOSYNTHETIC_PROCESS	0.319	0.179
		GO_NUCLEOTIDE_PHOSPHORYLATION	0.472	0.208
		GO_NUCLEOSIDE_TRIPHOSPHATE_METABOLIC_PROCESS	0.366	0.198
		GO_NUCLEOSIDE_MONOPHOSPHATE_METABOLIC_PROCESS	0.348	0.240
		GO_MUCOPOLYSACCHARIDE_METABOLIC_PROCESS	0.441	0.151
		GO_MONOSACCHARIDE_METABOLIC_PROCESS	0.361	0.198
		GO_HEXOSE_METABOLIC_PROCESS	0.389	0.167
		GO_GLUTAMINE_FAMILY_AMINO_ACID_METABOLIC_PROCESS	0.523	0.097
		GO_GLUCOSE_METABOLIC_PROCESS	0.378	0.240
		GO_GLUCAN_METABOLIC_PROCESS	0.482	0.174
		GO_GENERATION_OF_PRECURSOR_METABOLITES_AND_ENERGY	0.349	0.175
		GO_ENERGY_DERIVATION_BY_OXIDATION_OF_ORGANIC_COMPOUNDS	0.366	0.186
		GO_ELECTRON_TRANSPORT_CHAIN	0.462	0.184
		GO_CYCLIC_NUCLEOTIDE_METABOLIC_PROCESS	0.480	0.121
		GO_CYCLIC_NUCLEOTIDE_BIOSYNTHETIC_PROCESS	0.587	0.074
		GO_CELLULAR_AMIDE_METABOLIC_PROCESS	0.321	0.198
		GO_CARBOHYDRATE_DERIVATIVE_METABOLIC_PROCESS	0.298	0.232
		GO_CARBOHYDRATE_CATABOLIC_PROCESS	0.426	0.164
		GO_CARBOHYDRATE_BIOSYNTHETIC_PROCESS	0.422	0.191
		GO_AMMONIUM_ION_METABOLIC_PROCESS	0.376	0.192
		GO_AMINO_ACID_ACTIVATION	0.556	0.094
		GO_AMINOGLYCAN_METABOLIC_PROCESS	0.473	0.070
		GO_AMINOGLYCAN_CATABOLIC_PROCESS	0.574	0.045
		GO_AMINOGLYCAN_BIOSYNTHETIC_PROCESS	0.492	0.145
		GO_AMIDE_BIOSYNTHETIC_PROCESS	0.374	0.125
		GO_ADP_METABOLIC_PROCESS	0.468	0.213
macromolecular complex organization	7	GO_PROTEIN_TETRAMERIZATION	0.546	0.034
		GO_PROTEIN_OLIGOMERIZATION	0.417	0.061
		GO_PROTEIN_HOMOTETRAMERIZATION	0.621	0.035
		GO_PROTEIN_HOMOOLIGOMERIZATION	0.443	0.069
		GO_PROTEIN_COMPLEX_SUBUNIT_ORGANIZATION	0.331	0.145
		GO_PROTEIN_COMPLEX_BIOGENESIS	0.342	0.133
		GO_MACROMOLECULAR_COMPLEX_ASSEMBLY	0.335	0.142
snrna metabolic process	2	GO_SNRNA_METABOLIC_PROCESS	0.438	0.236
		GO_NCRNA_TRANSCRIPTION	0.444	0.197
regulation protein binding	2	GO_REGULATION_OF_PROTEIN_BINDING	0.360	0.228
		GO_REGULATION_OF_BINDING	0.363	0.149
oxide synthase monooxygenase	2	GO_REGULATION_OF_NITRIC_OXIDE_SYNTHASE_ACTIVITY	0.461	0.219
		GO_REGULATION_OF_MONOOXYGENASE_ACTIVITY	0.425	0.236

cellular biogenesis complex	2	GO_REGULATION_OF_CELLULAR_COMPONENT_BIOGENESIS	0.301	0.247
		GO_NEGATIVE_REGULATION_OF_PROTEIN_COMPLEX_ASSEMBLY	0.502	0.128
homeostasis water transition	21	GO_TISSUE_HOMEOSTASIS	0.376	0.186
		GO_WATER_HOMEOSTASIS	0.487	0.125
		GO_TRANSITION_METAL_ION_TRANSPORT	0.445	0.121
		GO_ION_HOMEOSTASIS	0.352	0.124
		GO_HOMEOSTATIC_PROCESS	0.328	0.160
		GO_MULTICELLULAR_ORGANISMAL_HOMEOSTASIS	0.387	0.121
		GO_REGULATION_OF_RENAL_SYSTEM_PROCESS	0.510	0.176
		GO_CHEMICAL_HOMEOSTASIS	0.346	0.121
		GO_MONOVALENT_INORGANIC_CATION_HOMEOSTASIS	0.470	0.125
		GO_DIVALENT_INORGANIC_CATION_HOMEOSTASIS	0.350	0.147
		GO_REGULATION_OF_PH	0.579	0.076
		GO_CARBOHYDRATE_HOMEOSTASIS	0.400	0.164
		GO_CELLULAR_TRANSITION_METAL_ION_HOMEOSTASIS	0.465	0.136
		GO_TRANSITION_METAL_ION_HOMEOSTASIS	0.445	0.128
		GO_CELLULAR_MONOVALENT_INORGANIC_CATION_HOMEOSTASIS	0.533	0.077
		GO_CELLULAR_CHEMICAL_HOMEOSTASIS	0.384	0.081
		GO_RENAL_SYSTEM_PROCESS	0.493	0.051
		GO_MULTICELLULAR_ORGANISMAL_WATER_HOMEOSTASIS	0.538	0.079
		GO_LIPID_HOMEOSTASIS	0.404	0.200
		GO_IRON_ION_TRANSPORT	0.579	0.075
		GO_CELLULAR_HOMEOSTASIS	0.375	0.081
Lipid metabolism and Transport				
regulation lipid biosynthetic	3	GO_REGULATION_OF_LIPID_METABOLIC_PROCESS	0.340	0.209
		GO_REGULATION_OF_LIPID_BIOSYNTHETIC_PROCESS	0.449	0.144
		GO_POSITIVE_REGULATION_OF_LIPID_BIOSYNTHETIC_PROCESS	0.513	0.144
steroid biosynthetic alcohol	2	GO_STEROID_BIOSYNTHETIC_PROCESS	-0.383	0.222
		GO_ALCOHOL_BIOSYNTHETIC_PROCESS	-0.344	0.208
lipoprotein metabolic biosynthetic	2	GO_LIPOPROTEIN_METABOLIC_PROCESS	0.436	0.173
		GO_LIPOPROTEIN_BIOSYNTHETIC_PROCESS	0.546	0.093
particle sterol ester	6	GO_STEROL_TRANSPORT	0.567	0.092
		GO_REGULATION_OF_PLASMA_LIPOPROTEIN_PARTICLE_LEVELS	0.475	0.200
		GO_ORGANOPHOSPHATE_ESTER_TRANSPORT	0.548	0.084
		GO_ORGANIC_HYDROXY_COMPOUND_TRANSPORT	0.444	0.078
		GO_MONOCARBOXYLIC_ACID_TRANSPORT	0.389	0.232
		GO_LIPID_LOCALIZATION	0.326	0.241
Signal transduction				
response purine cellular	50	GO_VASCULAR_ENDOTHELIAL_GROWTH_FACTOR_RECEPTOR_SIGNALING_PATHWAY	0.526	0.079
		GO_TRANSMEMBRANE_RECEPTOR_PROTEIN_T	0.343	0.160

YROSINE_KINASE_SIGNALING_PATHWAY		
GO_TRANSMEMBRANE_RECEPTOR_PROTEIN_SERINE_THREONINE_KINASE_SIGNALING_PATHWAY	0.397	0.140
GO_RESPONSE_TO_RETINOIC_ACID	0.459	0.119
GO_RESPONSE_TO_REACTIVE_OXYGEN_SPECIES	0.490	0.035
GO_RESPONSE_TO_PURINE_CONTAINING_COMPOUND	0.422	0.118
GO_RESPONSE_TO_PEPTIDE	0.393	0.077
GO_RESPONSE_TO_OXYGEN_CONTAINING_COMPOUND	0.340	0.125
GO_RESPONSE_TO_OXIDATIVE_STRESS	0.361	0.148
GO_RESPONSE_TO_ORGANOPHOSPHORUS	0.438	0.088
GO_RESPONSE_TO_ORGANIC_CYCLIC_COMPOUND	0.328	0.151
GO_RESPONSE_TO_NITROGEN_COMPOUND	0.345	0.128
GO_RESPONSE_TO_LIPID	0.308	0.209
GO_RESPONSE_TO_KETONE	0.392	0.140
GO_RESPONSE_TO_INSULIN	0.407	0.100
GO_RESPONSE_TO_HYDROGEN_PEROXIDE	0.474	0.103
GO_RESPONSE_TO_HORMONE	0.338	0.132
GO_RESPONSE_TO_GROWTH_FACTOR	0.342	0.157
GO_RESPONSE_TO_GLUCAGON	0.455	0.244
GO_RESPONSE_TO_FIBROBLAST_GROWTH_FACTOR	0.461	0.081
GO_RESPONSE_TO_ETHANOL	0.360	0.201
GO_RESPONSE_TO_ENDOGENOUS_STIMULUS	0.324	0.151
GO_RESPONSE_TO_CORTICOSTEROID	0.375	0.164
GO_RESPONSE_TO_CARBOHYDRATE	0.390	0.171
GO_RESPONSE_TO_CAMP	0.380	0.229
GO_RESPONSE_TO_AMINO_ACID	0.412	0.178
GO_RESPONSE_TO_ALCOHOL	0.340	0.164
GO_RESPONSE_TO_ACID_CHEMICAL	0.376	0.123
GO_INSULIN_RECEPTOR_SIGNALING_PATHWAY	0.513	0.075
GO_FIBROBLAST_GROWTH_FACTOR_RECEPTOR_SIGNALING_PATHWAY	0.435	0.177
GO_ERBB_SIGNALING_PATHWAY	0.424	0.195
GO_EPIDERMAL_GROWTH_FACTOR_RECEPTOR_SIGNALING_PATHWAY	0.477	0.206
GO_ENZYME_LINKED_RECEPTOR_PROTEIN_SIGNALING_PATHWAY	0.334	0.154
GO_CELLULAR_RESPONSE_TO_RETINOIC_ACID	0.526	0.089
GO_CELLULAR_RESPONSE_TO_REACTIVE_OXYGEN_SPECIES	0.534	0.056
GO_CELLULAR_RESPONSE_TO_PEPTIDE	0.375	0.112
GO_CELLULAR_RESPONSE_TO_OXYGEN_CONTAINING_COMPOUND	0.343	0.130
GO_CELLULAR_RESPONSE_TO_OXIDATIVE_STRESS	0.416	0.132
GO_CELLULAR_RESPONSE_TO_ORGANIC_CYCLIC_COMPOUND	0.354	0.134
GO_CELLULAR_RESPONSE_TO_NITROGEN_COMPOUND	0.369	0.094
GO_CELLULAR_RESPONSE_TO_LIPID	0.318	0.198
GO_CELLULAR_RESPONSE_TO_KETONE	0.463	0.147

		GO_CELLULAR_RESPONSE_TO_INSULIN_STIMULUS	0.479	0.049
		GO_CELLULAR_RESPONSE_TO_HYDROGEN_PEROXIDE	0.524	0.127
		GO_CELLULAR_RESPONSE_TO_HORMONE_STIMULUS	0.328	0.167
		GO_CELLULAR_RESPONSE_TO_ENDOGENOUS_STIMULUS	0.321	0.173
		GO_CELLULAR_RESPONSE_TO_CORTICOSTEROID_STIMULUS	0.424	0.214
		GO_CELLULAR_RESPONSE_TO_AMINO_ACID_STIMULUS	0.511	0.137
		GO_CELLULAR_RESPONSE_TO_ALCOHOL	0.416	0.159
		GO_CELLULAR_RESPONSE_TO_ACID_CHEMICAL	0.450	0.070
detection light mechanical	6	GO_RESPONSE_TO_OXYGEN_LEVELS	0.344	0.171
		GO_RESPONSE_TO_MECHANICAL_STIMULUS	0.519	0.015
		GO_RESPONSE_TO_COLD	0.533	0.141
		GO_RESPONSE_TO_ABIOTIC_STIMULUS	0.294	0.233
		GO_DETECTION_OF_LIGHT_STIMULUS	-0.457	0.187
		GO_CELLULAR_RESPONSE_TO_MECHANICAL_STIMULUS	0.564	0.029
communication negative stimulus	3	GO_NEGATIVE_REGULATION_OF_RESPONSE_TO_STIMULUS	0.328	0.145
		GO_NEGATIVE_REGULATION_OF_INTRACELLULAR_SIGNAL_TRANSDUCTION	0.428	0.049
		GO_NEGATIVE_REGULATION_OF_CELL_COMMUNICATION	0.319	0.167
response toxic substance	2	GO_RESPONSE_TO_TOXIC_SUBSTANCE	0.484	0.027
		GO_DETOXIFICATION	0.617	0.033
response exogenous dsrna	2	GO_RESPONSE_TO_EXOGENOUS_DSRNA	0.489	0.172
		GO_RESPONSE_TO_DSRNA	0.410	0.240
external starvation biotic	12	GO_RESPONSE_TO_NUTRIENT	0.361	0.185
		GO_RESPONSE_TO_EXTERNAL_STIMULUS	0.300	0.206
		GO_RESPONSE_TO_VIRUS	0.421	0.089
		GO_CELLULAR_RESPONSE_TO_BIOTIC_STIMULUS	0.452	0.093
		GO_RESPONSE_TO_MOLECULE_OF_BACTERIAL_ORIGIN	0.452	0.045
		GO_CELLULAR_RESPONSE_TO_STARVATION	0.413	0.176
		GO_DEFENSE_RESPONSE_TO_VIRUS	0.404	0.146
		GO_RESPONSE_TO_BIOTIC_STIMULUS	0.352	0.118
		GO_RESPONSE_TO_EXTRACELLULAR_STIMULUS	0.341	0.158
		GO_RESPONSE_TO_STARVATION	0.404	0.160
		GO_RESPONSE_TO_BACTERIUM	0.359	0.142
		GO_CELLULAR_RESPONSE_TO_EXTERNAL_STIMULUS	0.402	0.085
rho protein kinase	26	GO_STRESS_ACTIVATED_PROTEIN_KINASE_SIGNALING_CASCADE	0.443	0.185
		GO_REGULATION_OF_TRANSFERASE_ACTIVITY	0.318	0.184
		GO_REGULATION_OF_TOR_SIGNALING	0.488	0.198
		GO_REGULATION_OF_SMALL_GTPASE_MEDIATED_SIGNAL_TRANSDUCTION	0.421	0.078
		GO_REGULATION_OF_RHO_PROTEIN_SIGNAL_TRANSDUCTION	0.446	0.092
		GO_REGULATION_OF_RAS_PROTEIN_SIGNAL_TRANSDUCTION	0.450	0.068
		GO_REGULATION_OF_PROTEIN_MODIFICATION_PROCESS	0.297	0.213

		GO_REGULATION_OF_PROTEIN_KINASE_B_SIGNALING	0.385	0.216
		GO_REGULATION_OF_KINASE_ACTIVITY	0.317	0.197
		GO_REGULATION_OF_I_KAPPAB_KINASE_NF_KAPPAB_SIGNALING	0.427	0.076
		GO_REGULATION_OF_INTRACELLULAR_SIGNAL_TRANSDUCTION	0.315	0.176
		GO_POSITIVE_REGULATION_OF_TRANSFERASE_ACTIVITY	0.314	0.220
		GO_POSITIVE_REGULATION_OF_PROTEIN_MODIFICATION_PROCESS	0.306	0.199
		GO_POSITIVE_REGULATION_OF_PROTEIN_METABOLIC_PROCESS	0.301	0.217
		GO_POSITIVE_REGULATION_OF_PROTEIN_KINASE_B_SIGNALING	0.475	0.136
		GO_POSITIVE_REGULATION_OF_KINASE_ACTIVITY	0.314	0.225
		GO_POSITIVE_REGULATION_OF_I_KAPPAB_KINASE_NF_KAPPAB_SIGNALING	0.414	0.111
		GO_POSITIVE_REGULATION_OF_INTRACELLULAR_SIGNAL_TRANSDUCTION	0.315	0.183
		GO_POSITIVE_REGULATION_OF_ERK1_AND_ERK2_CASCADE	0.364	0.234
		GO_NEGATIVE_REGULATION_OF_TRANSFERASE_ACTIVITY	0.363	0.177
		GO_NEGATIVE_REGULATION_OF_PROTEIN_SERINE_THREONINE_KINASE_ACTIVITY	0.413	0.196
		GO_NEGATIVE_REGULATION_OF_PROTEIN_MODIFICATION_PROCESS	0.325	0.195
		GO_NEGATIVE_REGULATION_OF_PHOSPHORYLATION	0.337	0.189
mediated signaling messenger	6	GO_SMALL_GTPASE_MEDIATED_SIGNAL_TRANSDUCTION	0.332	0.214
		GO_SECOND_MESSENGER_MEDIATED_SIGNALING	0.499	0.030
		GO_INTRACELLULAR_SIGNAL_TRANSDUCTION	0.353	0.100
		GO_CYCLIC_NUCLEOTIDE_MEDIATED_SIGNALING	0.577	0.048
		GO_CAMP_MEDIATED_SIGNALING	0.442	0.240
		GO_CALCIUM_MEDIATED_SIGNALING	0.517	0.078
peptidyl autophosphorylation phosphorylation	4	GO_SIGNAL_TRANSDUCTION_BY_PROTEIN_PHOSPHORYLATION	0.389	0.089
		GO_PROTEIN_AUTOPHOSPHORYLATION	0.363	0.205
		GO_PHOSPHORYLATION	0.295	0.232
		GO_PEPTIDYL_THREONINE_MODIFICATION	0.520	0.164
Cytoskeleton and Motility				
migration subcellular motility	6	GO_TISSUE_MIGRATION	0.424	0.223
		GO_NEURON_MIGRATION	0.544	0.036
		GO_MYELOID_LEUKOCYTE_MIGRATION	-0.312	0.228
		GO_MOVEMENT_OF_CELL_OR_SUBCELLULAR_COMPONENT	0.289	0.239
		GO_ENDOTHELIAL_CELL_MIGRATION	0.510	0.142
		GO_CELL_MOTILITY	0.293	0.238
smooth migration locomotion	3	GO_REGULATION_OF_SMOOTH_MUSCLE_CELL_MIGRATION	0.511	0.164
		GO_REGULATION_OF_CELLULAR_COMPONENT_MOVEMENT	0.303	0.236

		GO_NEGATIVE_REGULATION_OF_LOCOMOTION	0.360	0.164
single cell adhesion	11	GO_THYMOCYTE_AGGREGATION	0.591	0.067
		GO_SINGLE_ORGANISM_CELL_ADHESION	0.365	0.122
		GO_RESPONSE_TO_WOUNDING	0.379	0.084
		GO_REGULATION_OF_BODY_FLUID_LEVELS	0.328	0.175
		GO_PLATELET_ACTIVATION	0.401	0.149
		GO_LEUKOCYTE_CELL_CELL_ADHESION	0.351	0.184
		GO_HOMOTYPIC_CELL_CELL_ADHESION	0.535	0.125
		GO_CELL_SUBSTRATE_ADHESION	0.545	0.015
		GO_CELL_MATRIX_ADHESION	0.549	0.014
		GO_CELL_CELL_ADHESION	0.310	0.211
		GO_BIOLOGICAL_ADHESION	0.319	0.175
filament bundle actin	6	GO_INTERMEDIATE_FILAMENT_BASED_PROCESS	0.482	0.179
		GO_CYTOSKELETON_ORGANIZATION	0.329	0.174
		GO_ACTOMYOSIN_STRUCTURE_ORGANIZATION	0.472	0.178
		GO_ACTIN_FILAMENT_ORGANIZATION	0.417	0.132
		GO_ACTIN_FILAMENT_BUNDLE_ORGANIZATION	0.489	0.166
		GO_ACTIN_FILAMENT_BASED_PROCESS	0.393	0.085
actin contraction muscle	4	GO_MUSCLE_SYSTEM_PROCESS	0.346	0.178
		GO_MUSCLE_CONTRACTION	0.374	0.136
		GO_ACTIN_MEDIATED_CELL_CONTRACTION	0.471	0.140
		GO_ACTIN_FILAMENT_BASED_MOVEMENT	0.445	0.173
cytoskeleton dependent intracellular	2	GO_ESTABLISHMENT_OF_LOCALIZATION_BY_MOVEMENT_ALONG_MICROTUBULE	0.546	0.076
		GO_CYTOSKELETON_DEPENDENT_INTRACELLULAR_TRANSPORT	0.525	0.087
Membrane dynamics				
		GO_REGULATION_OF_MEMBRANE_PERMEABILITY	0.436	0.184
mitochondrial membrane permeability	4	GO_MITOCHONDRION_ORGANIZATION	0.358	0.142
		GO_MITOCHONDRIAL_TRANSPORT	0.370	0.240
		GO_MITOCHONDRIAL_MEMBRANE_ORGANIZATION	0.439	0.165
		GO_POSITIVE_REGULATION_OF_PROTEIN_SECRETION	0.342	0.240
regulation mitochondrion transport	30	GO_NEGATIVE_REGULATION_OF_INTRACELLULAR_TRANSPORT	0.396	0.208
		GO_NEGATIVE_REGULATION_OF_CYTOPLASMIC_TRANSPORT	0.428	0.174
		GO_REGULATION_OF_CYTOPLASMIC_TRANSPORT	0.389	0.080
		GO_REGULATION_OF_LIPID_TRANSPORT	0.401	0.194
		GO_NEGATIVE_REGULATION_OF_NUCLEOCYTOPLASMIC_TRANSPORT	0.465	0.184
		GO_POSITIVE_REGULATION_OF_CELLULAR_PROTEIN_LOCALIZATION	0.464	0.028
		GO_NEGATIVE_REGULATION_OF_TRANSPORT	0.322	0.206
		GO_REGULATION_OF_PROTEIN_TARGETING_TO_MITOCHONDRION	0.562	0.055
		GO_REGULATION_OF_INTRACELLULAR_TRANSPORT	0.391	0.069
		GO_REGULATION_OF_CELLULAR_PROTEIN_LOCALIZATION	0.453	0.027

		GO_REGULATION_OF_ESTABLISHMENT_OF_PROTEIN_LOCALIZATION_TO_MITOCHONDRION	0.475	0.084
		GO_REGULATION_OF_MITOCHONDRION_ORGANIZATION	0.397	0.134
		GO_POSITIVE_REGULATION_OF_INSULIN_SECRETION	0.487	0.173
		GO_NEGATIVE_REGULATION_OF_CELLULAR_PROTEIN_LOCALIZATION	0.495	0.065
		GO_POSITIVE_REGULATION_OF_CYTOPLASMIC_TRANSPORT	0.382	0.138
		GO_REGULATION_OF_PROTEIN_LOCALIZATION	0.349	0.125
		GO_REGULATION_OF_PLASMA_MEMBRANE_ORGANIZATION	0.479	0.160
		GO_NEGATIVE_REGULATION_OF_INTRACELLULAR_PROTEIN_TRANSPORT	0.487	0.126
		GO_POSITIVE_REGULATION_OF_TRANSPORT	0.378	0.078
		GO_POSITIVE_REGULATION_OF_MITOCHONDRION_ORGANIZATION	0.382	0.196
		GO_REGULATION_OF_CELLULAR_LOCALIZATION	0.301	0.219
		GO_REGULATION_OF_PROTEIN_IMPORT	0.365	0.207
		GO_REGULATION_OF_INTRACELLULAR_PROTEIN_TRANSPORT	0.446	0.046
		GO_POSITIVE_REGULATION_OF_INTRACELLULAR_PROTEIN_TRANSPORT	0.454	0.056
		GO_REGULATION_OF_PROTEIN_LOCALIZATION_TO_NUCLEUS	0.389	0.137
		GO_POSITIVE_REGULATION_OF_INTRACELLULAR_TRANSPORT	0.424	0.063
		GO_REGULATION_OF_NUCLEOCYTOPLASMIC_TRANSPORT	0.397	0.121
		GO_REGULATION_OF_PROTEIN_TARGETING	0.435	0.070
		GO_POSITIVE_REGULATION_OF_ESTABLISHMENT_OF_PROTEIN_LOCALIZATION	0.400	0.076
localization membrane budding	28	GO_PROTEIN_LOCALIZATION_TO_CELL_PERIPHERY	0.515	0.038
		GO_VACUOLAR_TRANSPORT	0.458	0.077
		GO_NUCLEAR_IMPORT	0.439	0.134
		GO_PROTEIN_TARGETING	0.320	0.238
		GO_NUCLEUS_ORGANIZATION	0.401	0.240
		GO_INTRACELLULAR_PROTEIN_TRANSPORT	0.389	0.075
		GO_MEMBRANE_ORGANIZATION	0.372	0.084
		GO_MAINTENANCE_OF_LOCATION_IN_CELL	0.464	0.178
		GO_PROTEIN_LOCALIZATION_TO_NUCLEUS	0.421	0.129
		GO_SINGLE_ORGANISM_CELLULAR_LOCALIZATION	0.380	0.080
		GO_ESTABLISHMENT_OF_PROTEIN_LOCALIZATION_TO_MEMBRANE	0.478	0.048
		GO_NUCLEAR_TRANSPORT	0.384	0.126
		GO_SINGLE_ORGANISM_MEMBRANE_BUDDING	0.461	0.187
		GO_ESTABLISHMENT_OF_LOCALIZATION_IN_CELL	0.345	0.126
		GO_VESICLE_COATING	0.468	0.177
		GO_PROTEIN_LOCALIZATION_TO_MEMBRANE	0.434	0.051
		GO_PROTEIN_LOCALIZATION	0.378	0.070
		GO_PLASMA_MEMBRANE_ORGANIZATION	0.500	0.034
		GO_VESICLE_ORGANIZATION	0.465	0.066
		GO_PROTEIN_IMPORT	0.473	0.075
		GO_ENDOMEMBRANE_SYSTEM_ORGANIZATION	0.463	0.029

		GO_CELLULAR_MACROMOLECULE_LOCALIZATION	0.375	0.078
		GO_GOLGI_VESICLE_TRANSPORT	0.347	0.206
		GO_ESTABLISHMENT_OF_PROTEIN_LOCALIZATION	0.399	0.054
		GO_ESTABLISHMENT_OF_PROTEIN_LOCALIZATION_TO_PLASMA_MEMBRANE	0.613	0.021
		GO_MEMBRANE_BUDDING	0.505	0.078
		GO_ER_TO_GOLGI_VESICLE_MEDIATED_TRANSPORT	0.385	0.203
		GO_LOCALIZATION_WITHIN_MEMBRANE	0.487	0.076
regulated exocytosis secretion	7	GO_VESICLE_MEDIATED_TRANSPORT	0.328	0.160
		GO_SECRETION	0.370	0.110
		GO_EXOCYTOSIS	0.437	0.077
		GO_REGULATED_EXOCYTOSIS	0.481	0.061
		GO_PROTEIN_SECRETION	0.479	0.086
		GO_PLATELET_DEGRANULATION	0.527	0.031
		GO_SECRETION_BY_CELL	0.394	0.076
vacuole organization autophagy	2	GO_AUTOPHAGY	0.341	0.198
		GO_VACUOLE_ORGANIZATION	0.445	0.127
positive regulation endocytosis	2	GO_POSITIVE_REGULATION_OF_ENDOCYTOSIS	0.424	0.165
		GO_REGULATION_OF_ENDOCYTOSIS	0.352	0.240
Stress response				
stress hydrolase peptidase	23	GO_REGULATION_OF_PROTEIN_MATURATION	0.548	0.078
		GO_REGULATION_OF_CELLULAR_RESPONSE_TO_STRESS	0.335	0.159
		GO_REGULATION_OF_ACUTE_INFLAMMATORY_RESPONSE	0.505	0.134
		GO_REGULATION_OF_OXIDATIVE_STRESS_INDUCED_CELL_DEATH	0.457	0.211
		GO_REGULATION_OF_RESPONSE_TO_OXIDATIVE_STRESS	0.431	0.233
		GO_REGULATION_OF_PROTEOLYSIS	0.351	0.129
		GO_NEGATIVE_REGULATION_OF_HYDROLASE_ACTIVITY	0.387	0.093
		GO_REGULATION_OF_DEFENSE_RESPONSE	0.306	0.217
		GO_REGULATION_OF_INTERLEUKIN_1_PRODUCTION	0.490	0.179
		GO_REGULATION_OF_RESPONSE_TO_DNA_DAMAGE_STIMULUS	0.397	0.198
		GO_NEGATIVE_REGULATION_OF_CYSTEINE_TYPE_ENDOPEPTIDASE_ACTIVITY	0.449	0.141
		GO_NEGATIVE_REGULATION_OF_PEPTIDASE_ACTIVITY	0.440	0.066
		GO_REGULATION_OF_AUTOPHAGY	0.450	0.062
		GO_NEGATIVE_REGULATION_OF_IMMUNE_RESPONSE	0.493	0.085
		GO_REGULATION_OF_RESPONSE_TO_STRESS	0.319	0.172
		GO_NEGATIVE_REGULATION_OF_PROTEIN_METABOLIC_PROCESS	0.361	0.089
		GO_NEGATIVE_REGULATION_OF_CATALYTIC_ACTIVITY	0.366	0.093
		GO_NEGATIVE_REGULATION_OF_MOLECULAR_FUNCTION	0.371	0.081
		GO_NEGATIVE_REGULATION_OF_IMMUNE_EFFECTOR_PROCESS	0.513	0.075
		GO_NEGATIVE_REGULATION_OF_DEFENSE_RESPONSE	0.374	0.240

		GO_REGULATION_OF_HYDROLASE_ACTIVITY	0.315	0.176
		GO_NEGATIVE_REGULATION_OF_PROTEOLYSIS	0.406	0.078
		GO_REGULATION_OF_PEPTIDASE_ACTIVITY	0.407	0.070
reactive oxygen species	3	GO_REGULATION_OF_REACTIVE_OXYGEN_SPECIES_BIOSYNTHETIC_PROCESS	0.520	0.097
		GO_POSITIVE_REGULATION_OF_REACTIVE_OXYGEN_SPECIES_BIOSYNTHETIC_PROCESS	0.467	0.216
		GO_REGULATION_OF_NITRIC_OXIDE_BIOSYNTHETIC_PROCESS	0.507	0.160
wound healing coagulation	3	GO_REGULATION_OF_WOUND_HEALING	0.422	0.142
		GO_NEGATIVE_REGULATION_OF_WOUND_HEALING	0.496	0.090
		GO_NEGATIVE_REGULATION_OF_COAGULATION	0.421	0.236
Proteostasis				
catabolic proteasomal process	13	GO_REGULATION_OF_PROTEIN_CATABOLIC_PROCESS	0.460	0.035
		GO_REGULATION_OF_PROTEASOMAL_UBIQUITIN_DEPENDENT_PROTEIN_CATABOLIC_PROCESS	0.461	0.108
		GO_REGULATION_OF_PROTEASOMAL_PROTEIN_CATABOLIC_PROCESS	0.416	0.145
		GO_REGULATION_OF_CELLULAR_PROTEIN_CATABOLIC_PROCESS	0.455	0.049
		GO_REGULATION_OF_CATABOLIC_PROCESS	0.434	0.036
		GO_POSITIVE_REGULATION_OF_PROTEOLYSIS	0.335	0.216
		GO_POSITIVE_REGULATION_OF_PROTEIN_CATABOLIC_PROCESS	0.492	0.034
		GO_POSITIVE_REGULATION_OF_PROTEASOMAL_PROTEIN_CATABOLIC_PROCESS	0.521	0.115
		GO_POSITIVE_REGULATION_OF_CELLULAR_PROTEIN_CATABOLIC_PROCESS	0.501	0.049
		GO_POSITIVE_REGULATION_OF_CATABOLIC_PROCESS	0.410	0.077
		GO_NEGATIVE_REGULATION_OF_PROTEIN_CATABOLIC_PROCESS	0.420	0.192
		GO_NEGATIVE_REGULATION_OF_CELLULAR_CATABOLIC_PROCESS	0.414	0.145
		GO_NEGATIVE_REGULATION_OF_CATABOLIC_PROCESS	0.402	0.121
macromolecule catabolic polyubiquitination	12	GO_PROTEIN_POLYUBIQUITINATION	0.437	0.077
		GO_PROTEIN_CATABOLIC_PROCESS	0.414	0.055
		GO_PROTEASOMAL_PROTEIN_CATABOLIC_PROCESS	0.505	0.024
		GO_ORGANONITROGEN_COMPOUND_CATABOLIC_PROCESS	0.368	0.127
		GO_ORGANIC_HYDROXY_COMPOUND_CATABOLIC_PROCESS	0.488	0.144
		GO_MONOCARBOXYLIC_ACID_CATABOLIC_PROCESS	0.457	0.141
		GO_MACROMOLECULE_CATABOLIC_PROCESS	0.395	0.061
		GO_FATTY_ACID_CATABOLIC_PROCESS	0.439	0.241
		GO_ERAD_PATHWAY	0.580	0.067
		GO_CELLULAR_CATABOLIC_PROCESS	0.338	0.137
		GO_CATABOLIC_PROCESS	0.310	0.185
		GO_CARBOHYDRATE_DERIVATIVE_CATABOLIC_PROCESS	0.405	0.136
regulation stabilization stability	2	GO_REGULATION_OF_PROTEIN_STABILITY	0.352	0.205
		GO_PROTEIN_STABILIZATION	0.409	0.141

Synaptic transmission and calcium signalling				
regulation ion calcium	20	GO_REGULATION_OF_CATION_CHANNEL_ACTIVITY	0.427	0.206
		GO_REGULATION_OF_RECEPTOR_ACTIVITY	0.386	0.233
		GO_REGULATION_OF_CALCIUM_ION_TRANSMEMBRANE_TRANSPORTER_ACTIVITY	0.493	0.142
		GO_NEGATIVE_REGULATION_OF_HOMEOSTATIC_PROCESS	0.529	0.045
		GO_REGULATION_OF_TRANSPORTER_ACTIVITY	0.361	0.216
		GO_REGULATION_OF_CALCIUM_ION_IMPORT	0.510	0.075
		GO_POSITIVE_REGULATION_OF_ION_TRANSPORT	0.348	0.228
		GO_REGULATION_OF_ION_TRANSPORT	0.310	0.217
		GO_REGULATION_OF_METAL_ION_TRANSPORT	0.400	0.093
		GO_REGULATION_OF_TRANSMEMBRANE_TRANSPORT	0.319	0.224
		GO_REGULATION_OF_ION_HOMEOSTASIS	0.486	0.036
		GO_REGULATION_OF_CALCIUM_ION_TRANSPORT_INTO_CYTOSOL	0.498	0.094
		GO_REGULATION_OF_RELEASE_OF_SEQUESTERED_CALCIUM_ION_INTO_CYTOSOL	0.576	0.076
		GO_REGULATION_OF_CATION_TRANSMEMBRANE_TRANSPORT	0.395	0.145
		GO_REGULATION_OF_SEQUESTERING_OF_CALCIUM_ION	0.568	0.039
		GO_REGULATION_OF_HOMEOSTATIC_PROCESS	0.343	0.145
		GO_NEGATIVE_REGULATION_OF_ION_TRANSPORT	0.484	0.070
		GO_REGULATION_OF_SODIUM_ION_TRANSPORT	0.541	0.097
		GO_REGULATION_OF_CALCIUM_ION_TRANSPORT	0.424	0.086
		GO_REGULATION_OF_CALCIUM_ION_TRANSMEMBRANE_TRANSPORT	0.463	0.146
nanoparticle inorganic substance	6	GO_CELLULAR_RESPONSE_TO_CALCIUM_ION	0.503	0.174
		GO_RESPONSE_TO_METAL_ION	0.348	0.165
		GO_RESPONSE_TO_ZINC_ION	0.516	0.136
		GO_RESPONSE_TO_TRANSITION_METAL_NANOPARTICLE	0.398	0.144
		GO_CELLULAR_RESPONSE_TO_INORGANIC_SUBSTANCE	0.352	0.246
		GO_RESPONSE_TO_INORGANIC_SUBSTANCE	0.348	0.129
divalent cation calcium	3	GO_DIVALENT_INORGANIC_CATION_TRANSPORT	0.331	0.250
		GO_CALCIUM_ION_IMPORT	0.559	0.078
		GO_CALCIUM_ION_TRANSPORT	0.358	0.196
Death				
apoptotic death neuron	16	GO_REGULATION_OF_LEUKOCYTE_APOPTOTIC_PROCESS	0.428	0.208
		GO_NEGATIVE_REGULATION_OF_NEURON_DEATH	0.449	0.082
		GO_REGULATION_OF_INTRINSIC_APOPTOTIC_SIGNALING_PATHWAY	0.510	0.044
		GO_POSITIVE_REGULATION_OF_CELL_DEATH	0.330	0.175
		GO_NEGATIVE_REGULATION_OF_CELL_DEATH	0.324	0.176
		GO_NEGATIVE_REGULATION_OF_LEUKOCYTE_APOPTOTIC_PROCESS	0.463	0.232
		GO_REGULATION_OF_APOPTOTIC_SIGNALING_PATHWAY	0.330	0.194

		GO_REGULATION_OF_CELL_DEATH	0.317	0.175
		GO_NEGATIVE_REGULATION_OF_APOPTOTIC_SIGNALING_PATHWAY	0.403	0.117
		GO_POSITIVE_REGULATION_OF_NEURON_DEATH	0.576	0.056
		GO_NEGATIVE_REGULATION_OF_NEURON_APOPTOTIC_PROCESS	0.514	0.049
		GO_NEGATIVE_REGULATION_OF_INTRINSIC_APOPTOTIC_SIGNALING_PATHWAY	0.645	0.014
		GO_REGULATION_OF_NEURON_APOPTOTIC_PROCESS	0.459	0.062
		GO_REGULATION_OF_NEURON_DEATH	0.407	0.086
		GO_REGULATION_OF_LYMPHOCYTE_APOPTOTIC_PROCESS	0.450	0.233
		GO_POSITIVE_REGULATION_OF_INTRINSIC_APOPTOTIC_SIGNALING_PATHWAY	0.543	0.121
apoptotic pathway intrinsic	6	GO_APOPTOTIC_SIGNALING_PATHWAY	0.422	0.069
		GO_INTRINSIC_APOPTOTIC_SIGNALING_PATHWAY_BY_P53_CLASS_MEDIATOR	0.529	0.126
		GO_INTRINSIC_APOPTOTIC_SIGNALING_PATHWAY	0.522	0.033
		GO_CELL_DEATH	0.342	0.138
		GO_EXTRINSIC_APOPTOTIC_SIGNALING_PATHWAY	0.486	0.086
		GO_INTRINSIC_APOPTOTIC_SIGNALING_PATHWAY_IN_RESPONSE_TO_DNA_DAMAGE	0.515	0.078
Cell junction				
substrate junction assembly	5	GO_CELL_JUNCTION_ORGANIZATION	0.433	0.077
		GO_CELL_JUNCTION_ASSEMBLY	0.520	0.034
		GO_ADHERENS_JUNCTION_ORGANIZATION	0.593	0.037
		GO_CELL_SUBSTRATE_JUNCTION_ASSEMBLY	0.516	0.094
		GO_CELL_CELL_JUNCTION_ASSEMBLY	0.557	0.076
adherens junction matrix	4	GO_REGULATION_OF_ADHERENS_JUNCTION_ORGANIZATION	0.487	0.197
		GO_REGULATION_OF_CELL_MATRIX_ADHESION	0.453	0.121
		GO_REGULATION_OF_CELL_SUBSTRATE_ADHESION	0.358	0.232
		GO_REGULATION_OF_CELL_JUNCTION_ASSEMBLY	0.522	0.089
Transcription/replication/gene expression				
telomere organelle chromosome	8	GO_REGULATION_OF_DNA_BIOSYNTHETIC_PROCESS	0.437	0.175
		GO_REGULATION_OF_DNA_METABOLIC_PROCESS	0.322	0.240
		GO_POSITIVE_REGULATION_OF_ORGANELLE_ORGANIZATION	0.306	0.236
		GO_REGULATION_OF_CHROMOSOME_ORGANIZATION	0.360	0.176
		GO_POSITIVE_REGULATION_OF_CHROMOSOME_ORGANIZATION	0.439	0.145
		GO_POSITIVE_REGULATION_OF_DNA_BIOSYNTHETIC_PROCESS	0.469	0.206
		GO_REGULATION_OF_TELOMERE_MAINTENANCE	0.446	0.233
		GO_POSITIVE_REGULATION_OF_CELLULAR_COMPONENT_ORGANIZATION	0.324	0.168
ire1 topologically incorrect	8	GO_SIGNAL_TRANSDUCTION_BY_P53_CLASS_MEDIATOR	0.412	0.188
		GO_IRE1_MEDIATED_UNFOLDED_PROTEIN_RESPONSE	0.570	0.085
		GO_CELLULAR_RESPONSE_TO_DNA_DAMAGE_	0.328	0.178

		STIMULUS		
		GO_CELLULAR_RESPONSE_TO_STRESS	0.362	0.086
		GO_RESPONSE_TO_TOPOLOGICALLY_INCORRECT_PROTEIN	0.466	0.076
		GO_RESPONSE_TO_ENDOPLASMIC_RETICULUM_STRESS	0.482	0.037
		GO_CELLULAR_RESPONSE_TO_TOPOLOGICALLY_INCORRECT_PROTEIN	0.457	0.119
		GO_TRANSCRIPTION_COUPLED_NUCLEOTIDE_EXCISION_REPAIR	0.448	0.216
rna splicing mrna	6	GO_DNA_TEMPLATED_TRANSCRIPTION_TERMINATION	0.508	0.159
		GO_RNA_SPLICING	0.369	0.167
		GO_MRNA_METABOLIC_PROCESS	0.336	0.176
		GO_MRNA_PROCESSING	0.359	0.165
		GO_RNA_PROCESSING	0.310	0.210
		GO_RNA_SPLICING_VIA_TRANSESTERIFICATION_REACTIONS	0.379	0.177
posttranscriptional gene expression	4	GO_REGULATION_OF_CELLULAR_AMIDE_METABOLIC_PROCESS	0.350	0.176
		GO_REGULATION_OF_RNA_STABILITY	0.480	0.077
		GO_NEGATIVE_REGULATION_OF_CELLULAR_AMIDE_METABOLIC_PROCESS	0.413	0.173
		GO_POSTTRANSCRIPTIONAL_REGULATION_OF_GENE_EXPRESSION	0.336	0.186
sequence specific binding	3	GO_POSITIVE_REGULATION_OF_NF_KAPPAB_TRANSCRIPTION_FACTOR_ACTIVITY	0.444	0.142
		GO_NEGATIVE_REGULATION_OF_SEQUENCE_SPECIFIC_DNA_BINDING_TRANSCRIPTION_FACTOR_ACTIVITY	0.450	0.142
		GO_REGULATION_OF_SEQUENCE_SPECIFIC_DNA_BINDING_TRANSCRIPTION_FACTOR_ACTIVITY	0.351	0.164
nucleobase compound transport	2	GO_RNA_LOCALIZATION	0.401	0.197
		GO_NUCLEOBASE_CONTAINING_COMPOUND_TRANSPORT	0.433	0.135
Cell cycle				
mitotic nuclear cycle	4	GO_CELL_CYCLE	0.301	0.216
		GO_CELL_CYCLE_PROCESS	0.299	0.234
		GO_MITOTIC_CELL_CYCLE	0.343	0.142
		GO_MITOTIC_NUCLEAR_DIVISION	0.344	0.195
Circadian rhythm				
circadian rhythm rhythmic	2	GO_CIRCADIAN_RHYTHM	0.353	0.238
		GO_RHYTHMIC_PROCESS	0.350	0.163
Miscellaneous				
positive regulation vasodilation	2	GO_REGULATION_OF_VASODILATION	0.457	0.219
		GO_POSITIVE_REGULATION_OF_VASODILATION	0.490	0.185
cardiac conduction contraction	5	GO_REGULATION_OF_STRIATED_MUSCLE_CONTRACTION	0.398	0.238
		GO_REGULATION_OF_HEART_CONTRACTION	0.338	0.205
		GO_REGULATION_OF_CARDIAC_MUSCLE_CONTRACTION	0.437	0.184
		GO_REGULATION_OF_CARDIAC_CONDUCTION	0.568	0.041

		GO_CARDIAC_CONDUCTION	0.447	0.150
digestive system process	2	GO_DIGESTIVE_SYSTEM_PROCESS	0.496	0.121
		GO_DIGESTION	0.387	0.203

Cytoscape plugin Enrichment map in combination with Autoannotate plugin was used to cluster significantly enriched GOs (FDR q-value<0.25) according to their similarity coefficient. Clusters were manually classified in categories depending on the GOs they contain. Enrichment score from GSEA analysis for each GO is also shown.

Supplementary table 2. Categories and clusters enriched in X-ALD adults.

Cluster	Nodes	GOs	ES	FDR q-val
Immune system				
cell regulation activation	99	GO_IMMUNE_RESPONSE_REGULATING_CELL_SURFACE_RECEPTOR_SIGNALING_PATHWAY	0.443	0.038
		GO_NEGATIVE_REGULATION_OF_INNATE_IMMUNE_RESPONSE	0.587	0.052
		GO_POSITIVE_REGULATION_OF_IMMUNE_SYSTEM_PROCESS	0.508	0.001
		GO_REGULATION_OF_B_CELL_ACTIVATION	0.482	0.071
		GO_REGULATION_OF_PROTEIN_ACTIVATION_CASCADE	0.688	0.008
		GO_POSITIVE_REGULATION_OF_IMMUNE_RESPONSE	0.527	0.001
		GO_REGULATION_OF_NATURAL_KILLER_CELL_MEDIATED_IMMUNITY	0.493	0.230
		GO_POSITIVE_REGULATION_OF_ALPHA_BETA_T_CELL_DIFFERENTIATION	0.589	0.071
		GO_REGULATION_OF_ADAPTIVE_IMMUNE_RESPONSE	0.550	0.008
		GO_REGULATION_OF_RESPONSE_TO_BIOTIC_STIMULUS	0.369	0.190
		GO_REGULATION_OF_INTERLEUKIN_4_PRODUCTION	0.634	0.041
		GO_REGULATION_OF_PRODUCTION_OF_MOLECULAR_MEDIATOR_OF_IMMUNE_RESPONSE	0.518	0.037
		GO_REGULATION_OF_INNATE_IMMUNE_RESPONSE	0.529	0.002
		GO_POSITIVE_REGULATION_OF_LYMPHOCYTE_MEDIATED_IMMUNITY	0.519	0.051
		GO_REGULATION_OF_COAGULATION	0.506	0.035
		GO_REGULATION_OF_CELL_ADHESION	0.453	0.020
		GO_REGULATION_OF_T_CELL_MEDIATED_IMMUNITY	0.533	0.069
		GO_NEGATIVE_REGULATION_OF_CELL_CELL_ADHESION	0.539	0.014
		GO_REGULATION_OF_LEUKOCYTE_PROLIFERATION	0.547	0.005
		GO_NEGATIVE_REGULATION_OF_WOUND_HEALING	0.478	0.109
		GO_NEGATIVE_REGULATION_OF_IMMUNE_EFFECTOR_PROCESS	0.594	0.002
		GO_POSITIVE_REGULATION_OF_SUBSTRATE_ADHESION_DEPENDENT_CELL_SPREADING	0.492	0.207
		GO_PATTERN_RECOGNITION_RECEPTOR_SIGNALING_PATHWAY	0.621	0.001
		GO_POSITIVE_REGULATION_OF_INFLAMMATORY_RESPONSE	0.497	0.036
		GO_REGULATION_OF_DNA_RECOMBINATION	0.473	0.234
		GO_POSITIVE_REGULATION_OF_INNATE_IMMUNE_RESPONSE	0.514	0.008
		GO_POSITIVE_REGULATION_OF_ADAPTIVE_IMMUNE_RESPONSE	0.584	0.007
		GO_REGULATION_OF_INFLAMMATORY_RESPONSE	0.451	0.034

GO_TOLL_LIKE_RECEPTOR_SIGNALING_PATHWAY	0.670	0.000
GO_REGULATION_OF_LYMPHOCYTE_DIFFERENTIATION	0.531	0.021
GO_REGULATION_OF_IMMUNE_EFFECTOR_PROCESS	0.407	0.064
GO_POSITIVE_REGULATION_OF_LEUKOCYTE_DIFFERENTIATION	0.531	0.015
GO_REGULATION_OF_ANTIGEN_RECEPTOR_MEDIATED_SIGNALING_PATHWAY	0.504	0.159
GO_REGULATION_OF_CELL_SUBSTRATE_ADHESION	0.389	0.159
GO_REGULATION_OF_CD4_POSITIVE_ALPHA_BETA_T_CELL_ACTIVATION	0.586	0.076
GO_FC_GAMMA_RECEPTOR_SIGNALING_PATHWAY	0.499	0.081
GO_ANTIGEN_RECEPTOR_MEDIATED_SIGNALING_PATHWAY	0.413	0.109
GO_POSITIVE_REGULATION_OF_LYMPHOCYTE_DIFFERENTIATION	0.558	0.041
GO_REGULATION_OF_CELL_ACTIVATION	0.466	0.016
GO_NEGATIVE_REGULATION_OF_LYMPHOCYTE_MEDIATED_IMMUNITY	0.627	0.035
GO_POSITIVE_REGULATION_OF_IMMUNE_EFFECTOR_PROCESS	0.438	0.063
GO_POSITIVE_REGULATION_OF_T_CELL_MEDIATED_IMMUNITY	0.638	0.036
GO_REGULATION_OF_CYTOKINE_PRODUCTION_INVOLVED_IN_IMMUNE_RESPONSE	0.592	0.025
GO_REGULATION_OF_ALPHA_BETA_T_CELL_DIFFERENTIATION	0.640	0.021
GO_POSITIVE_REGULATION_OF_IMMUNOGLOBULIN_PRODUCTION	0.534	0.155
GO_REGULATION_OF_SUBSTRATE_ADHESION_DEPENDENT_CELL_SPREADING	0.489	0.126
GO_REGULATION_OF_T_CELL_DIFFERENTIATION	0.540	0.025
GO_NEGATIVE_REGULATION_OF_COAGULATION	0.472	0.174
GO_POSITIVE_REGULATION_OF_LEUKOCYTE_MEDIATED_IMMUNITY	0.475	0.065
GO_REGULATION_OF_T_CELL_PROLIFERATION	0.561	0.006
GO_REGULATION_OF_IMMUNE_RESPONSE	0.523	0.001
GO_POSITIVE_REGULATION_OF_CELL_ACTIVATION	0.531	0.002
GO_REGULATION_OF_ALPHA_BETA_T_CELL_ACTIVATION	0.616	0.005
GO_NEGATIVE_REGULATION_OF_LEUKOCYTE_PROLIFERATION	0.569	0.058
GO_ACTIVATION_OF_IMMUNE_RESPONSE	0.545	0.000
GO_REGULATION_OF_RESPONSE_TO_EXTERNAL_STIMULUS	0.343	0.176
GO_POSITIVE_REGULATION_OF_PRODUCTION_OF_MOLECULAR_MEDIATOR_OF_IMMUNE_RESPONSE	0.476	0.110
GO_NEGATIVE_REGULATION_OF_CELL_ADHESION	0.485	0.025
GO_REGULATION_OF_LEUKOCYTE_MEDIATED_IMMUNITY	0.428	0.088
GO_REGULATION_OF_HOMOTYPIC_CELL_CELL_ADHESION	0.538	0.002
GO_NEGATIVE_REGULATION_OF_HOMOTYPIC_CELL_CELL_ADHESION	0.621	0.004
GO_REGULATION_OF_TOLL_LIKE_RECEPTOR_SIGNALING_PATHWAY	0.649	0.014
GO_NEGATIVE_REGULATION_OF_IMMUNE_RESPONSE	0.615	0.000
GO_NEGATIVE_REGULATION_OF_IMMUNE_SYSTEM_PROCESS	0.553	0.000

		GO_NEGATIVE_REGULATION_OF_LEUKOCYTE_MEDIATED_IMMUNITY	0.616	0.020
		GO_POSITIVE_REGULATION_OF_RESPONSE_TO_WOUNDING	0.503	0.018
		GO_POSITIVE_REGULATION_OF_RESPONSE_TO_EXTERNAL_STIMULUS	0.415	0.071
		GO_LYMPHOCYTE_COSTIMULATION	0.584	0.026
		GO_REGULATION_OF_DEFENSE_RESPONSE	0.456	0.015
		GO_REGULATION_OF_LEUKOCYTE_MEDIATED_CYTOTOXICITY	0.523	0.076
		GO_POSITIVE_REGULATION_OF_B_CELL_ACTIVATION	0.579	0.022
		GO_POSITIVE_REGULATION_OF_DEFENSE_RESPONSE	0.512	0.003
		GO_REGULATION_OF_CELL_KILLING	0.461	0.139
		GO_NEGATIVE_REGULATION_OF_DEFENSE_RESPONSE	0.412	0.132
		GO_CYTOPLASMIC_PATTERN_RECOGNITION_RECEPTOR_SIGNALING_PATHWAY	0.543	0.072
		GO_POSITIVE_REGULATION_OF_CELL_KILLING	0.602	0.032
		GO_REGULATION_OF_RESPONSE_TO_WOUNDING	0.420	0.049
		GO_REGULATION_OF_WOUND_HEALING	0.484	0.034
		GO_REGULATION_OF_CELL_ADHESION_MEDIATED_BY_INTEGRIN	0.527	0.135
		GO_T_CELL_RECEPTOR_SIGNALING_PATHWAY	0.444	0.074
		GO_REGULATION_OF_LYMPHOCYTE_MEDIATED_IMMUNITY	0.500	0.034
		GO_REGULATION_OF_IMMUNOGLOBULIN_PRODUCTION	0.572	0.070
		GO_POSITIVE_REGULATION_OF_ALPHA_BETA_T_CELL_ACTIVATION	0.626	0.006
		GO_NEGATIVE_REGULATION_OF_CELL_SUBSTRATE_ADHESION	0.451	0.212
		GO_ACTIVATION_OF_INNATE_IMMUNE_RESPONSE	0.536	0.005
		GO_NEGATIVE_REGULATION_OF_CELL_ACTIVATION	0.529	0.011
		GO_REGULATION_OF_CELL_JUNCTION_ASSEMBLY	0.461	0.103
		GO_POSITIVE_REGULATION_OF_RESPONSE_TO_BIOTIC_STIMULUS	0.535	0.116
		GO_REGULATION_OF_CELL_CELL_ADHESION	0.477	0.013
		GO_REGULATION_OF_B_CELL_PROLIFERATION	0.560	0.094
		GO_POSITIVE_REGULATION_OF_CELL_ADHESION	0.499	0.006
		GO_REGULATION_OF_B_CELL_MEDIATED_IMMUNITY	0.583	0.068
		GO_POSITIVE_REGULATION_OF_CELL_CELL_ADHESION	0.517	0.007
		GO_REGULATION_OF_ACUTE_INFLAMMATORY_RESPONSE	0.546	0.023
		GO_POSITIVE_REGULATION_OF_WOUND_HEALING	0.565	0.041
		GO_FC_RECEPTOR_SIGNALING_PATHWAY	0.424	0.087
		GO_POSITIVE_REGULATION_OF_T_CELL_PROLIFERATION	0.537	0.036
		GO_POSITIVE_REGULATION_OF_LEUKOCYTE_PROLIFERATION	0.557	0.010
		GO_REGULATION_OF_HUMORAL_IMMUNE_RESPONSE	0.620	0.014
immune response humoral	30	GO_INNATE_IMMUNE_RESPONSE	0.586	0.000
		GO_DEFENSE_RESPONSE	0.510	0.001
		GO_INFLAMMATORY_RESPONSE	0.582	0.000

		GO_RESPONSE_TO_VIRUS	0.588	0.000
		GO_LEUKOCYTE_MEDIATED_IMMUNITY	0.624	0.000
		GO_RESPONSE_TO_BIOTIC_STIMULUS	0.478	0.007
		GO_DEFENSE_RESPONSE_TO_BACTERIUM	0.513	0.015
		GO_CELLULAR_RESPONSE_TO_BIOTIC_STIMULUS	0.512	0.016
		GO_DEFENSE_RESPONSE_TO_OTHER_ORGANISM	0.467	0.017
		GO_RESPONSE_TO_BACTERIUM	0.489	0.006
		GO_LEUKOCYTE_MEDIATED_CYTOTOXICITY	0.513	0.190
		GO_ACUTE_INFLAMMATORY_RESPONSE	0.656	0.000
		GO_RESPONSE_TO_MOLECULE_OF_BACTERIAL_ORIGIN	0.486	0.011
		GO_RESPONSE_TO_TYPE_I_INTERFERON	0.733	0.000
		GO_ANTIMICROBIAL_HUMORAL_RESPONSE	0.507	0.138
		GO_ADAPTIVE_IMMUNE_RESPONSE	0.590	0.000
		GO_COMPLEMENT_ACTIVATION	0.757	0.000
		GO_T_CELL_MEDIATED_IMMUNITY	0.637	0.032
		GO_B_CELL_MEDIATED_IMMUNITY	0.771	0.000
		GO_LYMPHOCYTE_MEDIATED_IMMUNITY	0.679	0.000
		GO_ADAPTIVE_IMMUNE_RESPONSE_BASED_ON_SOMATIC_RECOMBINATION_OF_IMMUNE_RECEPTORS_BUILT_FROM_IMMUNOGLOBULIN_SUPERFAMILY_DOMAINS	0.703	0.000
		GO_IMMUNE_RESPONSE	0.524	0.001
		GO_RESPONSE_TO_FUNGUS	0.596	0.069
		GO_CELL_KILLING	0.484	0.170
		GO_ACUTE_PHASE_RESPONSE	0.680	0.002
		GO_HUMORAL_IMMUNE_RESPONSE_MEDIATED_BY_CIRCULATING_IMMUNOGLOBULIN	0.823	0.000
		GO_DEFENSE_RESPONSE_TO_VIRUS	0.606	0.000
		GO_HUMORAL_IMMUNE_RESPONSE	0.614	0.000
		GO_PROTEIN_ACTIVATION_CASCADE	0.707	0.000
		GO_IMMUNE_EFFECTOR_PROCESS	0.539	0.001
cytokine chemokine production	20	GO_REGULATION_OF_INTERLEUKIN_8_PRODUCTION	0.597	0.041
		GO_POSITIVE_REGULATION_OF_TUMOR_NECROSIS_FACTOR_SUPERFAMILY_CYTOKINE_PRODUCTION	0.689	0.002
		GO_POSITIVE_REGULATION_OF_CYTOKINE_PRODUCTION	0.559	0.000
		GO_POSITIVE_REGULATION_OF_CHEMOKINE_PRODUCTION	0.527	0.111
		GO_REGULATION_OF_INTERLEUKIN_6_PRODUCTION	0.440	0.130
		GO_REGULATION_OF_INTERLEUKIN_2_PRODUCTION	0.510	0.163
		GO_POSITIVE_REGULATION_OF_CYTOKINE_BIOSYNTHETIC_PROCESS	0.549	0.091
		GO_REGULATION_OF_INTERLEUKIN_12_PRODUCTION	0.601	0.064
		GO_REGULATION_OF_CYTOKINE_BIOSYNTHETIC_PROCESS	0.542	0.026
		GO_REGULATION_OF_INTERLEUKIN_10_PRODUCTION	0.620	0.050
		GO_POSITIVE_REGULATION_OF_INTERFERON_GAMMA_PRODUCTION	0.630	0.024
		GO_REGULATION_OF_TUMOR_NECROSIS_FACTOR_SUPERFAMILY_CYTOKINE_PRODUCTION	0.685	0.000

		GO_REGULATION_OF_INTERFERON_BETA_PRODUCTION	0.584	0.055
		GO_POSITIVE_REGULATION_OF_TYPE_I_INTERFERON_PRODUCTION	0.603	0.006
		GO_REGULATION_OF_CYTOKINE_PRODUCTION	0.546	0.000
		GO_POSITIVE_REGULATION_OF_INTERLEUKIN_6_PRODUCTION	0.469	0.146
		GO_REGULATION_OF_TYPE_I_INTERFERON_PRODUCTION	0.553	0.015
		GO_REGULATION_OF_VASCULAR_ENDOTHELIAL_GROWTH_FACTOR_PRODUCTION	0.648	0.021
		GO_REGULATION_OF_INTERFERON_GAMMA_PRODUCTION	0.644	0.002
		GO_NEGATIVE_REGULATION_OF_CYTOKINE_PRODUCTION	0.554	0.002
gamma interleukin 1	12	GO_RESPONSE_TO_INTERLEUKIN_6	0.680	0.013
		GO_TUMOR_NECROSIS_FACTOR_MEDIATED_SIGNALING_PATHWAY	0.388	0.216
		GO_INTERFERON_GAMMA_MEDIATED_SIGNALING_PATHWAY	0.757	0.000
		GO_RESPONSE_TO_INTERLEUKIN_4	0.579	0.084
		GO_CELLULAR_RESPONSE_TO_CYTOKINE_STIMULUS	0.542	0.000
		GO_RESPONSE_TO_INTERFERON_GAMMA	0.721	0.000
		GO_CELLULAR_RESPONSE_TO_INTERFERON_GAMMA	0.725	0.000
		GO_CELLULAR_RESPONSE_TO_INTERLEUKIN_1	0.619	0.006
		GO_CYTOKINE_MEDIATED_SIGNALING_PATHWAY	0.549	0.000
		GO_RESPONSE_TO_TUMOR_NECROSIS_FACTOR	0.464	0.038
		GO_RESPONSE_TO_CYTOKINE	0.541	0.000
		GO_RESPONSE_TO_INTERLEUKIN_1	0.606	0.001
growth factor beta	11	GO_ERBB_SIGNALING_PATHWAY	0.446	0.149
		GO_TRANSFORMING_GROWTH_FACTOR_BETA_RECEPTOR_SIGNALING_PATHWAY	0.488	0.059
		GO_VASCULAR_ENDOTHELIAL_GROWTH_FACTOR_RECEPTOR_SIGNALING_PATHWAY	0.546	0.032
		GO_RESPONSE_TO_TRANSFORMING_GROWTH_FACTOR_BETA	0.409	0.123
		GO_SMAD_PROTEIN_SIGNAL_TRANSDUCTION	0.520	0.081
		GO_ENZYME_LINKED_RECEPTOR_PROTEIN_SIGNALING_PATHWAY	0.369	0.115
		GO_RESPONSE_TO_GROWTH_FACTOR	0.362	0.136
		GO_TRANSMEMBRANE_RECEPTOR_PROTEIN_TYROSINE_KINASE_SIGNALING_PATHWAY	0.368	0.125
		GO_TRANSMEMBRANE_RECEPTOR_PROTEIN_SERINE_THREONINE_KINASE_SIGNALING_PATHWAY	0.409	0.107
		GO_EPIDERMAL_GROWTH_FACTOR_RECEPTOR_SIGNALING_PATHWAY	0.479	0.195
		GO_RESPONSE_TO_FIBROBLAST_GROWTH_FACTOR	0.388	0.227
presentation antigen mhc	5	GO_REGULATION_OF_CELLULAR_AMINE_METABOLIC_PROCESS	0.456	0.112
		GO_ANTIGEN_PROCESSING_AND_PRESENTATION_OF_EXOGENOUS_PEPTIDE_ANTIGEN_VIA_MHC_CLASS_I	0.632	0.002
		GO_NIK_NF_KAPPAB_SIGNALING	0.454	0.136
		GO_REGULATION_OF_RNA_STABILITY	0.422	0.121
		GO_ANTIGEN_PROCESSING_AND_PRESENTATION_OF_PEPTIDE_ANTIGEN_VIA_MHC_CLASS_I	0.543	0.010
peptide polysaccharide antigen	3	GO_ANTIGEN_PROCESSING_AND_PRESENTATION_OF_PEPTIDE_ANTIGEN	0.518	0.006

		GO_ANTIGEN_PROCESSING_AND_PRESENTATION	0.492	0.014
		GO_ANTIGEN_PROCESSING_AND_PRESENTATION_OF_PEPTIDE_OR_POLYSACCHARIDE_ANTIGEN_VIA_MHC_CLASS_II	0.534	0.026
tumor necrosis factor	2	GO_REGULATION_OF_TUMOR_NECROSIS_FACTOR_MEDIATED_SIGNALING_PATHWAY	0.649	0.016
		GO_REGULATION_OF_RESPONSE_TO_CYTOKINE_STIMULUS	0.526	0.015
transforming growth stimulus	2	GO_REGULATION_OF_CELLULAR_RESPONSE_TO_TRANSFORMING_GROWTH_FACTOR_BETA_STIMULUS	0.417	0.184
		GO_REGULATION_OF_CELLULAR_RESPONSE_TO_GROWTH_FACTOR_STIMULUS	0.382	0.167
production molecular immune	2	GO_IMMUNOGLOBULIN_PRODUCTION	0.583	0.029
		GO_PRODUCTION_OF_MOLECULAR_MEDIATOR_OF_IMMUNE_RESPONSE	0.555	0.029
nik kappab signaling	2	GO_POSITIVE_REGULATION_OF_INTRACELLULAR_SIGNAL_TRANSDUCTION	0.427	0.034
		GO_REGULATION_OF_NIK_NF_KAPPAB_SIGNALING	0.574	0.061
lymphocyte apoptotic process	2	GO_REGULATION_OF_LYMPHOCYTE_APOPTOTIC_PROCESS	0.700	0.006
		GO_REGULATION_OF_LEUKOCYTE_APOPTOTIC_PROCESS	0.704	0.000
cytokine secretion production	2	GO_CYTOKINE_PRODUCTION	0.544	0.010
		GO_CYTOKINE_SECRETION	0.665	0.015
viral genome replication	6	GO_NEGATIVE_REGULATION_OF_VIRAL_PROCESS	0.550	0.018
		GO_REGULATION_OF_VIRAL_GENOME_REPLICATION	0.592	0.006
		GO_NEGATIVE_REGULATION_OF_MULTI_ORGANISM_PROCESS	0.516	0.014
		GO_REGULATION_OF_MULTI_ORGANISM_PROCESS	0.361	0.149
		GO_REGULATION_OF_SYMBIOSIS_ENCOMPASSING_MUTUALISM_THROUGH_PARASITISM	0.425	0.071
		GO_NEGATIVE_REGULATION_OF_VIRAL_GENOME_REPLICATION	0.671	0.005
Development/regeneration/differentiation/proliferation				
projection regeneration platelet	12	GO_RESPONSE_TO_AXON_INJURY	0.512	0.094
		GO_PLATELET_AGGREGATION	0.582	0.053
		GO_NEURON_PROJECTION_REGENERATION	0.721	0.006
		GO_HEMOSTASIS	0.437	0.052
		GO_TISSUE_REGENERATION	0.426	0.236
		GO_PLATELET_ACTIVATION	0.413	0.128
		GO_SKELETAL_MUSCLE_TISSUE_REGENERATION	0.620	0.050
		GO_HOMOTYPIC_CELL_CELL_ADHESION	0.540	0.066
		GO_ORGAN_REGENERATION	0.544	0.013
		GO_REGENERATION	0.531	0.005
		GO_WOUND_HEALING	0.447	0.025
		GO_RESPONSE_TO_WOUNDING	0.457	0.015
projection negative differentiation	8	GO_NEGATIVE_REGULATION_OF_LEUKOCYTE_DIFFERENTIATION	0.574	0.013
		GO_NEGATIVE_REGULATION_OF_CELL_DIFFERENTIATION	0.355	0.160
		GO_NEGATIVE_REGULATION_OF_LYMPHOCYTE_DIFFERENTIATION	0.576	0.086
		GO_NEGATIVE_REGULATION_OF_CELL_PROJECTION_ORGANIZATION	0.379	0.205

		GO_NEGATIVE_REGULATION_OF_MULTICELLULAR_ORGANISMAL_PROCESS	0.394	0.069
		GO_NEGATIVE_REGULATION_OF_MYELOID_CELL_DIFFERENTIATION	0.408	0.235
		GO_NEGATIVE_REGULATION_OF_HEMOPOIESIS	0.533	0.017
		GO_NEGATIVE_REGULATION_OF_DEVELOPMENTAL_PROCESS	0.356	0.146
mesenchymal transition stem	8	GO_REGULATION_OF_EPITHELIAL_TO_MESENCHYMAL_TRANSITION	0.459	0.164
		GO_POSITIVE_REGULATION_OF_CELL_DIFFERENTIATION	0.380	0.092
		GO_POSITIVE_REGULATION_OF_DEVELOPMENTAL_PROCESS	0.365	0.111
		GO_REGULATION_OF_STEM_CELL_DIFFERENTIATION	0.412	0.188
		GO_POSITIVE_REGULATION_OF_EPITHELIAL_TO_MESENCHYMAL_TRANSITION	0.608	0.049
		GO_REGULATION_OF_EPITHELIAL_CELL_DIFFERENTIATION	0.457	0.068
		GO_POSITIVE_REGULATION_OF_STEM_CELL_DIFFERENTIATION	0.595	0.028
		GO_POSITIVE_REGULATION_OF_CELL_MORPHOGENESIS_INVOLVED_IN_DIFFERENTIATION	0.379	0.197
morphogenesis branching kidney	19	GO_UROGENITAL_SYSTEM_DEVELOPMENT	0.437	0.055
		GO_TISSUE_MORPHOGENESIS	0.353	0.176
		GO_REGULATION_OF_KIDNEY_DEVELOPMENT	0.528	0.086
		GO_MESODERM_DEVELOPMENT	0.387	0.233
		GO_SKIN_DEVELOPMENT	0.386	0.160
		GO_EPITHELIAL_CELL_DEVELOPMENT	0.423	0.080
		GO_ODONTOGENESIS	0.388	0.222
		GO_ORGAN_MORPHOGENESIS	0.369	0.121
		GO_LUNG_MORPHOGENESIS	0.535	0.147
		GO_EPIDERMIS_DEVELOPMENT	0.428	0.071
		GO_EPITHELIUM_DEVELOPMENT	0.376	0.097
		GO_MORPHOGENESIS_OF_AN_EPITHELIUM	0.352	0.188
		GO_GLOMERULUS_DEVELOPMENT	0.498	0.109
		GO_KIDNEY_MORPHOGENESIS	0.443	0.216
		GO_KERATINOCYTE_DIFFERENTIATION	0.518	0.066
		GO_GLAND_MORPHOGENESIS	0.504	0.035
		GO_MORPHOGENESIS_OF_A_BRANCHING_STRUCTURE	0.377	0.206
		GO_EPITHELIAL_CELL_DIFFERENTIATION	0.395	0.070
		GO_RESPIRATORY_SYSTEM_DEVELOPMENT	0.401	0.123
formation valve angiogenesis	8	GO_CIRCULATORY_SYSTEM_DEVELOPMENT	0.382	0.094
		GO_VASCULOGENESIS	0.620	0.046
		GO_CELLULAR_RESPONSE_TO_VASCULAR_ENDOTHELIAL_GROWTH_FACTOR_STIMULUS	0.521	0.164
		GO_ANGIOGENESIS	0.422	0.063
		GO_VASCULATURE_DEVELOPMENT	0.412	0.057
		GO_BLOOD_VESSEL_MORPHOGENESIS	0.448	0.026
		GO_ANATOMICAL_STRUCTURE_FORMATION_INVOLVED_IN_MORPHOGENESIS	0.327	0.222
		GO_HEART_VALVE_DEVELOPMENT	0.570	0.078
utero embryonic placenta	6	GO_IN_UTERO_EMBRYONIC_DEVELOPMENT	0.422	0.062
		GO_EMBRYONIC_PLACENTA_DEVELOPMENT	0.517	0.066
		GO_DEVELOPMENTAL_PROCESS_INVOLVED_IN	0.327	0.249

		_REPRODUCTION		
		GO_LABYRINTHINE_LAYER_DEVELOPMENT	0.568	0.055
		GO_PLACENTA_DEVELOPMENT	0.460	0.069
		GO_REPRODUCTIVE_SYSTEM_DEVELOPMENT	0.378	0.125
osteoclast hemopoiesis myeloid	6	GO_POSITIVE_REGULATION_OF_HEMOPOIESIS	0.507	0.022
		GO_REGULATION_OF_LEUKOCYTE_DIFFERENTIATION	0.531	0.006
		GO_REGULATION_OF_HEMOPOIESIS	0.511	0.006
		GO_REGULATION_OF_MYELOID_LEUKOCYTE_DIFFERENTIATION	0.421	0.149
		GO_REGULATION_OF_MYELOID_CELL_DIFFERENTIATION	0.427	0.087
		GO_REGULATION_OF_OSTEOCLAST_DIFFERENTIATION	0.515	0.080
ossification biomineral osteoblast	6	GO_NEGATIVE_REGULATION_OF_OSSIFICATION	0.569	0.028
		GO_POSITIVE_REGULATION_OF_OSSIFICATION	0.544	0.020
		GO_POSITIVE_REGULATION_OF_OSTEOBLAST_DIFFERENTIATION	0.606	0.010
		GO_REGULATION_OF_OSTEOBLAST_DIFFERENTIATION	0.531	0.015
		GO_REGULATION_OF_OSSIFICATION	0.509	0.011
		GO_REGULATION_OF_BIOMINERAL_TISSUE_DEVELOPMENT	0.534	0.050
muscle tissue development	6	GO_MUSCLE_ORGAN_DEVELOPMENT	0.440	0.055
		GO_MUSCLE_TISSUE_DEVELOPMENT	0.392	0.126
		GO_CARDIAC_CHAMBER_MORPHOGENESIS	0.401	0.221
		GO_SKELETAL_MUSCLE_ORGAN_DEVELOPMENT	0.528	0.020
		GO_MUSCLE_STRUCTURE_DEVELOPMENT	0.393	0.089
		GO_SKELETAL_MUSCLE_CELL_DIFFERENTIATION	0.663	0.017
connective tissue development	5	GO_BONE_DEVELOPMENT	0.369	0.234
		GO_SKELETAL_SYSTEM_DEVELOPMENT	0.357	0.165
		GO_CARTILAGE_DEVELOPMENT	0.505	0.016
		GO_CONNECTIVE_TISSUE_DEVELOPMENT	0.499	0.014
		GO_CHONDROCYTE_DIFFERENTIATION	0.467	0.146
vasculature development shape	4	GO_REGULATION_OF_ANATOMICAL_STRUCTURE_MORPHOGENESIS	0.330	0.222
		GO_POSITIVE_REGULATION_OF_VASCULATURE_DEVELOPMENT	0.534	0.008
		GO_REGULATION_OF_CELL_SHAPE	0.393	0.191
		GO_REGULATION_OF_VASCULATURE_DEVELOPMENT	0.476	0.026
prostate gland hepaticobiliary	4	GO_PROSTATE_GLAND_DEVELOPMENT	0.543	0.078
		GO_HEPATICOBILIARY_SYSTEM_DEVELOPMENT	0.495	0.033
		GO_GLAND_DEVELOPMENT	0.384	0.101
		GO_EXOCRINE_SYSTEM_DEVELOPMENT	0.473	0.118
fibroblast regulation proliferation	4	GO_NEGATIVE_REGULATION_OF_CELL_PROLIFERATION	0.404	0.065
		GO_POSITIVE_REGULATION_OF_FIBROBLAST_PROLIFERATION	0.589	0.034
		GO_REGULATION_OF_FIBROBLAST_PROLIFERATION	0.570	0.011
		GO_NEGATIVE_REGULATION_OF_FIBROBLAST_PROLIFERATION	0.521	0.190
female maternal placenta	4	GO_MATERNAL_PROCESS_INVOLVED_IN_FEMALE_PREGNANCY	0.544	0.048
		GO_EMBRYO_IMPLANTATION	0.518	0.127

		GO_MULTI_MULTICELLULAR_ORGANISM_PROCESS	0.420	0.075
		GO_MATERNAL_PLACENTA_DEVELOPMENT	0.488	0.209
cell size growth	4	GO_REGULATION_OF_CELL_SIZE	0.377	0.213
		GO_REGULATION_OF_CELL_GROWTH	0.340	0.218
		GO_REGULATION_OF_GROWTH	0.344	0.189
		GO_NEGATIVE_REGULATION_OF_GROWTH	0.413	0.093
regulation endothelial proliferation	3	GO_REGULATION_OF_ENDOTHELIAL_CELL_PROLIFERATION	0.435	0.110
		GO_POSITIVE_REGULATION_OF_ENDOTHELIAL_CELL_PROLIFERATION	0.412	0.240
		GO_NEGATIVE_REGULATION_OF_ENDOTHELIAL_CELL_PROLIFERATION	0.548	0.108
organ growth cell	3	GO_CELL_GROWTH	0.502	0.022
		GO_GROWTH	0.390	0.099
		GO_ORGAN_GROWTH	0.516	0.069
cartilage development chondrocyte	3	GO_REGULATION_OF_CHONDROCYTE_DIFFERENTIATION	0.521	0.207
		GO_POSITIVE_REGULATION_OF_CARTILAGE_DEVELOPMENT	0.492	0.232
		GO_REGULATION_OF_CARTILAGE_DEVELOPMENT	0.467	0.132
astrocyte differentiation glial	3	GO_GLIOGENESIS	0.404	0.135
		GO_GLIAL_CELL_DEVELOPMENT	0.425	0.191
		GO_ASTROCYTE_DIFFERENTIATION	0.672	0.022
smooth muscle proliferation	2	GO_REGULATION_OF_SMOOTH_MUSCLE_CELL_PROLIFERATION	0.377	0.233
		GO_POSITIVE_REGULATION_OF_SMOOTH_MUSCLE_CELL_PROLIFERATION	0.455	0.132
regulation remodeling bone	2	GO_REGULATION_OF_TISSUE_REMODELING	0.440	0.239
		GO_REGULATION_OF_BONE_REMODELING	0.501	0.188
osteoblast differentiation ossification	2	GO_OSTEOBLAST_DIFFERENTIATION	0.428	0.105
		GO_OSSIFICATION	0.384	0.132
negative muscle differentiation	2	GO_REGULATION_OF_MUSCLE_CELL_DIFFERENTIATION	0.385	0.212
		GO_NEGATIVE_REGULATION_OF_MUSCLE_CELL_DIFFERENTIATION	0.490	0.172
muscle hypertrophy adaptation	2	GO_REGULATION_OF_MUSCLE_HYPERTROPHY	0.581	0.065
		GO_REGULATION_OF_MUSCLE_ADAPTATION	0.486	0.120
epithelial cell proliferation	2	GO_CELL_PROLIFERATION	0.336	0.220
		GO_EPITHELIAL_CELL_PROLIFERATION	0.404	0.238
endocrine pancreas development	2	GO_ENDOCRINE_PANCREAS_DEVELOPMENT	0.500	0.152
		GO_PANCREAS_DEVELOPMENT	0.590	0.014
tissue remodeling	1	GO_TISSUE_REMODELING	0.539	0.021
neuromuscular junction development	1	GO_NEUROMUSCULAR_JUNCTION_DEVELOPMENT	0.510	0.191
post embryonic development	1	GO_POST_EMBRYONIC_DEVELOPMENT	0.465	0.129
lens development camera	1	GO_LENS_DEVELOPMENT_IN_CAMERA_TYPE_EYE	0.439	0.235
positive regulation cell	1	GO_POSITIVE_REGULATION_OF_CELL_PROLIFERATION	0.391	0.076
fat cell differentiation	1	GO_FAT_CELL_DIFFERENTIATION	0.426	0.163
renal homeostasis number	52	GO_B_CELL_DIFFERENTIATION	0.514	0.057
		GO_TISSUE_HOMEOSTASIS	0.469	0.046
		GO_LEUKOCYTE_ACTIVATION	0.387	0.109
		GO_TRANSITION_METAL_ION_HOMEOSTASIS	0.560	0.011

GO_ALPHA_BETA_T_CELL_ACTIVATION	0.580	0.041
GO_CELLULAR_HOMEOSTASIS	0.438	0.027
GO_CELLULAR_RESPONSE_TO_CARBOHYDRATE_STIMULUS	0.484	0.089
GO_T_CELL_ACTIVATION_INVOLVED_IN_IMMUNE_RESPONSE	0.517	0.147
GO_IRON_ION_HOMEOSTASIS	0.526	0.052
GO_CYTOSOLIC_CALCIUM_ION_TRANSPORT	0.619	0.034
GO_MYELOID_CELL_DEVELOPMENT	0.596	0.064
GO_CELLULAR_TRANSITION_METAL_ION_HOMEOSTASIS	0.591	0.007
GO_CHEMICAL_HOMEOSTASIS	0.387	0.084
GO_HOMEOSTASIS_OF_NUMBER_OF_CELLS	0.425	0.101
GO_CALCIUM_ION_IMPORT	0.559	0.053
GO_OSTEOCLAST_DIFFERENTIATION	0.489	0.200
GO_MULTICELLULAR_ORGANISMAL_HOMEOSTASIS	0.420	0.066
GO_B_CELL_ACTIVATION	0.445	0.099
GO_LEUKOCYTE_HOMEOSTASIS	0.560	0.033
GO_T_CELL_DIFFERENTIATION	0.484	0.059
GO_RENAL_WATER_HOMEOSTASIS	0.520	0.111
GO_REGULATION_OF_CYTOSOLIC_CALCIUM_ION_CONCENTRATION	0.392	0.166
GO_T_CELL_PROLIFERATION	0.500	0.212
GO_CELLULAR_GLUCOSE_HOMEOSTASIS	0.485	0.102
GO_CELL_CELL_ADHESION	0.403	0.065
GO_CELL_REDOX_HOMEOSTASIS	0.574	0.021
GO_ALPHA_BETA_T_CELL_DIFFERENTIATION	0.519	0.154
GO_ERYTHROCYTE_HOMEOSTASIS	0.434	0.160
GO_LYMPHOCYTE_DIFFERENTIATION	0.483	0.025
GO_CALCIUM_ION_IMPORT_INTO_CYTOSOL	0.668	0.027
GO_CARBOHYDRATE_HOMEOSTASIS	0.448	0.072
GO_DIVALENT_INORGANIC_CATION_HOMEOSTASIS	0.430	0.050
GO_MYELOID_CELL_DIFFERENTIATION	0.392	0.146
GO_RENAL_SYSTEM_PROCESS	0.453	0.094
GO_HOMEOSTATIC_PROCESS	0.377	0.088
GO_ION_HOMEOSTASIS	0.407	0.066
GO_CELL_ACTIVATION	0.411	0.056
GO_MYELOID_CELL_HOMEOSTASIS	0.508	0.044
GO_THYMOCYTE_AGGREGATION	0.654	0.017
GO_LEUKOCYTE_DIFFERENTIATION	0.450	0.034
GO_ANATOMICAL_STRUCTURE_HOMEOSTASIS	0.415	0.094
GO_SINGLE_ORGANISM_CELL_ADHESION	0.453	0.023
GO_CELLULAR_CHEMICAL_HOMEOSTASIS	0.441	0.027
GO_IMMUNE_SYSTEM_DEVELOPMENT	0.360	0.146
GO_LYMPHOCYTE_ACTIVATION_INVOLVED_IN_IMMUNE_RESPONSE	0.472	0.108
GO_CELLULAR_IRON_ION_HOMEOSTASIS	0.581	0.031
GO_LEUKOCYTE_CELL_CELL_ADHESION	0.475	0.023
GO_LYMPHOCYTE_ACTIVATION	0.407	0.080

		GO_ANION_HOMEOSTASIS	0.468	0.216
		GO_RETINA_HOMEOSTASIS	0.526	0.074
		GO_LEUKOCYTE_PROLIFERATION	0.448	0.154
		GO_RESPONSE_TO_CARBOHYDRATE	0.404	0.112
General Metabolism				
cysteine type endopeptidase	5	GO_ACTIVATION_OF_CYSTEINE_TYPE_ENDOPEPTIDASE_ACTIVITY	0.530	0.029
		GO_PROTEIN_MATURATION	0.351	0.218
		GO_ZYMOGEN_ACTIVATION	0.465	0.071
		GO_REGULATION_OF_CYSTEINE_TYPE_ENDOPEPTIDASE_ACTIVITY	0.480	0.020
		GO_POSITIVE_REGULATION_OF_PEPTIDASE_ACTIVITY	0.474	0.040
amide posttranscriptional gene	5	GO_NEGATIVE_REGULATION_OF_CELLULAR_AMIDE_METABOLIC_PROCESS	0.389	0.213
		GO_POSITIVE_REGULATION_OF_CELLULAR_AMIDE_METABOLIC_PROCESS	0.404	0.189
		GO_POSTTRANSCRIPTIONAL_GENE_SILENCING	0.496	0.159
		GO_REGULATION_OF_TRANSLATIONAL_INITIATION	0.411	0.188
		GO_REGULATION_OF_CELLULAR_AMIDE_METABOLIC_PROCESS	0.376	0.128
tetramerization oligomerization homotetramerization	4	GO_PROTEIN_HOMOTETRAMERIZATION	0.468	0.140
		GO_PROTEIN_TETRAMERIZATION	0.486	0.040
		GO_PROTEIN_HOMOOLIGOMERIZATION	0.395	0.142
		GO_PROTEIN_OLIGOMERIZATION	0.389	0.090
chondroitin sulfate proteoglycan	3	GO_AMINOGLYCAN_METABOLIC_PROCESS	0.530	0.008
		GO_MUCOPOLYSACCHARIDE_METABOLIC_PROCESS	0.517	0.041
		GO_CHONDROITIN_SULFATE_PROTEOGLYCAN_METABOLIC_PROCESS	0.556	0.109
carbohydrate derivative organonitrogen	3	GO_ORGANONITROGEN_COMPOUND_CATABOLIC_PROCESS	0.401	0.084
		GO_AMINOGLYCAN_CATABOLIC_PROCESS	0.649	0.002
		GO_CARBOHYDRATE_DERIVATIVE_CATABOLIC_PROCESS	0.462	0.061
regulation stabilization stability	2	GO_REGULATION_OF_PROTEIN_STABILITY	0.471	0.031
		GO_PROTEIN_STABILIZATION	0.585	0.002
regulation phospholipase lipase	2	GO_REGULATION_OF_LIPASE_ACTIVITY	0.485	0.092
		GO_REGULATION_OF_PHOSPHOLIPASE_ACTIVITY	0.480	0.108
regulation glucose import	2	GO_REGULATION_OF_GLUCOSE_IMPORT	0.499	0.154
		GO_REGULATION_OF_GLUCOSE_TRANSPORT	0.404	0.231
regulation atpase activity	2	GO_REGULATION_OF_ATPASE_ACTIVITY	0.577	0.026
		GO_POSITIVE_REGULATION_OF_ATPASE_ACTIVITY	0.577	0.060
peptidyl serine phosphorylation	2	GO_REGULATION_OF_PEPTIDYL_SERINE_PHOSPHORYLATION	0.463	0.087
		GO_POSITIVE_REGULATION_OF_PEPTIDYL_SERINE_PHOSPHORYLATION	0.544	0.029
oxidoreduction coenzyme nad	2	GO_OXIDOREDUCTION_COENZYME_METABOLIC_PROCESS	0.416	0.188
		GO_NAD_METABOLIC_PROCESS	0.510	0.123
nucleoside monophosphate biosynthetic	2	GO_NUCLEOSIDE_MONOPHOSPHATE_BIOSYNTHETIC_PROCESS	-0.423	0.145
		GO_PURINE_NUCLEOSIDE_MONOPHOSPHATE_BIOSYNTHETIC_PROCESS	-0.516	0.046

multicellular organismal macromolecule	2	GO_MULTICELLULAR_ORGANISM_METABOLIC_PROCESS	0.542	0.020
		GO_MULTICELLULAR_ORGANISMAL_MACROMOLECULE_METABOLIC_PROCESS	0.559	0.026
lipoprotein metabolic biosynthetic	2	GO_LIPOPROTEIN_BIOSYNTHETIC_PROCESS	0.426	0.240
		GO_LIPOPROTEIN_METABOLIC_PROCESS	0.415	0.163
ammonium ion amine	2	GO_AMINE_METABOLIC_PROCESS	0.392	0.214
		GO_AMMONIUM_ION_METABOLIC_PROCESS	0.407	0.152
water soluble vitamin	1	GO_WATER_SOLUBLE_VITAMIN_METABOLIC_PROCESS	0.402	0.249
thioester metabolic process	1	GO_THIOESTER_METABOLIC_PROCESS	-0.427	0.112
oxidative phosphorylation	1	GO_OXIDATIVE_PHOSPHORYLATION	-0.453	0.032
cyclic nucleotide metabolic	1	GO_CYCLIC_NUCLEOTIDE_METABOLIC_PROCESS	0.489	0.154
isoprenoid biosynthetic process	1	GO_ISOPRENOID_BIOSYNTHETIC_PROCESS	-0.633	0.010
amino sugar metabolic	1	GO_AMINO_SUGAR_METABOLIC_PROCESS	0.611	0.034
organic hydroxy compound	1	GO_ORGANIC_HYDROXY_COMPOUND_CATABOLIC_PROCESS	0.411	0.234
regulation hydrolase activity	1	GO_REGULATION_OF_HYDROLASE_ACTIVITY	0.387	0.074
regulation protein deacetylation	1	GO_REGULATION_OF_PROTEIN_DEACETYLATION	0.490	0.210
Lipid Metabolism and Transport				
biosynthetic sterol steroid	6	GO_STEROL_METABOLIC_PROCESS	-0.384	0.022
		GO_STEROID_BIOSYNTHETIC_PROCESS	-0.480	0.002
		GO_STEROL_BIOSYNTHETIC_PROCESS	-0.803	0.000
		GO_ORGANIC_HYDROXY_COMPOUND_BIOSYNTHETIC_PROCESS	-0.330	0.108
		GO_STEROID_METABOLIC_PROCESS	-0.287	0.149
		GO_ALCOHOL_BIOSYNTHETIC_PROCESS	-0.427	0.016
lipid biosynthetic metabolic	5	GO_REGULATION_OF_LIPID_BIOSYNTHETIC_PROCESS	0.578	0.008
		GO_REGULATION_OF_STEROID_METABOLIC_PROCESS	0.456	0.218
		GO_POSITIVE_REGULATION_OF_LIPID_BIOSYNTHETIC_PROCESS	0.603	0.014
		GO_REGULATION_OF_LIPID_METABOLIC_PROCESS	0.412	0.097
		GO_POSITIVE_REGULATION_OF_LIPID_METABOLIC_PROCESS	0.440	0.096
fatty acid biosynthetic	1	GO_FATTY_ACID_BIOSYNTHETIC_PROCESS	-0.365	0.109
neutral lipid metabolic	1	GO_NEUTRAL_LIPID_METABOLIC_PROCESS	0.424	0.228
particle complex subunit	7	GO_PROTEIN_LIPID_COMPLEX_SUBUNIT_ORGANIZATION	0.736	0.006
		GO_STEROL_TRANSPORT	0.550	0.066
		GO_ORGANIC_HYDROXY_COMPOUND_TRANSPORT	0.476	0.049
		GO_STEROL_HOMEOSTASIS	0.465	0.202
		GO_LIPID_LOCALIZATION	0.404	0.105
		GO_REGULATION_OF_PLASMA_LIPOPROTEIN_PARTICLE_LEVELS	0.673	0.006
		GO_FATTY_ACID_TRANSPORT	0.569	0.060
sterol transport lipid	3	GO_REGULATION_OF_LIPID_TRANSPORT	0.507	0.060
		GO_REGULATION_OF_STEROL_TRANSPORT	0.657	0.025
		GO_POSITIVE_REGULATION_OF_LIPID_TRANSPORT	0.555	0.052
organophosphate ester phospholipid	2	GO_ORGANOPHOSPHATE_ESTER_TRANSPORT	0.480	0.150

		GO_PHOSPHOLIPID_TRANSPORT	0.550	0.099
toxin transport	1	GO_TOXIN_TRANSPORT	0.603	0.051
regulation lipid storage	1	GO_REGULATION_OF_LIPID_STORAGE	0.606	0.030
regulation intracellular steroid	1	GO_REGULATION_OF_INTRACELLULAR_STEROID_HORMONE_RECEPTOR_SIGNALING_PATHWAY	0.465	0.224
Signal Transduction				
retinoic acid response	31	GO_RESPONSE_TO_DSRNA	0.554	0.032
		GO_CELLULAR_RESPONSE_TO_RETINOIC_ACID	0.496	0.081
		GO_RESPONSE_TO_ETHANOL	0.377	0.219
		GO_RESPONSE_TO_ALCOHOL	0.423	0.048
		GO_CELLULAR_RESPONSE_TO_LIPID	0.379	0.105
		GO_CELLULAR_RESPONSE_TO_KETONE	0.500	0.094
		GO_RESPONSE_TO_CORTICOSTEROID	0.542	0.003
		GO_RESPONSE_TO_HORMONE	0.374	0.104
		GO_RESPONSE_TO_STEROID_HORMONE	0.362	0.145
		GO_RESPONSE_TO_ATP	0.600	0.064
		GO_RESPONSE_TO_ACID_CHEMICAL	0.417	0.066
		GO_CELLULAR_RESPONSE_TO_FATTY_ACID	0.588	0.066
		GO_CELLULAR_RESPONSE_TO_AMINO_ACID_STIMULUS	0.615	0.009
		GO_RESPONSE_TO_PROGESTERONE	0.539	0.045
		GO_RESPONSE_TO_AMINO_ACID	0.460	0.060
		GO_RESPONSE_TO_ORGANIC_CYCLIC_COMPOUND	0.369	0.105
		GO_CELLULAR_RESPONSE_TO_ALCOHOL	0.428	0.122
		GO_CELLULAR_RESPONSE_TO_ACID_CHEMICAL	0.525	0.008
		GO_RESPONSE_TO_RETINOIC_ACID	0.432	0.128
		GO_CELLULAR_RESPONSE_TO_ORGANIC_CYCLIC_COMPOUND	0.375	0.123
		GO_RESPONSE_TO_PURINE_CONTAINING_COMPOUND	0.359	0.233
		GO_RESPONSE_TO_LIPID	0.383	0.092
		GO_RESPONSE_TO_EXOGENOUS_DSRNA	0.640	0.023
		GO_RESPONSE_TO_ESTROGEN	0.379	0.189
		GO_CELLULAR_RESPONSE_TO_CORTICOSTEROID_STIMULUS	0.589	0.027
		GO_CELLULAR_RESPONSE_TO_DSRNA	0.516	0.154
		GO_INTRACELLULAR_RECEPTOR_SIGNALING_PATHWAY	0.380	0.190
		GO_RESPONSE_TO_VITAMIN_D	0.496	0.177
		GO_RESPONSE_TO_NICOTINE	0.473	0.212
		GO_RESPONSE_TO_KETONE	0.461	0.041
		GO_RESPONSE_TO_FATTY_ACID	0.440	0.198
radiation abiotic ionizing	14	GO_RESPONSE_TO_RADIATION	0.384	0.104
		GO_RESPONSE_TO_X_RAY	0.535	0.132
		GO_RESPONSE_TO_ABIOTIC_STIMULUS	0.411	0.047
		GO_RESPONSE_TO_MECHANICAL_STIMULUS	0.604	0.000
		GO_CELLULAR_RESPONSE_TO_MECHANICAL_STIMULUS	0.615	0.002
		GO_RESPONSE_TO_HEAT	0.598	0.002

		GO_CELLULAR_RESPONSE_TO_IONIZING_RADIATION	0.481	0.208
		GO_RESPONSE_TO_IONIZING_RADIATION	0.493	0.034
		GO_CELLULAR_RESPONSE_TO_ABIOTIC_STIMULUS	0.381	0.142
		GO_RESPONSE_TO_COLD	0.493	0.164
		GO_RESPONSE_TO_GAMMA_RADIATION	0.559	0.062
		GO_CELLULAR_RESPONSE_TO_HEAT	0.702	0.006
		GO_RESPONSE_TO_OXYGEN_LEVELS	0.403	0.074
		GO_RESPONSE_TO_TEMPERATURE_STIMULUS	0.548	0.005
insulin nitrogen glucagon	11	GO_INSULIN_RECEPTOR_SIGNALING_PATHWAY	0.417	0.235
		GO_CELLULAR_RESPONSE_TO_INSULIN_STIMULUS	0.389	0.163
		GO_RESPONSE_TO_NITROGEN_COMPOUND	0.367	0.114
		GO_CELLULAR_RESPONSE_TO_GLUCAGON_STIMULUS	0.534	0.112
		GO_CELLULAR_RESPONSE_TO_ENDOGENOUS_STIMULUS	0.338	0.188
		GO_RESPONSE_TO_PEPTIDE	0.418	0.057
		GO_CELLULAR_RESPONSE_TO_PEPTIDE	0.355	0.209
		GO_RESPONSE_TO_GLUCAGON	0.471	0.190
		GO_RESPONSE_TO_INSULIN	0.395	0.128
		GO_CELLULAR_RESPONSE_TO_HORMONE_STIMULUS	0.362	0.133
		GO_CELLULAR_RESPONSE_TO_NITROGEN_COMPOUND	0.371	0.125
starvation nutrient extracellular	8	GO_RESPONSE_TO_EXTRACELLULAR_STIMULUS	0.366	0.135
		GO_RESPONSE_TO_STARVATION	0.455	0.055
		GO_RESPONSE_TO_NUTRIENT	0.363	0.189
		GO_CELLULAR_RESPONSE_TO_NUTRIENT	0.472	0.190
		GO_CELLULAR_RESPONSE_TO_EXTERNAL_STIMULUS	0.496	0.008
		GO_CELLULAR_RESPONSE_TO_STARVATION	0.460	0.054
		GO_CELLULAR_RESPONSE_TO_EXTRACELLULAR_STIMULUS	0.445	0.052
		GO_CELLULAR_RESPONSE_TO_GLUCOSE_STARVATION	0.552	0.059
toxic detoxification antibiotic	3	GO_RESPONSE_TO_ANTIBIOTIC	0.587	0.070
		GO_DETOXIFICATION	0.407	0.215
		GO_RESPONSE_TO_TOXIC_SUBSTANCE	0.460	0.030
response drug	1	GO_RESPONSE_TO_DRUG	0.376	0.128
negative function catalytic	12	GO_NEGATIVE_REGULATION_OF_PHOSPHORUS_METABOLIC_PROCESS	0.329	0.234
		GO_NEGATIVE_REGULATION_OF_ERK1_AND_ERK2_CASCADE	0.515	0.110
		GO_NEGATIVE_REGULATION_OF_CATALYTIC_ACTIVITY	0.436	0.027
		GO_NEGATIVE_REGULATION_OF_TRANSFERASE_ACTIVITY	0.391	0.111
		GO_NEGATIVE_REGULATION_OF_PROTEIN_MODIFICATION_PROCESS	0.334	0.224
		GO_NEGATIVE_REGULATION_OF_MOLECULAR_FUNCTION	0.419	0.037
		GO_NEGATIVE_REGULATION_OF_PROTEIN_SERINE_THREONINE_KINASE_ACTIVITY	0.474	0.055
		GO_NEGATIVE_REGULATION_OF_PROTEIN_METABOLIC_PROCESS	0.413	0.041
		GO_NEGATIVE_REGULATION_OF_MAPK_CASCADE	0.428	0.111

		GO_NEGATIVE_REGULATION_OF_KINASE_ACTIVITY	0.449	0.041
		GO_NEGATIVE_REGULATION_OF_PHOSPHORYLATION	0.370	0.140
		GO_NEGATIVE_REGULATION_OF_MAP_KINASE_ACTIVITY	0.463	0.135
camp messenger nucleotide	3	GO_CYCLIC_NUCLEOTIDE_MEDIATED_SIGNALING	0.592	0.027
		GO_SECOND_MESSENGER_MEDIATED_SIGNALING	0.443	0.084
stat cascade	1	GO_STAT_CASCADE	0.469	0.188
map kinase activity	21	GO_REGULATION_OF_PROTEIN_TYROSINE_KINASE_ACTIVITY	0.420	0.235
		GO_POSITIVE_REGULATION_OF_MAP_KINASE_ACTIVITY	0.379	0.207
		GO_POSITIVE_REGULATION_OF_TRANSFERASE_ACTIVITY	0.368	0.125
		GO_POSITIVE_REGULATION_OF_MAPK_CASCADE	0.389	0.092
		GO_REGULATION_OF_KINASE_ACTIVITY	0.379	0.096
		GO_ACTIVATION_OF_MAPK_ACTIVITY	0.436	0.126
		GO_POSITIVE_REGULATION_OF_PEPTIDYL_TYROSINE_PHOSPHORYLATION	0.392	0.168
		GO_ACTIVATION_OF_PROTEIN_KINASE_ACTIVITY	0.420	0.071
		GO_POSITIVE_REGULATION_OF_PHOSPHORUS_METABOLIC_PROCESS	0.380	0.087
		GO_REGULATION_OF_PEPTIDYL_TYROSINE_PHOSPHORYLATION	0.372	0.160
		GO_REGULATION_OF_ERK1_AND_ERK2_CASCADE	0.456	0.044
		GO_REGULATION_OF_MAPK_CASCADE	0.377	0.100
		GO_REGULATION_OF_MAP_KINASE_ACTIVITY	0.399	0.109
		GO_STRESS_ACTIVATED_PROTEIN_KINASE_SIGNALING_CASCADE	0.415	0.197
		GO_POSITIVE_REGULATION_OF_PROTEIN_MODIFICATION_PROCESS	0.369	0.108
		GO_POSITIVE_REGULATION_OF_KINASE_ACTIVITY	0.413	0.065
		GO_REGULATION_OF_PROTEIN_SERINE_THREONINE_KINASE_ACTIVITY	0.416	0.057
		GO_POSITIVE_REGULATION_OF_PROTEIN_SERINE_THREONINE_KINASE_ACTIVITY	0.438	0.047
		GO_REGULATION_OF_PEPTIDYL_THREONINE_PHOSPHORYLATION	0.537	0.121
		GO_REGULATION_OF_TRANSFERASE_ACTIVITY	0.352	0.159
		GO_POSITIVE_REGULATION_OF_ERK1_AND_ERK2_CASCADE	0.464	0.049
kappab kinase nf	3	GO_I_KAPPAB_KINASE_NF_KAPPAB_SIGNALING	0.624	0.014
		GO_POSITIVE_REGULATION_OF_I_KAPPAB_KINASE_NF_KAPPAB_SIGNALING	0.455	0.050
		GO_REGULATION_OF_I_KAPPAB_KINASE_NF_KAPPAB_SIGNALING	0.476	0.028
protein kinase signaling	2	GO_REGULATION_OF_PROTEIN_KINASE_B_SIGNALING	0.569	0.007
		GO_POSITIVE_REGULATION_OF_PROTEIN_KINASE_B_SIGNALING	0.646	0.002
rho transduction ras	2	GO_REGULATION_OF_RAS_PROTEIN_SIGNAL_TRANSDUCTION	0.422	0.097
		GO_REGULATION_OF_RHO_PROTEIN_SIGNAL_TRANSDUCTION	0.443	0.114
Cytoskeleton and Motility				
filament actin reorganization	6	GO_ACTIN_FILAMENT_BUNDLE_ORGANIZATION	0.520	0.095

		GO_ACTIN_FILAMENT_ORGANIZATION	0.448	0.064
		GO_ACTIN_CYTOSKELETON_REORGANIZATION	0.437	0.182
		GO_ACTIN_FILAMENT_BASED_PROCESS	0.409	0.060
		GO_INTERMEDIATE_FILAMENT_BASED_PROCESS	0.571	0.064
		GO_CYTOSKELETON_ORGANIZATION	0.338	0.207
contraction striated muscle	5	GO_ACTIN_MEDIATED_CELL_CONTRACTION	0.427	0.235
		GO_HEART_PROCESS	0.425	0.191
		GO_MUSCLE_SYSTEM_PROCESS	0.399	0.099
		GO_MUSCLE_CONTRACTION	0.398	0.126
		GO_STRIATED_MUSCLE_CONTRACTION	0.446	0.140
lamellipodium organization	1	GO_LAMELLIPODIUM_ORGANIZATION	0.521	0.146
migration leukocyte chemotaxis	12	GO_CELL_MOTILITY	0.386	0.081
		GO_LOCOMOTION	0.398	0.064
		GO_CELL_CHEMOTAXIS	0.433	0.103
		GO_TISSUE_MIGRATION	0.424	0.188
		GO_GRANULOCYTE_MIGRATION	0.660	0.006
		GO_MYELOID_LEUKOCYTE_MIGRATION	0.525	0.053
		GO_TAXIS	0.362	0.163
		GO_MOVEMENT_OF_CELL_OR_SUBCELLULAR_COMPONENT	0.352	0.147
		GO_NEURON_MIGRATION	0.549	0.032
		GO_ENDOTHELIAL_CELL_MIGRATION	0.493	0.099
		GO_LEUKOCYTE_MIGRATION	0.485	0.016
		GO_LEUKOCYTE_CHEMOTAXIS	0.536	0.032
epithelial migration locomotion	9	GO_REGULATION_OF_BLOOD_VESSEL_ENDOTHELIAL_CELL_MIGRATION	0.511	0.064
		GO_POSITIVE_REGULATION_OF_ENDOTHELIAL_CELL_MIGRATION	0.442	0.178
		GO_POSITIVE_REGULATION_OF_EPITHELIAL_CELL_MIGRATION	0.415	0.146
		GO_NEGATIVE_REGULATION_OF_LOCOMOTION	0.351	0.219
		GO_REGULATION_OF_ENDOTHELIAL_CELL_MIGRATION	0.422	0.121
		GO_POSITIVE_REGULATION_OF_CHEMOTAXIS	0.442	0.106
		GO_POSITIVE_REGULATION_OF_LOCOMOTION	0.364	0.161
		GO_REGULATION_OF_CELLULAR_COMPONENT_MOVEMENT	0.387	0.078
		GO_REGULATION_OF_EPITHELIAL_CELL_MIGRATION	0.388	0.144
collagen fibril disassembly	3	GO_EXTRACELLULAR_MATRIX_DISASSEMBLY	0.524	0.071
		GO_EXTRACELLULAR_STRUCTURE_ORGANIZATION	0.402	0.094
		GO_COLLAGEN_FIBRIL_ORGANIZATION	0.510	0.098
Membrane dynamics				
membrane biogenesis assembly	2	GO_MEMBRANE_BIOGENESIS	0.539	0.068
		GO_MEMBRANE_ASSEMBLY	0.592	0.049
regulation mitochondrial membrane	1	GO_REGULATION_OF_MITOCHONDRIAL_MEMBRANE_POTENTIAL	0.460	0.161
plasma membrane organization	1	GO_PLASMA_MEMBRANE_ORGANIZATION	0.417	0.094
regulation localization secretion	39	GO_POSITIVE_REGULATION_OF_CELLULAR_PROTEIN_LOCALIZATION	0.394	0.102
		GO_REGULATION_OF_CYTOKINE_SECRETION	0.573	0.008

GO_REGULATION_OF_PROTEIN_LOCALIZATION	0.384	0.084
GO_REGULATION_OF_INTERLEUKIN_1_PRODUCTION	0.702	0.012
GO_POSITIVE_REGULATION_OF_PEPTIDE_SECRETION	0.510	0.043
GO_POSITIVE_REGULATION_OF_TRANSPORT	0.397	0.066
GO_POSITIVE_REGULATION_OF_SECRETION	0.385	0.111
GO_POSITIVE_REGULATION_OF_HORMONE_SECRETION	0.433	0.147
GO_REGULATION_OF_PLASMA_MEMBRANE_ORGANIZATION	0.462	0.136
GO_REGULATION_OF_CELLULAR_PROTEIN_LOCALIZATION	0.398	0.074
GO_REGULATION_OF_MITOCHONDRION_ORGANIZATION	0.384	0.182
GO_POSITIVE_REGULATION_OF_CYTOKINE_SECRETION	0.475	0.121
GO_REGULATION_OF_SECRETION	0.334	0.216
GO_NEGATIVE_REGULATION_OF_INTRACELLULAR_TRANSPORT	0.394	0.190
GO_NEGATIVE_REGULATION_OF_PROTEIN_SECRETION	0.470	0.146
GO_POSITIVE_REGULATION_OF_INTRACELLULAR_TRANSPORT	0.355	0.198
GO_POSITIVE_REGULATION_OF_PROTEIN_SECRETION	0.450	0.059
GO_REGULATION_OF_INTRACELLULAR_PROTEIN_TRANSPORT	0.385	0.126
GO_REGULATION_OF_PROTEIN_SECRETION	0.388	0.109
GO_REGULATION_OF_PROTEIN_IMPORT	0.483	0.032
GO_REGULATION_OF_PROTEIN_LOCALIZATION_TO_NUCLEUS	0.466	0.035
GO_REGULATION_OF_CALCIUM_ION_DEPENDENT_EXOCYTOSIS	-0.509	0.046
GO_POSITIVE_REGULATION_OF_NUCLEOCYTOPLASMIC_TRANSPORT	0.453	0.109
GO_NEGATIVE_REGULATION_OF_ESTABLISHMENT_OF_PROTEIN_LOCALIZATION	0.439	0.066
GO_POSITIVE_REGULATION_OF_PROTEIN_IMPORT	0.495	0.071
GO_POSITIVE_REGULATION_OF_ESTABLISHMENT_OF_PROTEIN_LOCALIZATION	0.426	0.046
GO_REGULATION_OF_MITOCHONDRIAL_OUTER_MEMBRANE_PERMEABILIZATION_INVOLVED_IN_APOPTOTIC_SIGNALING_PATHWAY	0.561	0.102
GO_POSITIVE_REGULATION_OF_INSULIN_SECRETION	0.578	0.027
GO_NEGATIVE_REGULATION_OF_CELLULAR_PROTEIN_LOCALIZATION	0.430	0.112
GO_POSITIVE_REGULATION_OF_INTRACELLULAR_PROTEIN_TRANSPORT	0.387	0.147
GO_POSITIVE_REGULATION_OF_CYTOPLASMIC_TRANSPORT	0.353	0.219
GO_REGULATION_OF_PROTEIN_TARGETING	0.412	0.076
GO_NEGATIVE_REGULATION_OF_SECRETION	0.402	0.137
GO_REGULATION_OF_NUCLEOCYTOPLASMIC_TRANSPORT	0.478	0.023
GO_REGULATION_OF_CYTOPLASMIC_TRANSPORT	0.381	0.111
GO_REGULATION_OF_TRANSCRIPTION_FACTOR_IMPORT_INTO_NUCLEUS	0.468	0.132
GO_POSITIVE_REGULATION_OF_PROTEIN_LOCALIZATION_TO_NUCLEUS	0.499	0.036
GO_REGULATION_OF_INTRACELLULAR_TRANSPORT	0.364	0.136
GO_REGULATION_OF_CELLULAR_LOCALIZATION	0.335	0.198

regulated exocytosis secretion	9	GO_HORMONE_TRANSPORT	0.459	0.122
		GO_PEPTIDE_SECRETION	0.436	0.249
		GO_PROTEIN_SECRETION	0.511	0.027
		GO_PLATELET_DEGRANULATION	0.552	0.007
		GO_SECRETION_BY_CELL	0.409	0.065
		GO_SECRETION	0.405	0.069
		GO_EXOCYTOSIS	0.396	0.098
		GO_BODY_FLUID_SECRETION	0.491	0.096
		GO_REGULATED_EXOCYTOSIS	0.441	0.061
endocytosis internalization phagocytosis	8	GO_REGULATION_OF_ENDOCYTOSIS	0.432	0.060
		GO_REGULATION_OF_PHAGOCYTOSIS	0.529	0.046
		GO_POSITIVE_REGULATION_OF_CELLULAR_COMPONENT_ORGANIZATION	0.340	0.190
		GO_REGULATION_OF_RECEPTOR_INTERNALIZATION	0.562	0.094
		GO_REGULATION_OF_RECEPTOR_MEDIATED_ENDOCYTOSIS	0.425	0.209
		GO_POSITIVE_REGULATION_OF_PHAGOCYTOSIS	0.636	0.014
		GO_POSITIVE_REGULATION_OF_ENDOCYTOSIS	0.502	0.030
		GO_NEGATIVE_REGULATION_OF_ENDOCYTOSIS	0.492	0.146
phagocytosis engulfment clearance	6	GO_APOPTOTIC_CELL_CLEARANCE	0.561	0.102
		GO_ENDOCYTOSIS	0.375	0.120
		GO_RECEPTOR_MEDIATED_ENDOCYTOSIS	0.430	0.067
		GO_MEMBRANE_INVAGINATION	0.475	0.222
		GO_PHAGOCYTOSIS	0.507	0.015
		GO_PHAGOCYTOSIS_ENGULFMENT	0.544	0.146
nuclear import nucleus	3	GO_NUCLEAR_IMPORT	0.483	0.043
		GO_PROTEIN_LOCALIZATION_TO_NUCLEUS	0.512	0.017
		GO_PROTEIN_IMPORT	0.453	0.063
monosaccharide transport carbohydrate	2	GO_CARBOHYDRATE_TRANSPORT	0.611	0.010
		GO_MONOSACCHARIDE_TRANSPORT	0.566	0.057
maintenance location cell	2	GO_MAINTENANCE_OF_LOCATION	0.491	0.034
		GO_MAINTENANCE_OF_LOCATION_IN_CELL	0.456	0.124
bicarbonate transport	1	GO_BICARBONATE_TRANSPORT	-0.464	0.118
regulation vesicle fusion	1	GO_REGULATION_OF_VESICLE_FUSION	0.547	0.105
lytic vacuole organization	1	GO_LYTIC_VACUOLE_ORGANIZATION	0.565	0.070
Stress response				
endoplasmic reticulum stress	8	GO_NEGATIVE_REGULATION_OF_RESPONSE_TO_OXIDATIVE_STRESS	0.631	0.020
		GO_REGULATION_OF_CELLULAR_RESPONSE_TO_HEAT	0.638	0.001
		GO_REGULATION_OF_OXIDATIVE_STRESS_INDUCED_CELL_DEATH	0.609	0.015
		GO_REGULATION_OF_ENDOPLASMIC_RETICULUM_STRESS_INDUCED_INTRINSIC_APOPTOTIC_SIGNALING_PATHWAY	0.533	0.136
		GO_REGULATION_OF_CELLULAR_RESPONSE_TO_STRESS	0.376	0.102
		GO_NEGATIVE_REGULATION_OF_RESPONSE_TO_DNA_DAMAGE_STIMULUS	0.514	0.104
		GO_REGULATION_OF_RESPONSE_TO_OXIDATI	0.535	0.040

		VE_STRESS		
		GO_NEGATIVE_REGULATION_OF_RESPONSE_TO_ENDOPLASMIC_RETICULUM_STRESS	0.531	0.098
reactive oxygen species	5	GO_POSITIVE_REGULATION_OF_REACTIVE_OXYGEN_SPECIES_BIOSYNTHETIC_PROCESS	0.517	0.066
		GO_POSITIVE_REGULATION_OF_REACTIVE_OXYGEN_SPECIES_METABOLIC_PROCESS	0.540	0.019
		GO_REGULATION_OF_NITRIC_OXIDE_BIOSYNTHETIC_PROCESS	0.537	0.060
		GO_REGULATION_OF_REACTIVE_OXYGEN_SPECIES_BIOSYNTHETIC_PROCESS	0.515	0.055
		GO_REGULATION_OF_REACTIVE_OXYGEN_SPECIES_METABOLIC_PROCESS	0.462	0.034
synthase oxidoreductase monooxygenase	4	GO_REGULATION_OF_NITRIC_OXIDE_SYNTHASE_ACTIVITY	0.571	0.049
		GO_REGULATION_OF_MONOOXYGENASE_ACTIVITY	0.528	0.069
		GO_POSITIVE_REGULATION_OF_OXIDOREDUCTASE_ACTIVITY	0.568	0.089
		GO_REGULATION_OF_OXIDOREDUCTASE_ACTIVITY	0.492	0.084
cellular response oxygen	1	GO_CELLULAR_RESPONSE_TO_OXYGEN_CONTAINING_COMPOUND	0.387	0.081
reactive oxygen species	1	GO_REACTIVE_OXYGEN_SPECIES_METABOLIC_PROCESS	0.490	0.060
response fluid shear	1	GO_RESPONSE_TO_FLUID_SHEAR_STRESS	0.635	0.017
erad catabolic process	6	GO_PROTEASOMAL_PROTEIN_CATABOLIC_PROCESS	0.383	0.150
		GO_ER_ASSOCIATED_UBIQUITIN_DEPENDENT_PROTEIN_CATABOLIC_PROCESS	0.484	0.135
		GO_ERAD_PATHWAY	0.444	0.205
		GO_MACROMOLECULE_CATABOLIC_PROCESS	0.353	0.153
		GO_PROTEIN_CATABOLIC_PROCESS	0.346	0.191
		GO_REGULATION_OF_ERAD_PATHWAY	0.493	0.229
hydrogen peroxide response	14	GO_RESPONSE_TO_METAL_ION	0.488	0.008
		GO_RESPONSE_TO_CALCIUM_ION	0.385	0.240
		GO_CELLULAR_RESPONSE_TO_INORGANIC_SUBSTANCE	0.478	0.037
		GO_RESPONSE_TO_REACTIVE_OXYGEN_SPECIES	0.518	0.007
		GO_RESPONSE_TO_CADMIUM_ION	0.545	0.076
		GO_RESPONSE_TO_HYDROGEN_PEROXIDE	0.473	0.046
		GO_CELLULAR_RESPONSE_TO_REACTIVE_OXYGEN_SPECIES	0.513	0.017
		GO_RESPONSE_TO_ZINC_ION	0.729	0.001
		GO_RESPONSE_TO_INORGANIC_SUBSTANCE	0.451	0.021
		GO_CELLULAR_RESPONSE_TO_OXIDATIVE_STRESS	0.504	0.013
		GO_RESPONSE_TO_OXIDATIVE_STRESS	0.457	0.025
Proteostasis				
maturation proteolysis peptidase	8	GO_CAMP_MEDIATED_SIGNALING	0.488	0.207
		GO_REGULATION_OF_PROTEOLYSIS	0.453	0.018
		GO_NEGATIVE_REGULATION_OF_CYSTEINE_TYPE_ENDOPEPTIDASE_ACTIVITY	0.553	0.009
		GO_NEGATIVE_REGULATION_OF_PEPTIDASE_ACTIVITY	0.583	0.000
		GO_NEGATIVE_REGULATION_OF_PROTEIN_MATURATION	0.625	0.037
		GO_REGULATION_OF_PROTEIN_MATURATION	0.486	0.070
		GO_REGULATION_OF_PEPTIDASE_ACTIVITY	0.545	0.001

		GO_NEGATIVE_REGULATION_OF_PROTEOLYSIS	0.532	0.002
catabolic small conjugation	11	GO_NEGATIVE_REGULATION_OF_PROTEIN_CATABOLIC_PROCESS	0.508	0.041
		GO_POSITIVE_REGULATION_OF_CELLULAR_PROTEIN_CATABOLIC_PROCESS	0.390	0.170
		GO_NEGATIVE_REGULATION_OF_CATABOLIC_PROCESS	0.414	0.116
		GO_POSITIVE_REGULATION_OF_CATABOLIC_PROCESS	0.345	0.208
		GO_REGULATION_OF_PROTEASOMAL_UBIQUITIN_DEPENDENT_PROTEIN_CATABOLIC_PROCESS	0.394	0.190
		GO_REGULATION_OF_PROTEIN_CATABOLIC_PROCESS	0.434	0.041
		GO_POSITIVE_REGULATION_OF_PROTEIN_CATABOLIC_PROCESS	0.385	0.157
		GO_REGULATION_OF_CATABOLIC_PROCESS	0.376	0.098
		GO_REGULATION_OF_CELLULAR_PROTEIN_CATABOLIC_PROCESS	0.391	0.135
		GO_REGULATION_OF_PROTEIN_MODIFICATION_BY_SMALL_PROTEIN_CONJUGATION_OR_REMOVAL	0.365	0.206
		GO_POSITIVE_REGULATION_OF_PROTEOLYSIS	0.401	0.084
erad catabolic process	6	GO_PROTEASOMAL_PROTEIN_CATABOLIC_PROCESS	0.383	0.150
		GO_ER_ASSOCIATED_UBIQUITIN_DEPENDENT_PROTEIN_CATABOLIC_PROCESS	0.484	0.135
		GO_ERAD_PATHWAY	0.444	0.205
		GO_MACROMOLECULE_CATABOLIC_PROCESS	0.353	0.153
		GO_PROTEIN_CATABOLIC_PROCESS	0.346	0.191
		GO_REGULATION_OF_ERAD_PATHWAY	0.493	0.229
chaperone refolding folding	3	GO_PROTEIN_FOLDING	0.611	0.000
		GO_PROTEIN_REFOLDING	0.730	0.006
		GO_CHAPERONE_MEDIATED_PROTEIN_FOLDING	0.667	0.003
topologically incorrect ire1	5	GO_CELLULAR_RESPONSE_TO_TOPOLOGICALLY_INCORRECT_PROTEIN	0.506	0.027
		GO_RESPONSE_TO_ENDOPLASMIC_RETICULUM_STRESS	0.515	0.008
		GO_ER_NUCLEUS_SIGNALING_PATHWAY	0.677	0.007
		GO_RESPONSE_TO_TOPOLOGICALLY_INCORRECT_PROTEIN	0.634	0.000
		GO_IRE1_MEDIATED_UNFOLDED_PROTEIN_RESPONSE	0.519	0.079
Synaptic transmission and calcium signalling				
		GO_REGULATION_OF_POSTSYNAPTIC_MEMBRANE_POTENTIAL	-0.549	0.053
regulation postsynaptic membrane	2	GO_CELL_SURFACE_RECEPTOR_SIGNALING_PATHWAY_INVOLVED_IN_CELL_CELL_SIGNALING	-0.543	0.018
		GO_NEURON_NEURON_SYNAPTIC_TRANSMISSION	-0.402	0.218
neuron synaptic transmission	1	GO_NEGATIVE_REGULATION_OF_CELL_COMMUNICATION	0.340	0.189
canonical wnt coupled	5	GO_NEGATIVE_REGULATION_OF_INTRACELLULAR_SIGNAL_TRANSDUCTION	0.457	0.020
		GO_NEGATIVE_REGULATION_OF_CANONICAL_WNT_SIGNALING_PATHWAY	0.415	0.121
		GO_NEGATIVE_REGULATION_OF_SYNAPTIC_TRANSMISSION	-0.444	0.109
		GO_NEGATIVE_REGULATION_OF_G_PROTEIN_COUPLED_RECEPTOR_PROTEIN_SIGNALING_PATHWAY	0.489	0.207
regulation depolarization homeostatic	4	GO_REGULATION_OF_ION_HOMEOSTASIS	0.432	0.078

		GO_REGULATION_OF_MEMBRANE_DEPOLARIZATION	0.673	0.010
		GO_NEGATIVE_REGULATION_OF_HOMEOSTATIC_PROCESS	0.433	0.104
		GO_REGULATION_OF_HOMEOSTATIC_PROCESS	0.370	0.131
sodium ion transmembrane	4	GO_REGULATION_OF_SODIUM_ION_TRANSMEMBRANE_TRANSPORT	0.650	0.022
		GO_REGULATION_OF_METAL_ION_TRANSPORT	0.371	0.154
		GO_REGULATION_OF_CALCIUM_ION_TRANSPORT	0.376	0.201
		GO_REGULATION_OF_SODIUM_ION_TRANSPORT	0.537	0.065
anion negative transport	3	GO_NEGATIVE_REGULATION_OF_ION_TRANSPORT	0.422	0.140
		GO_NEGATIVE_REGULATION_OF_TRANSPORT	0.390	0.098
		GO_NEGATIVE_REGULATION_OF_ANION_TRANSPORT	0.550	0.093
Death				
		GO_NEGATIVE_REGULATION_OF_INTRINSIC_APOPTOTIC_SIGNALING_PATHWAY	0.634	0.002
apoptotic pathway extrinsic	12	GO_NEGATIVE_REGULATION_OF_APOPTOTIC_SIGNALING_PATHWAY	0.564	0.001
		GO_POSITIVE_REGULATION_OF_INTRINSIC_APOPTOTIC_SIGNALING_PATHWAY	0.528	0.069
		GO_NEGATIVE_REGULATION_OF_EXTRINSIC_APOPTOTIC_SIGNALING_PATHWAY	0.579	0.006
		GO_POSITIVE_REGULATION_OF_APOPTOTIC_SIGNALING_PATHWAY	0.533	0.009
		GO_REGULATION_OF_EXTRINSIC_APOPTOTIC_SIGNALING_PATHWAY_IN_ABSENCE_OF_LIGAND	0.617	0.041
		GO_REGULATION_OF_INTRINSIC_APOPTOTIC_SIGNALING_PATHWAY	0.557	0.005
		GO_REGULATION_OF_APOPTOTIC_SIGNALING_PATHWAY	0.505	0.005
		GO_REGULATION_OF_EXTRINSIC_APOPTOTIC_SIGNALING_PATHWAY	0.572	0.002
		GO_POSITIVE_REGULATION_OF_EXTRINSIC_APOPTOTIC_SIGNALING_PATHWAY	0.671	0.009
		GO_POSITIVE_REGULATION_OF_CELL_DEATH	0.431	0.032
		GO_REGULATION_OF_EXTRINSIC_APOPTOTIC_SIGNALING_PATHWAY_VIA_DEATH_DOMAIN_RECEPTORS	0.543	0.069
extrinsic apoptotic intrinsic	8	GO_CELL_DEATH	0.413	0.046
		GO_APOPTOTIC_SIGNALING_PATHWAY	0.523	0.003
		GO_APOPTOTIC_MITOCHONDRIAL_CHANGES	0.543	0.064
		GO_EXTRINSIC_APOPTOTIC_SIGNALING_PATHWAY	0.564	0.012
		GO_INTRINSIC_APOPTOTIC_SIGNALING_PATHWAY_IN_RESPONSE_TO_DNA_DAMAGE	0.646	0.004
		GO_EXTRINSIC_APOPTOTIC_SIGNALING_PATHWAY_VIA_DEATH_DOMAIN_RECEPTORS	0.692	0.007
		GO_INTRINSIC_APOPTOTIC_SIGNALING_PATHWAY_BY_P53_CLASS_MEDIATOR	0.578	0.060
		GO_INTRINSIC_APOPTOTIC_SIGNALING_PATHWAY	0.611	0.000
neuron process death	5	GO_REGULATION_OF_NEURON_APOPTOTIC_PROCESS	0.470	0.033
		GO_NEGATIVE_REGULATION_OF_NEURON_APOPTOTIC_PROCESS	0.570	0.009
		GO_POSITIVE_REGULATION_OF_NEURON_DEATH	0.452	0.126
		GO_NEGATIVE_REGULATION_OF_NEURON_DEATH	0.524	0.011

		GO_REGULATION_OF_NEURON_DEATH	0.446	0.046
apoptotic process epithelial	3	GO_REGULATION_OF_ENDOTHELIAL_CELL_APOPTOTIC_PROCESS	0.649	0.012
		GO_REGULATION_OF_EPITHELIAL_CELL_APOPTOTIC_PROCESS	0.505	0.084
		GO_NEGATIVE_REGULATION_OF_EPITHELIAL_CELL_APOPTOTIC_PROCESS	0.557	0.071
muscle cell death	2	GO_NEGATIVE_REGULATION_OF_CELL_DEATH	0.470	0.010
		GO_REGULATION_OF_MUSCLE_CELL_APOPTOTIC_PROCESS	0.507	0.183
Cell junction				
substrate junction assembly	12	GO_CELL_CELL_JUNCTION_ASSEMBLY	0.461	0.188
		GO_CELL_MATRIX_ADHESION	0.520	0.020
		GO_BIOLOGICAL_ADHESION	0.384	0.086
		GO_CELL_SUBSTRATE_ADHESION	0.510	0.010
		GO_INTEGRIN_MEDIATED_SIGNALING_PATHWAY	0.458	0.130
		GO_CELL_JUNCTION_ASSEMBLY	0.511	0.023
		GO_CELL_SUBSTRATE_JUNCTION_ASSEMBLY	0.571	0.041
		GO_SUBSTRATE_ADHESION_DEPENDENT_CELL_SPREADING	0.480	0.196
		GO_ADHERENS_JUNCTION_ORGANIZATION	0.476	0.097
		GO_ADHERENS_JUNCTION_ASSEMBLY	0.618	0.038
		GO_CELL_JUNCTION_ORGANIZATION	0.400	0.126
		GO_CELL_SUBSTRATE_ADHERENS_JUNCTION_ASSEMBLY	0.629	0.037
Transcription/replication/gene expression				
sequence specific binding	4	GO_NEGATIVE_REGULATION_OF_SEQUENCE_SPECIFIC_DNA_BINDING_TRANSCRIPTION_FACTOR_ACTIVITY	0.438	0.100
		GO_REGULATION_OF_SEQUENCE_SPECIFIC_DNA_BINDING_TRANSCRIPTION_FACTOR_ACTIVITY	0.381	0.129
		GO_POSITIVE_REGULATION_OF_NF_KAPPAB_TRANSCRIPTION_FACTOR_ACTIVITY	0.452	0.057
		GO_POSITIVE_REGULATION_OF_SEQUENCE_SPECIFIC_DNA_BINDING_TRANSCRIPTION_FACTOR_ACTIVITY	0.371	0.176
telomere maintenance lengthening	3	GO_POSITIVE_REGULATION_OF_TELOMERE_MAINTENANCE_VIA_TELOMERE_LENGTHENING	0.464	0.225
		GO_REGULATION_OF_DNA_BIOSYNTHETIC_PROCESS	0.393	0.232
		GO_REGULATION_OF_DNA_REPLICATION	0.389	0.191
regulation dna binding	3	GO_NEGATIVE_REGULATION_OF_DNA_BINDING	0.507	0.139
		GO_REGULATION_OF_BINDING	0.367	0.155
		GO_NEGATIVE_REGULATION_OF_BINDING	0.379	0.234
templated polymerase promoter	2	GO_POSITIVE_REGULATION_OF_TRANSCRIPTION_FROM_RNA_POLYMERASE_II_PROMOTER_IN_RESPONSE_TO_STRESS	0.606	0.052
		GO_REGULATION_OF_DNA_TEMPLATED_TRANSCRIPTION_IN_RESPONSE_TO_STRESS	0.513	0.051
amino acid activation	1	GO_AMINO_ACID_ACTIVATION	0.467	0.206
Cell cycle				
regulation cell cycle	2	GO_REGULATION_OF_CELL_CYCLE_G1_S_PHAS	0.411	0.146

		E_TRANSITION		
		GO_SIGNAL_TRANSDUCTION_BY_P53_CLASS_MEDIATOR	0.428	0.135
Circadian rhythm				
circadian rhythm ovulation	3	GO_RHYTHMIC_PROCESS	0.406	0.081
		GO_OVULATION_CYCLE	0.496	0.050
		GO_CIRCADIAN_RHYTHM	0.425	0.104
Ageing				
cell aging	2	GO_CELL_AGING	0.452	0.188
		GO_AGING	0.482	0.015
Miscellaneous				
vasodilation circulation vasoconstriction	5	GO_VASCULAR_PROCESS_IN_CIRCULATORY_SYSTEM	0.410	0.097
		GO_REGULATION_OF_VASOCONSTRICTION	0.463	0.111
		GO_POSITIVE_REGULATION_OF_BLOOD_CIRCULATION	0.482	0.059
		GO_REGULATION_OF_ANATOMICAL_STRUCTURE_SIZE	0.343	0.209
		GO_REGULATION_OF_VASODILATION	0.542	0.104
systemic arterial pressure	2	GO_REGULATION_OF_SYSTEMIC_ARTERIAL_BLOOD_PRESSURE	0.419	0.201
		GO_REGULATION_OF_RENAL_SYSTEM_PROCESS	0.614	0.056
digestive system process	1	GO_DIGESTIVE_SYSTEM_PROCESS	0.575	0.036
heart rate conduction	3	GO_REGULATION_OF_HEART_RATE	0.497	0.098
		GO_REGULATION_OF_CARDIAC_CONDUCTION	0.465	0.167
		GO_REGULATION_OF_HEART_CONTRACTION	0.364	0.232
regulation body fluid	1	GO_REGULATION_OF_BODY_FLUID_LEVELS	0.427	0.041
		GO_NEGATIVE_REGULATION_OF_HYDROLASE_ACTIVITY	0.529	0.001
involved symbiotic interaction	8	GO_INTERACTION_WITH_SYMBIONT	0.584	0.030
		GO_TRANSLATIONAL_INITIATION	0.392	0.206
		GO_MULTI_ORGANISM_LOCALIZATION	0.456	0.154
		GO_MOVEMENT_IN_ENVIRONMENT_OF_OTHER_ORGANISM_INVOLVED_IN_SYMBIOTIC_INTERACTION	0.520	0.036
		GO_INTERSPECIES_INTERACTION_BETWEEN_ORGANISMS	0.380	0.105
		GO_INTERACTION_WITH_HOST	0.458	0.061
		GO_MODIFICATION_OF_MORPHOLOGY_OR_PHYSIOLOGY_OF_OTHER_ORGANISM	0.452	0.097
		GO_VIRAL_LIFE_CYCLE	0.408	0.093

Cytoscape plugin Enrichment map in combination with Autoannotate plugin was used to cluster significantly enriched GOs (FDR q-value<0.25) according to their similarity coefficient. Clusters were classified in categories depending on the GOs they contain. Enrichment score from GSEA analysis for each GO is also show